UFSC

Modeling and simulation of electric vehicles (EVs) and design of batteries for EVs

INEP

Prof. Gierri Waltrich, Dr.

Prof. Marcelo L. Heldwein, Dr. sc. ETH

E-mails: gierri.waltrich@ufsc.br / heldwein@inep.ufsc.br

COBEP 2015

NOVEMBER 29^{th} TO DECEMBER 2^{nd}, 2015

SPEC IEEE Power Electronics Society

SOUTHERN POWER ELECTRONICS CONFERENCE

Power Electronics Institute

Newsweek’s top 10 (world) hottest cities 2006

“Florianópolis, Brazil –

aka 'Silicon Valley of Brazil, with beaches', ban on heavy industry”

~380 000 people / 17 universities / 2 technological centers

Aim: create 40k tech jobs in 10 years

Federal University of Santa Catarina (2013)

Founded: **1961**

Built area: **651796 m²**

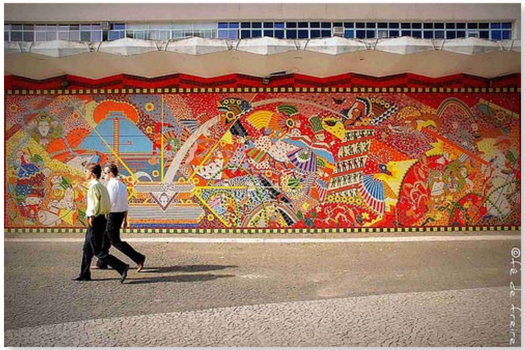

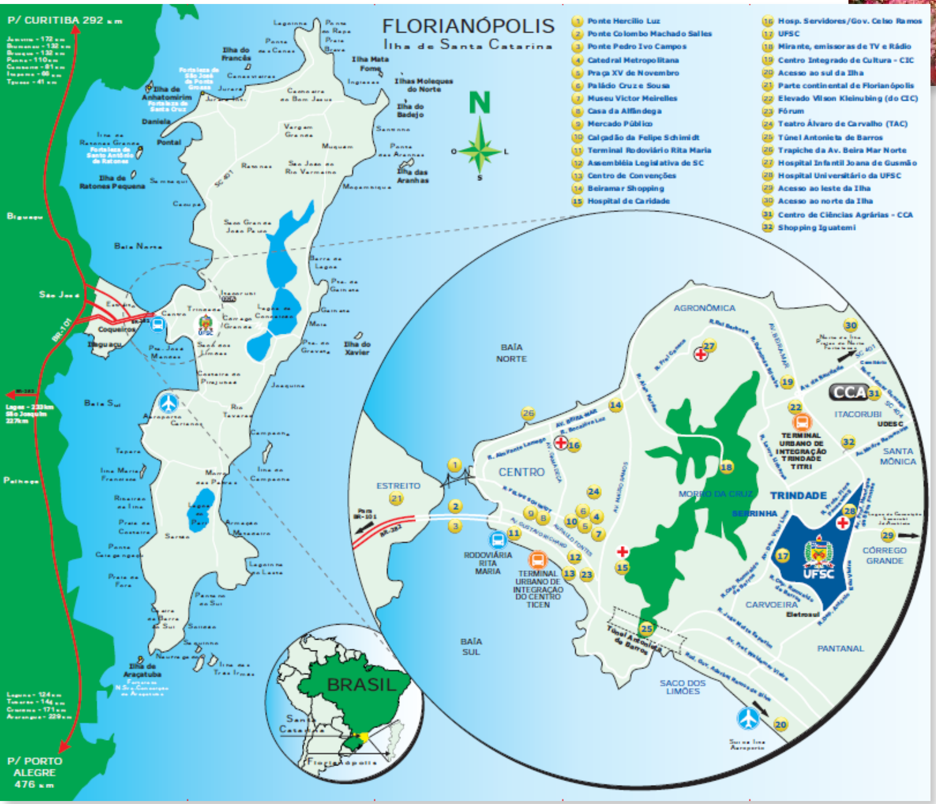

- Entry students /year:
- Total undergrad.: **30602**
- Total grad.: **7514**

  } = **38116**
- PhD: **2900**
- Publications/year (journals): **2023**
- Scholarships: **7521**
- Professors+lecturers: **2059**
- Other staff: **3137**
- Budget: **R$955.479.298,00**

Technological Center – CTC

Departments

Architecture and urbanism – ARQ

Automation and Systems – DAS

Civil Engineering – ECV

Electrical Engineering – EEL

Mechanical Engineering – EMC

Production Engineering – EPS

Chemical and Food Engineering – EQA

Environmental Engineering – ENS

Informatics and Statistics – INE

Numbers

360 Professors / lecturers

120 Employees

5100 Undergraduation students

2000 Graduation students

49 Professors / lecturers

13 Employees

498 Undergraduation students

145 Master students

89 PhD students

Power Electronics Institute – INEP

Founded: **1979 as LAMEP**

Re-structured: **1994 as INEP**

Supervisor
Prof. Denizar

Professors
Prof. Samir A. Mussa
Prof. Marcelo L. Heldwein
Prof. Telles B. Lazzarin
Prof. Roberto F. Coelho

Prof. Gierri Waltrich
Prof. Arnaldo J. Perin

Administrative staff — **2**

Technical staff — **3**

Students — **94**

Undergrad.	*Master*	*PhD*	*Postdoc*
41	**26**	**23**	**4**

INEP

Professors


Prof. Denizar C. Martins


Prof. Samir A. Mussa


Prof. Marcelo L. Heldwein


Prof. Telles B. Lazzarin


Prof. Roberto F. Coelho


Prof. Gierri Waltrich


Prof. Arnaldo J. Perin

Tutorial outline

- Part 1 – EVs infrastructure and required Power Electronics
  - EVs today
  - Power electronics systems for Evs
  - Introductions to battery systems for Evs, V2G and V2H
  - Recharge modes, stations and converters
- Part 2 - Modeling and simulation of EVs and design of batteries
  - Battery modelling
  - Motor modelling
  - Vehicle modelling
  - Electric vehicle range modelling

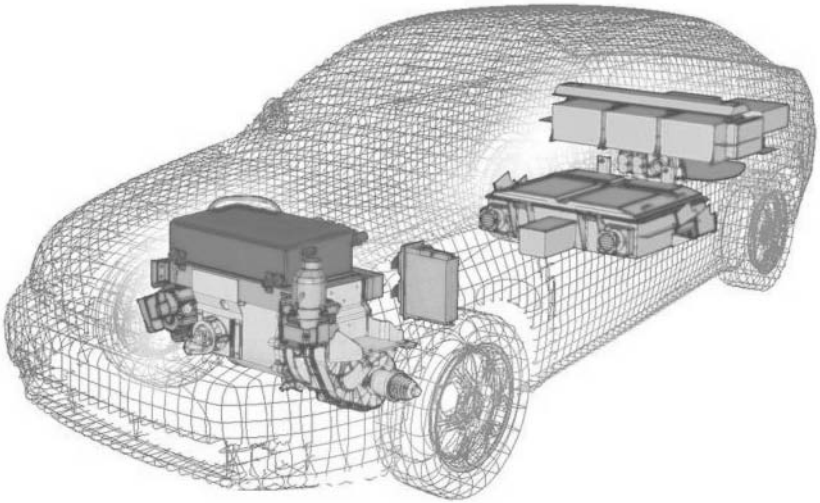

Modeling and simulation of electric vehicles (EVs) and design of batteries for Evs

Part 1 – EVs infrastructure and Power Electronics

Prof. Marcelo L. Heldwein, Dr. sc. ETH

E-mail: heldwein@inep.ufsc.br

UFSC

INEP

COBEP 2015

NOVEMBER 29th TO DECEMBER 2nd, 2015

SPEC IEEE Power Electronics Society

SOUTHERN POWER ELECTRONICS CONFERENCE

Charging stations

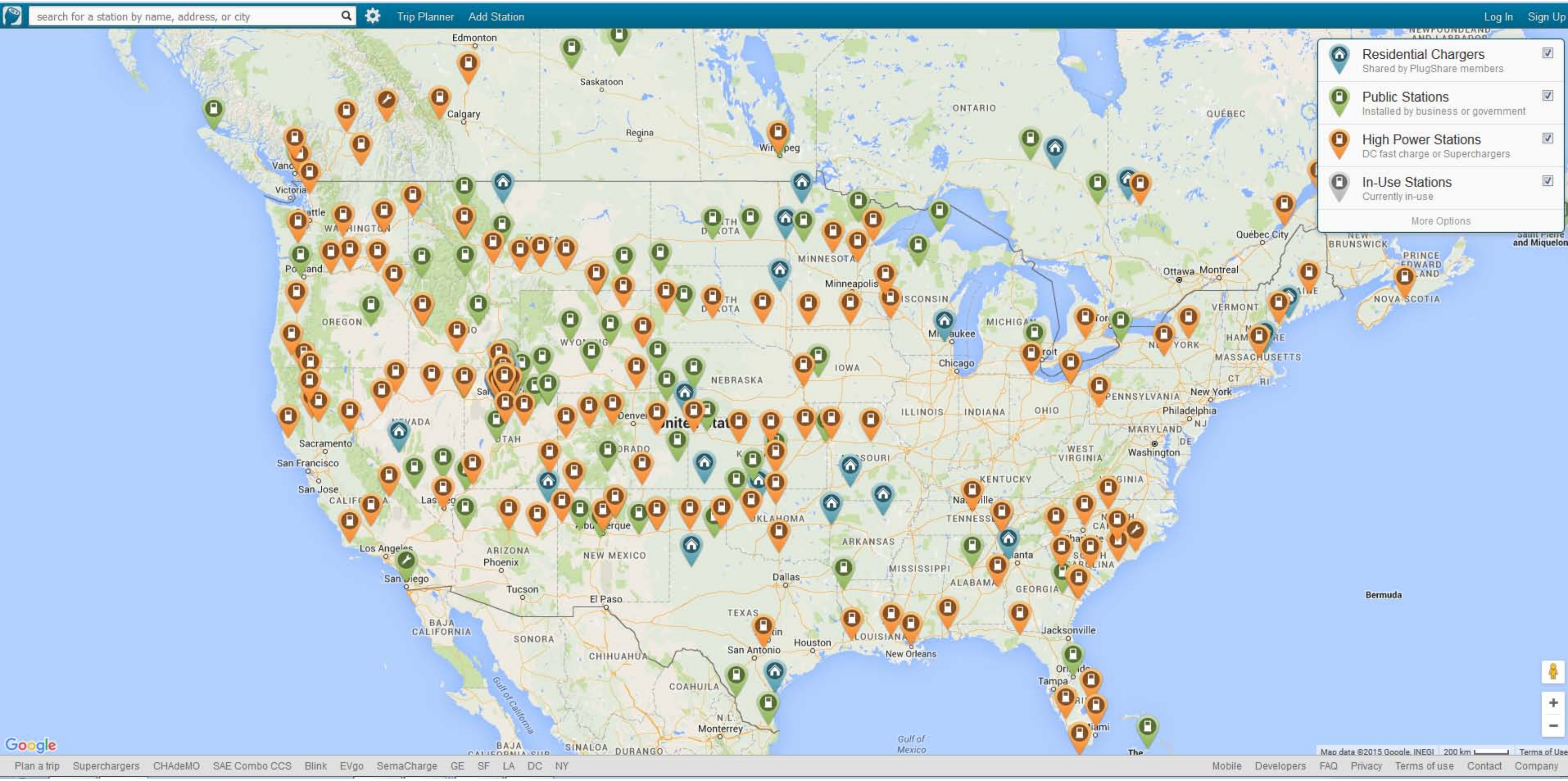

Charging stations

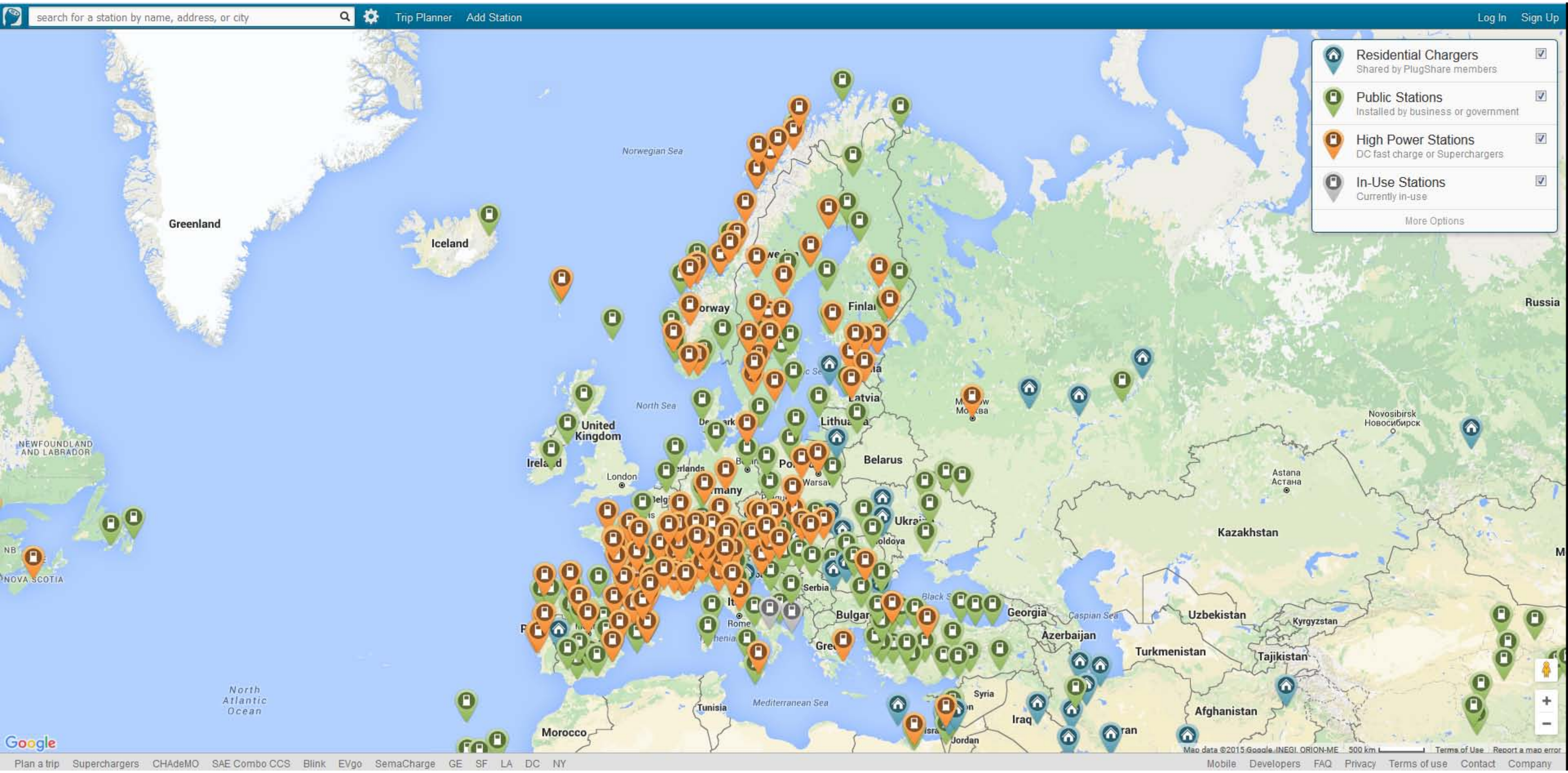

Charging stations

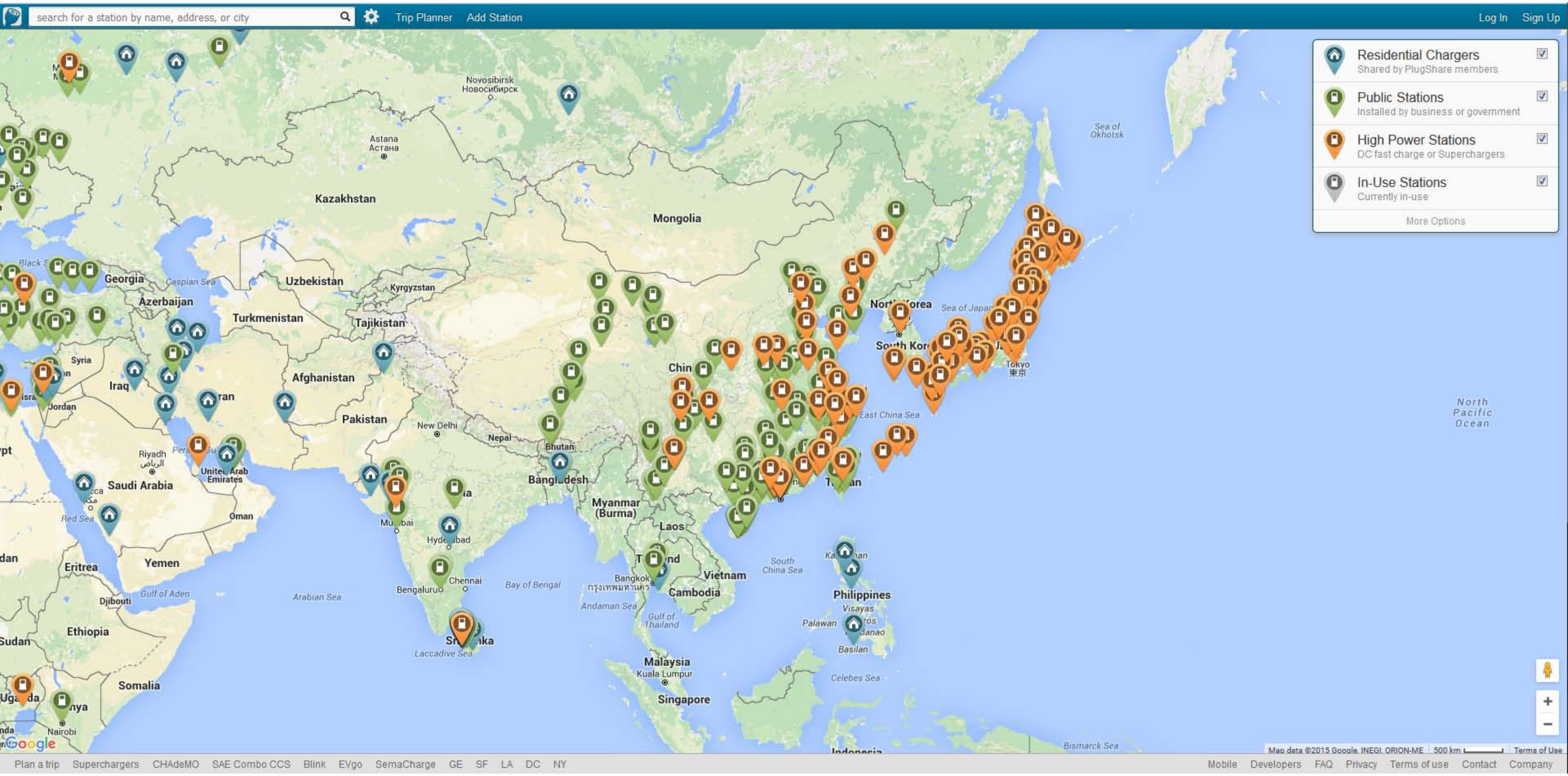

Charging stations

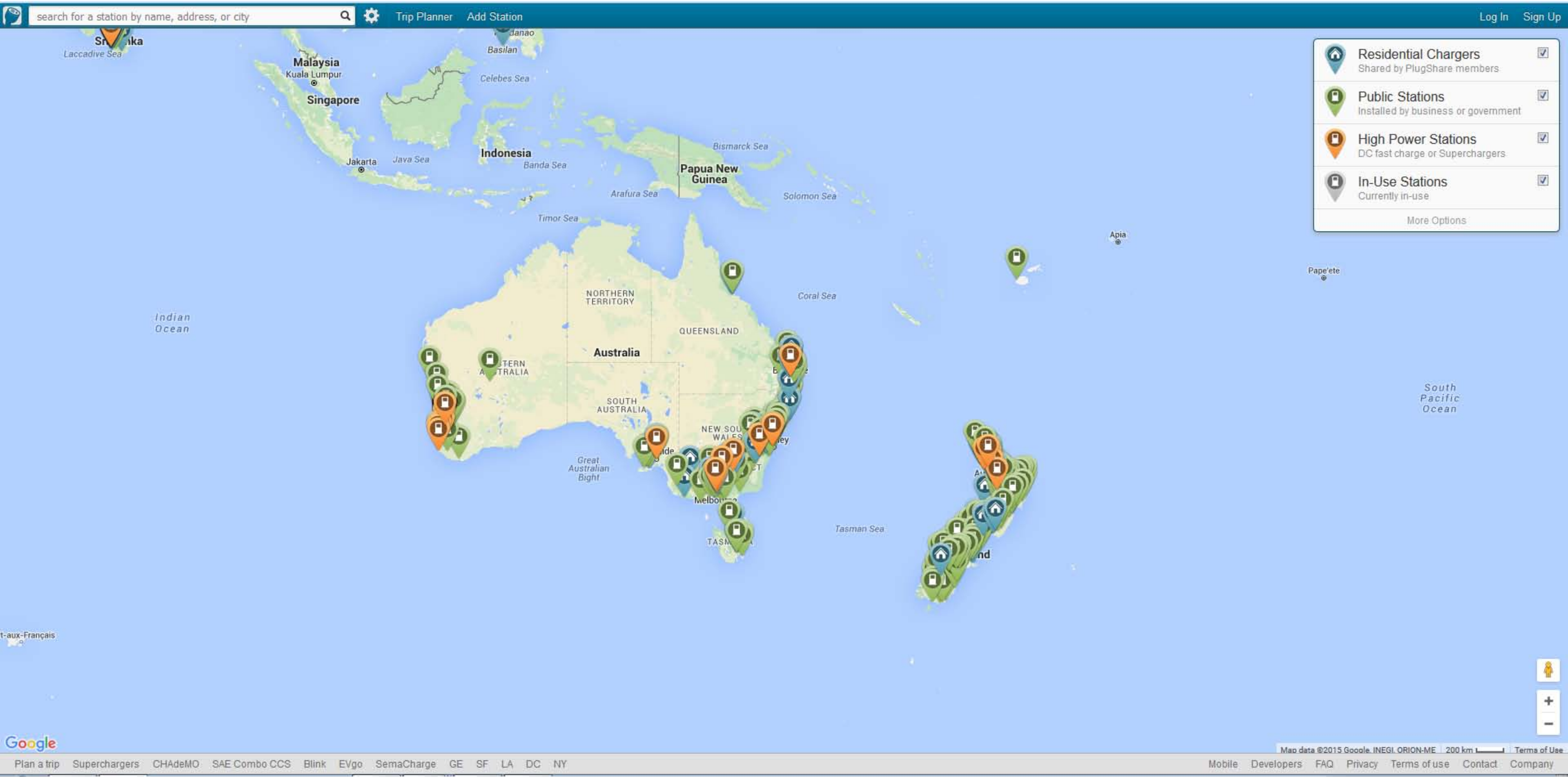

Charging stations

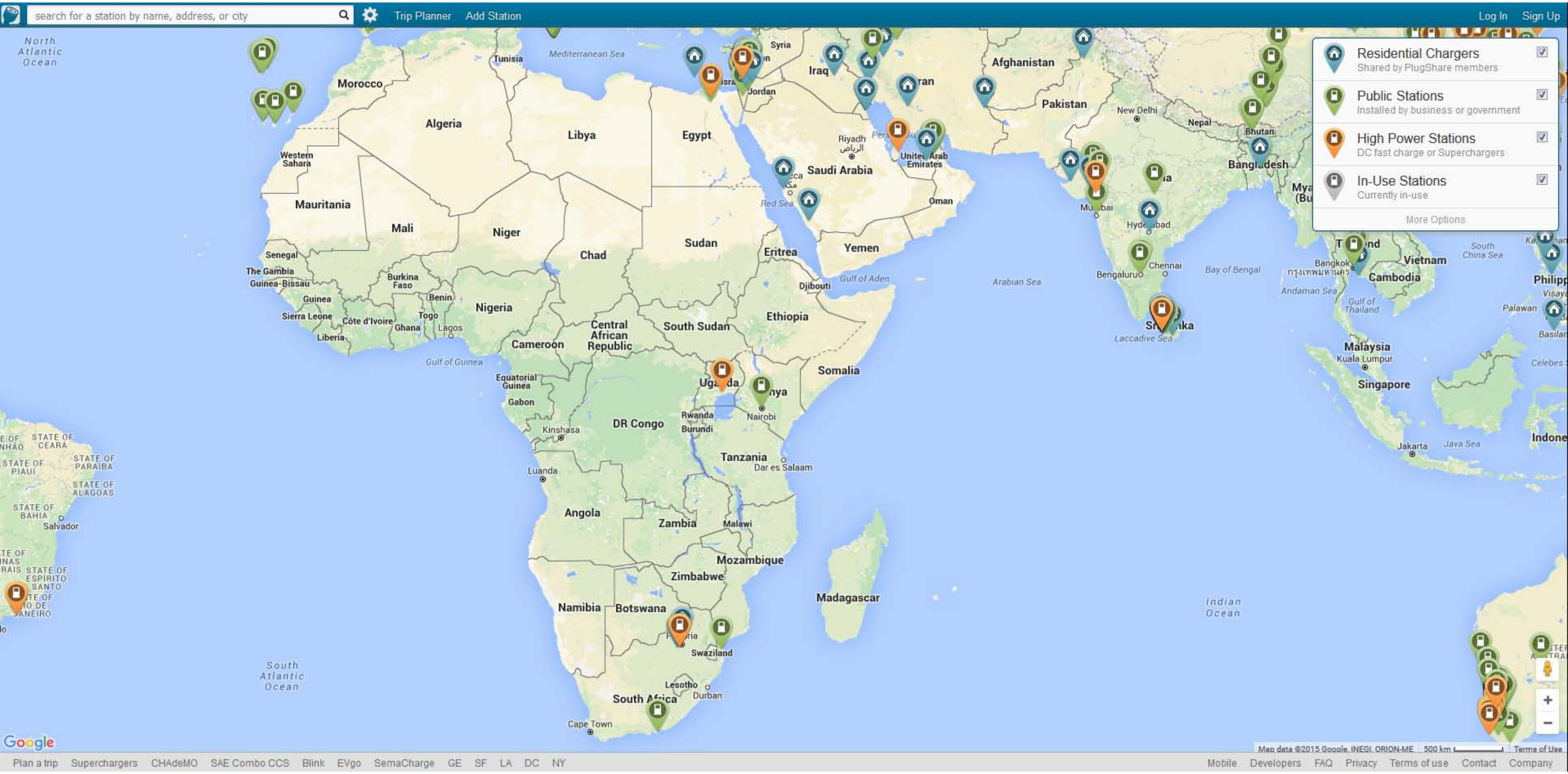

Charging stations

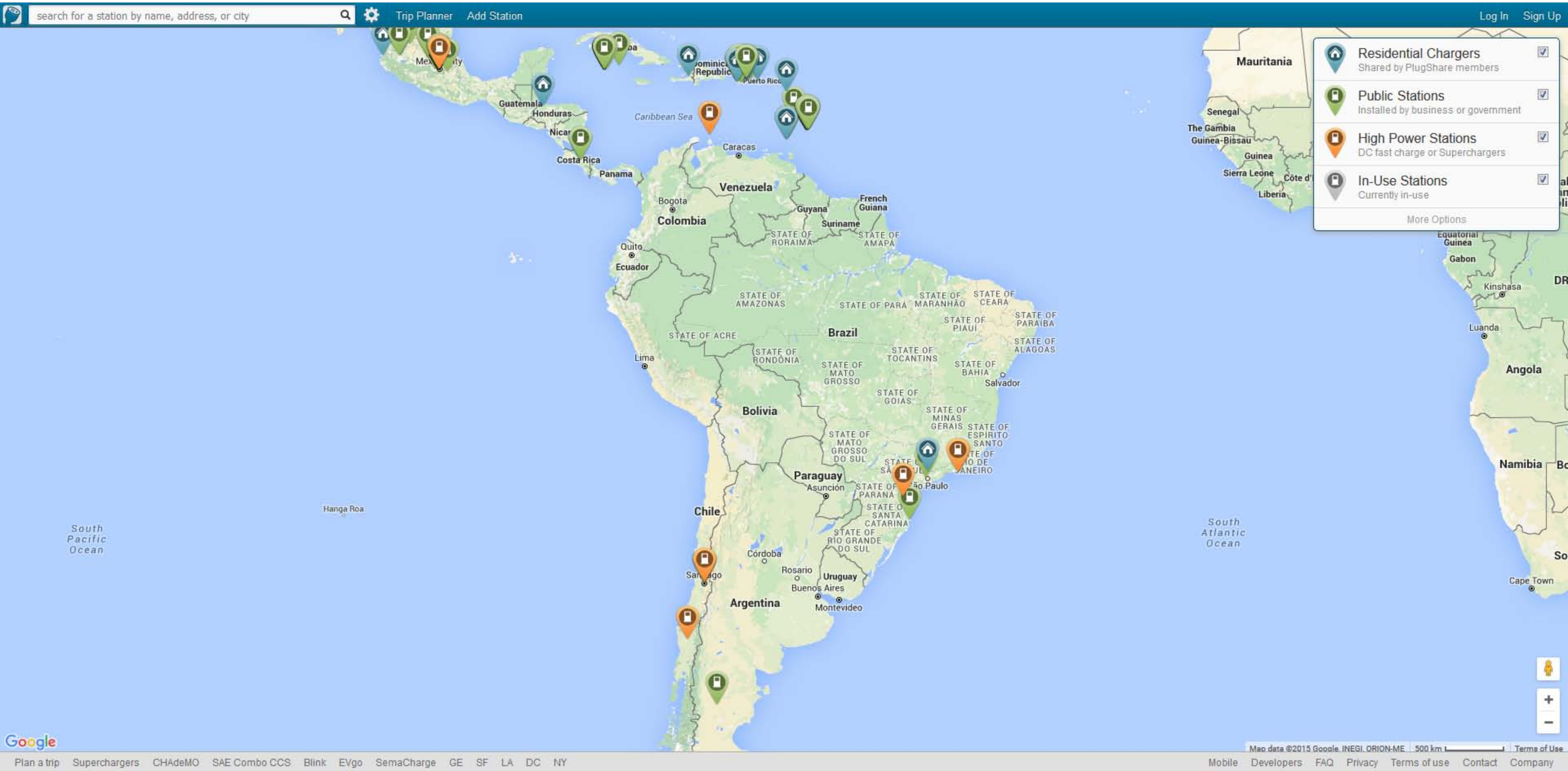

EV conditions

global EV sales

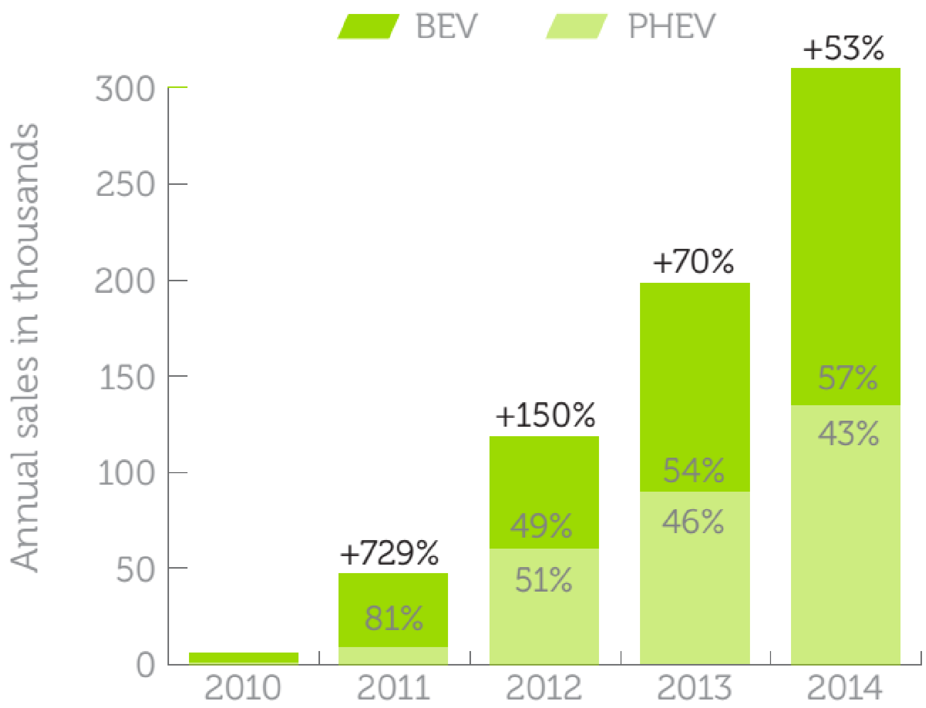

EV spending by category

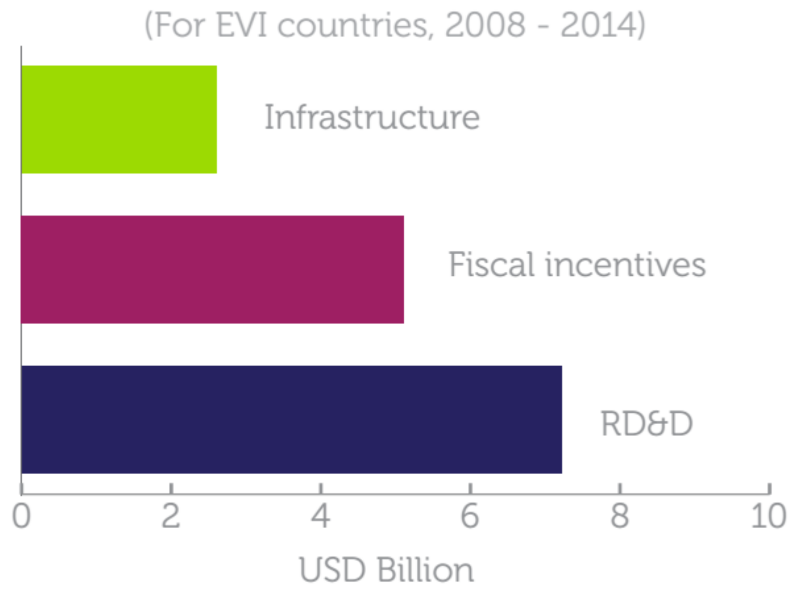

2015 Global EV Outlook (GEO 2015) OECD/IEA

EV conditions

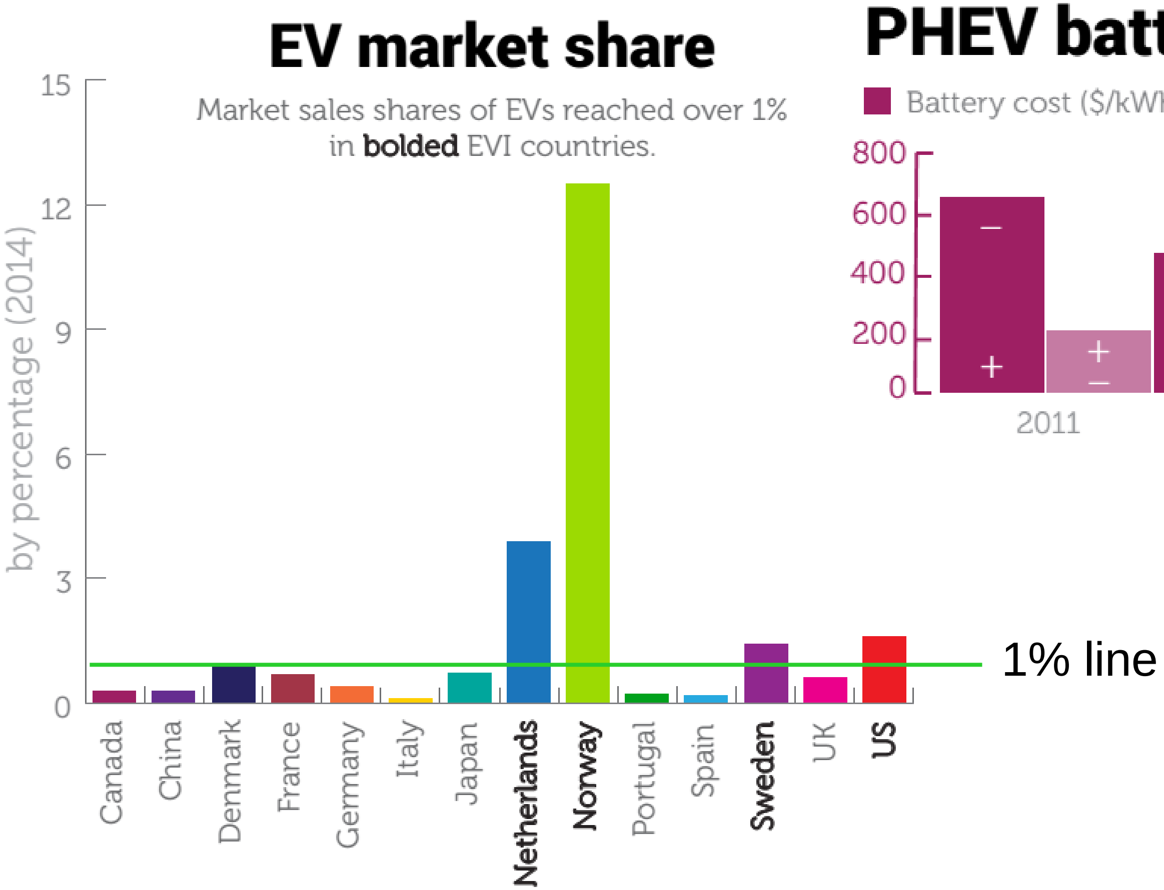

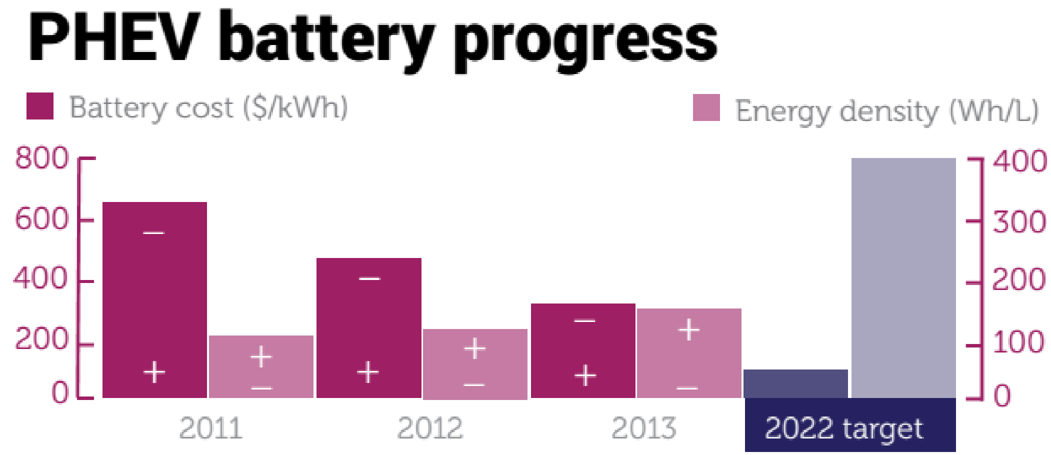

EVs are more popular (but not there yet)

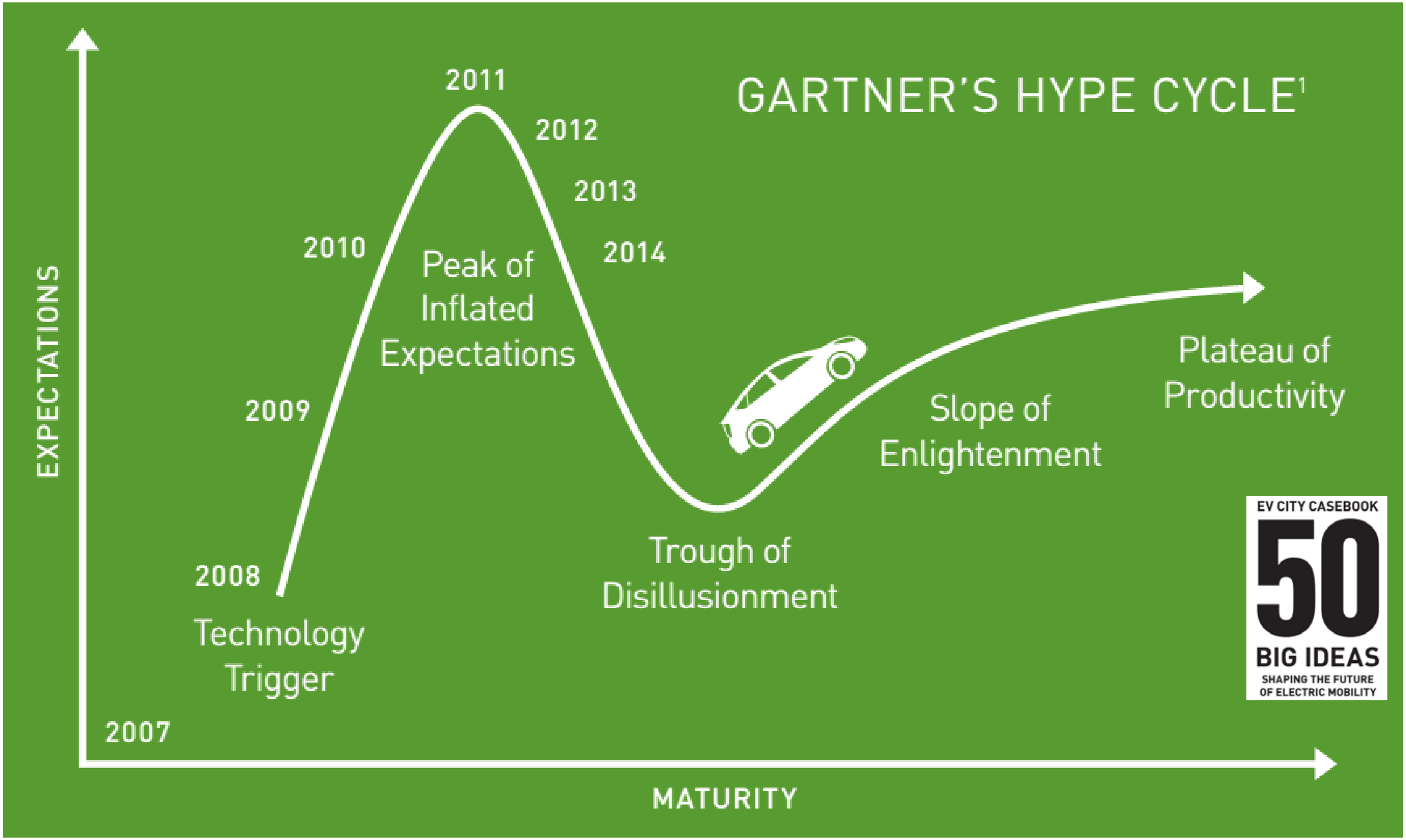

http://www.iea.org/topics/transport/subtopics/electricvehiclesinitiative/EVI_2014_Casebook.pdf

Electric vehicles

Electric Vehicle	EV	Vehicles that use an electric motor instead of a traditional internal combustion engine (ICE)
Battery Electric Vehicle	BEV	Electric Vehicles that run purely on electrical power from battery packs
Hybrid Electric Vehicle	HEV	Electric vehicles that use a gas-powered motor in addition to the electric motor
Plug-in Hybrid Electric Vehicle	PHEV	A type of Hybrid Electric Vehicle with powerful batteries that can be charged with a plug through a wall socket
Full Performance Battery Electric Vehicle	FCEV	An electric vehicle that uses a fuel cell rather than a battery to provide electricity that powers the car
Hydrogen Internal Combustion Vehicle	H2ICV	An altered version of the traditional gasoline internal combustion engine car. The hydrogen engine burns fuel in the same way as gasoline engines.

http://vancouver.ca/sustainability/documents/ElectricVehicleClassificationTable.pdf

Electric vehicles

City Electric Vehicle	CEV	Battery Electric Vehicles with limited acceleration and a top speed
Neighbourhood Electric Vehicle	NEV	Battery Electric Vehicles with limited acceleration and a top speed
Fuel Cell Auxiliary Power Unit Vehicle	FCAPUV	Fuel Cell Vehicles using a solid oxide fuel cell utilizing a solid ceramic material as the electrolyte
Neighbourhood Zero Emission Vehicle	NZEV	Battery Electric Vehicles with limited acceleration and a top speed
Low Speed Vehicles	LSV	Battery Electric Vehicles with limited acceleration and a top speed

INEP

http://vancouver.ca/sustainability/documents/ElectricVehicleClassificationTable.pdf

Electric vehicles

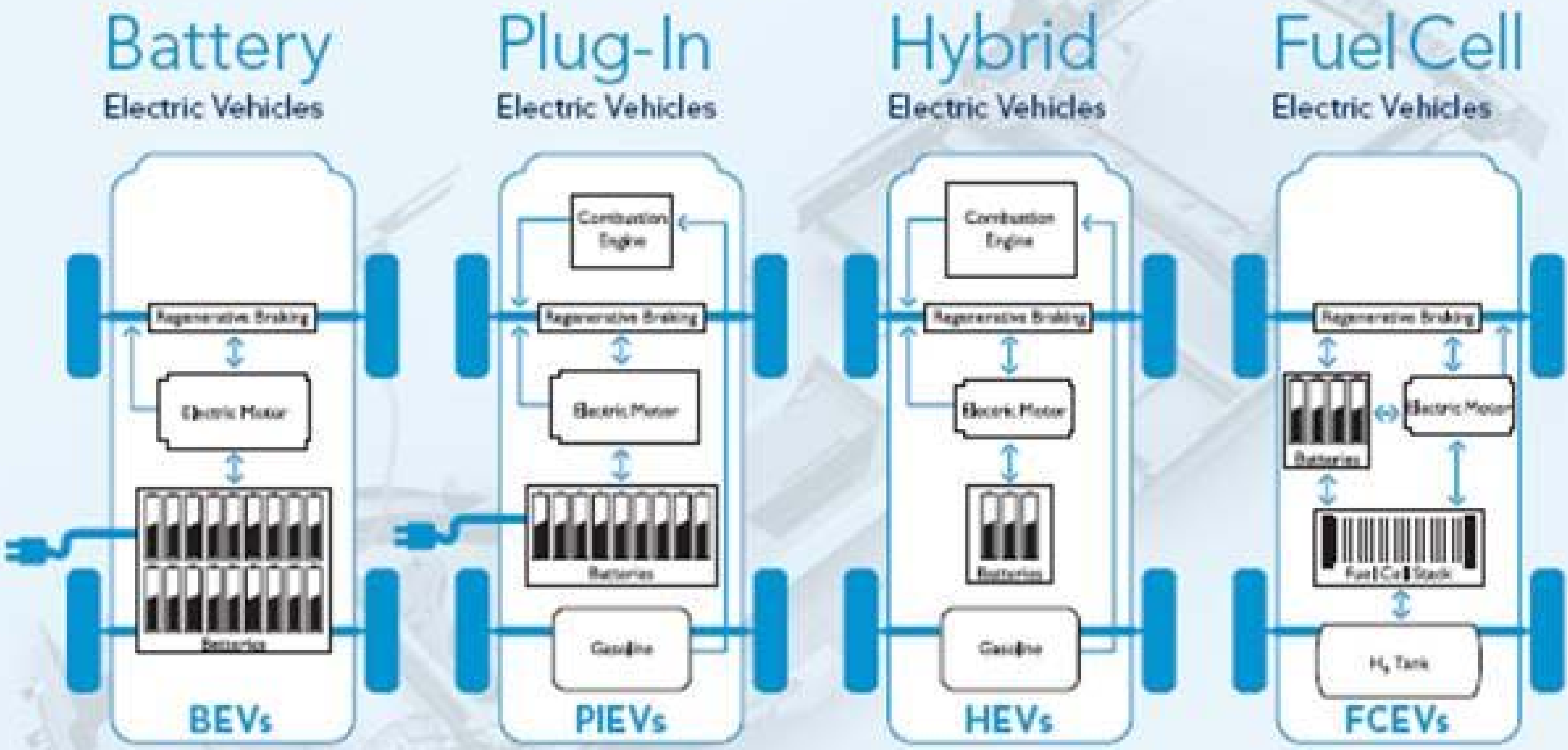

http://www.dolcera.com/wiki/index.php?title=Image:EV_vechicle_types.jpg

EV classification

Internal Combustion Engine

Belt Driven Integrated Starter Generator (ISG):
3-5kW With Idle Stop and Regenerative Braking

Integrated Starter Generator: 7-12kW With Idle Stop, Regenerative Braking & Downsized ICE

30-50 kW, 200-500 Volts With Electric Launch, Idle Stop, Regenerative Braking & Downsized ICE

Battery Powered Electric Vehicles

75-100 kW Fuel Cell Electric Vehicles

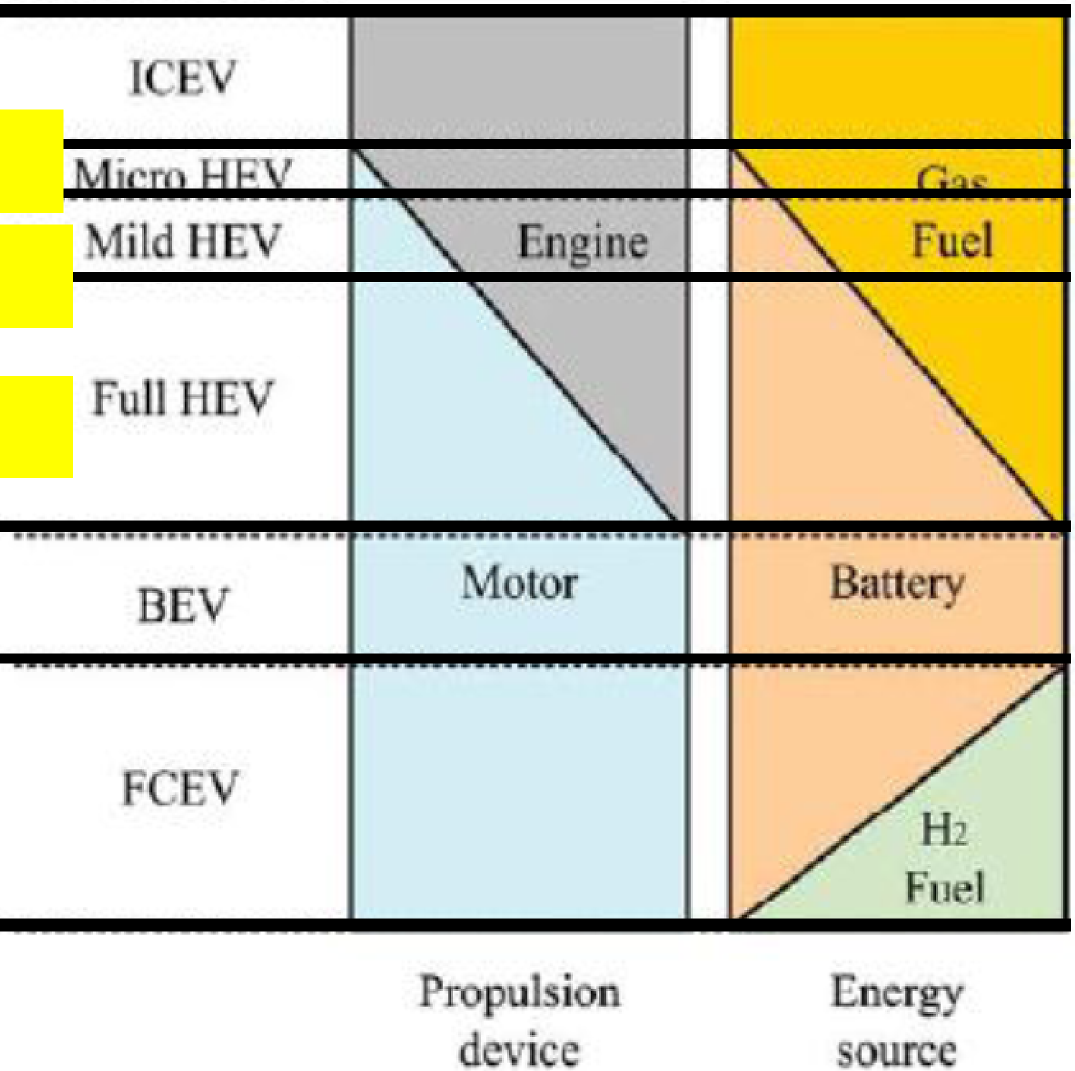

K. T. Chau and C.C. Chan, *Emerging Energy-Efficient Technologies for Hybrid Electric Vehicles*, Proceedings of the IEEE, April, 2007.

Power architectures

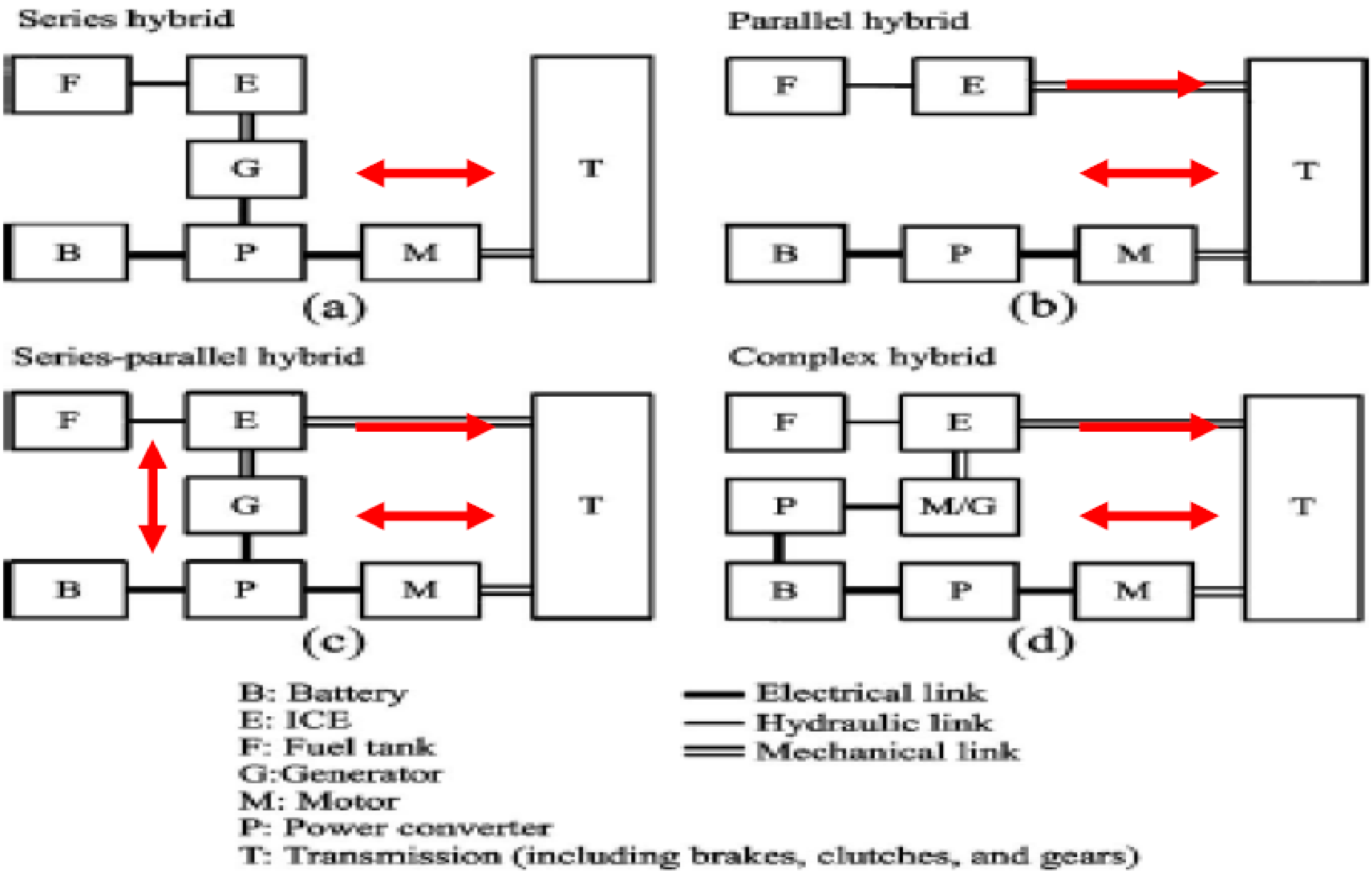

C.C. Chan, *The State of the Art of Electric Hybrid, and Fuel Cell Vehicles*, Proceedings of the IEEE, April, 2007.

Electronic systems in na EV

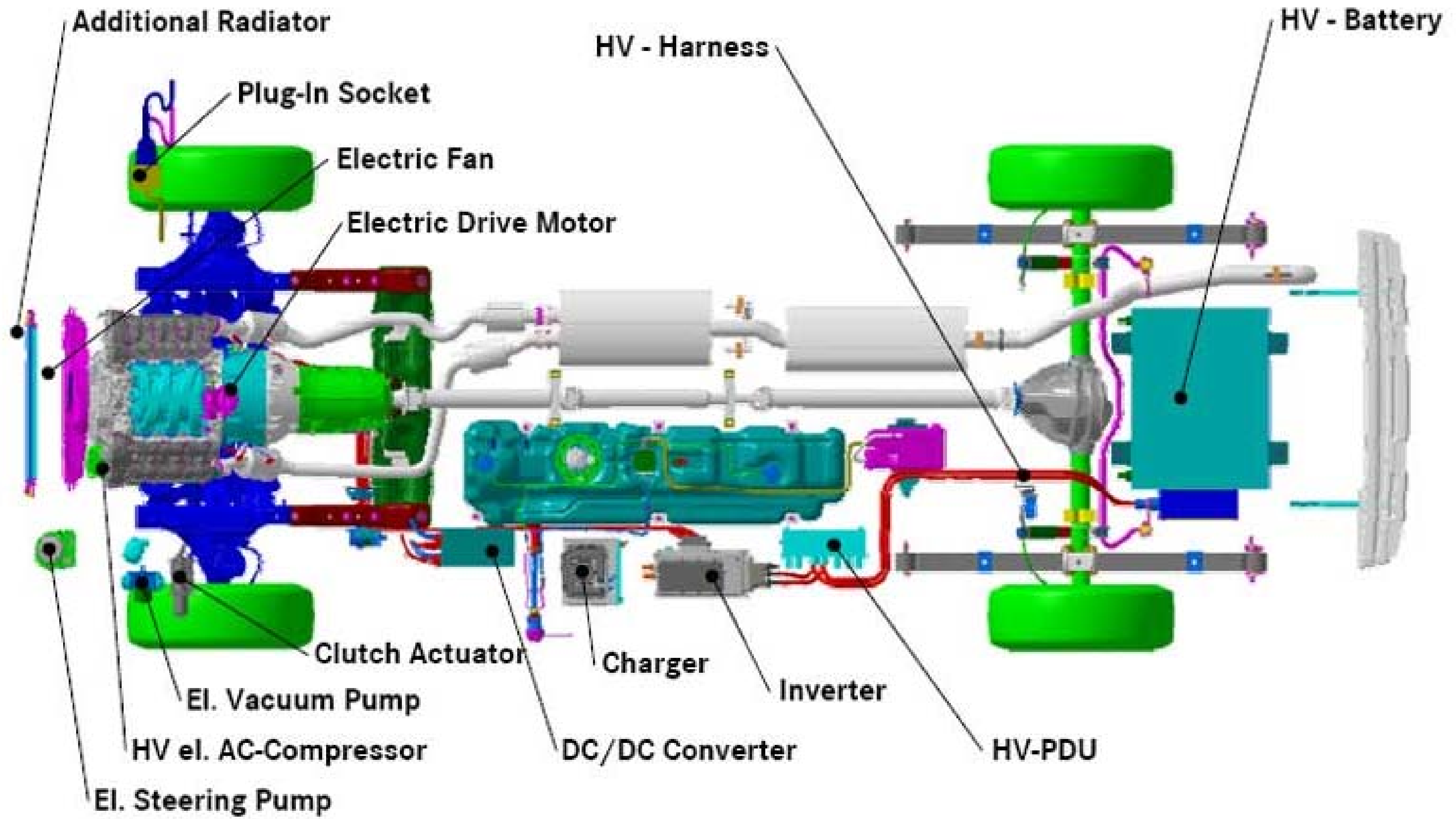

Power Electronics in a PHEV

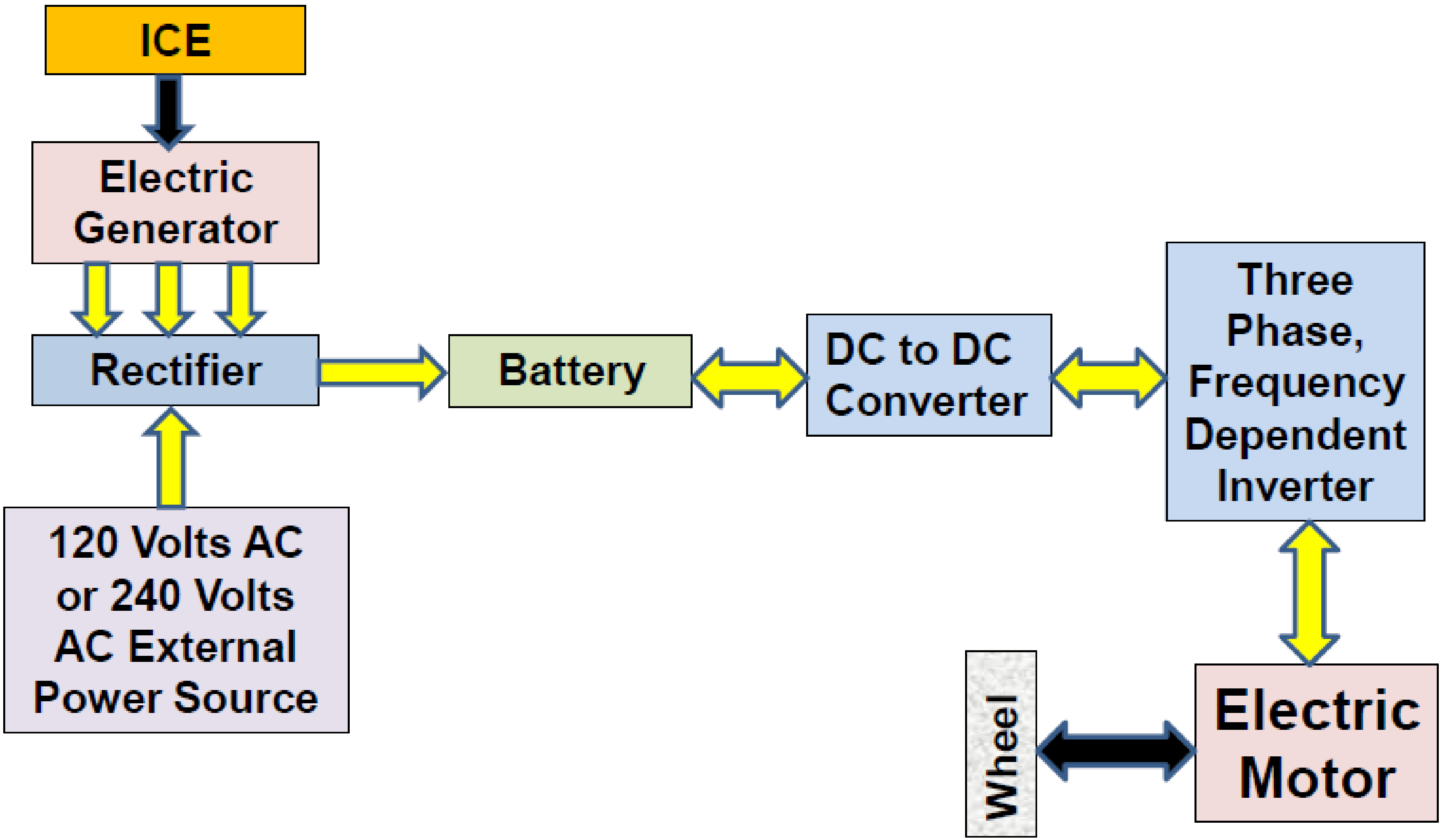

J. Gover, "A Tutorial on Hybrid Electric Vehicles: EV, HEV, PHEV and FCEV".

Power Electronics in a PHEV

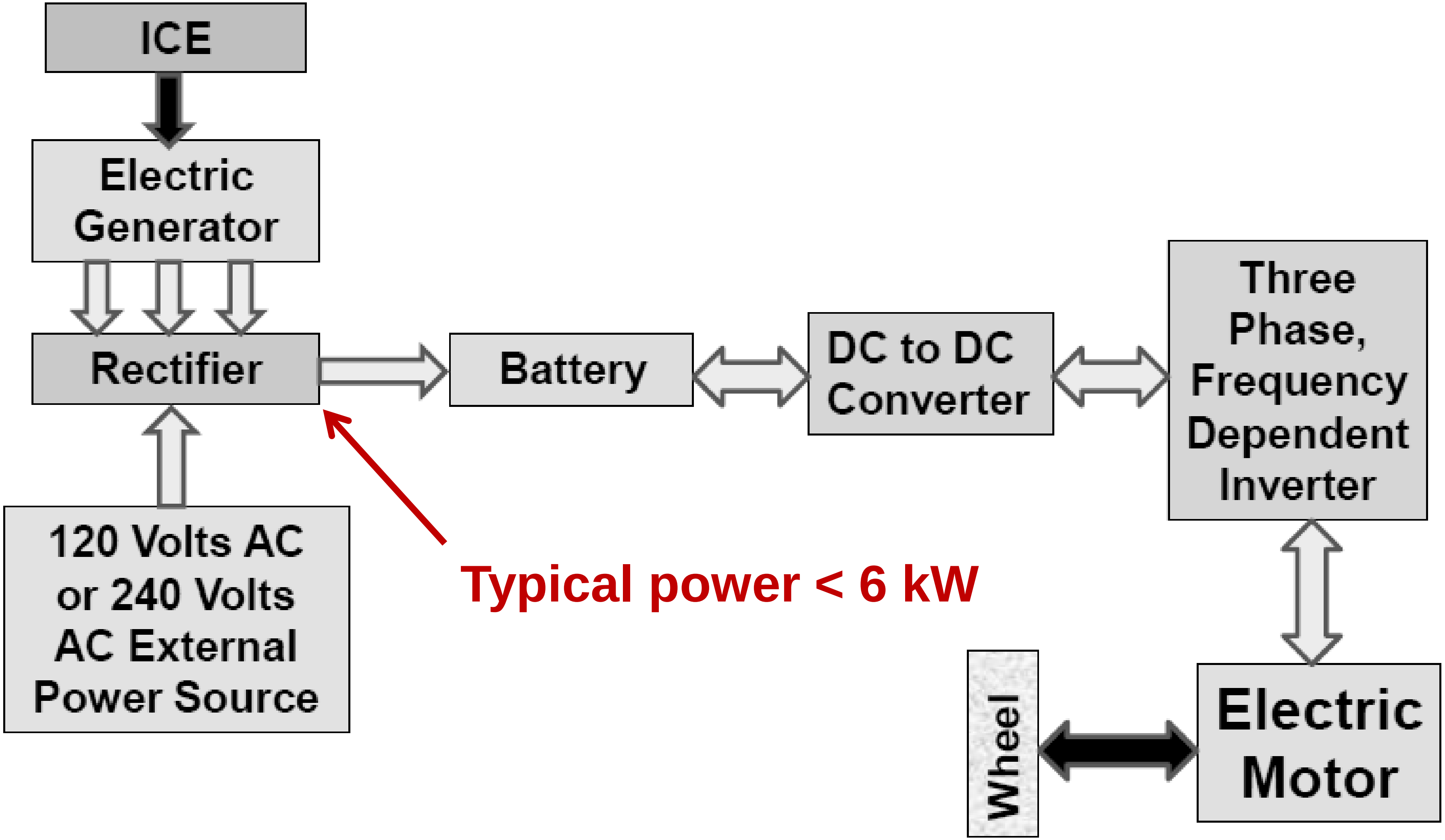

J. Gover, "A Tutorial on Hybrid Electric Vehicles: EV, HEV, PHEV and FCEV".

Evolution of the powertrain inverter technology

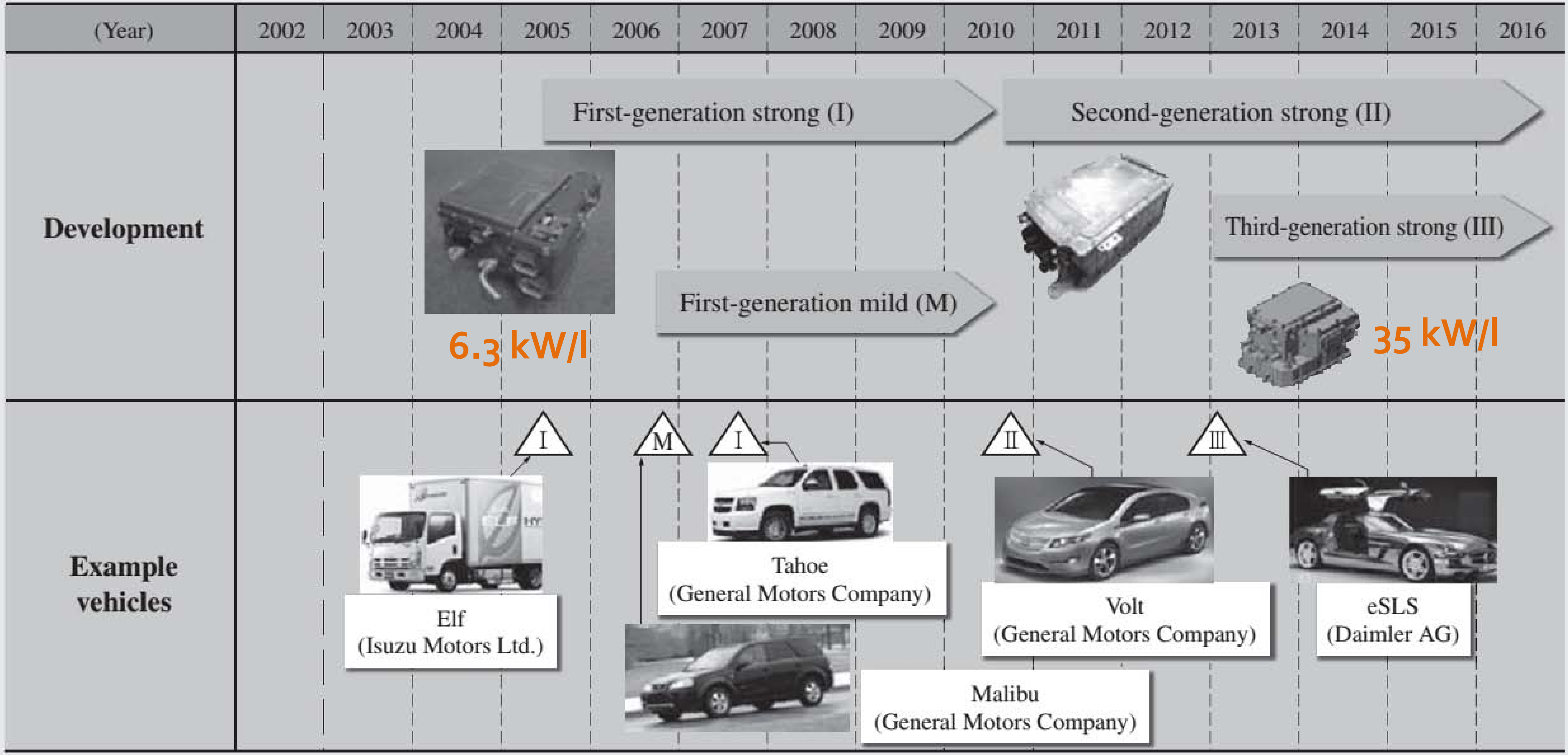

Hitachi Review Vol. 63 (2014), No. 2

INEP

High-power-density Inverter Technology for Hybrid and Electric Vehicle Applications

Takashi Kimura
Ryuichi Saitou
Kenji Kubo
Kinya Nakatsu
Hideaki Ishikawa
Kaname Sasaki

Evolution of the powertrain inverter technology

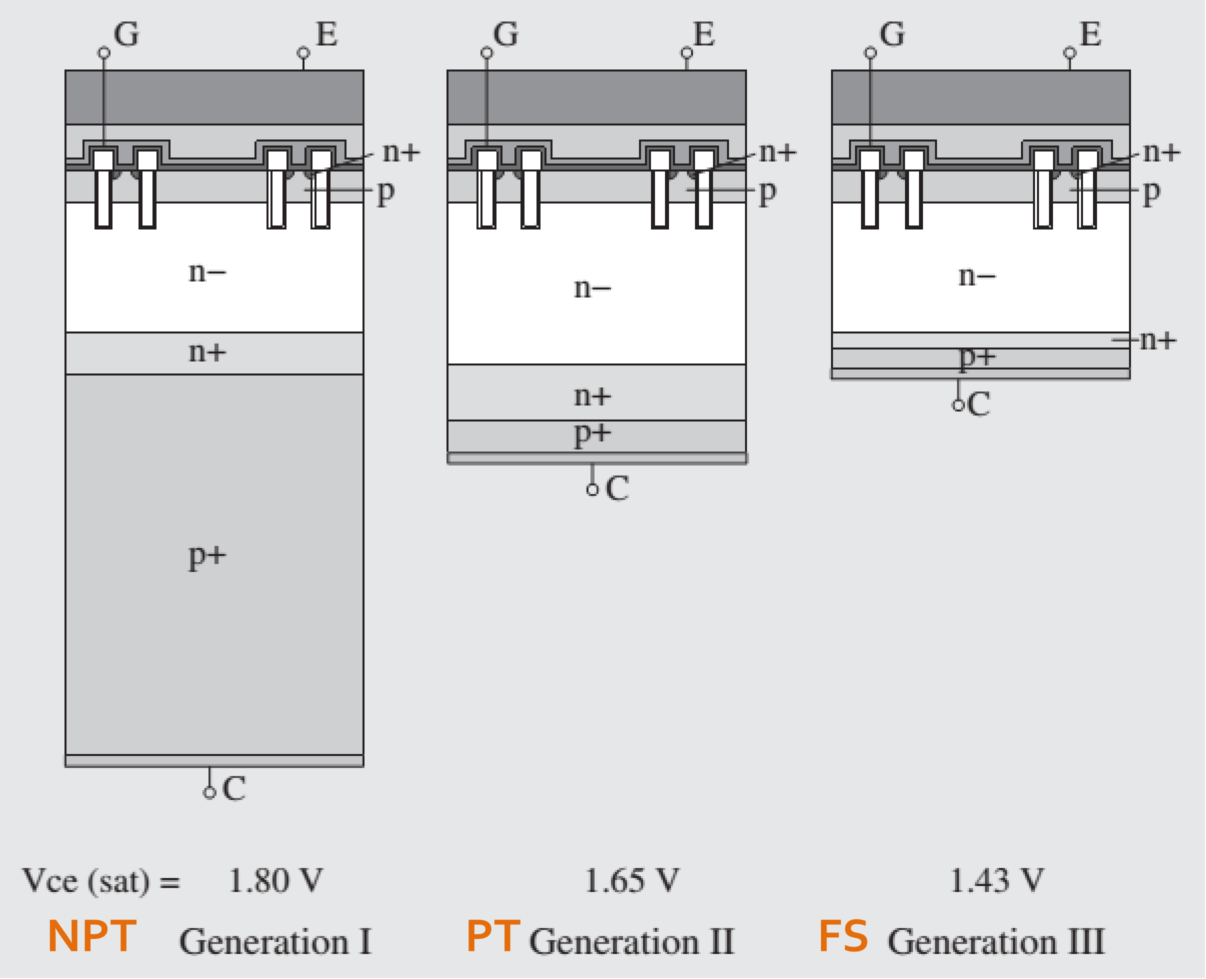

Hitachi Review Vol. 63 (2014), No. 2

High-power-density Inverter Technology for Hybrid and Electric Vehicle Applications

Takashi Kimura
Ryuichi Saitou
Kenji Kubo
Kinya Nakatsu
Hideaki Ishikawa
Kaname Sasaki

Evolution of the powertrain inverter technology

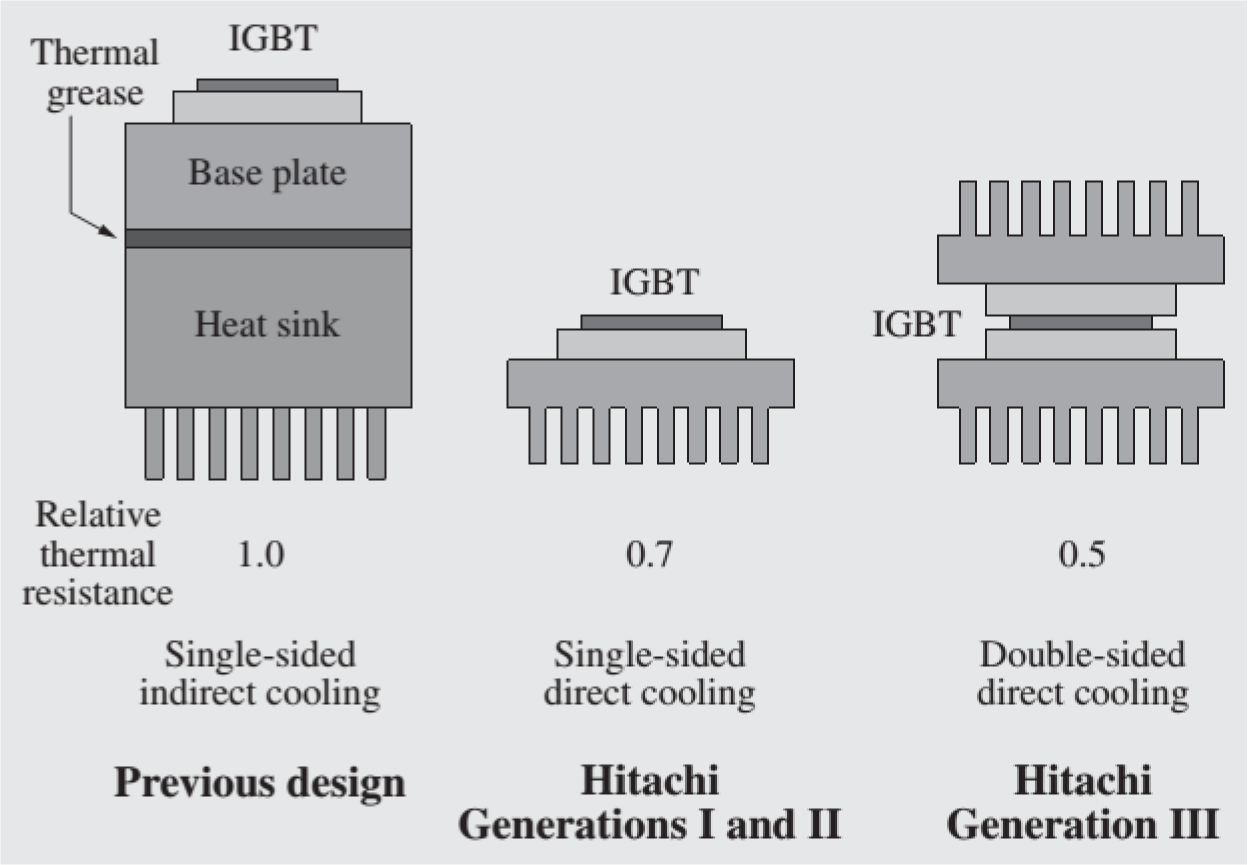

Hitachi Review Vol. 63 (2014), No. 2

High-power-density Inverter Technology for Hybrid and Electric Vehicle Applications

Takashi Kimura
Ryuichi Saitou
Kenji Kubo
Kinya Nakatsu
Hideaki Ishikawa
Kaname Sasaki

Evolution of the powertrain inverter technology

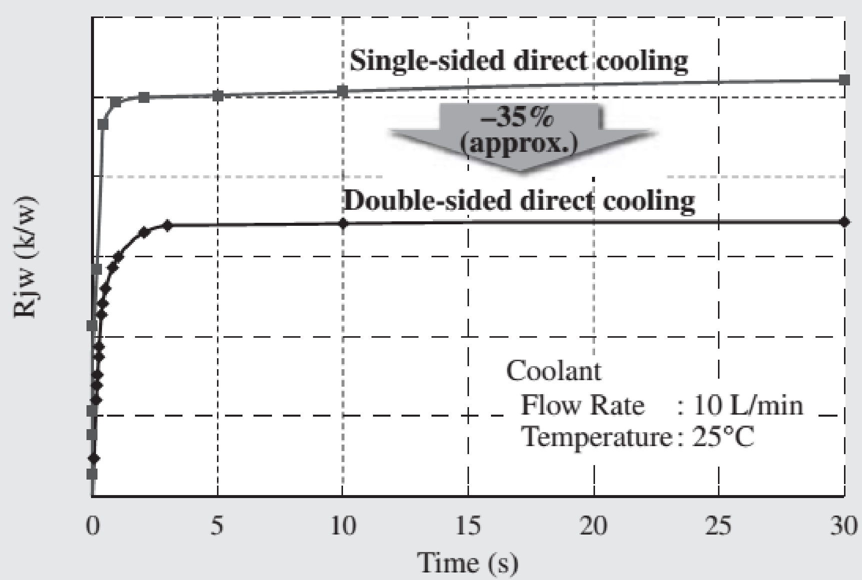

(a) Comparison of transient thermal resistance

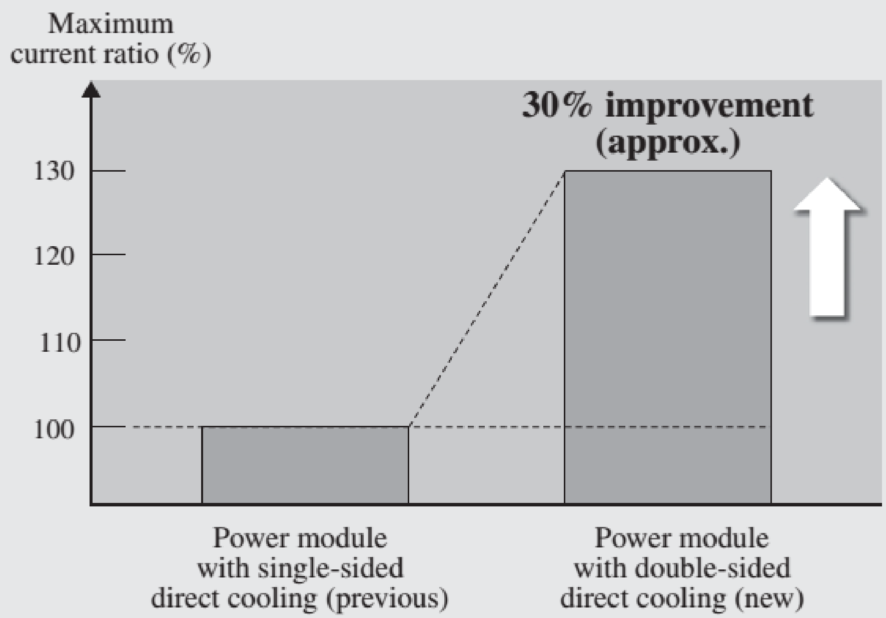

(b) Comparison of maximum current ratios

Hitachi Review Vol. 63 (2014), No. 2

INEP

High-power-density Inverter Technology for Hybrid and Electric Vehicle Applications

Takashi Kimura
Ryuichi Saitou
Kenji Kubo
Kinya Nakatsu
Hideaki Ishikawa
Kaname Sasaki

Evolution of the powertrain inverter technology

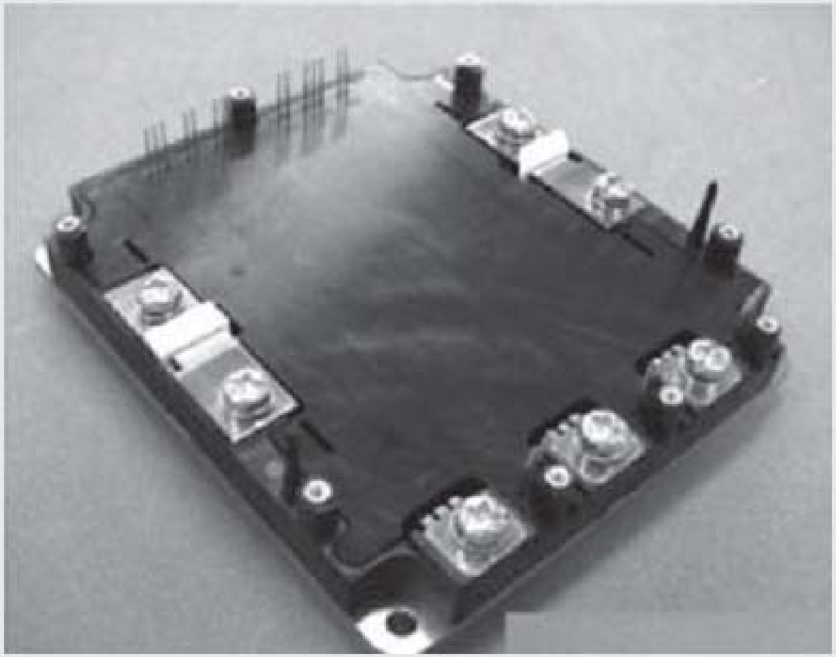

(a) Power module with single-sided direct cooling

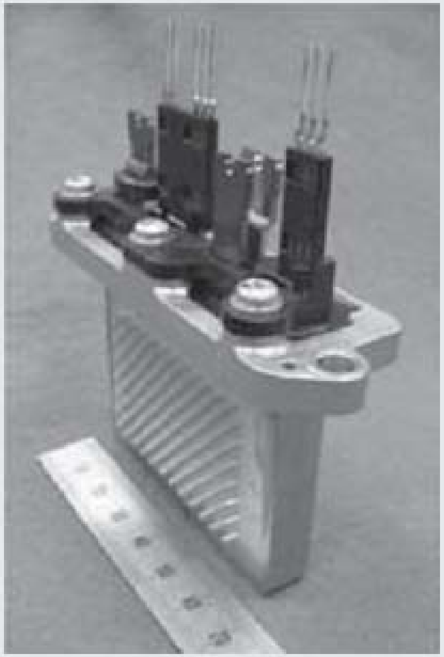

(b) Power module with double-sided direct cooling

Hitachi Review Vol. 63 (2014), No. 2

High-power-density Inverter Technology for Hybrid and Electric Vehicle Applications

Takashi Kimura
Ryuichi Saitou
Kenji Kubo
Kinya Nakatsu
Hideaki Ishikawa
Kaname Sasaki

In-wheel motor with integrated inverter

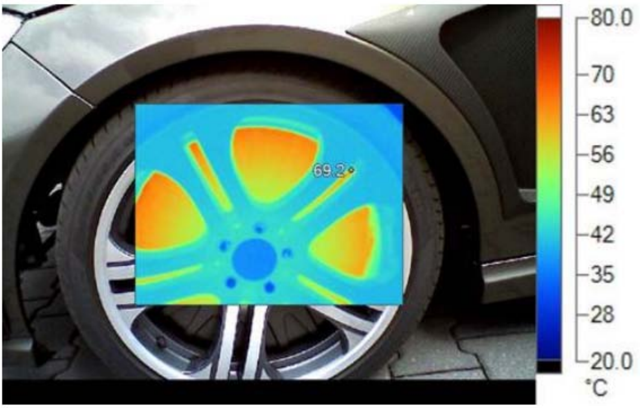

Fonte: http://www.proteanelectric.com/

Integrated inverter

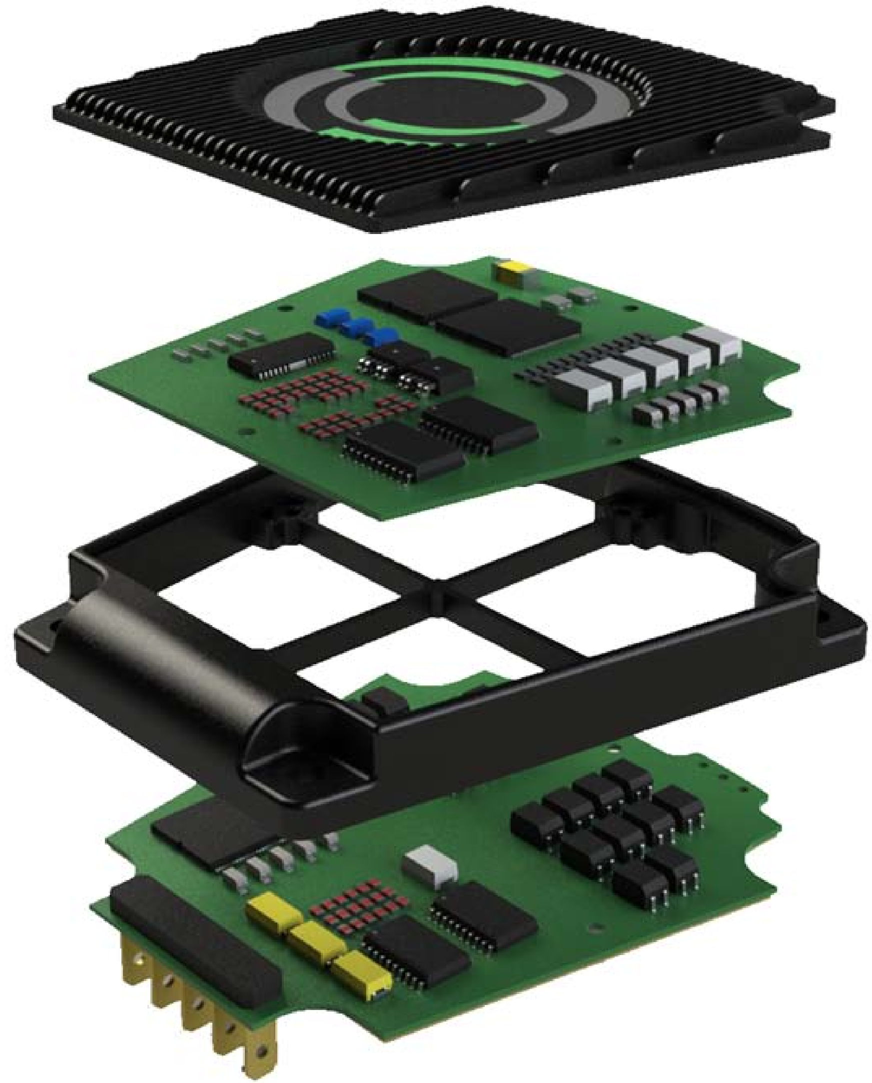

Challenges:

- Mechanical conditions
- Packaging and integration

Electric boat integrated drive

- Integrated inverter

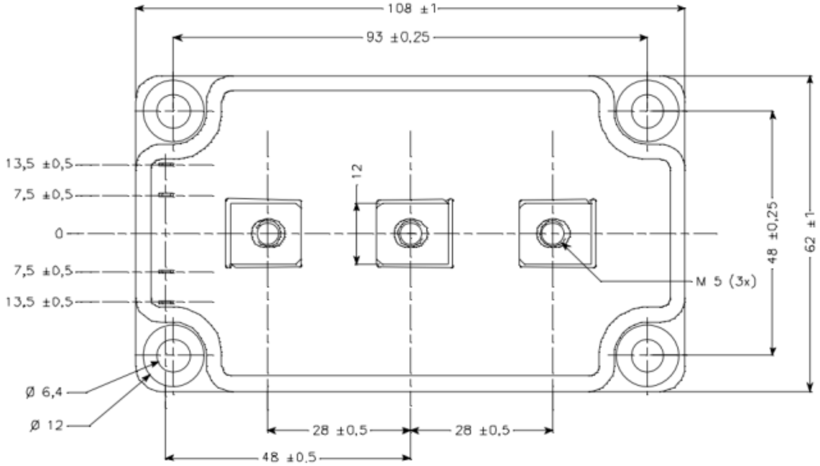

Electric boat integrated drive

- Integrated cooling system

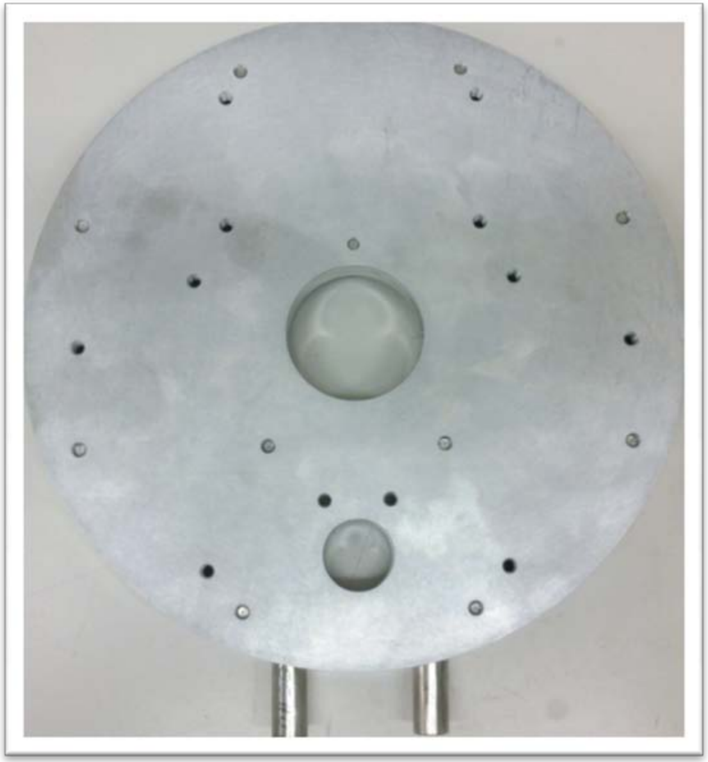

Electric boat integrated drive

- Control / modulation board

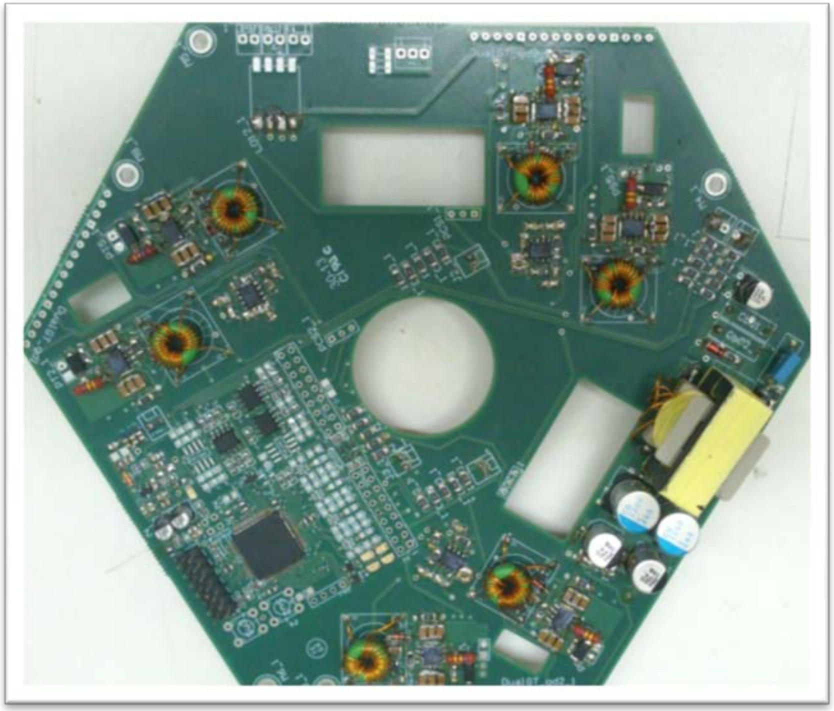

Electric boat integrated drive

- Assembly

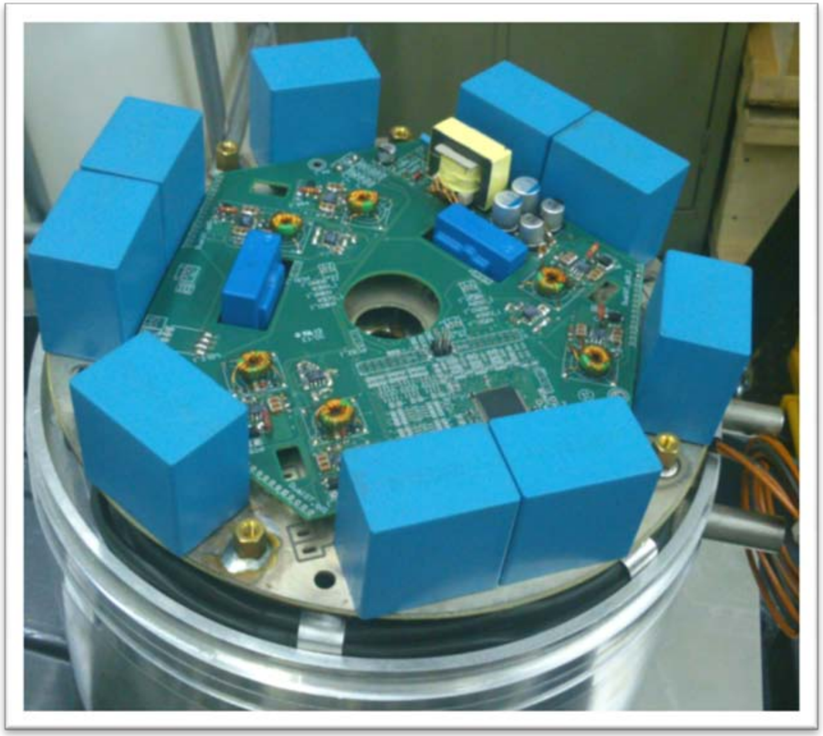

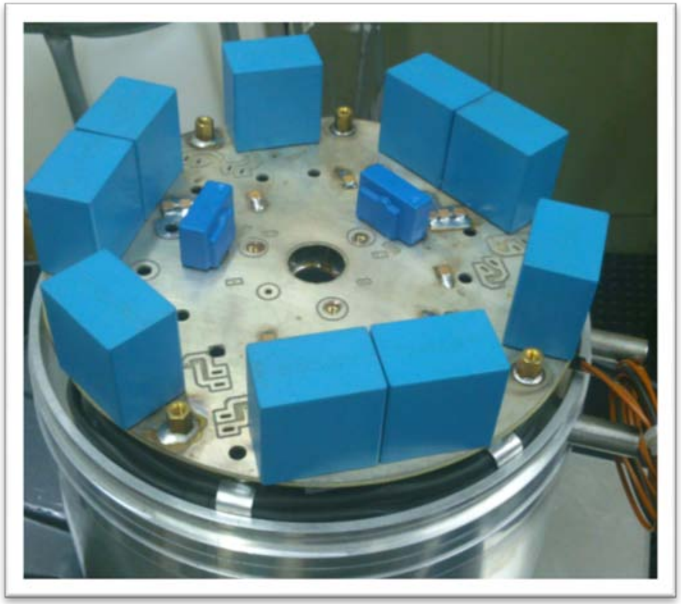

INEP

Electric boat integrated drive

- Assembly

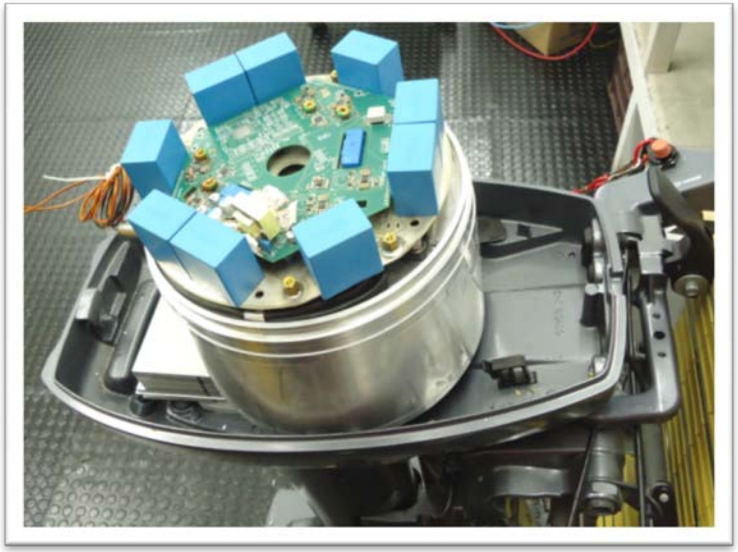

Li-ion batteries

HONDA

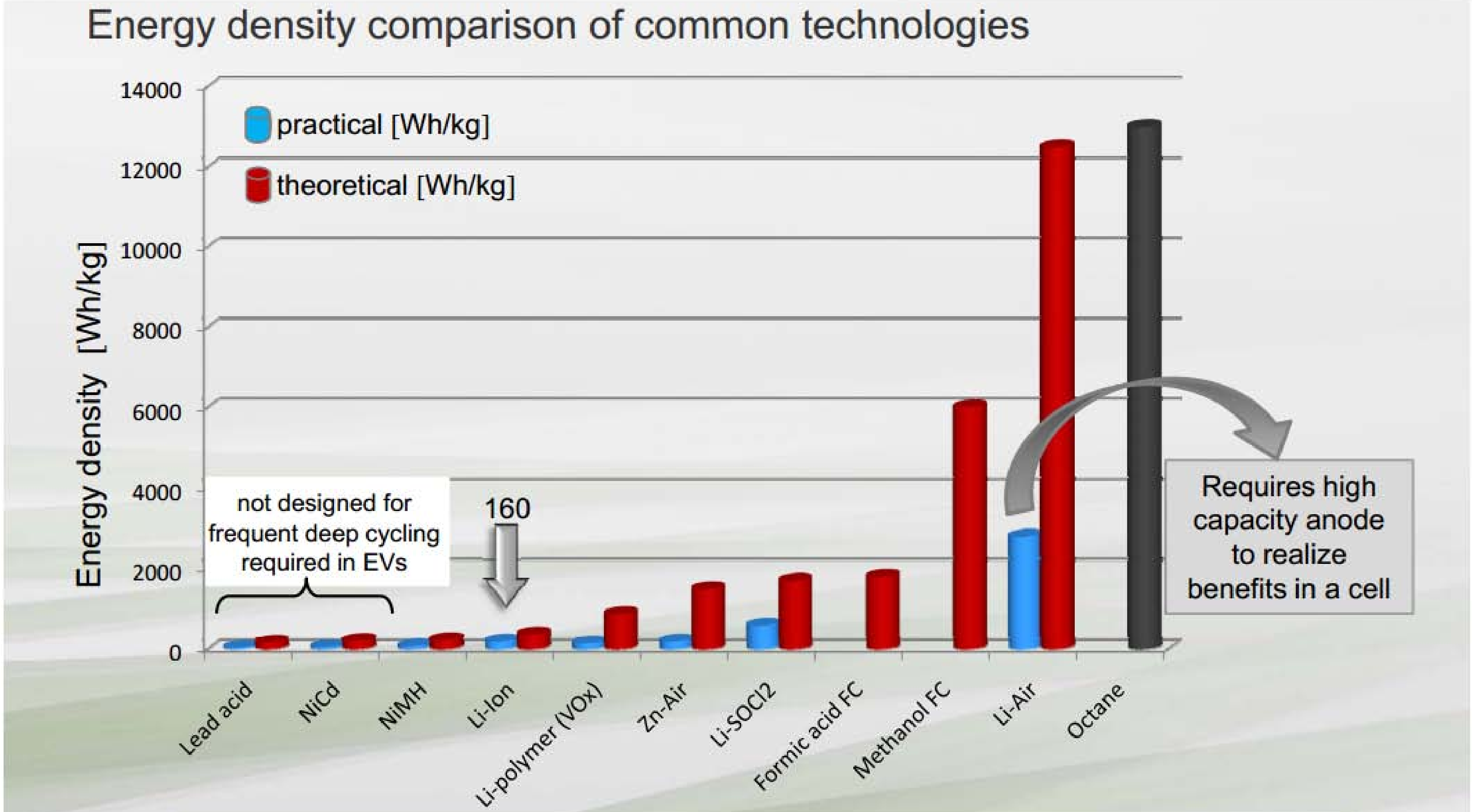

Huge difference between theoretical and practical energy density
There is a strong need for further research!

INEP

Li-ion batteries

HONDA

Battery requirements vs. vehicle application

Cycle life goals for batteries
HEV : 300,000 shallow cycles
PHEV (CD mode): 5,000 deep cycles
PHEV (CS mode): 300,000 shallow cycles
EV: 1,000 deep cycles

- ✓ High energy density
- ✓ High power density
- ✓ Calendar lifetime
- ✓ Good safety
- ✓ Low cost
- ✓ Material availability
- ✓ Recycling

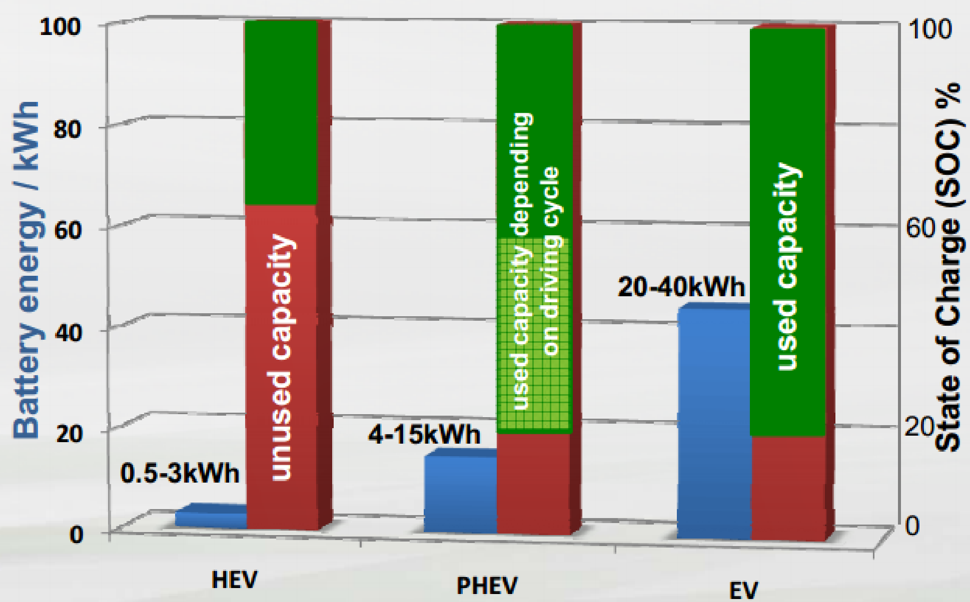

Different requirements guide the choice of the battery chemistry!

Currently, there is no unique material that meets all needs equally well!

INEP

Typical Li-ion cell (Voc x SoC)

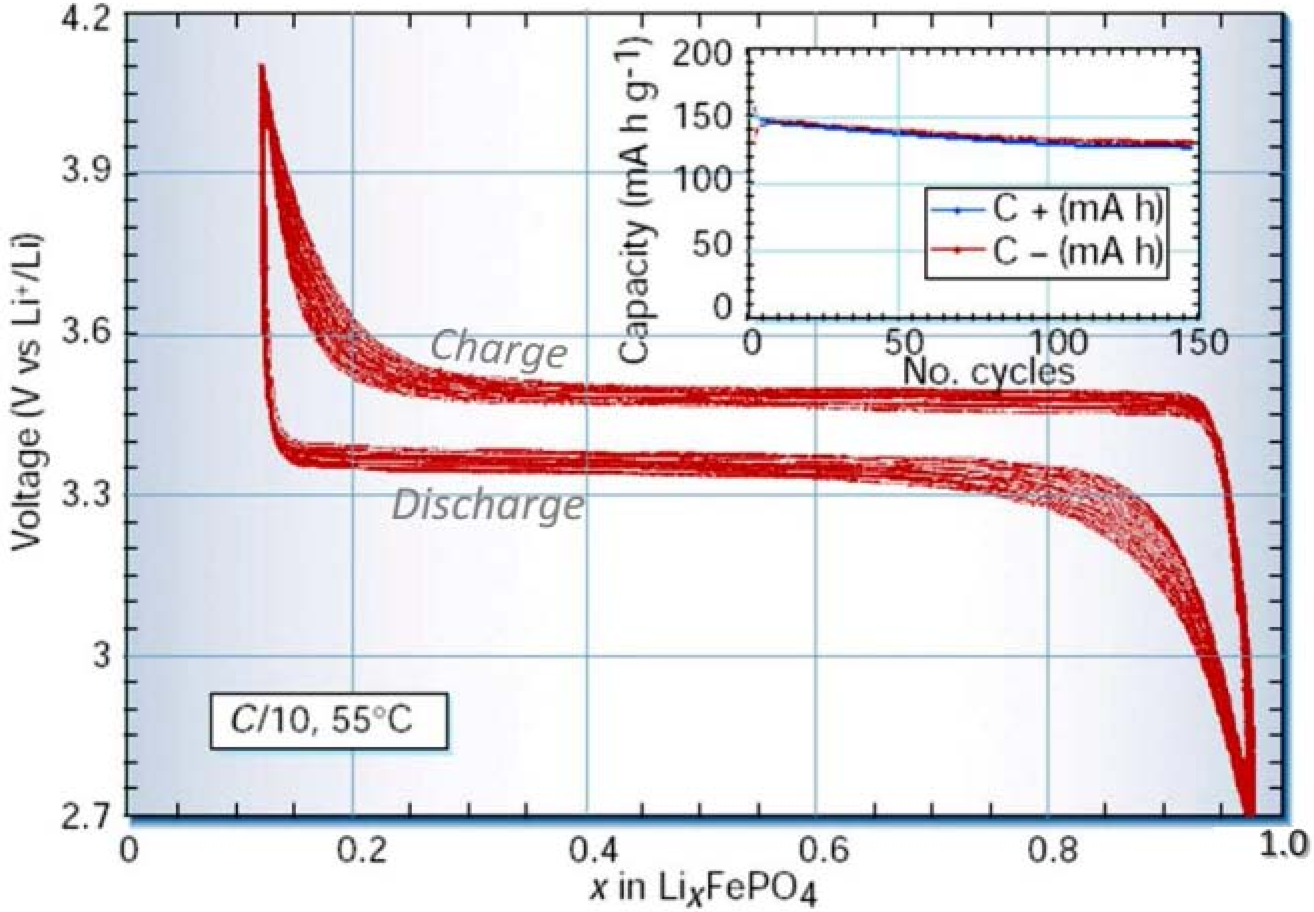

Figure 3.2: Charge and discharge curves of a $LiFePO_4$ battery cell (Wagemaker, 2011).

Battery packs

Figure 3.3: The battery pack of the Chevrolet Volt (General Motors, 2010).

DoD incluence on battery life

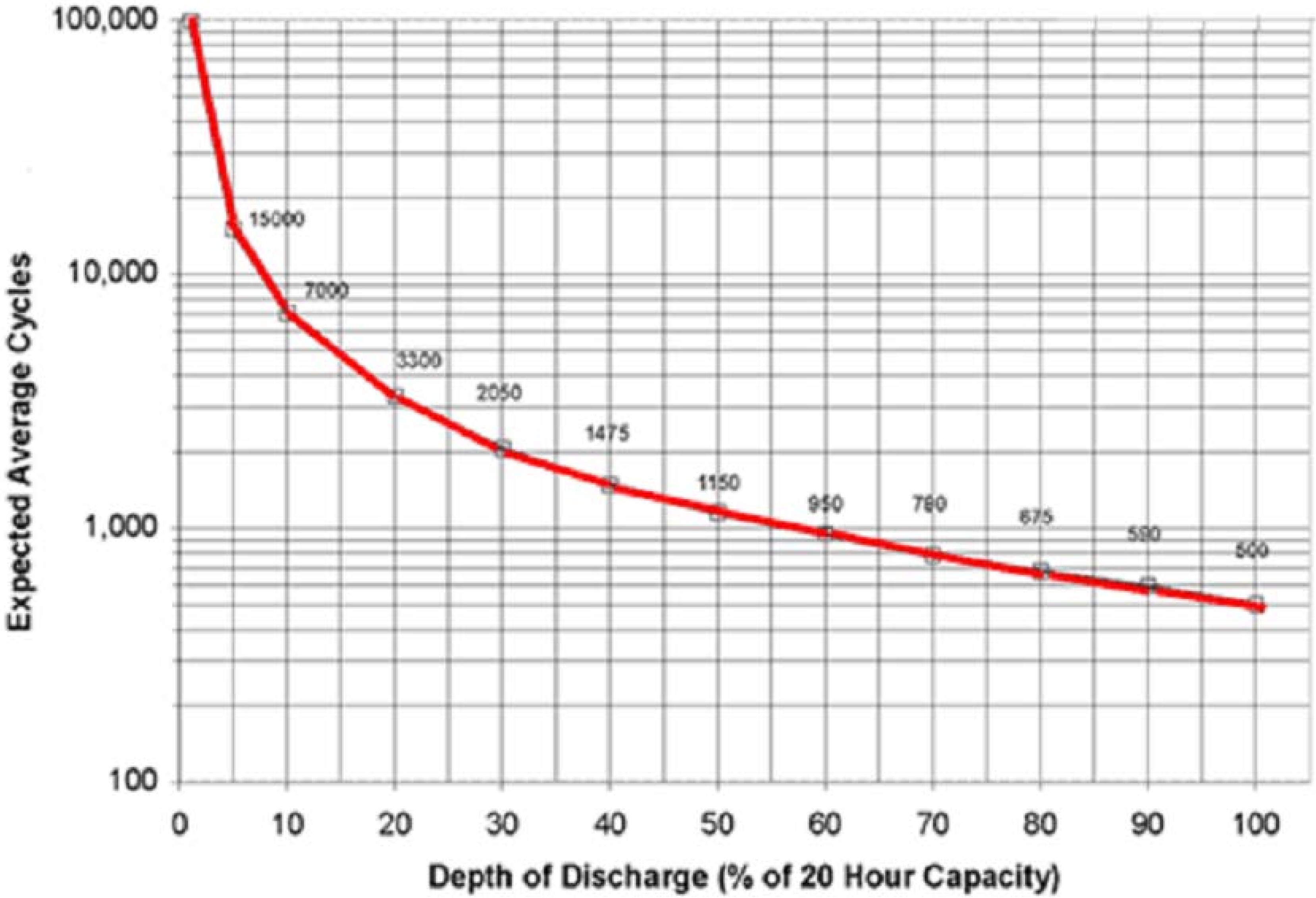

Battery charge profiles

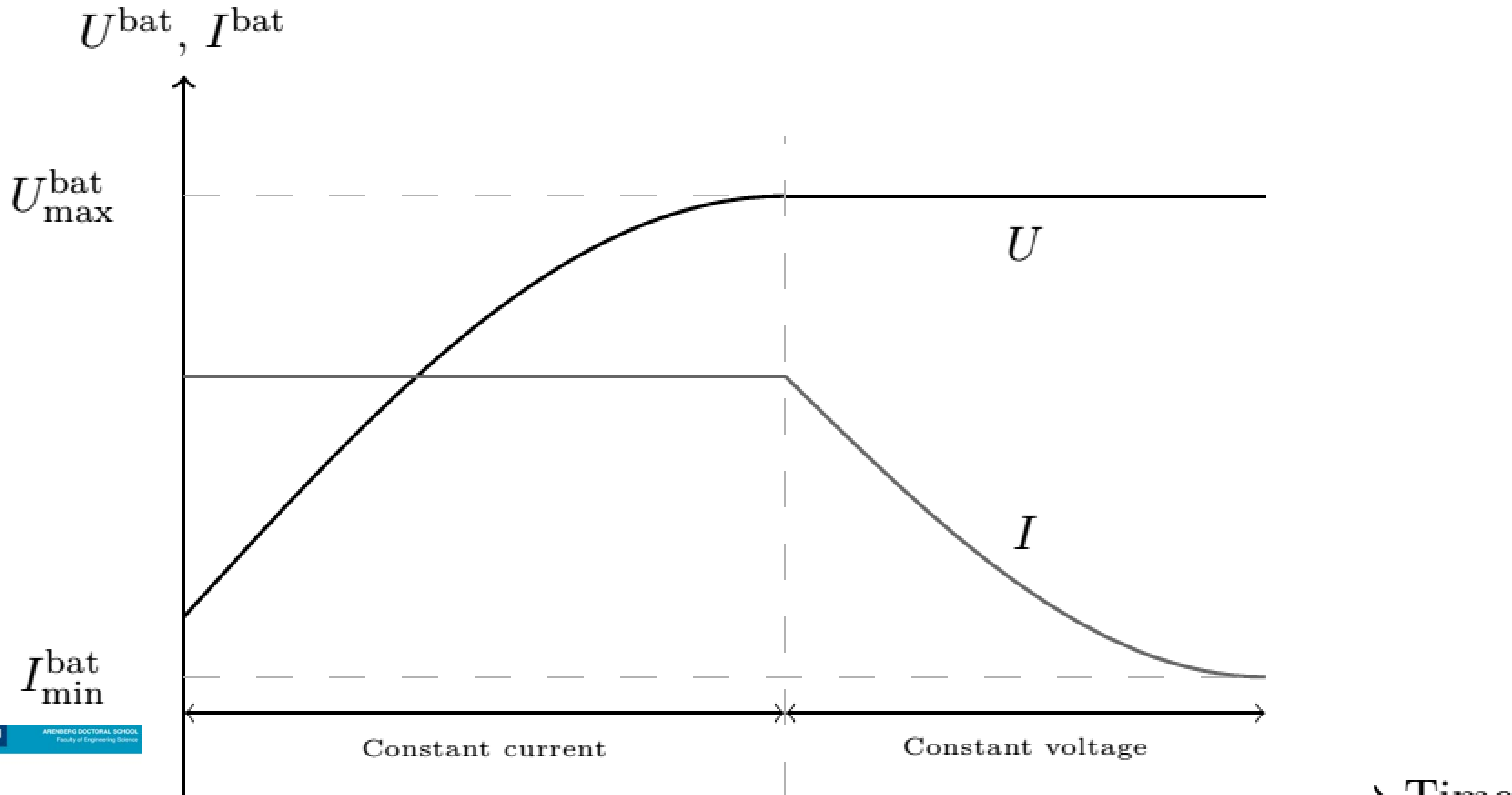

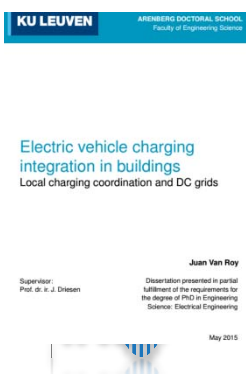
KU LEUVEN

ARENBERG DOCTORAL SCHOOL
Faculty of Engineering Science

Electric vehicle charging integration in buildings

Local charging coordination and DC grids

Juan Van Roy

Supervisor:
Prof. dr. ir. J. Driesen

Dissertation presented in partial fulfillment of the requirements for the degree of PhD in Engineering Science: Electrical Engineering

May 2015

Charging infrastructures

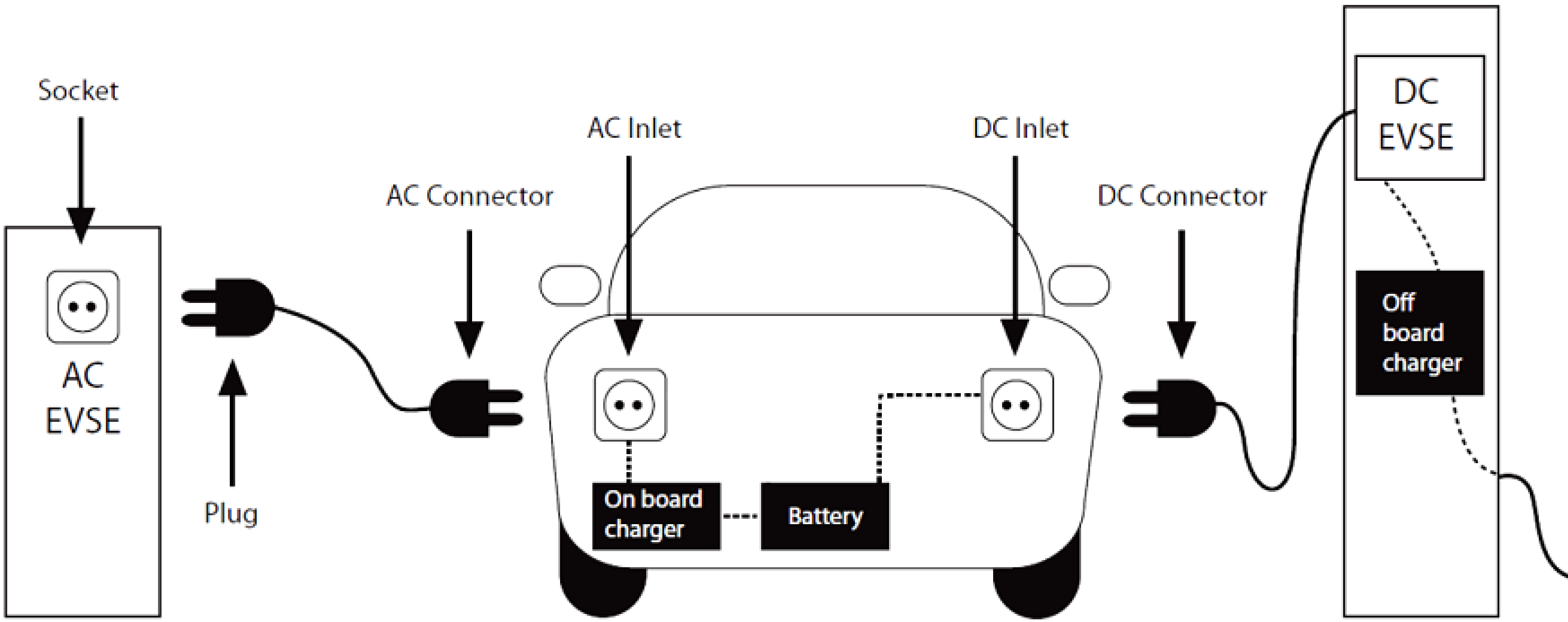

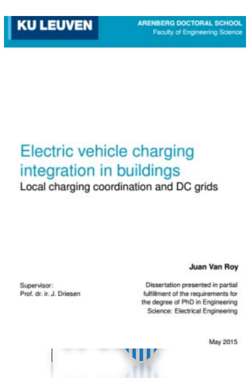
KU LEUVEN
ARENBERG DOCTORAL SCHOOL
Faculty of Engineering Science

Electric vehicle charging integration in buildings
Local charging coordination and DC grids

Juan Van Roy

Supervisor:
Prof. dr. ir. J. Driesen

Dissertation presented in partial fulfillment of the requirements for the degree of PhD in Engineering Science: Electrical Engineering

May 2015

EVSE: Electric vehicle supply equipment

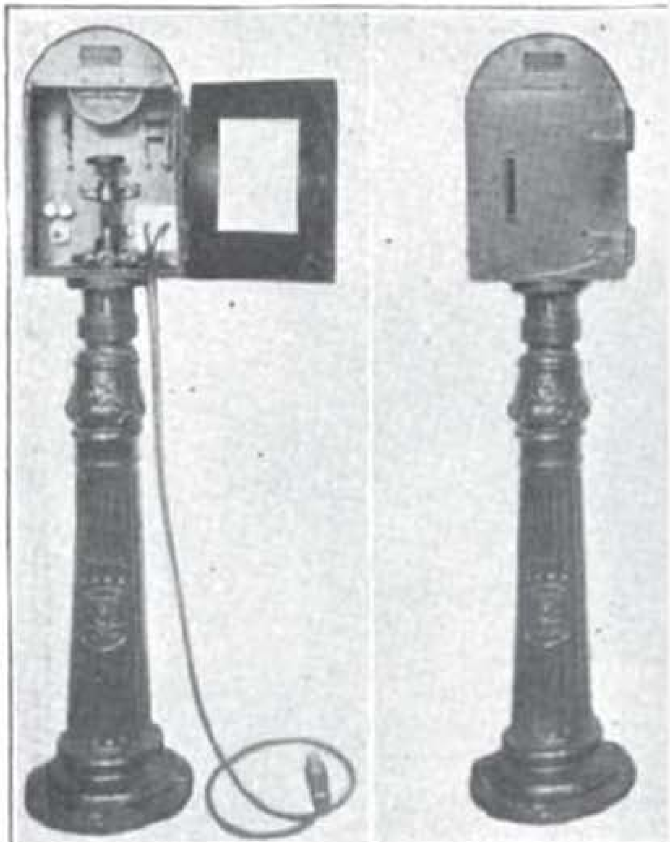

Public Electric-Vehicle-Charging Station

A compact charging station for electric automobiles, which is inclosed in a weatherproof box and is mounted on a pedestal so that it can be placed near the curb, is shown in the accompanying illustration. A charging cable and plug are provided, and while the battery is being charged the door can be closed and locked. A

FIGS. 1 AND 2—CURB CHARGING STATION FOR ELECTRIC AUTOMOBILES

regulating rheostat, ammeter, polarity indicator, lamp, switches, etc., are mounted on a slate panel as shown in Fig. 1. The box is of sheet steel and is electrically welded. The pedestal is of cast iron. Connection with the direct-current supply is made through conduit passing underneath the sidewalk. A prepayment meter may be used if desired, but on account of the numerous sizes and kinds of batteries and varying conditions an attendant is usually required.

This device for charging electric cars at the curb is made in two sizes with ratings of 100 amp and 150 amp and is being placed on the market by Clarence E. Ogden, 514 Mercantile Library Building, Cincinnati, Ohio.

Work Package (WP) No: **WP5**

WP title: Analysis of grid infrastructure

D5.2: Requirements for the infrastructure based on the defined model

Editors: N. VIDAL, (ENDESA), C. SILVESTRI, P.SCURO, S. BRAMBILLA (Enel)

Tipos de instalação

Case A: connection of an EV to the AC supply network utilizing a supply cable and plug permanently attached to the EV.

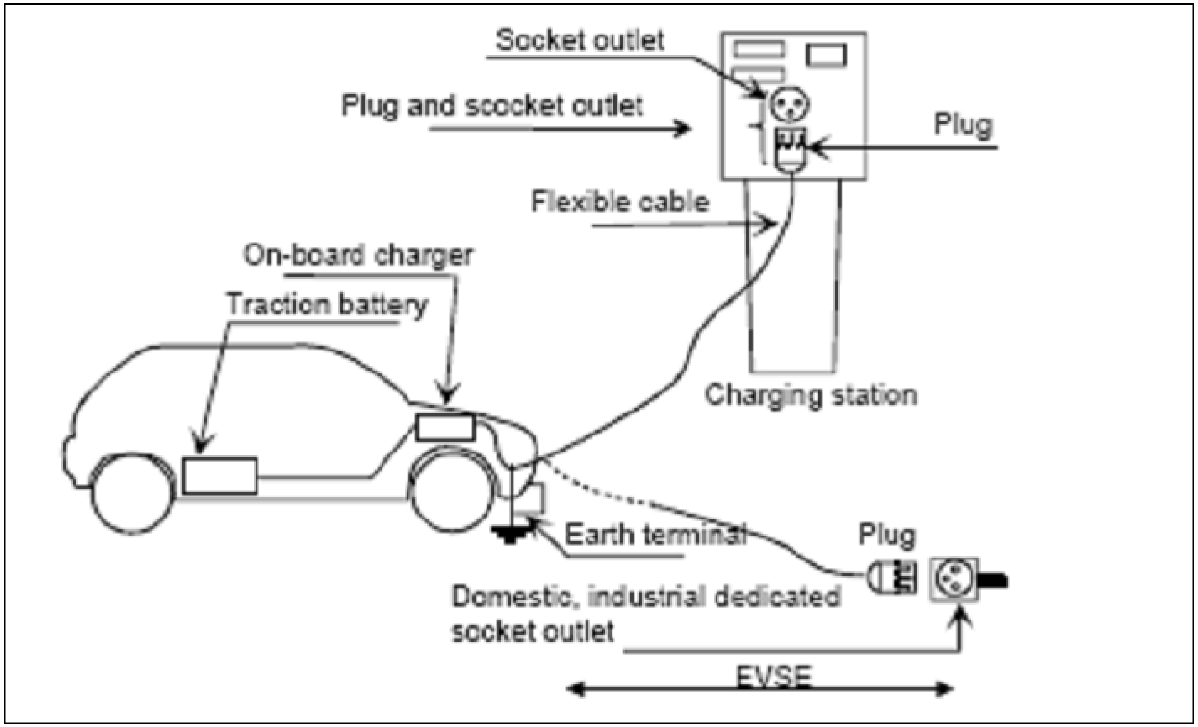

Tipos de instalação

Case B: connection of an EV to the AC supply network utilizing a cable set which can be completely taken off.

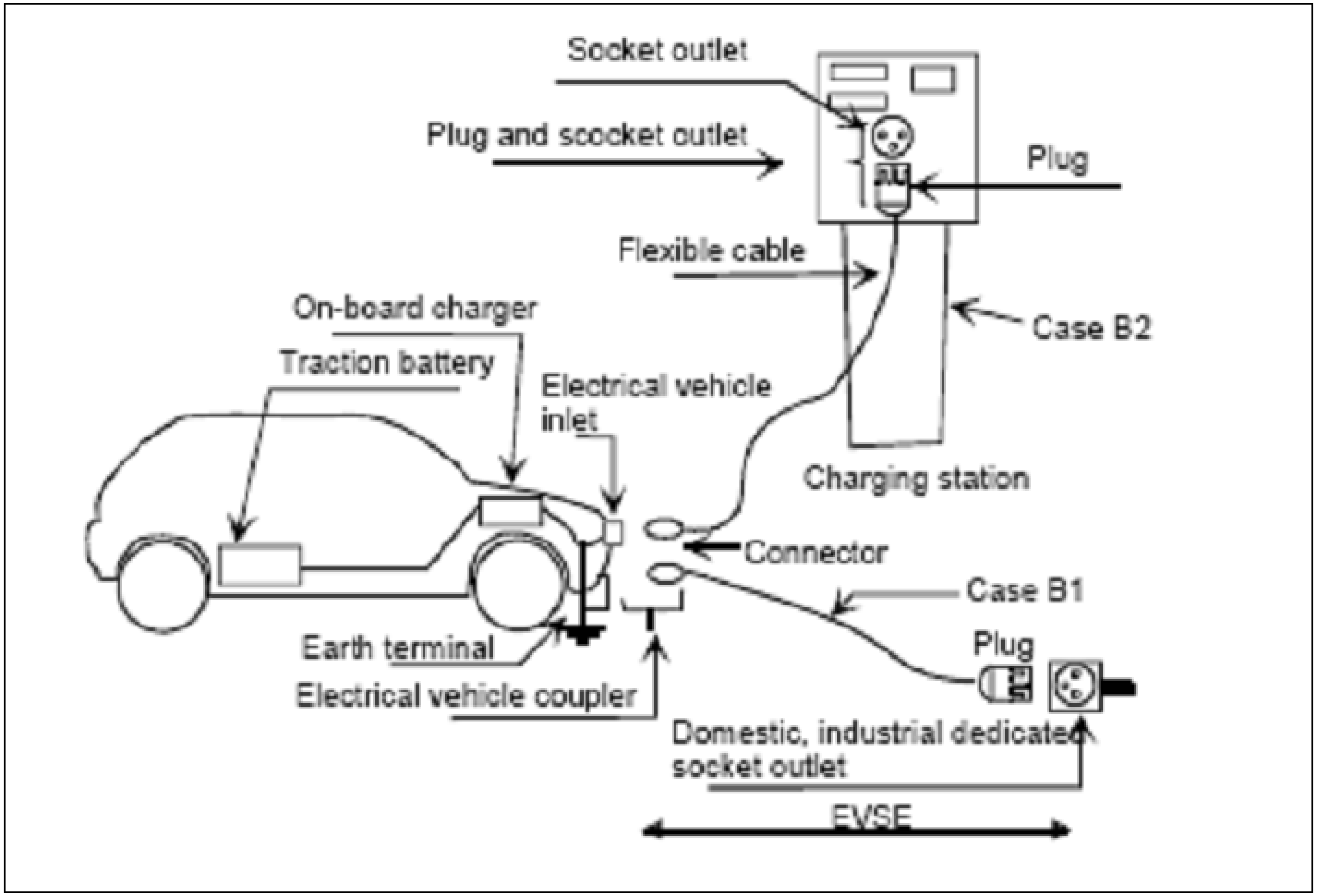

Tipos de instalação

Case C: connection of an EV to the AC supply network utilizing a supply cable and vehicle connector permanently attached to the supply equipment.

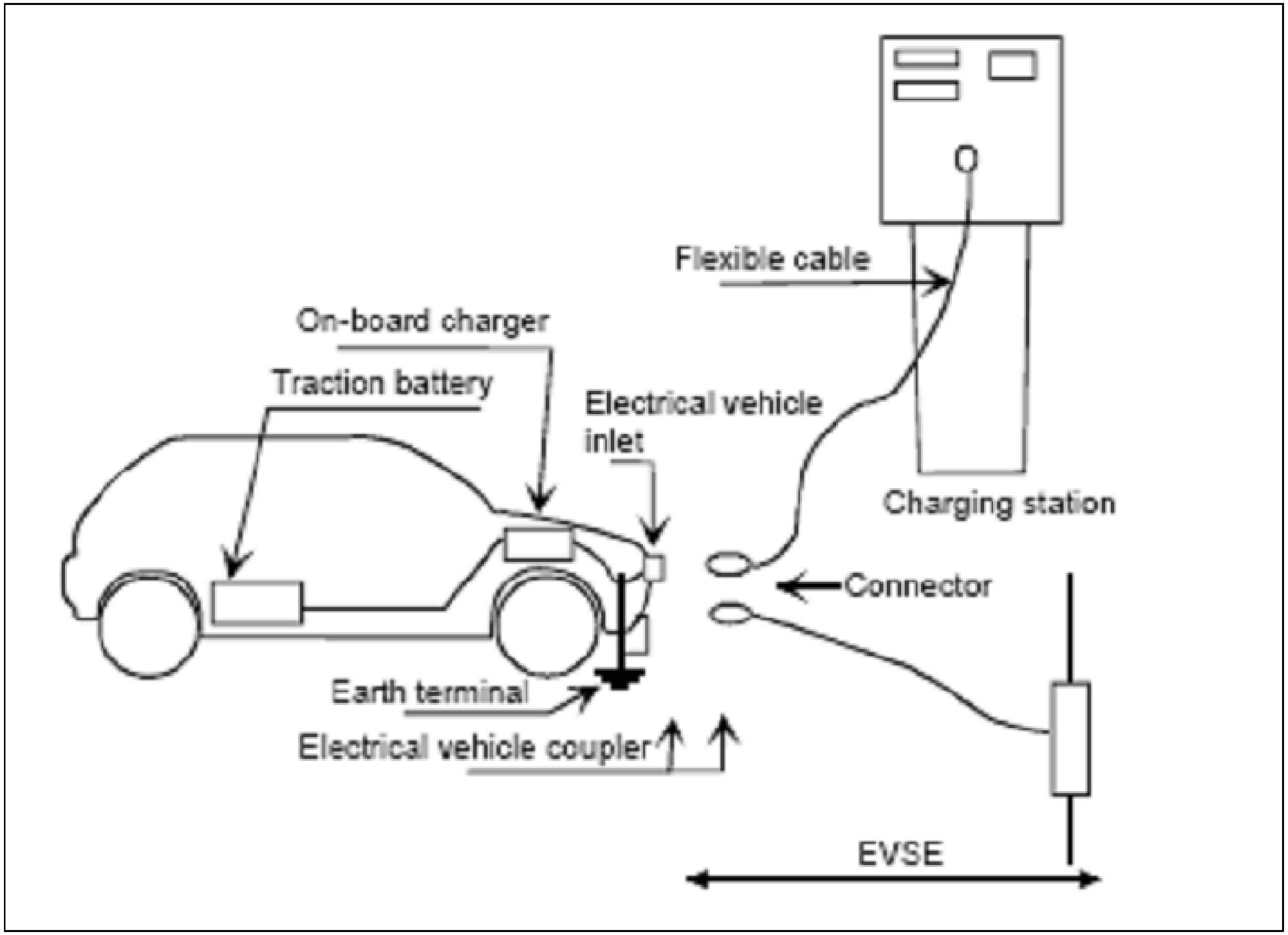

Charging stations

- Public station
  - Recharging infrastructure for use in public spaces with access allowed to more persons
  - Charge is to be permitted after identification or payment

- Private station
  - Use in private spaces
  - Does not require identification

Harmonics

UFSC

Table 3. Emission limits of currents. Source: IEC 61000-3-2.

Harmonic order (n)	Maximum permissible harmonic current (A)	Harmonic order (n)	Maximum permissible harmonic current (A)
Odd harmonics		**Even harmonics**	
3	2,30	2	1,08
5	1,14	4	0,43
7	0,77	6	0,30
9	0,40	$8 \leq n \leq 40$	0,23 8/n
11	0,33		
13	0,21		
$15 \leq n \leq 39$	0,15 15/n		

IEC 61000-3-2: Class A
Current ≤ 16 A per phase

INEP

Harmonics

Table 4. Emission limits of currents. Source: IEC 61000-3-12.

Minimum R_{cc}	Individual Distortion Rate of Current D (%)				Harmonic Distortion factor of admissible current (%)	
	I5	I7	I9	I11	THD	PWHD
33	10,7	7,2	3,1	2	13	22
66	14	9	5	3	16	25
120	19	12	7	4	22	28
250	31	20	12	7	37	38
≥ 350	40	25	15	10	48	46

IEC 61000-3-12: Class A
16 A < Current ≤ 75 A per phase

Harmonics

Table 5 shows the limits of voltage harmonics fixed at the standard 50160.

Table 5. Values of individual harmonic voltages at the supply terminals.

Odd harmonics				Even harmonics		Total Distortion Rate of Voltage
Not multiples of 3		Multiples of 3				
Order h	Relative voltage (%)	Order h	Relative voltage (%)	Order h	Relative voltage (%)	THD (%)
5	6	3	5	2	2	< 8%
7	5	9	1,5	4	1	
11	3,5	15	0,5	6	0,5	
13	3	21	0,5			
17	2					
19	1,5					
23	1,5					

EN 50160 *Voltage characteristics of electricity supplied by public distribution systems*

Table IV: EV charging modes (EMSD EV, 2011).

Mode	Description	Voltage type	Voltage level	Max Current	Max Power
Mode I	standard socket outlet on-board charger	AC	1φ: 220V	16 A	3.5 kW
Mode II	standard socket outlet in-cable control box with control pilot cable on-board charger	AC	1φ: 220V 3φ: 400V	32 A	22 kW
Mode III	dedicated socket outlet with pilot control cable, permanently connected to AC mains on-board charger	AC	1φ: 220V 3φ: 400V	80 A	55 kW
Mode IV	external fast charger	DC	50 - 600V	400 A	240 kW

Table V: Electric car battery parameters monitored by BMS.

Measurement	Battery Management System: computation	Battery Management System: action
Cell Voltage	Cell SoC	Cell balancing
Total Voltage	• Total SoC • Remaining charge • Remaining range	Initiate/stop charge, (dis)charging current, DoD warning
Temperature	Battery health	(dis)Charge current limit, required coolant flow, cell balancing
Coolant flow	Pump/fan speed	Feedback to BMS
Current	Energy delivery	Feedback to BMS

IEC 61851-1 Electric vehicle conductive charging system

Mode 1: the EV is connected to the AC supply network not exceeding 16A and not exceeding 250 V AC single-phase or 480 V AC three-phase utilizing standardized socket-outlets and utilizing the power and protective earth conductors.
Mode 2: the EV is connected to the AC supply network not exceeding 32A and not exceeding 250 V AC single-phase or 480 V AC three-phase utilizing standardized socket-outlets and utilizing the power and protective earth conductors together with a control pilot function.
Mode 3: the EV is connected to the AC supply network utilizing dedicated EV supply equipment which has a pilot function (conductor) leading all the way to the device continuously connected to the AC supply network.
Mode 4: the EV is connected to the AC supply network utilizing an off-board charger that delivers direct current and where the pilot function (conductor) has to lead all the way to the device continuously connected to the AC supply network.

DC Fast Chargers

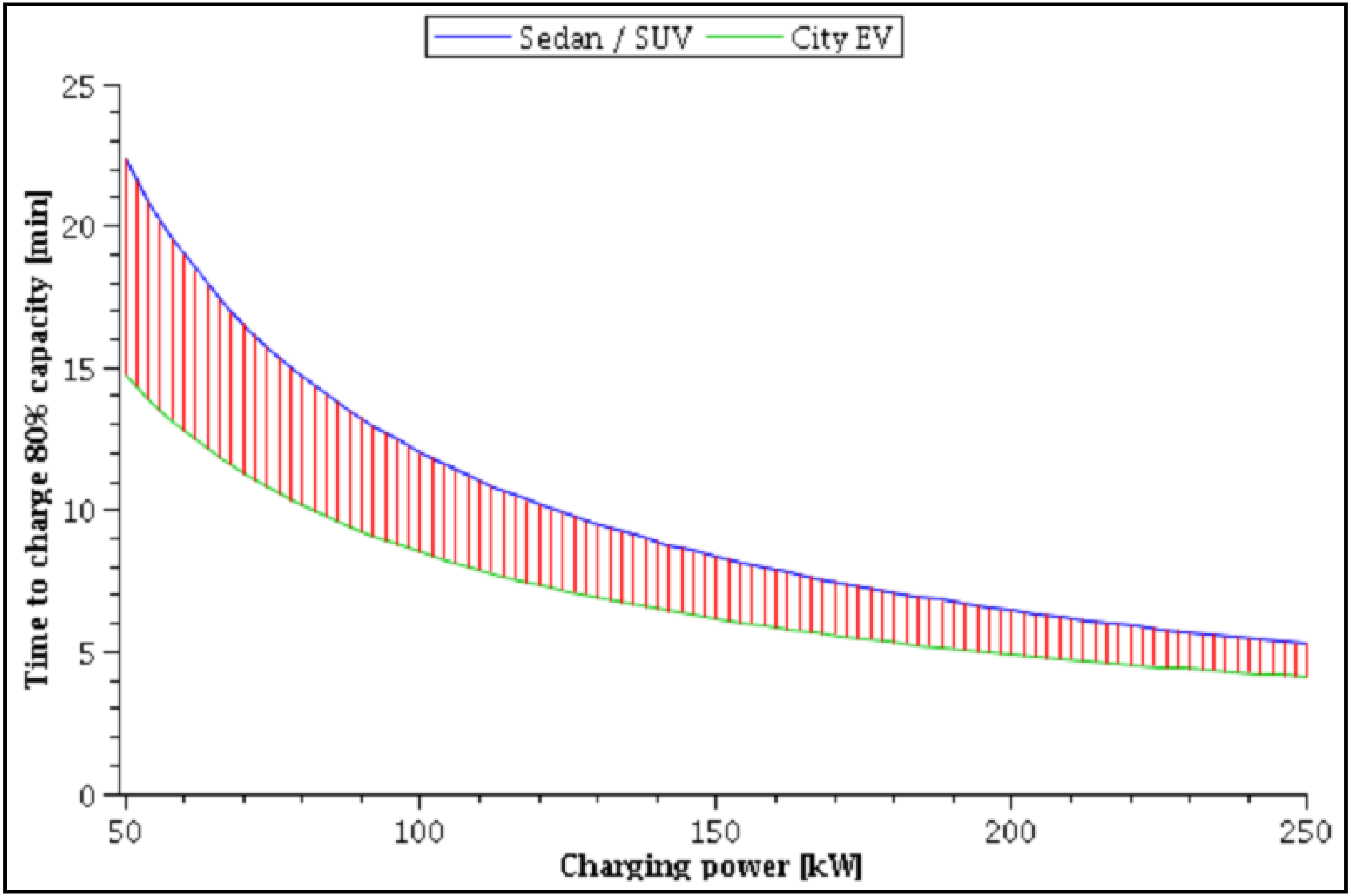

Figure 8. . Typical 80% charging time versus DC charger available power1.

DC Fast Charging Stations

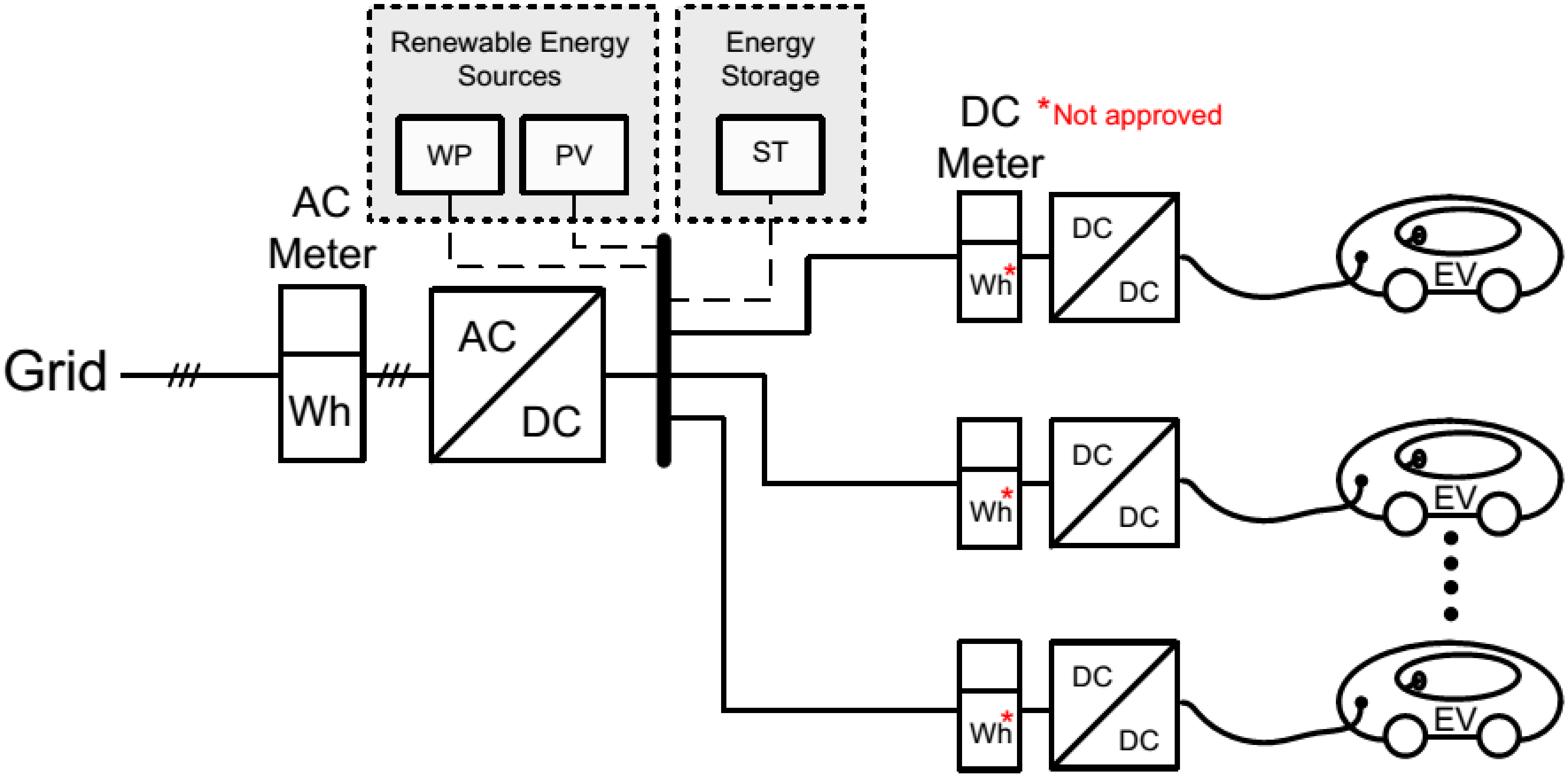

DC Fast Charging Stations

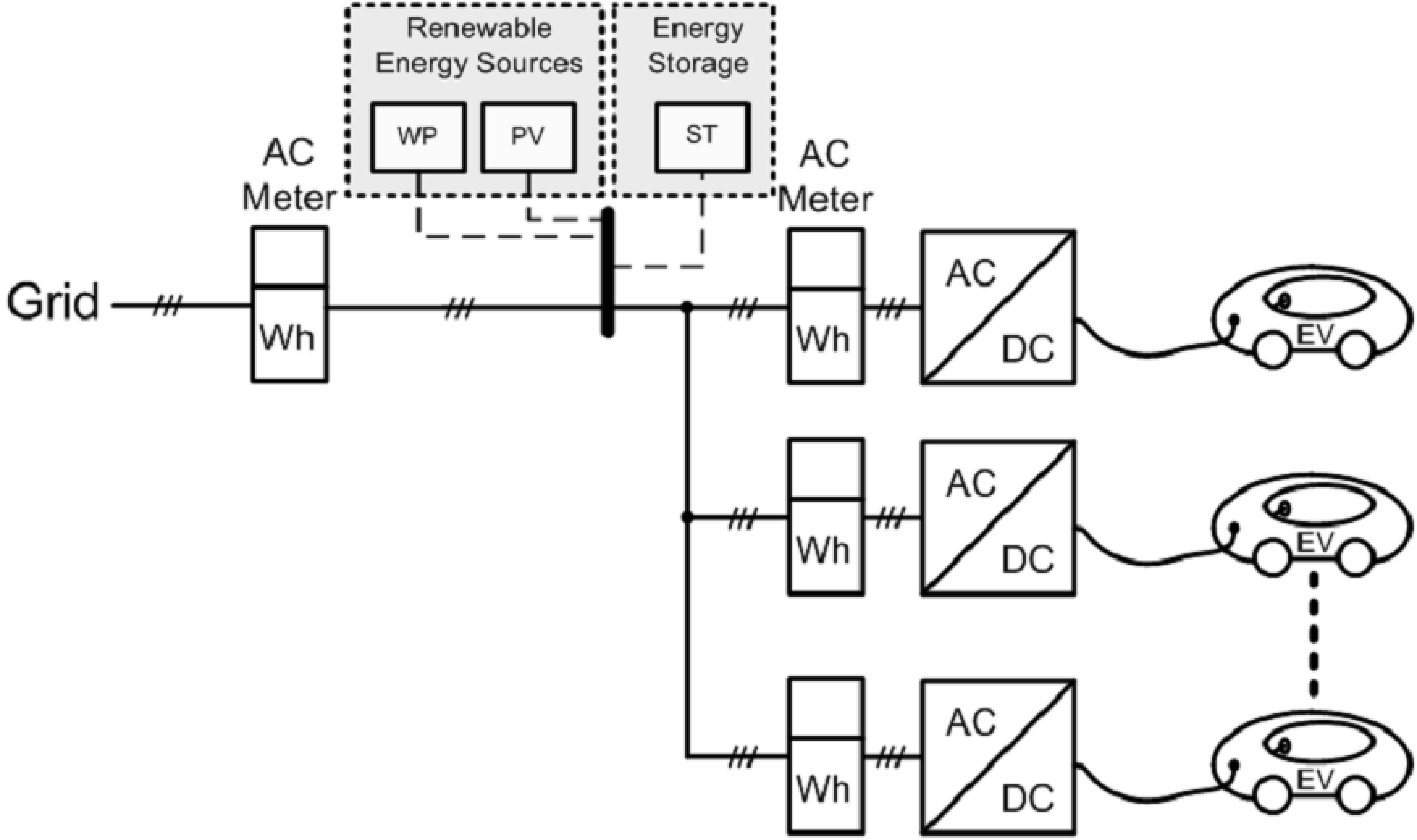

AC vs DC

It has been assumed an energy consumption of 600 kWh for a period of 24 hours

Table 10. Comparison of costs in 2020 for each configuration

Configuration	Fast charge in DC[2]		Slow charge in AC	
	Multi-Output	Single-Output	With Cost of Space	No Cost of Space
Cost of installation (€)	82.000 €	56.000 €	166.800 €	46.800 €
Energy charged per facility per day (kWh)	600 kWh	600 kWh	600 kWh	600 kWh
Charging duration	15 minutes	15 minutes	8 hours	8 hours
Power rate	25 kW	50 kW	4 kW	4 kW
Range Achieved per EV[3]	42 km	83 km	197 km	197 km
Chargers per Facility	4 x 25kW	2 x 50kW	18 x 4W	18 x 4kW
Utilization Factor	25%	25%	50%	50%
Number of EVs charged per facility per day	96	48	18	18

[2] Including the cost of the space needed for the installation and to park the EVs (without space cost, total facility costs would be: multi-output 32.000€, Single output 26.000€)

[3] Average EV consumes 15 kWh per 100km.

INEP

Table 2: Installation Costs for Residential and Publicly Available EVSE/Charge Stations[17]

	Residential Level 2 (Qty 1)	Publicly Available Charge Station Level 2 (Qty 2)	Publicly Available Charge Station Level 3 (Qty 2)
Labor	$1,050	$4,670	$7,020
Materials (EVSE, panels, breakers, signage, etc.)	$1,137	$6,840	$56,863
Permit	$85	$85	$85
Trenching and Repair	N/A	$4,500	$1,500
Concrete Work	N/A	N/A	$1,500
Total	**$2,272**	**$16,095**	**$66,968**

ENERGY STAR Market and Industry Scoping Report
Electric Vehicle Supply Equipment (EVSE)
September 2013

www.inl.gov

Idaho National Laboratory

DC Fast Charger Use, Fees, Battery Impacts and Temperature Impacts on Charge Rates - EV Roadmap 7

Jim Francfort

EV Roadmap 7 – Portland, Oregon

July 25, 2014

This presentation does not contain any proprietary, confidential, or otherwise restricted information

INL/CON-14-32496

DC Fast Charging Impact Study on 2012 Leafs

DC Fast Charging Impact Study on 2012 Leafs

- Two Goals
  - Determine DC Fast Charge (DCFC) impacts versus Level 2 impact
  - Compare on-road to laboratory test results
- Two on-road Nissan Leafs are exclusively Level 2 (L2) charged
- Two on-road Nissan Leafs are exclusively DCFC charged
- Identical on-road routes are driven
- Drivers' miles are balanced – all drive the four vehicles equally

- Each Leaf battery was tested when new (Base case)
- Each on-road battery is retested at 10,000-mile increments
- Battery temperature is tracked during normal charging operations
- 50,000 miles completed, going to 70,000 miles per on-road Leaf
- 24 battery tests completed on the on-road Leaf batteries

- Lab testing of two additional batteries (only preliminary results) @ 4,000 mile increments

DC Fast Charging Impact Study on 2012 Leafs

- All Leafs were the same color – avoid unequal solar loading
- Note very tight monthly efficiency results across all four Leafs during Level 2 and DCFC operations (red min & max bars)
- Leafs' climate control is set at 72°F year round
- Note seasonal efficiency impacts from heating and air conditioning
  - 39.8 DC kWh/mi delta for min vs. max month
  - Max month 19% higher than min month

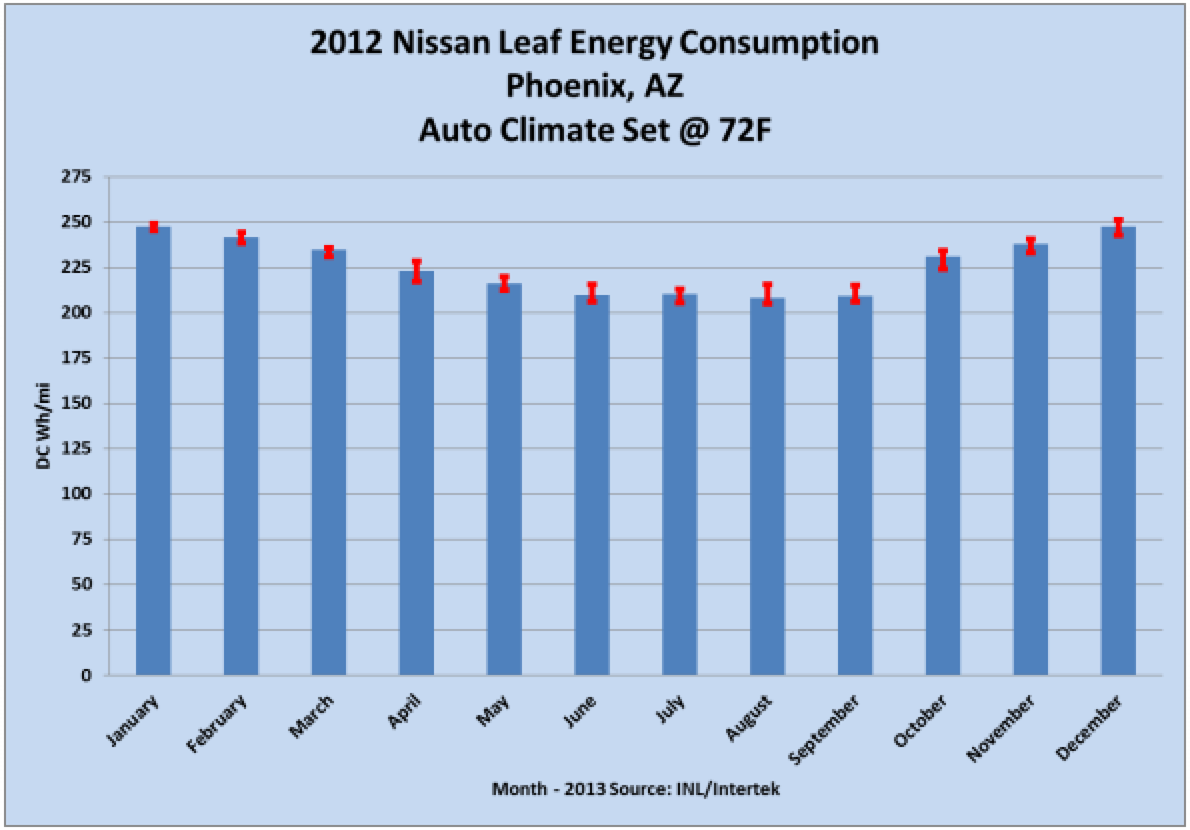

DC Fast Charging Impact Study on 2012 Leafs

- 0.6 kWh average capacity difference @ 50k miles between Level 2 and DCFC Leafs, probably not a significant difference
- Level 2 averaged 5.8 kWh loss @ 50k miles
- DCFC averaged 6.4 kWh @ 50k miles

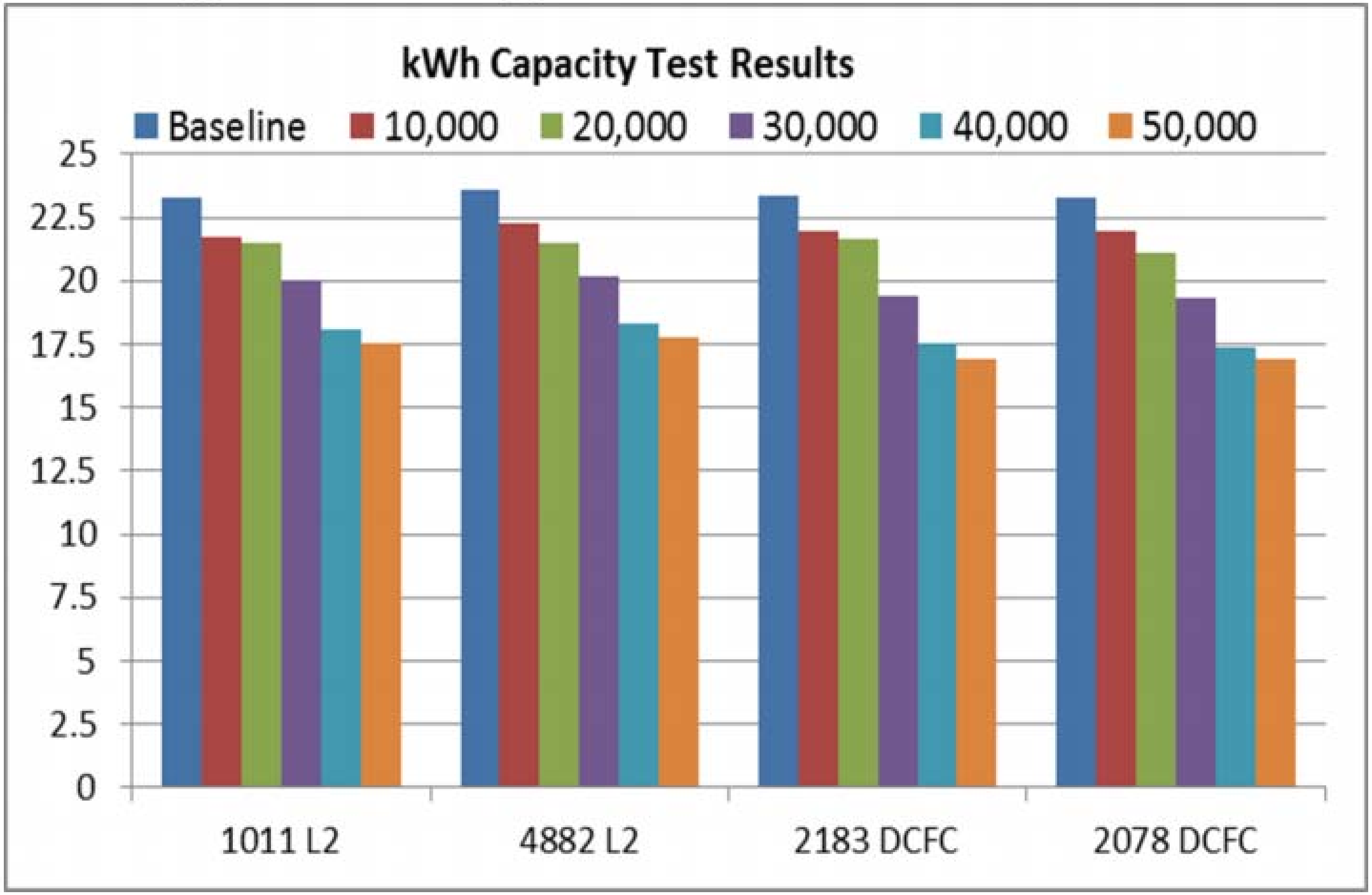

DC Fast Charging Impact Study on 2012 Leafs

- Level 2 averaged 75.2% SOC @ 50k miles
- DCFC averaged 72.6% SOC @ 50k miles
- 2.6% capacity difference @ 50k miles, probably not a significant difference

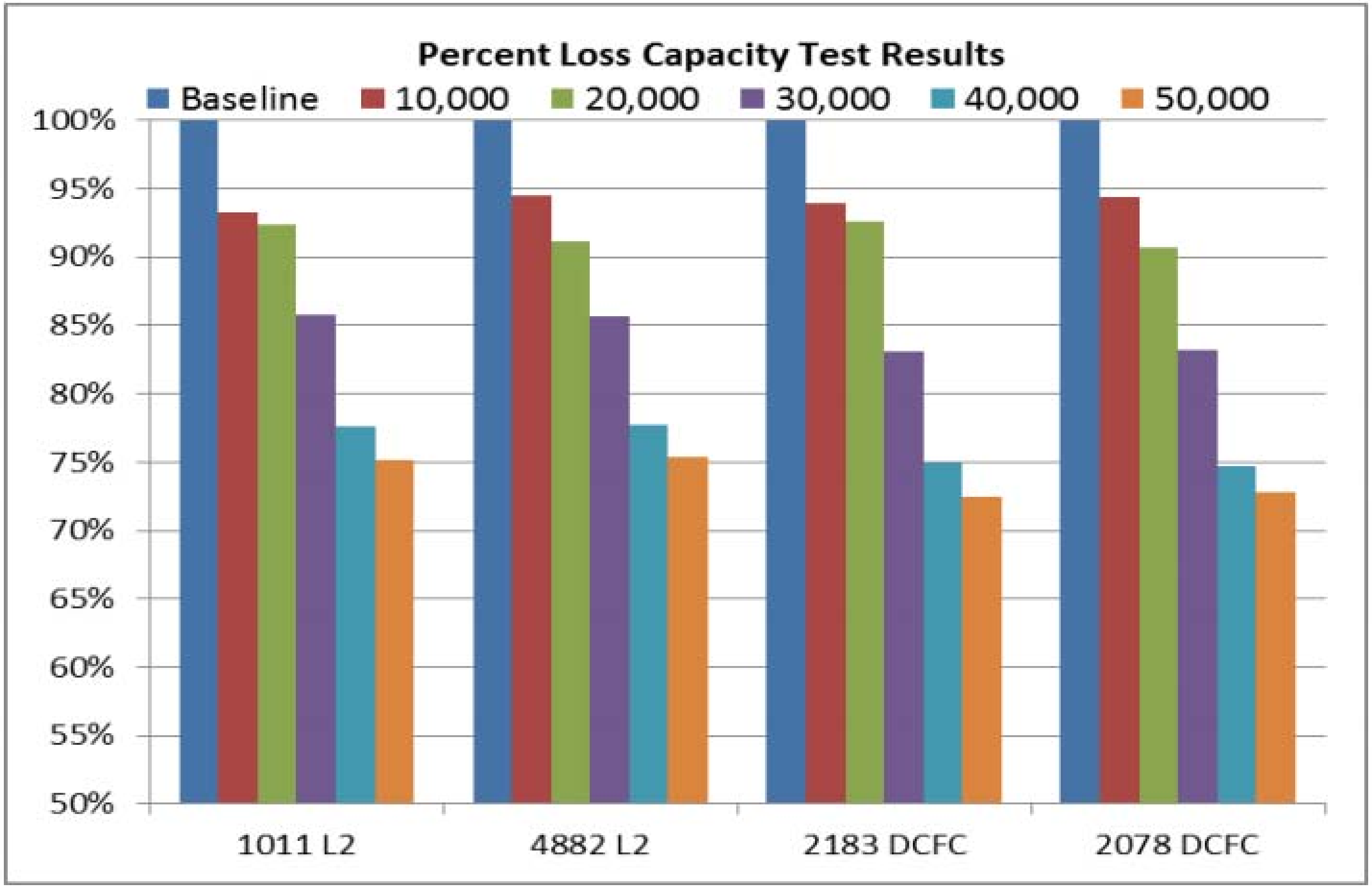

DC Fast Charging Impact Study on 2012 Leafs

- **Same data as last slide. Each line represents a single vehicle, plotted by capacity SOC for each battery test**

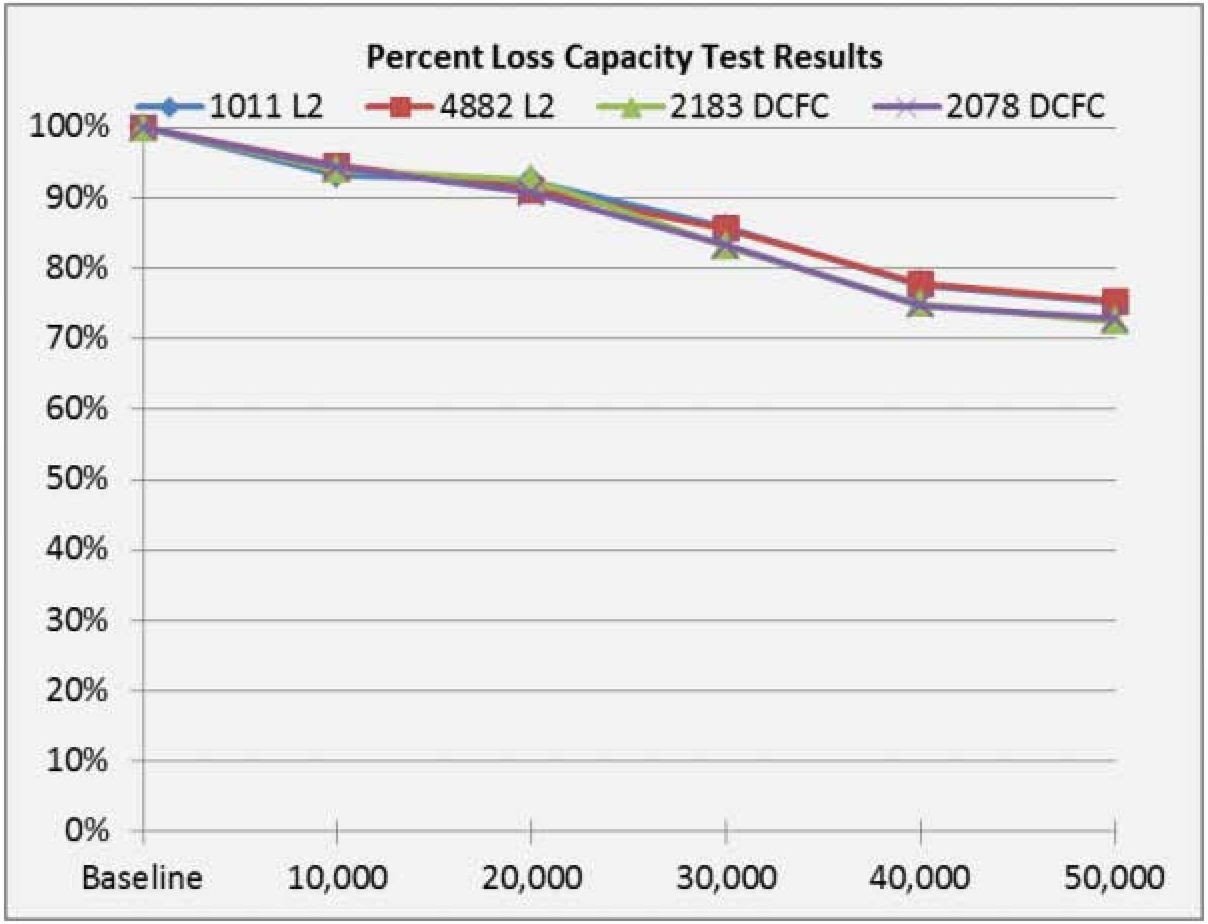

Idaho National Laboratory

DC Fast Charging Impact Study on 2012 Leafs

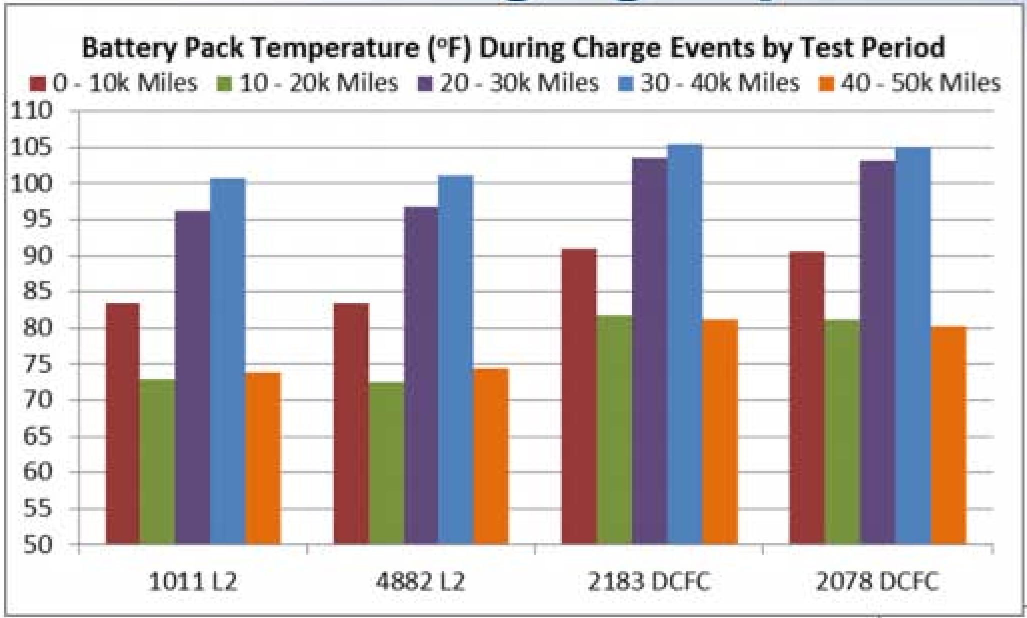

- **Largest decreases in capacity from test before, occurred during high heat charging operation**
- **Phoenix heat likely accelerates all results**

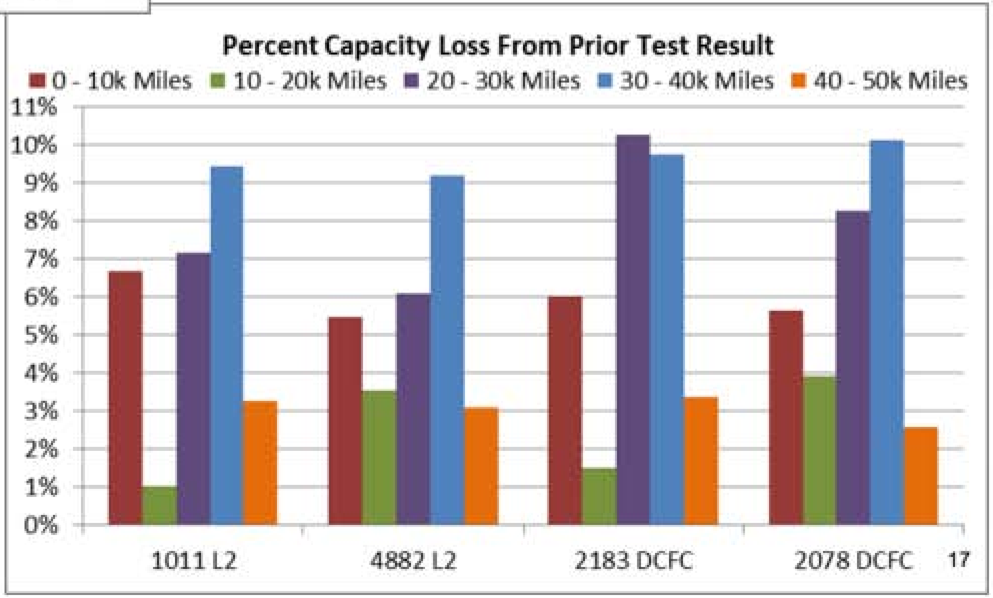

DC Fast Charging Impact Study on 2012 Leafs

- **Percentage Range and Capacity at 50,000 miles compared to testing when new**

	L2 Average	DCFC Average
Range	79.0%	69.3%
Capacity	75.2%	72.6%

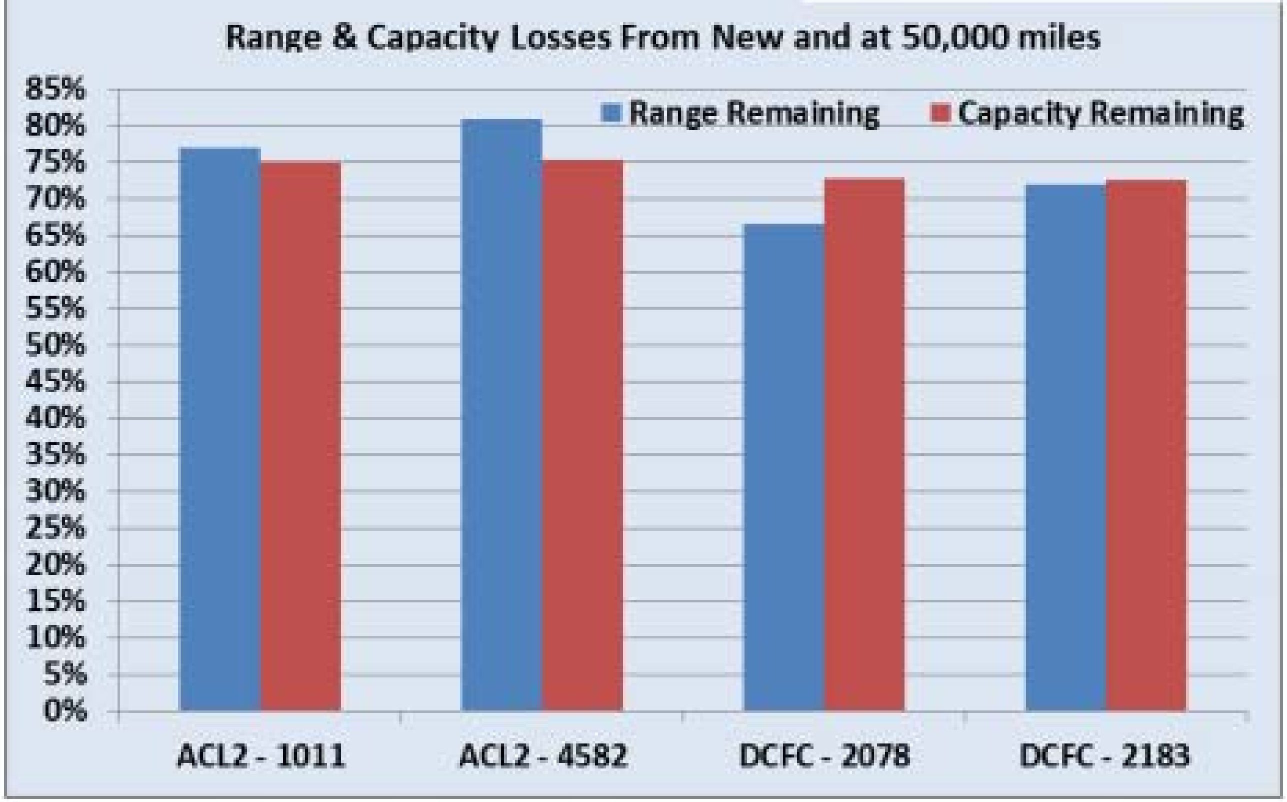

DC Fast Charging Acceptance Rates at Various Temperature

DC Fast Charging Acceptance Rates at Various Temperatures

- Objective is to develop a formal testing regime to examine battery charge acceptance rates at various ambient temperatures during DC Fast Charging
  - The results should be considered preliminary as the tests were undertaken to identify needed test procedures
  - 2013 Nissan Leaf at 6,000 miles was used
  - 2012 Mitsubishi i-MiEV at 5,700 miles was used
  - Vehicles temperature soaked for minimum of 12 hours
  - Used Intertek's soak chamber in Phoenix
- Identified additional instrumentation needed in additional proper test regime steps

2013 Leaf - DC Fast Charging @ 0, 25 & 50 C

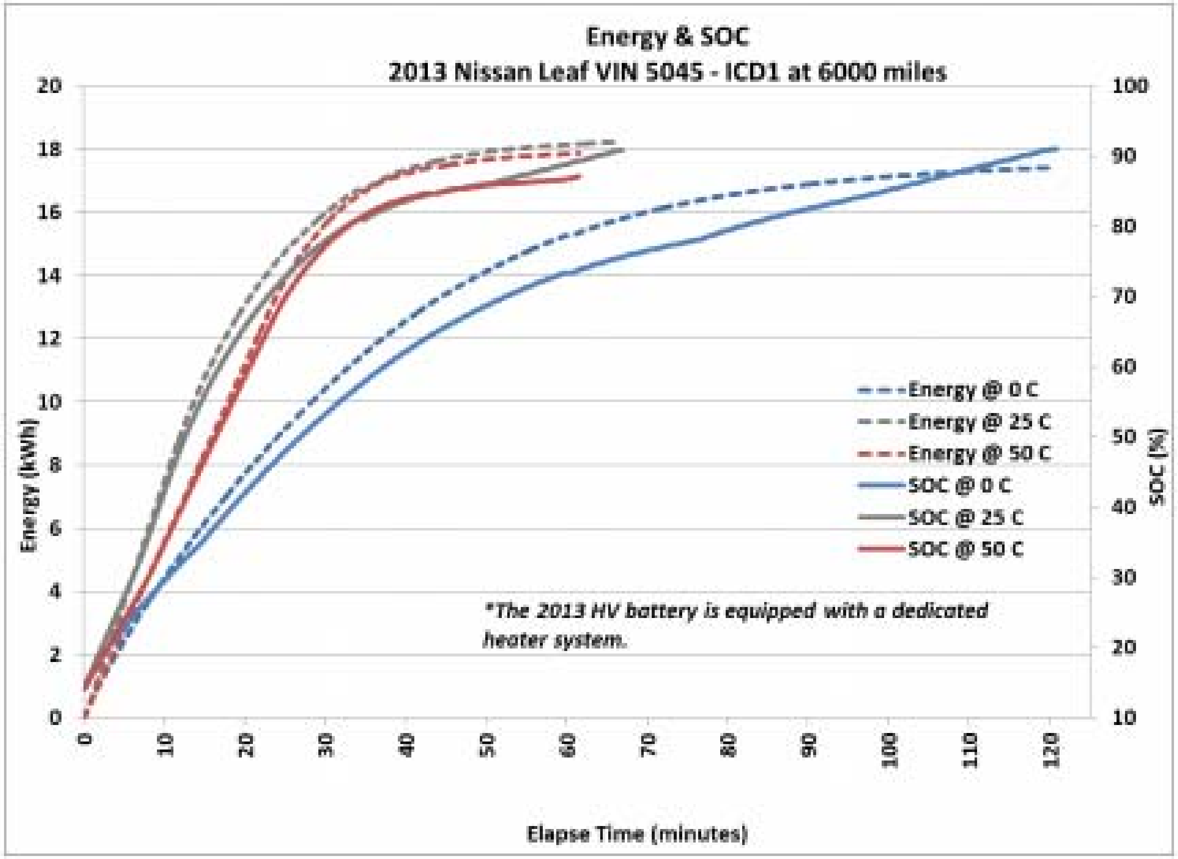

Preliminary Data Results

- After 30 minutes:
  - 50 C: 77% SOC
  - 25 C: 77% SOC
  - 0 C: 53% SOC
- At charge end:
  - 50 C: 87% SOC at 62 minutes
  - 25 C: 91% SOC at 67 minutes
  - 0 C: 91% SOC at 121 minutes
- Total kWh:
- 50 C: 17.9 kwh
- 25 C: 18.2 kWh
- 0 C: 17.4 kWh

0 C = 32 F
25 C = 77 F
50 C = 122 F

22

2012 iMiEV - DC Fast Charging @ 0, 25 & 50 C

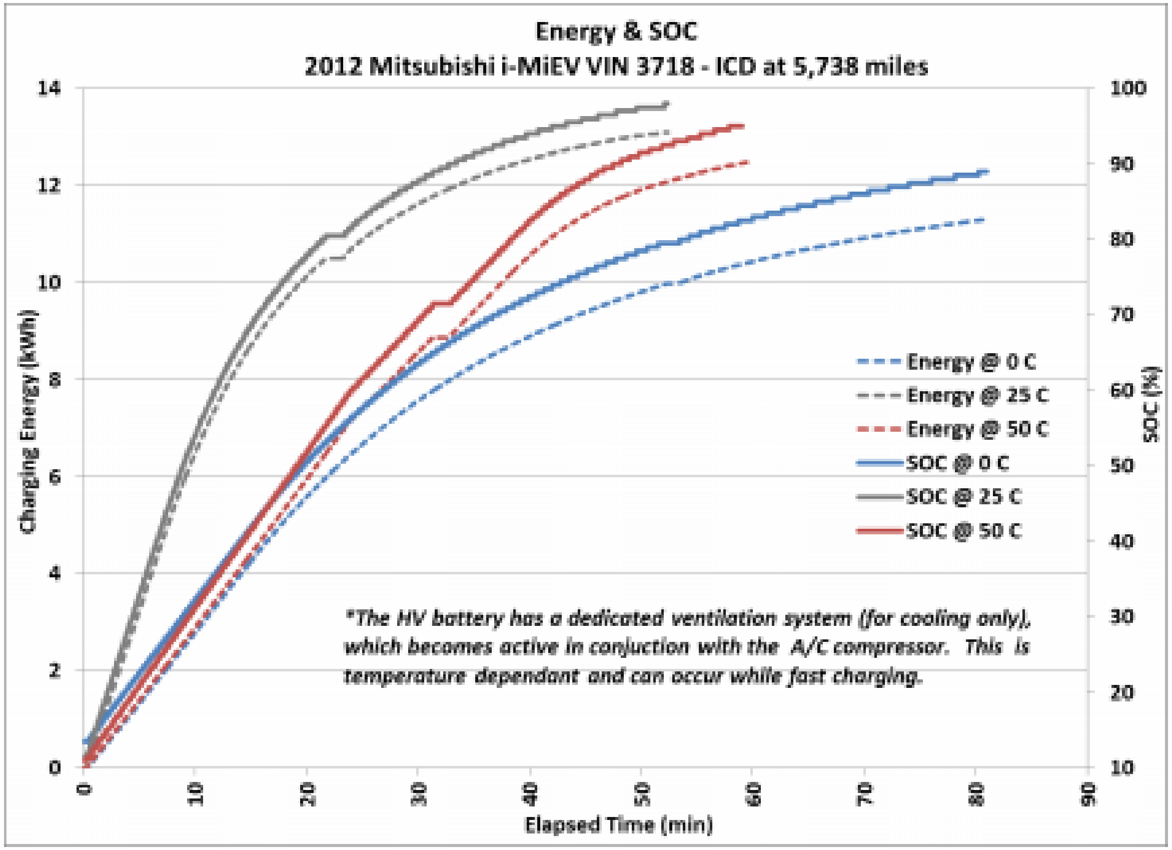

Preliminary Data Results

- **After 30 minutes:**
  - **50 C: 69% SOC**
  - **25 C: 88% SOC**
  - **0 C: 64% SOC**
- **At charge end:**
  - **50 C: 95% SOC at 59 minutes**
  - **25 C: 98% SOC at 67 minutes**
  - **0 C: 89% SOC at 81 minutes**
- **Total kWh:**
- **50 C: 12.5 kwh**
- **25 C: 13.1 kWh**
- **0 C: 11.5 kWh**

0 C = 32 F
25 C = 77 F
50 C = 122 F

2012 iMiEV - DC Fast Charging @ 0, 25 & 50 C

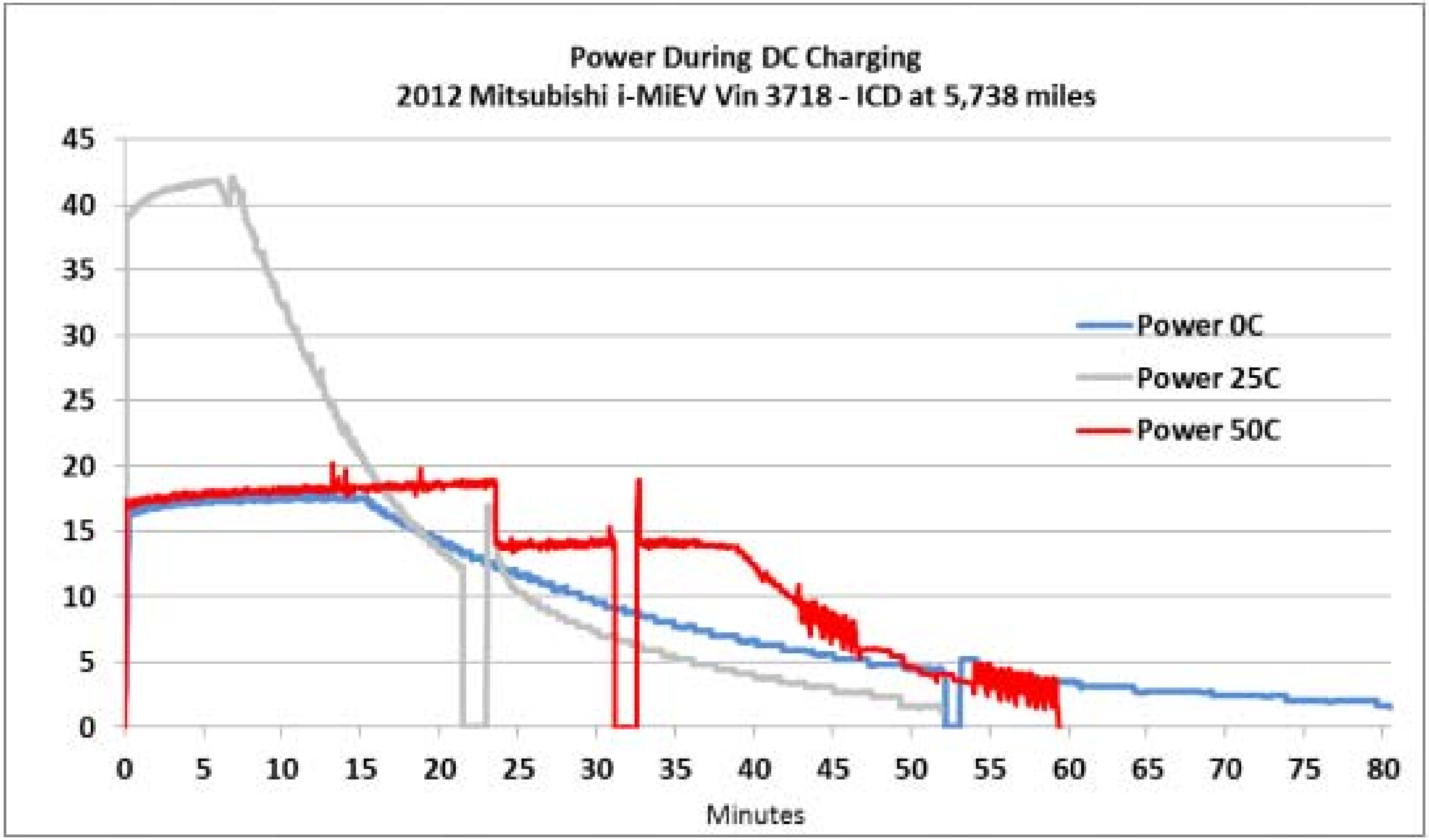

Preliminary Data Results

U.S. Department of Energy
Energy Efficiency and Renewable Energy
Bringing you a prosperous future where energy is clean, abundant, reliable, and affordable

INL Efficiency and Security Testing of EVSE, DC Fast Chargers, and Wireless Charging Systems

PI: Jim Francfort
Presenter: Jim Francfort
Idaho National Laboratory
Energy Storage & Transportation Systems
Advanced Vehicle Testing Activity (AVTA)

May 14, 2013

Project ID VSS096

2013 DOE Vehicle Technologies Program Annual Merit Review

INL/MIS-13-28724

This presentation does not contain any proprietary, confidential, or otherwise restricted information

www.inl.gov

Idaho National Laboratory

Idaho National Laboratory

INL's Level 1 and 2 EVSE and DCFC Testing

Conductive Efficiency? – It depends on where and when you measure it: 23% to 99.7%

EVSE Testing - Conductive

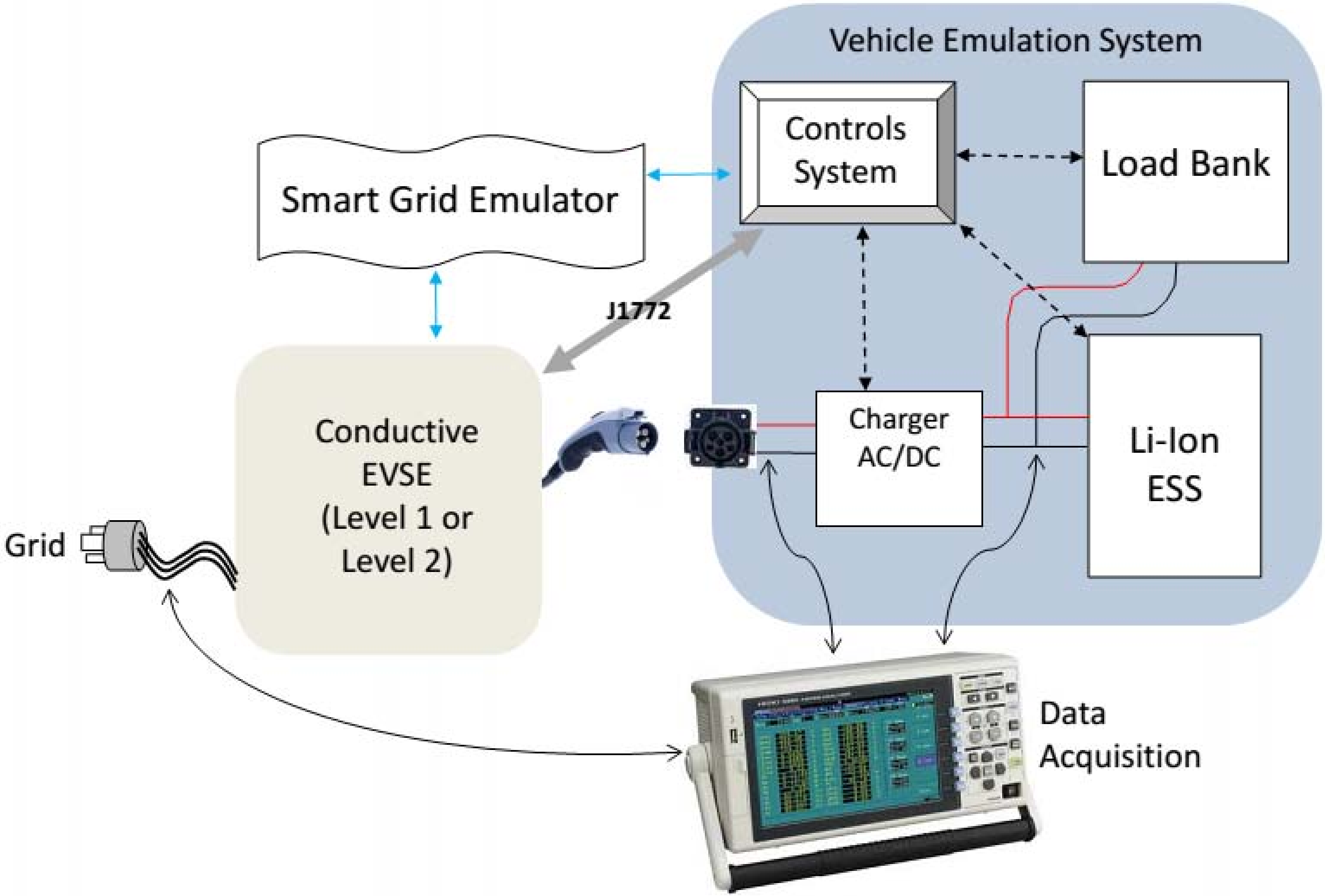

Conductive EVSE Energy Consumption

- AC energy consumption at rest and during Volt charging benchmarked

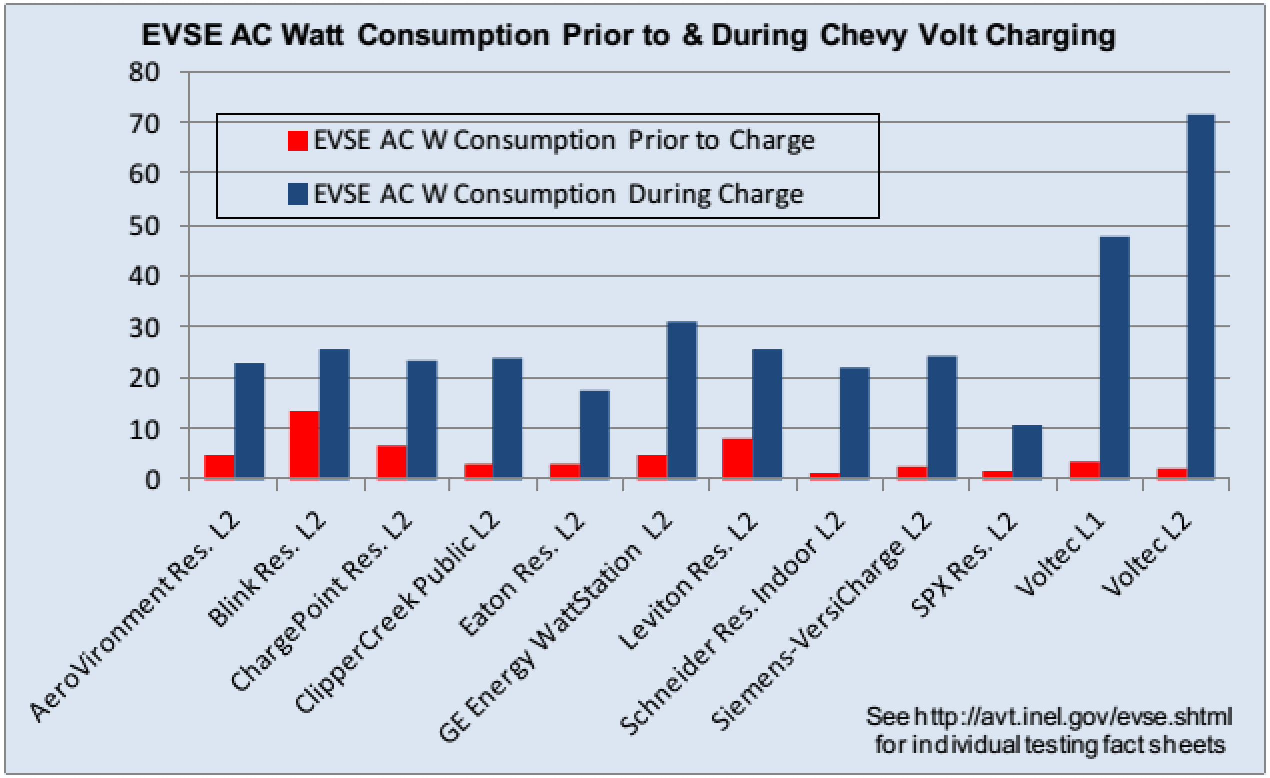

- Most EVSE consume 13 W or less at rest. Higher power use at rest is tied to greater EVSE features and functionality
- During charging, most EVSE power use is under 30 W

Conductive EVSE Charging Efficiency

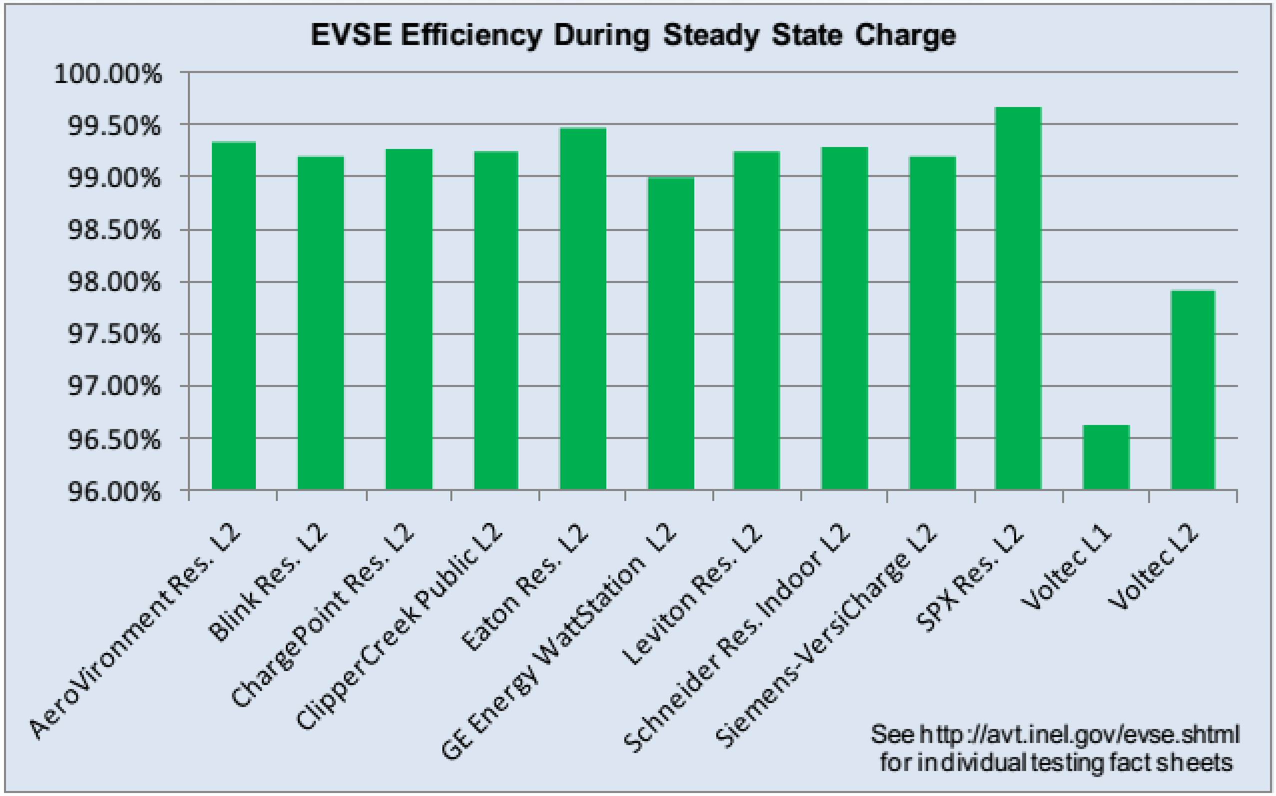

- **Steady state charging efficiency benchmarked for EVSE only (at meter and J1772 connector). No onboard components included**
- **Most conductive EVSE 99+% efficient during steady state charge of a Volt**

Charging Efficiency Can Be Difficult to Quantify With A Single Number For All Conditions

U.S. DEPARTMENT OF ENERGY | Energy Efficiency & Renewable Energy — VEHICLE TECHNOLOGIES PROGRAM

Electric Vehicle Supply Equipment (EVSE) Test Report: Blink

EVSE Features

Touch screen	PLC, WiFi, cellular, LAN communications
Backlit screen	Web-based bi-directional data flow
User charge scheduling via PDA, internet, and touchpad	

EVSE Tested

Blink Residential Wall-Mount Unit
AC Level 2
Model No. we-30cire

EVSE Specifications

Grid connection	Plug and cord NEMA 6-50
Connector type	J1772
Test lab certifications	UL listed
Approximate size (H x W x D inches)	18 x 22 x 6
Charge level	AC Level 2
Input voltage	208VAC to 240 VAC +/- 10%
Maximum input current	30 Amp
Circuit breaker rating	40 Amp

Test Conditions[1]

Test date	10/12/2011
Nominal supply voltage (Vrms)	210.6
Supply frequency (Hz)	60.00
Initial ambient temperature (°F)	88

Test Vehicle[1,3]

Make and model	2011 Chevrolet Volt
Battery type	Li-ion
Steady state charge power (AC kW)	3.12
Maximum charge power (AC kW)	3.30

EVSE Test Results[1,2,4]

EVSE consumption prior to charge (AC W)	13.4
EVSE consumption during steady state charge (AC W)	25.6
EVSE consumption post charge (AC W)	12.5
Efficiency during steady state charge	99.19%

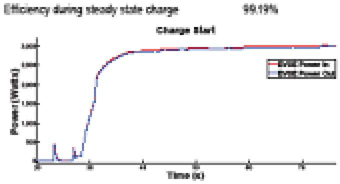

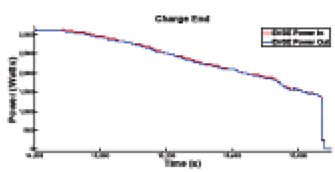

NOTE: Charge start and charge end power demand curves are dependent upon the vehicle

Features and Specifications Reference: http://www.blinknetwork.com/media/kit/Blink%20L2%20Wall%20Mount%20Charger.pdf

1. Hioki 3390 Power Meter used for all current and voltage measurements
2. Measurements were taken at EVSE grid connection and J1772 connection
3. Steady state charge power is the most common power level dictated by the vehicle during the charge
4. Steady state charge refers to the portion of the charge when power was greater than or equal to steady state charge power

INL/EXT-11-23986

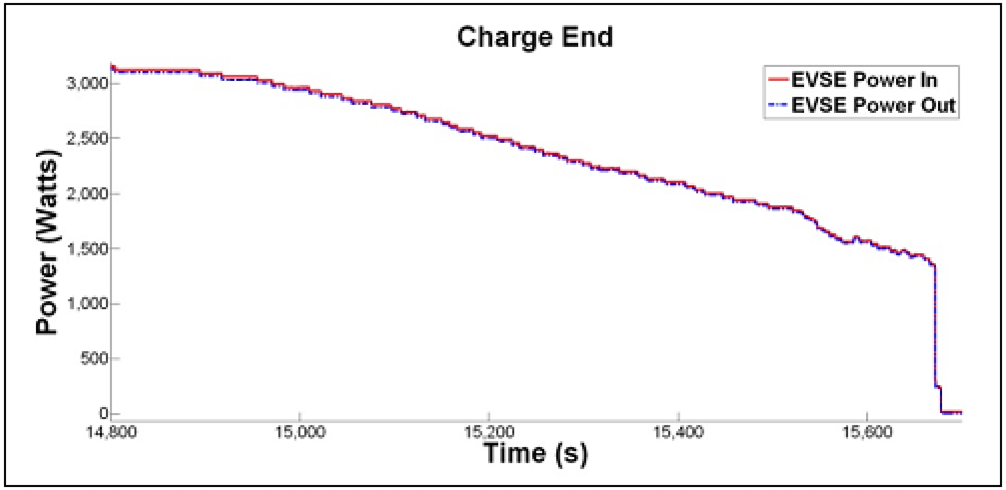

http://avt.inel.gov/pdf/evse/EVSEECOtalityBlink.pdf

Conductive System Benchmarking

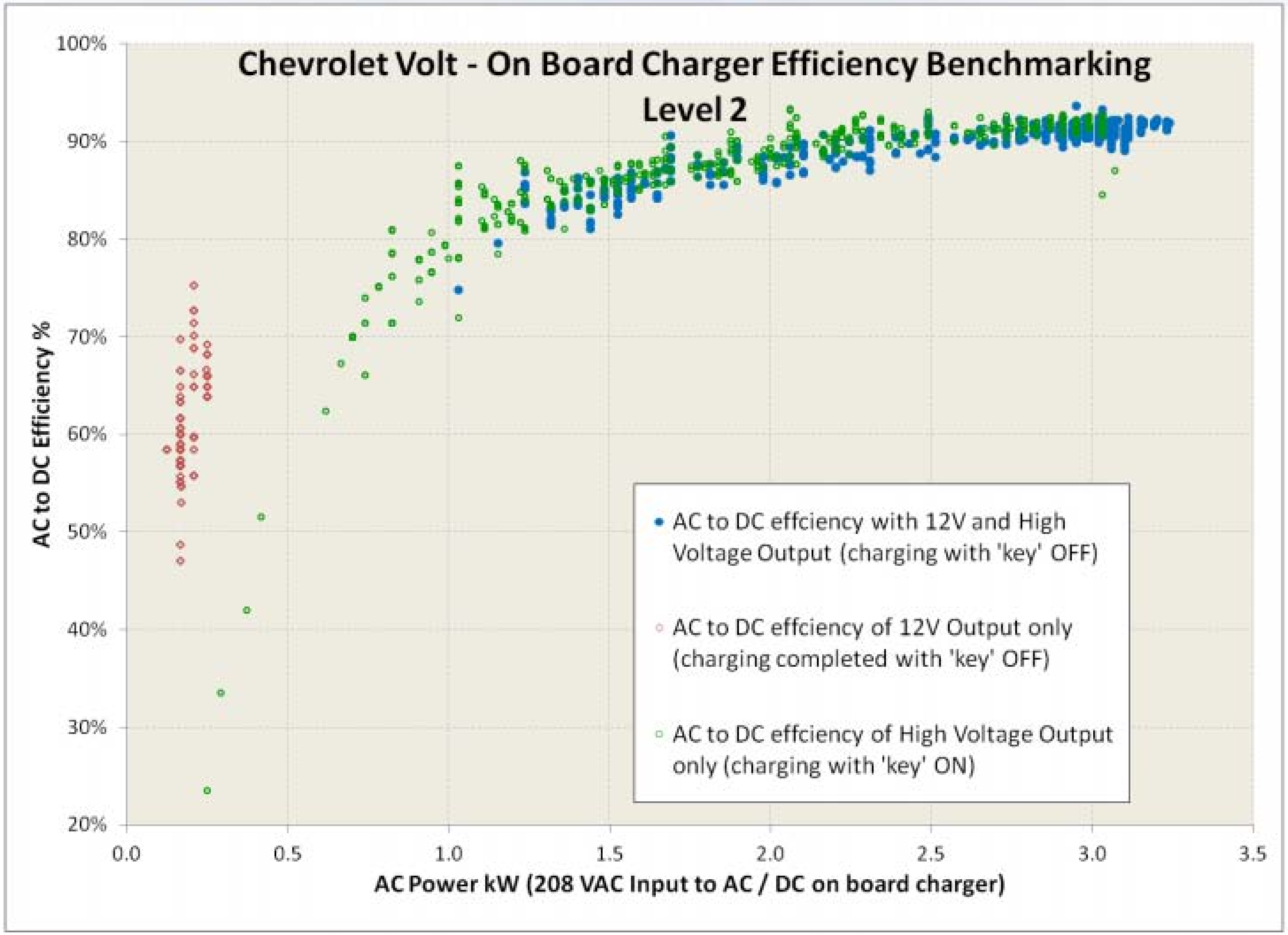

Entire report can be found at:
http://avt.inel.gov/pdf/phev/EfficiencyResultsChevroletVoltOnBoardCharger.pdf

Conductive System Benchmarking

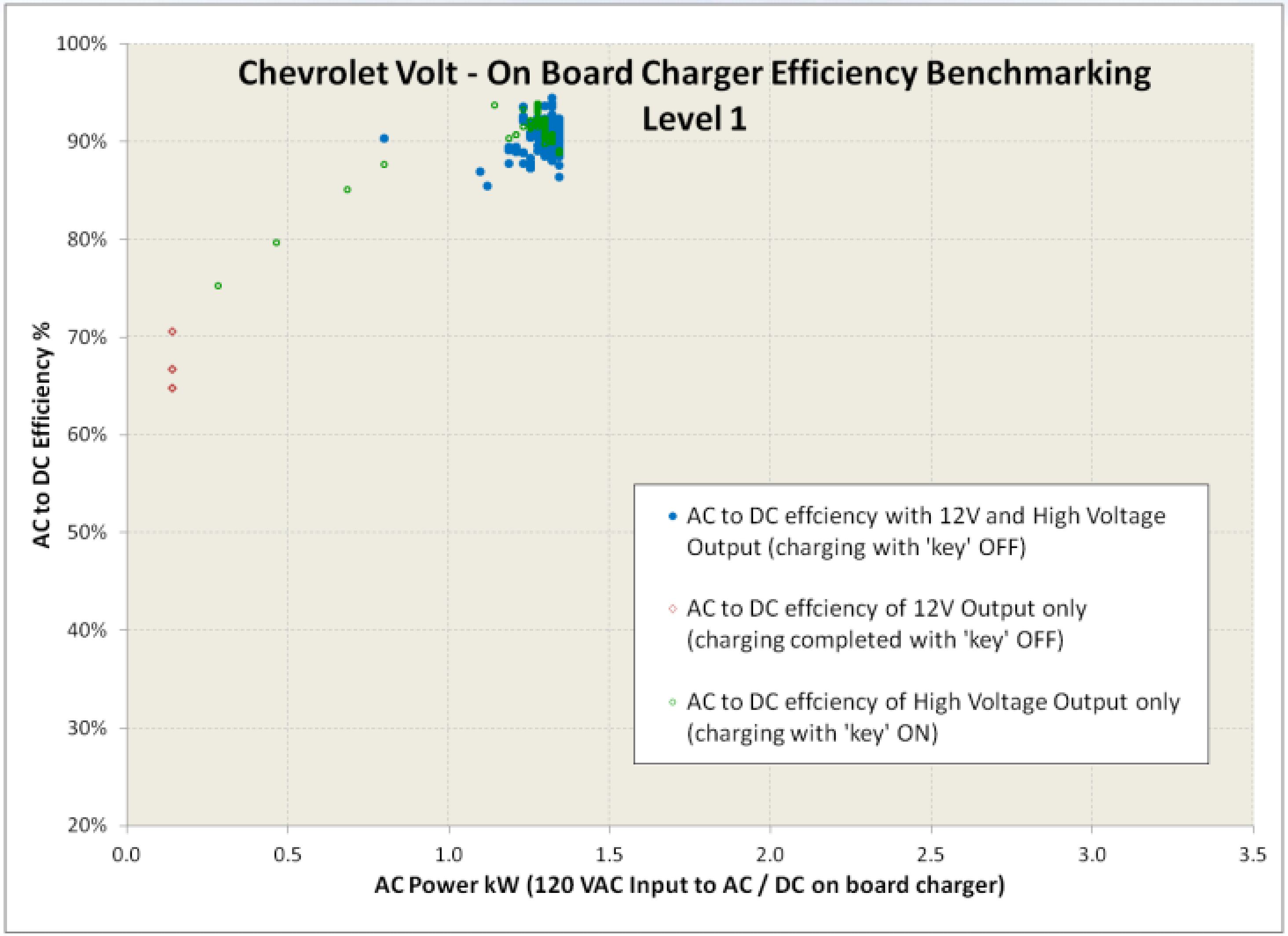

Entire report can be found at:
http://avt.inel.gov/pdf/phev/EfficiencyResultsChevroletVoltOnBoardCharger.pdf

Idaho National Laboratory

DCFC Benchmarking – Leaf Charging

U.S. DEPARTMENT OF ENERGY | Energy Efficiency & Renewable Energy — VEHICLE TECHNOLOGIES PROGRAM

Production EVSE Fact Sheet: DC Fast Charger: Hasetec

Specifications	
Grid connection	Hardwired
Connector type	CHAdeMo
Approximate size (H x W x D inches)	36 x 69 x 21
Charge level	DC Fast Charge
Input voltage	480 VAC - 3 Phase
Isolation Transformer[1]	75 kVA
Maximum input current[2]	120 Amp
Test Conditions	
Test date	10/23/2012
Supply frequency (Hz)	60
Initial ambient temperature (°F)	65
Vehicle Charged	
Make and model	2011 Nissan Leaf
Battery type	Li-ion
Initial Leaf ESS State of Charge[3]	9%
Final Leaf ESS State of Charge[3]	80%
DCFC Test Results[3, 4]	
Peak Power draw from Grid (AC kW)	53.1
Energy from grid (AC kWh)	15.0
Peak Charge Power to Leaf ESS (DC kW)	47.1
Energy delivered to Leaf ESS (DC kWh)	13.3
Charge time (min:sec)	31:40
Overall Charge Efficiency (480VAC to ESS DC)	88.7%

DC Fast Charger Tested

Hasetec LD6-3P3W 50KW

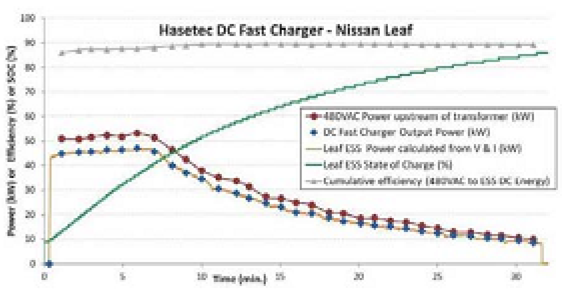

1. EPS Sentinel dry type Isolation Transformer
2. Manufacture specification = 125A max; this installation is configured to 120A max due to supply restrictions
3. Vehicle CAN message data acquisition and Hasetec DC output watthour meter used for DC measurements
4. Square D WattHour meter used for 480VAC energy measurement on feed to transformer

INL/EXT-11-23986

- 88.7% Overall charge efficiency (480VAC to ESS DC)
- 53.1 AC kW peak grid power
- 47.1 DC kW peak power to Leaf energy storage system (ESS)
- 15.0 Grid AC kWh and 13.3 DC kWh delivered to Leaf ESS

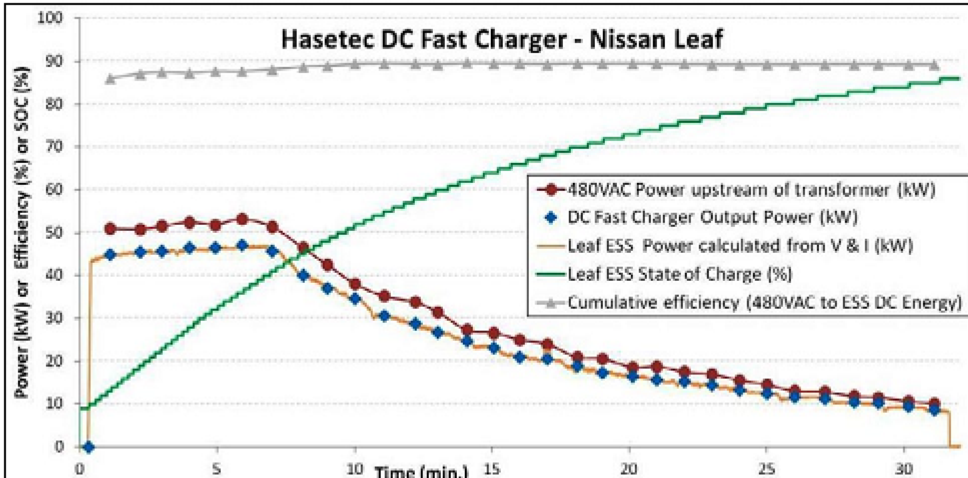

http://avt.inel.gov/pdf/evse/DCFCHasetec.pdf

First Brazilian power grid

- Rio de Janeiro Central Station
- 1878 – D. Pedro II hired Thomas Edison company

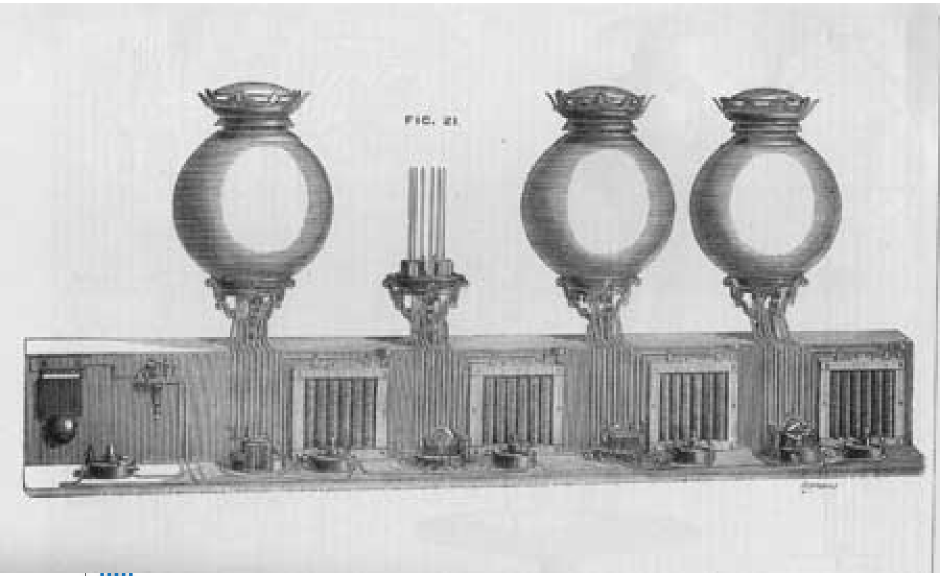

Fonte: http://www.theiet.org/about/libarc/archives/biographies/jablochkoff.cfm

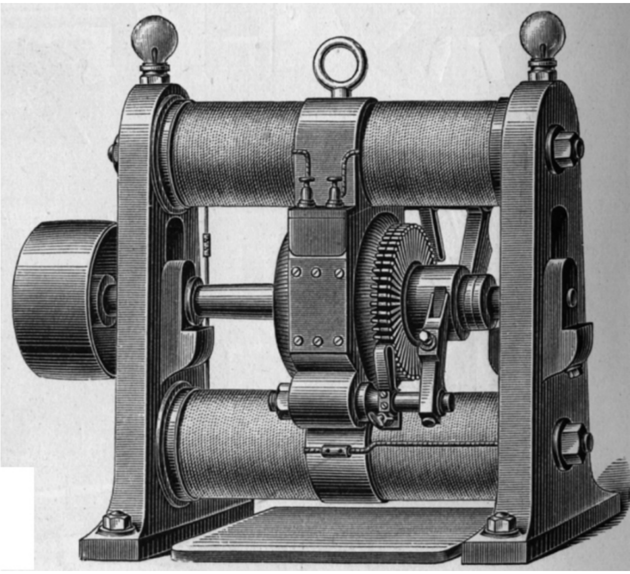

Fonte: http://pixii.com/gramme1.jpg

First Brazilian power grid

Stability:

Supply and demand balance !

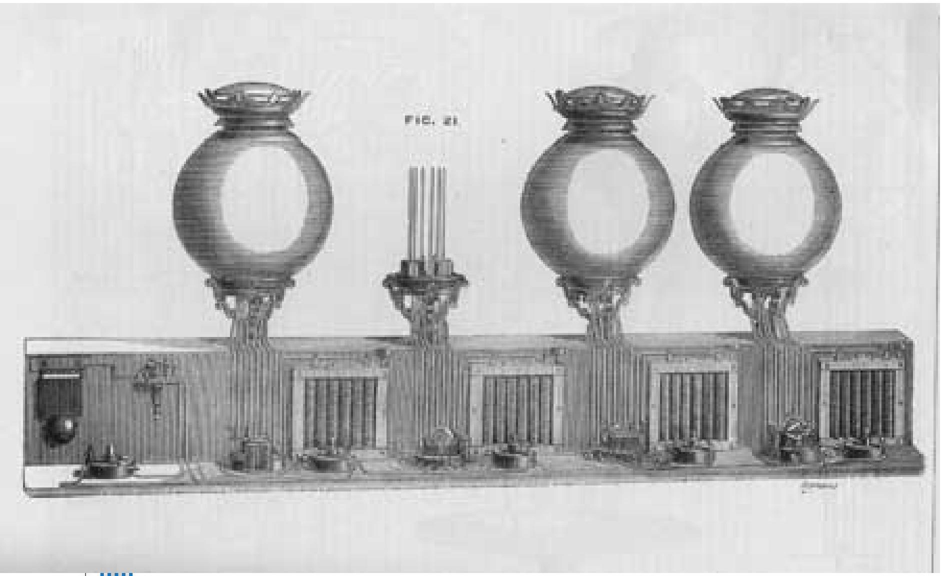

Fonte: http://www.theiet.org/about/libarc/archives/biographies/jablochkoff.cfm

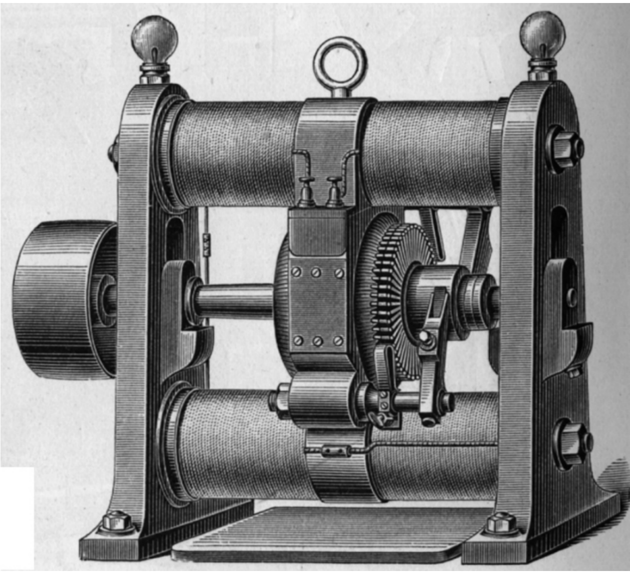

Fonte: http://pixii.com/gramme1.jpg

First Brazilian power grid

Stability:

Supply and demand balance !

First grid:

All was well known.

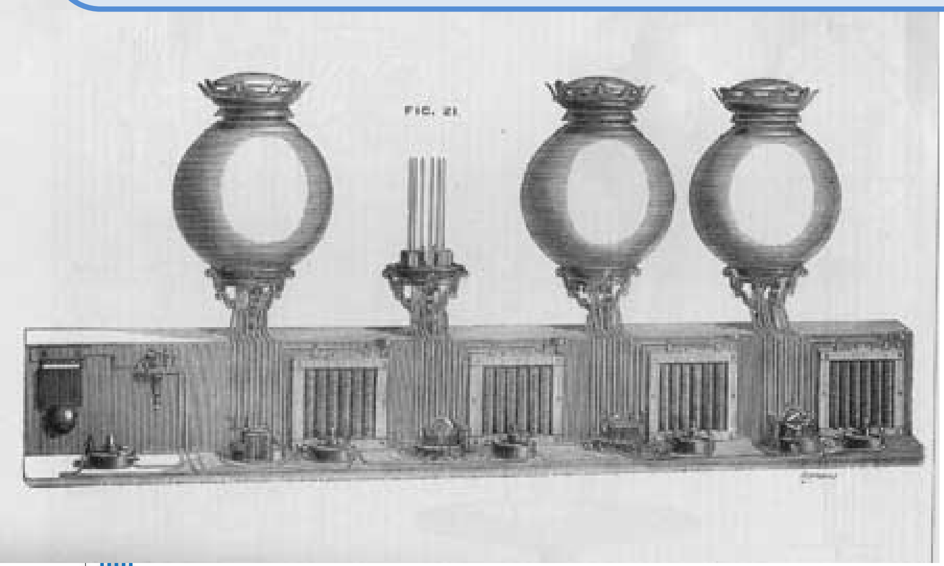

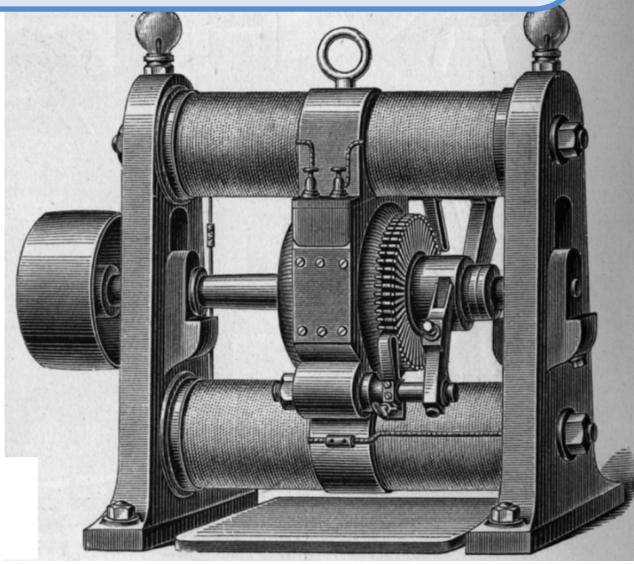

Fonte: http://www.theiet.org/about/libarc/archives/biographies/jablochkoff.cfm

Fonte: http://pixii.com/gramme1.jpg

First Brazilian power grid

Stability:

Supply and demand balance !

First grid:

All was well known.

How about the Smart Grid?

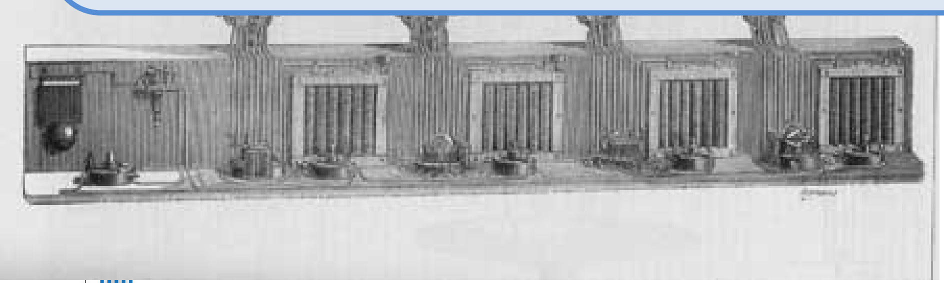

Fonte: http://www.theiet.org/about/libarc/archives/biographies/jablochkoff.cfm

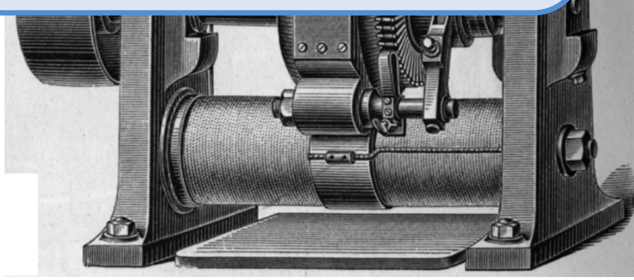

Fonte: http://pixii.com/gramme1.jpg

Safety Design of CHAdeMO Quick Charger and its impact on Power Grid

December 1 , 2010

TEPCO

Takafumi Anegawa

Optimal charging speed is different in each batteries

- Battery degradation is caused by over voltage and high temperature.
- Limit voltage and temperature depend on battery characteristics.
- On-board battery management system is watching the voltage and the temperature in real time.

Observing parameters
- Battery total voltage
- Cell voltage
- Battery temperature
- Input Current etc.

Charging process is controlled by EV in CHAdeMO

Problems:

- Battery improvement is so fast that it's **difficult to catch up every batteries' data.**
- Standardization to meet lowest speed battery disturbs battery improvement.

How CHAdeMO charger works:

- **EV computer unit decides** charging speed based on BMS observation.
- Charging current signal is sent to charger using CAN bus.
- Charger supplies DC current following the request from EV.

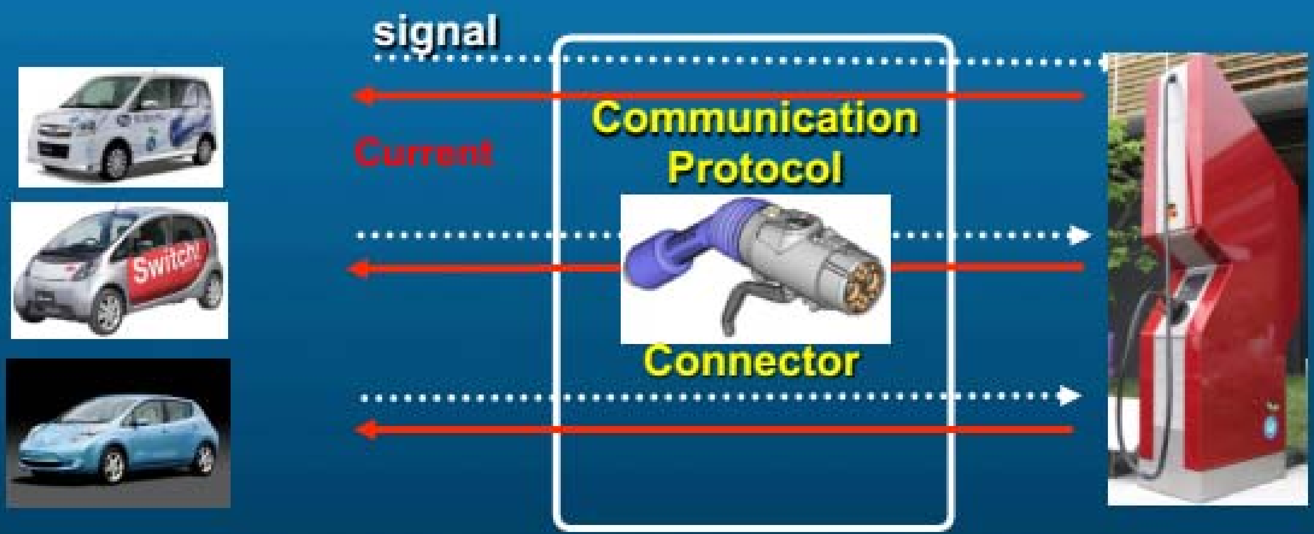

Location of quick chargers on power grid

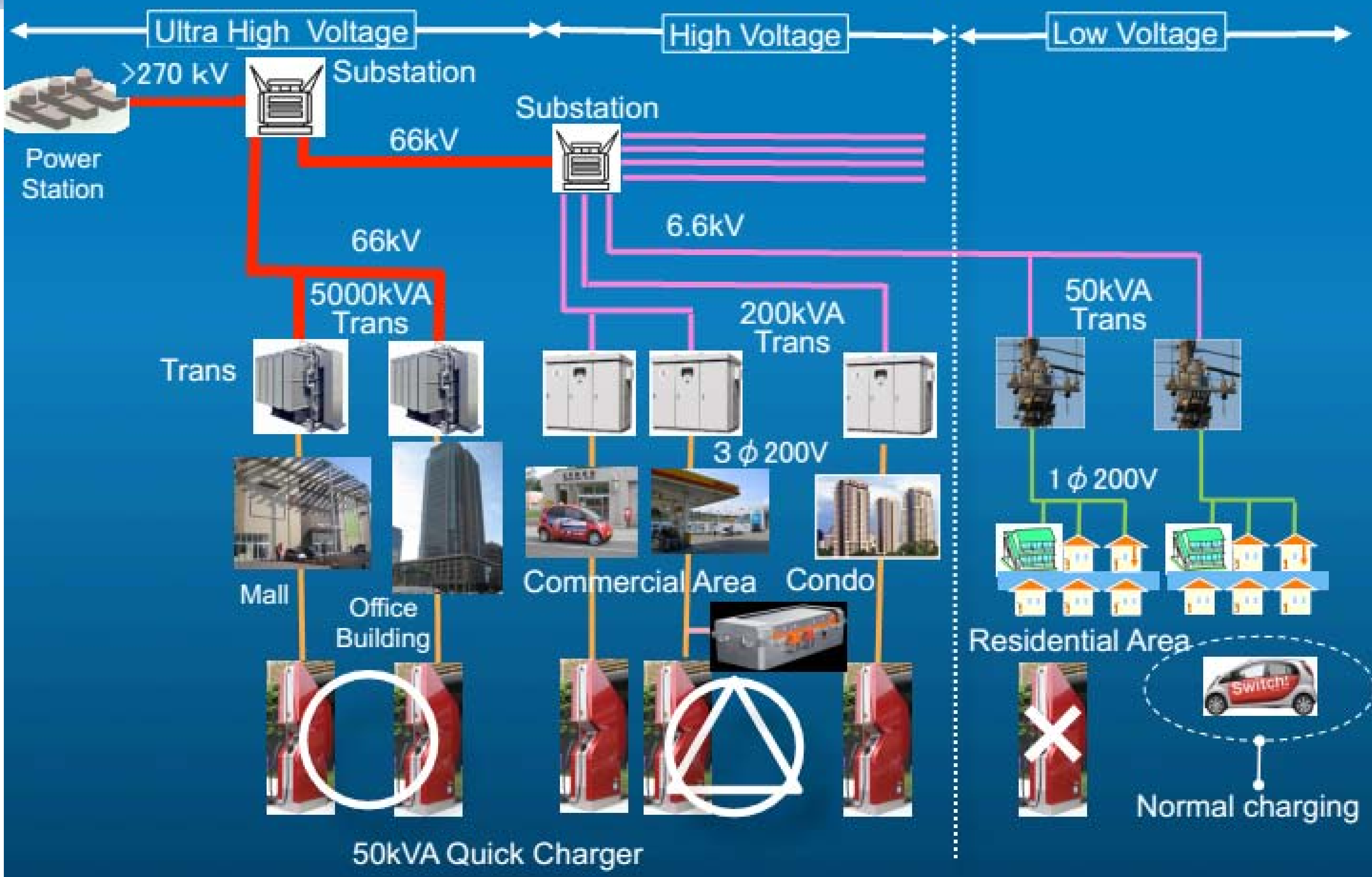

Impact on distribution grid (20% dissemination rate)

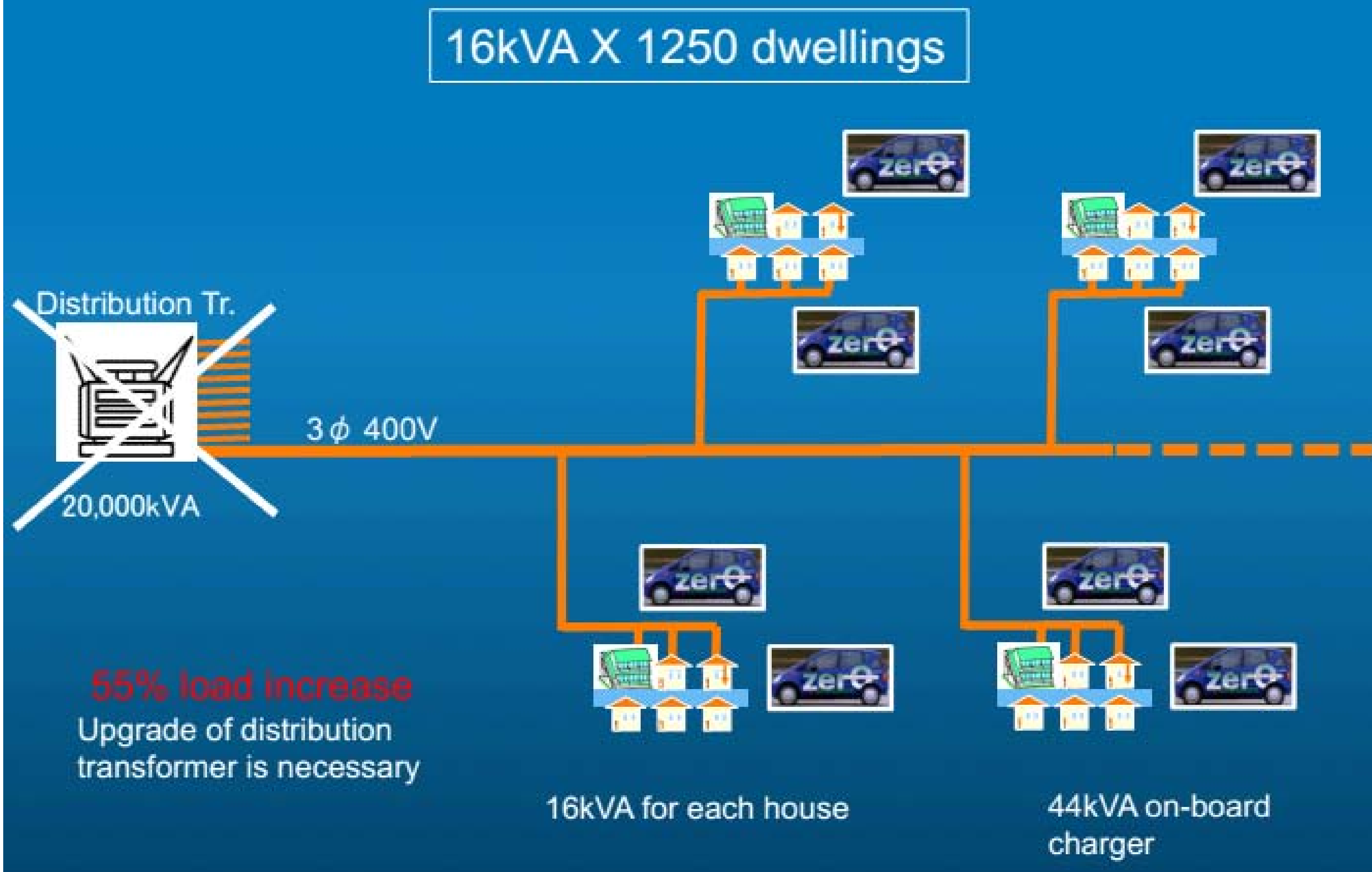

Impact on distribution grid (20% dissemination rate)

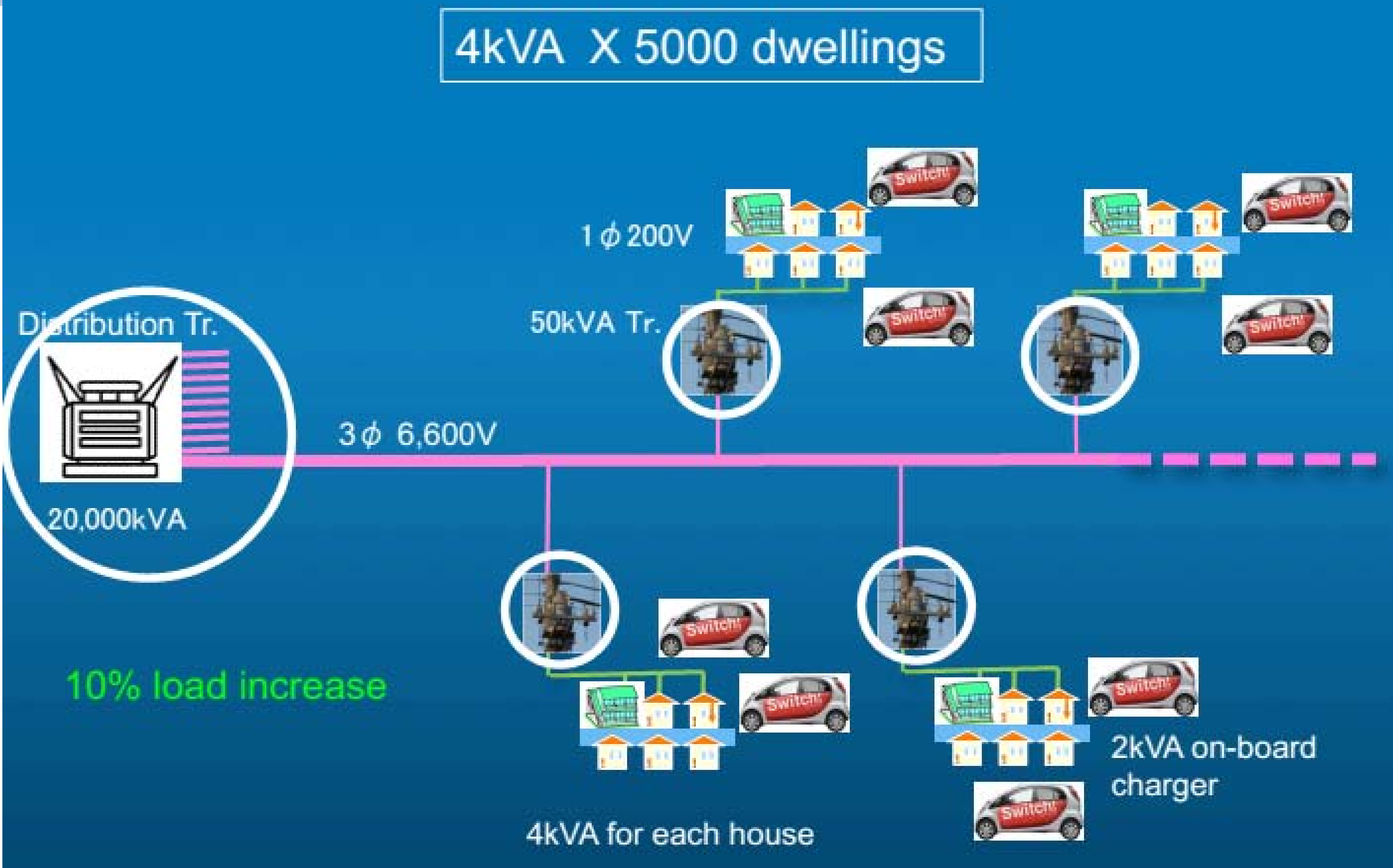

Slow AC and fast DC combination

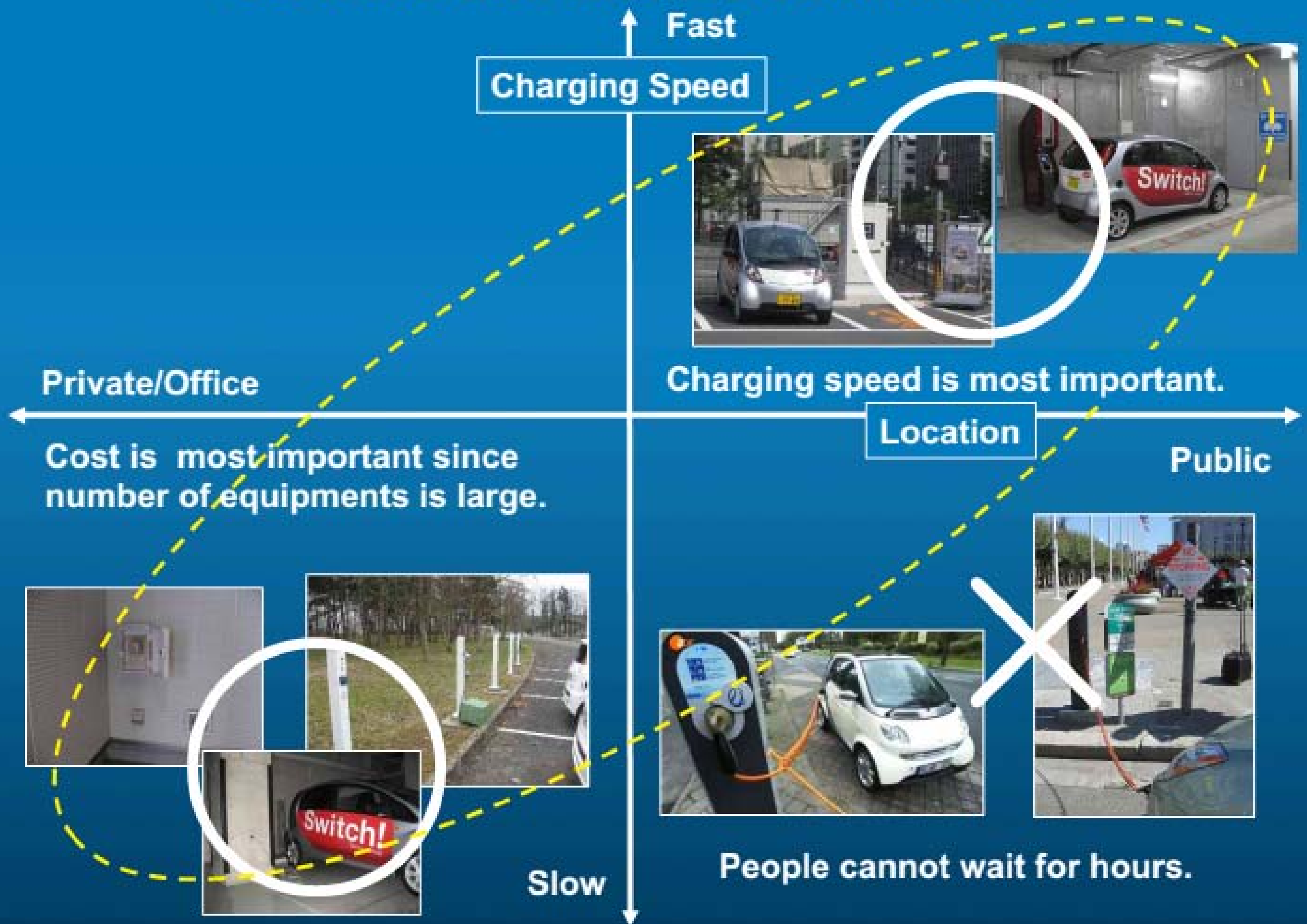

Is there negative impact on power grid?

- (Ultra) high voltage power grid can supply electricity to quick charger easily.
- Frequency to use quick charger is not often then impact on power grid is small.
- In order to minimize impact on distribution gird in residential area, on-board charger kW should be small.
- If there are moderate number of quick chargers in public area, drivers satisfy with small size on-board chargers.

INEP

Grid voltage variation range

- IEC

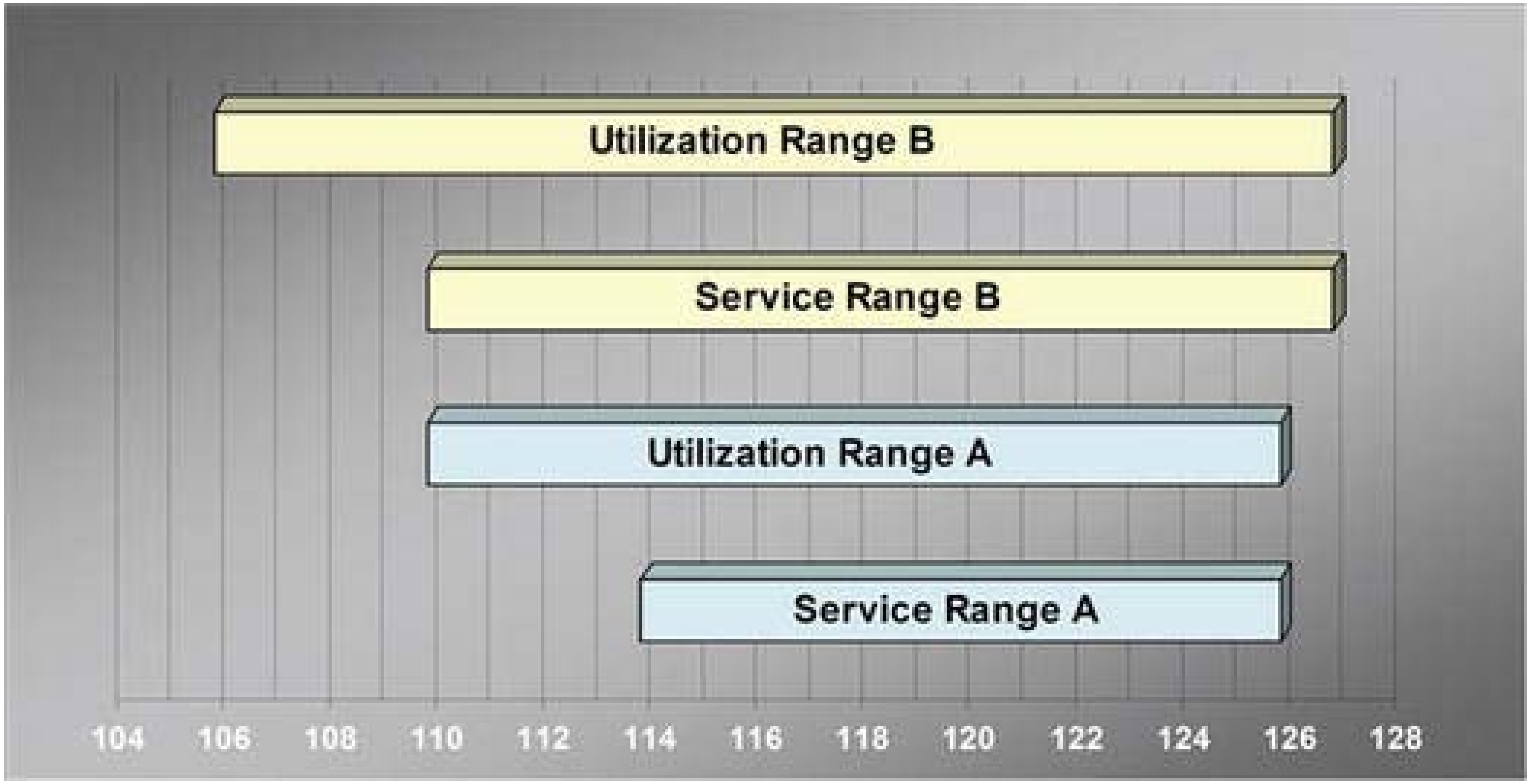

Grid frequency variation range

- IEC 61000-2-2
  - ±1 Hz

- ONS (Brazilian agency)

Desempenho	Tempo acumulado máximo de exposição a desvios de frequência (seg)
f > 66,0 Hz	0
63,5 Hz < f ≤ 66,0 Hz	30,0
62,0 Hz < f ≤ 63,5 Hz	150,0
60,5 Hz < f ≤ 62,0 Hz	270,0
58,5 Hz ≤ f < 59,5 Hz	390,0
57,5 Hz ≤ f < 58,5 Hz	45,0
56,5 Hz ≤ f < 57,5 Hz	15,0
f < 56,5 Hz	0

Eletronics

Labour saving device	Increase in ownership 1970-2004
Dishwashers	1 per cent in 1970 to 26 per cent in 2004
Microwaves	<1 per cent in 1977[5] to 84 per cent in 2004
Tumble dryers/washer dryers[6]	<1 per cent 1970 to 55 per cent in 2004
Vacuum cleaner	80 per cent in 1970 to 100 per cent in 2004

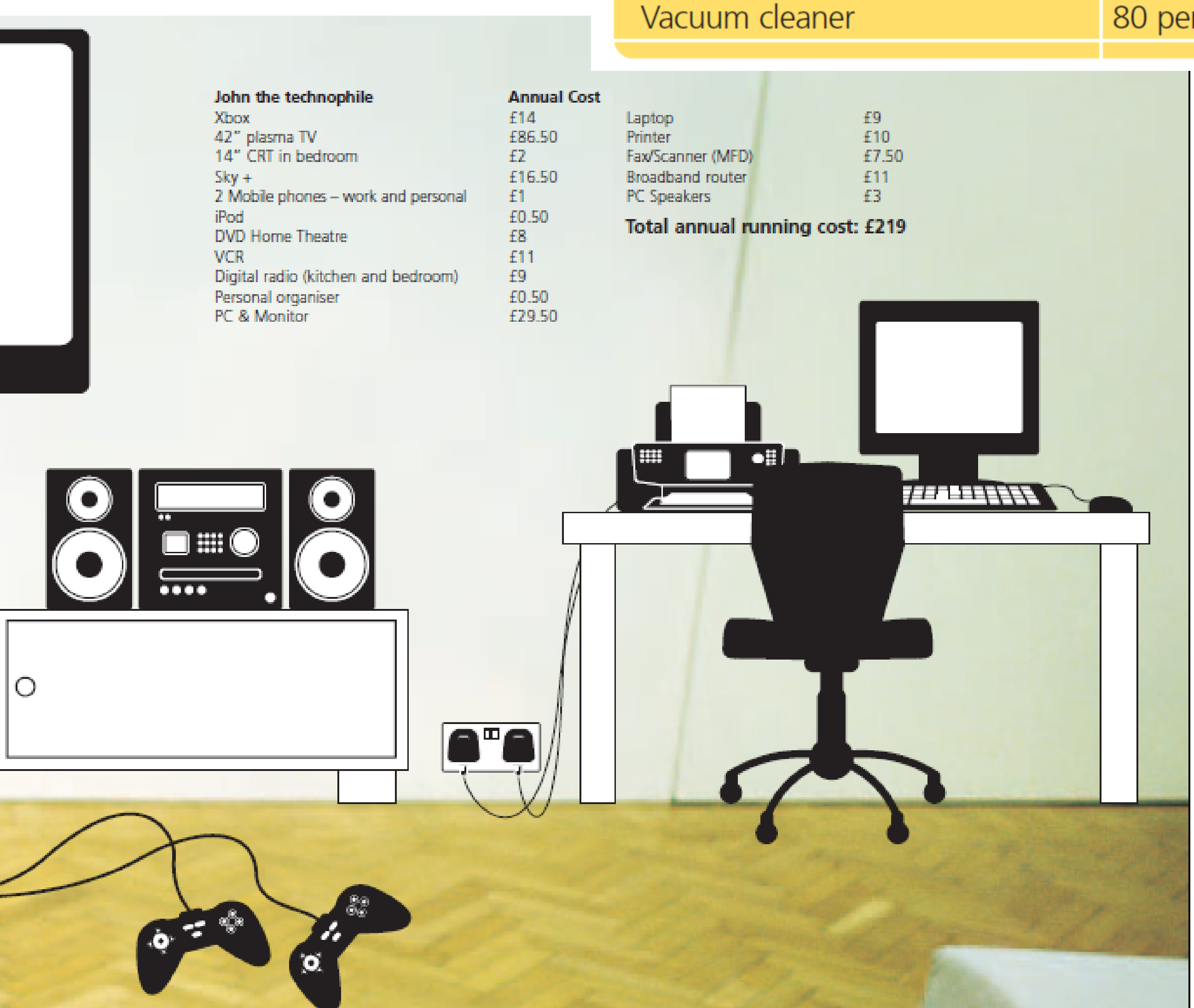

Energy saving trust, "The ampere strikes back How consumer electronics are taking over the world," 2007.

Smart Grid electric functions

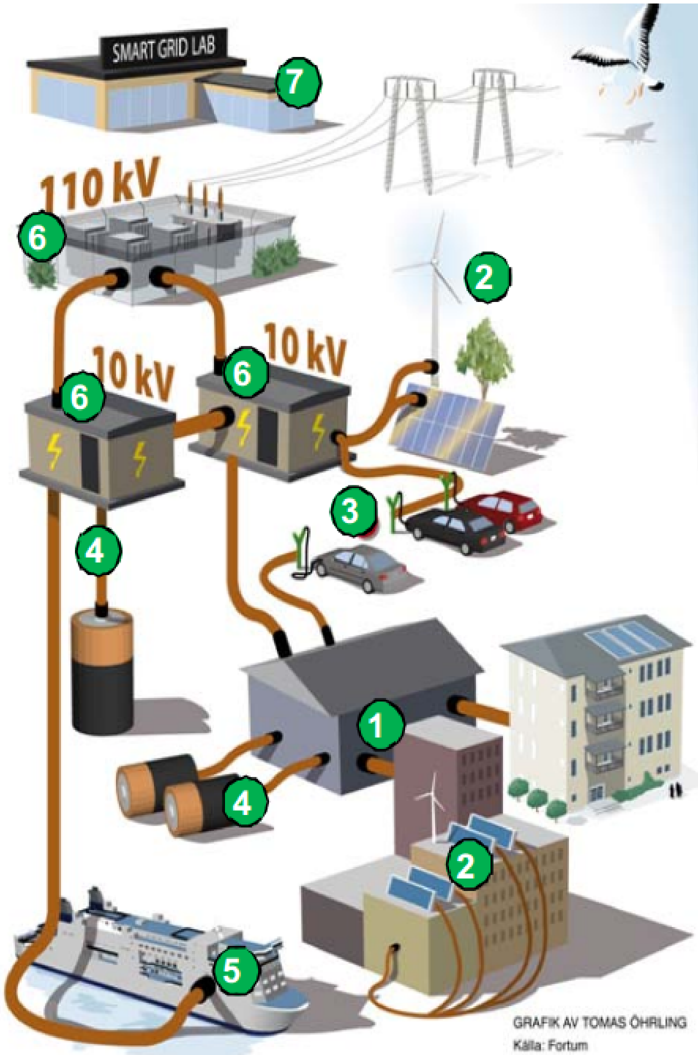

1 Smart home and "Demand response"

- Reduced peak load and improved energy efficiency through active consumers and home automation

2 Distributed generation

- Integration of solar panel and wind turbines

3 Integration and use of electric vehicles

- Including fast charging and load balancing

4 Energy storage

- Stability and power quality

5 Smart harbour

- Reduce CO_2 emissions by supplying vessel in the harbour with clean power from land ("Shore-to-Ship")

6 Smart substation

- Improved efficiency and stability through automation

7 Smart Grid Lab

- R&D, simulation and demonstration of smart grid applications

Home Area Networks (HAN)

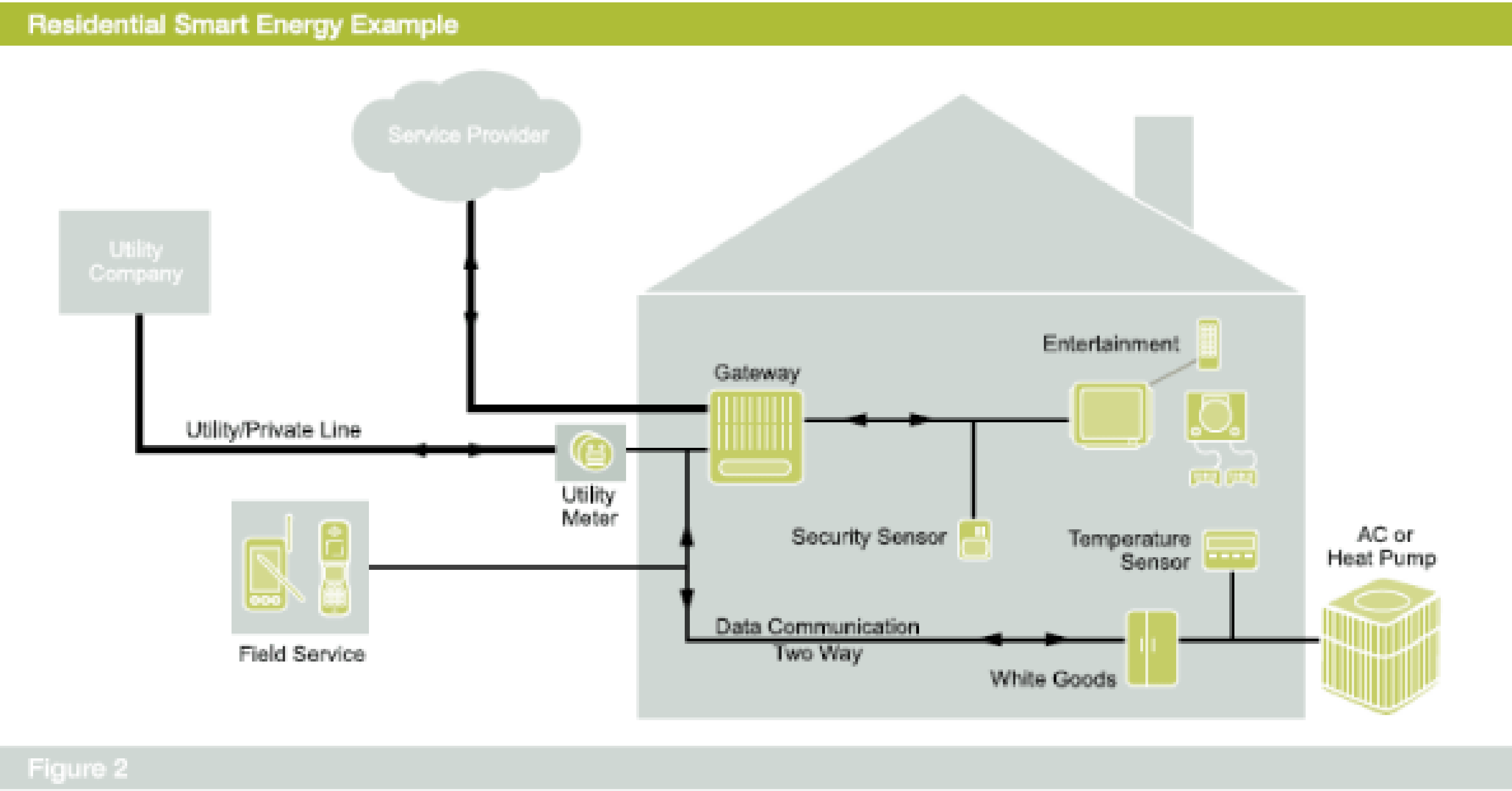

http://www.freescale.com/webapp/sps/site/overview.jsp?code=784_LPBBGREE

Improving homes

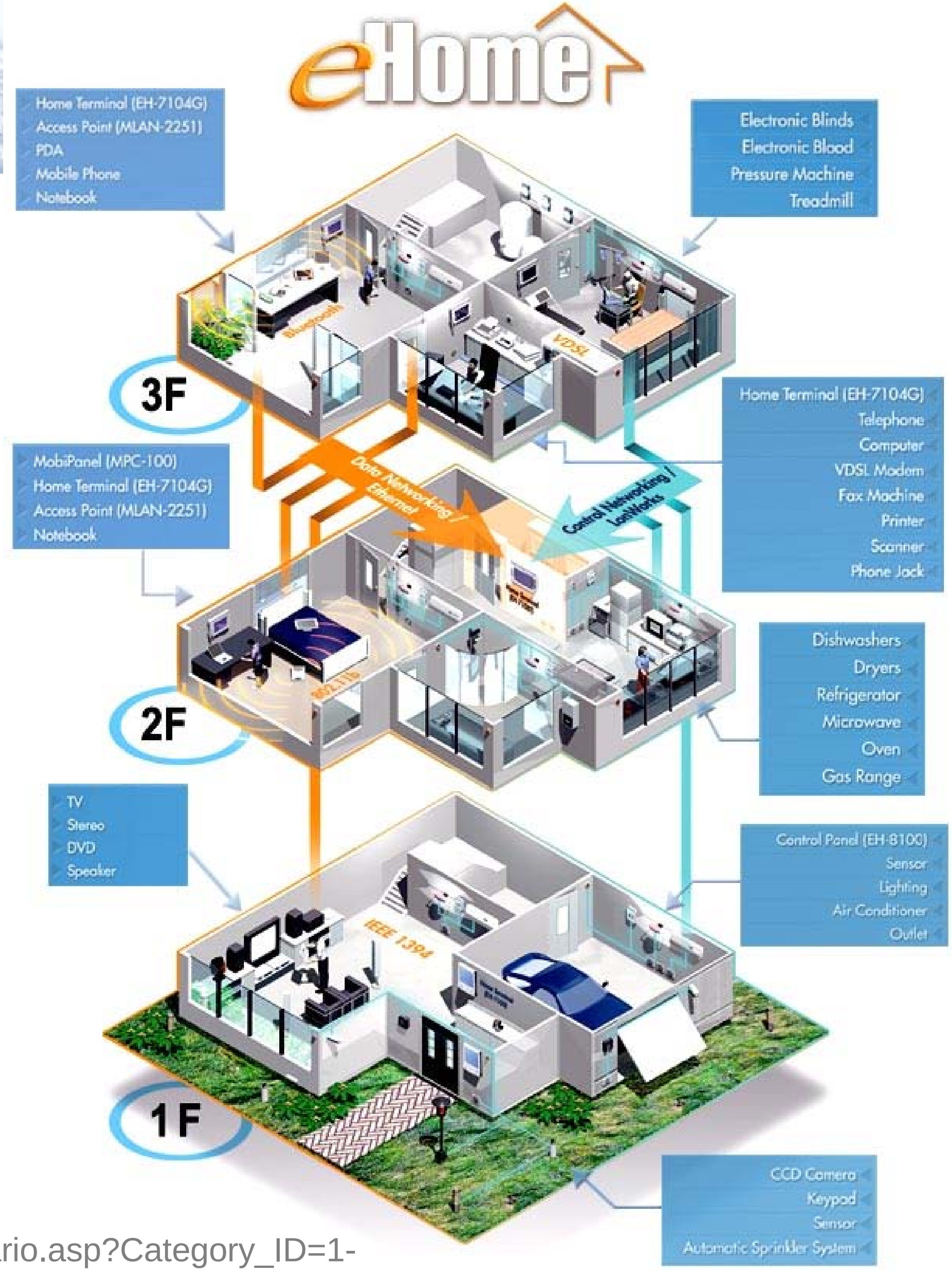

http://www.advantech.com/solutions/eHome/scenario.asp?Category_ID=1-

EVs are more popular

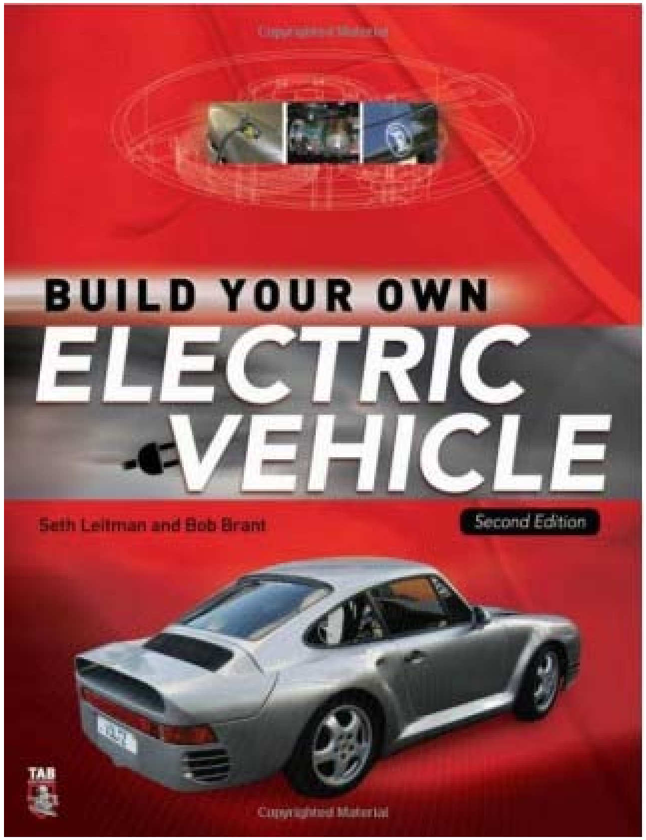

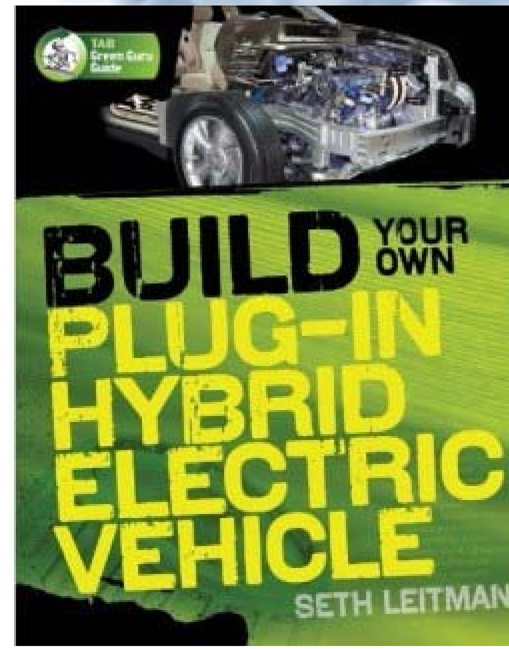

Vehicle-to-Grid (V2G)

- To integrate EVs to the grid not only as loads, but as storage systems
- Objective: reduce EVs impact to the grid

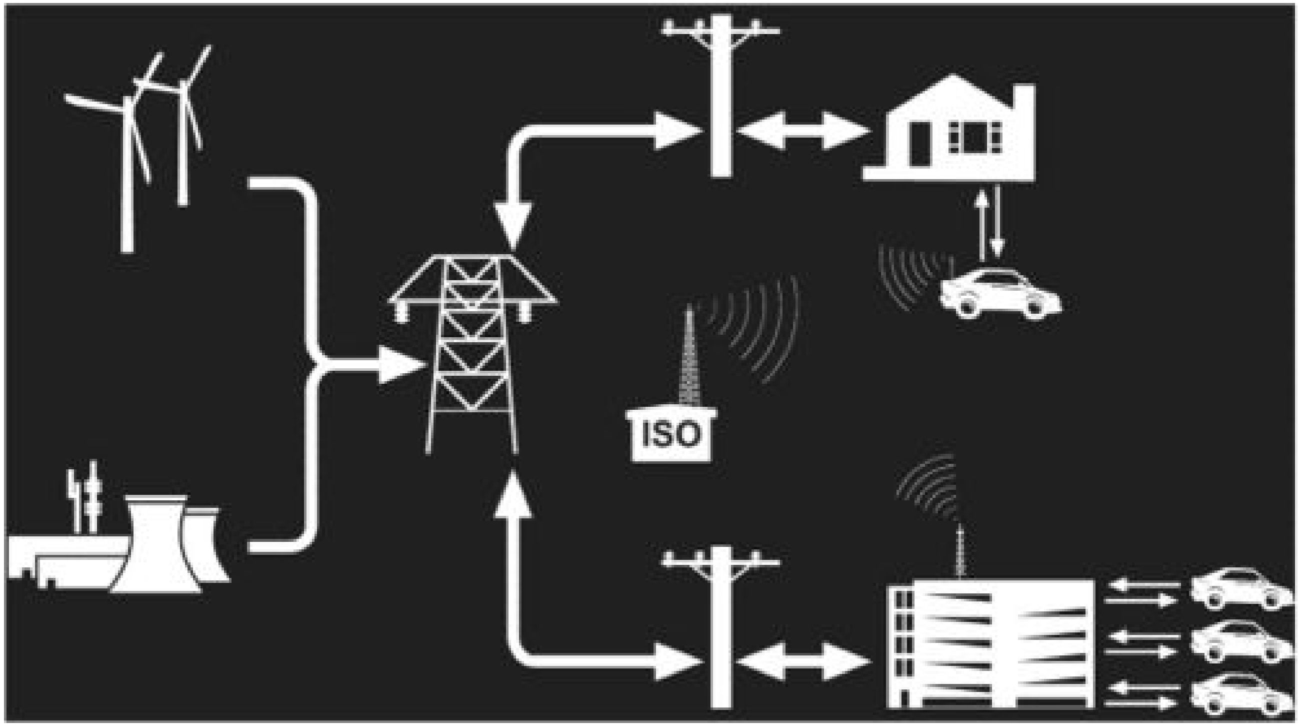

The Vehicle-to-Grid (V2G) concept

- Components:
  - Batteries
  - BMS (Battery management systems)
  - Battery charger (ac-dc)
  - Inverter (dc-ac)
  - Controller
  - GPS
  - Measurement

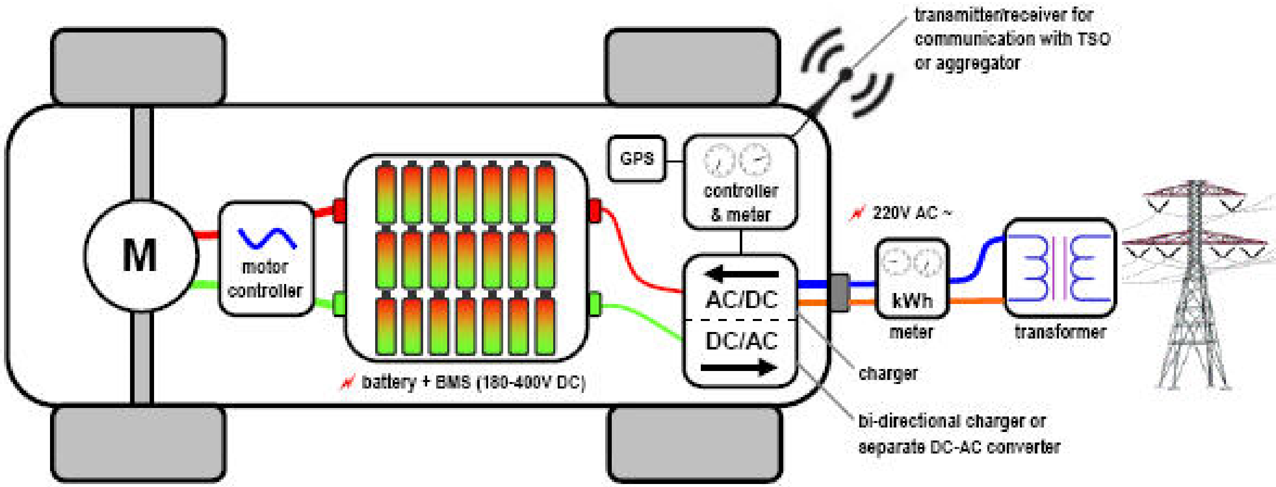

Schematic drawing of a V2G-capable vehicle

- Outside the vehicle:
  - Smart meter
  - Power grid

Vehicle-to-Grid (V2G)

- Aggregator:
  - service provider that receives information and takes decisions

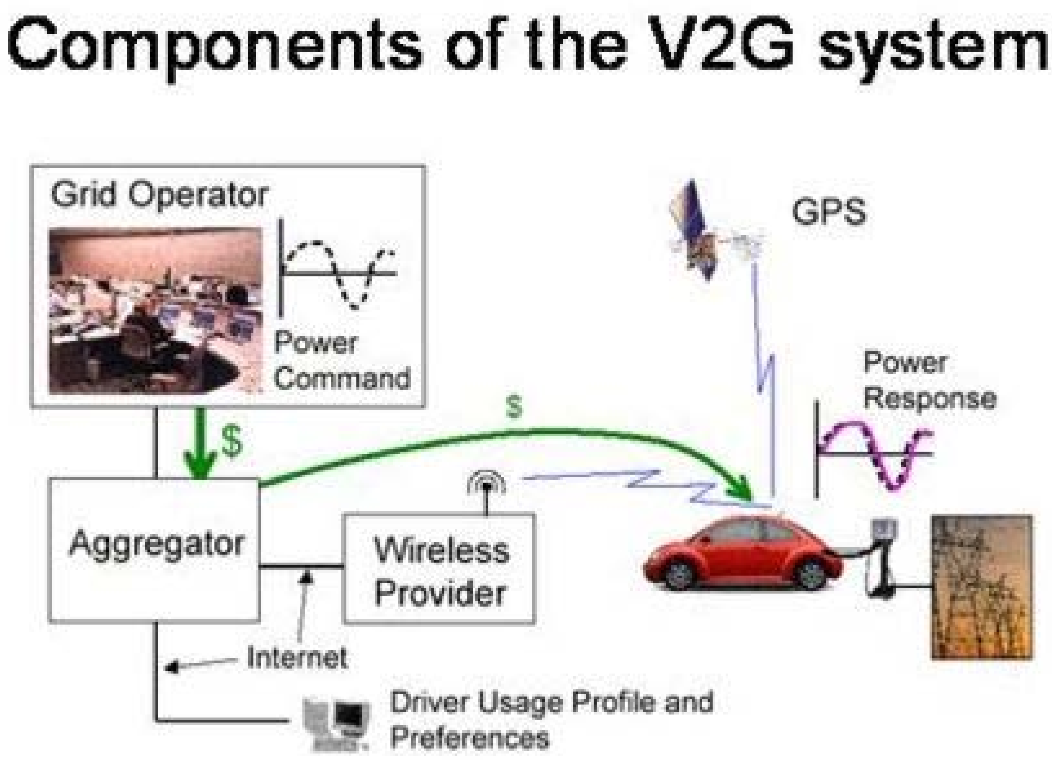

Nissan's home integrated storage

http://www.iea.org/topics/transport/subtopics/electricvehiclesinitiative/EVI_2014_Casebook.pdf

Analysis of different strategies to V2H

a) Business-as-usual
b) Local energy control
c) Iterative global energy controller

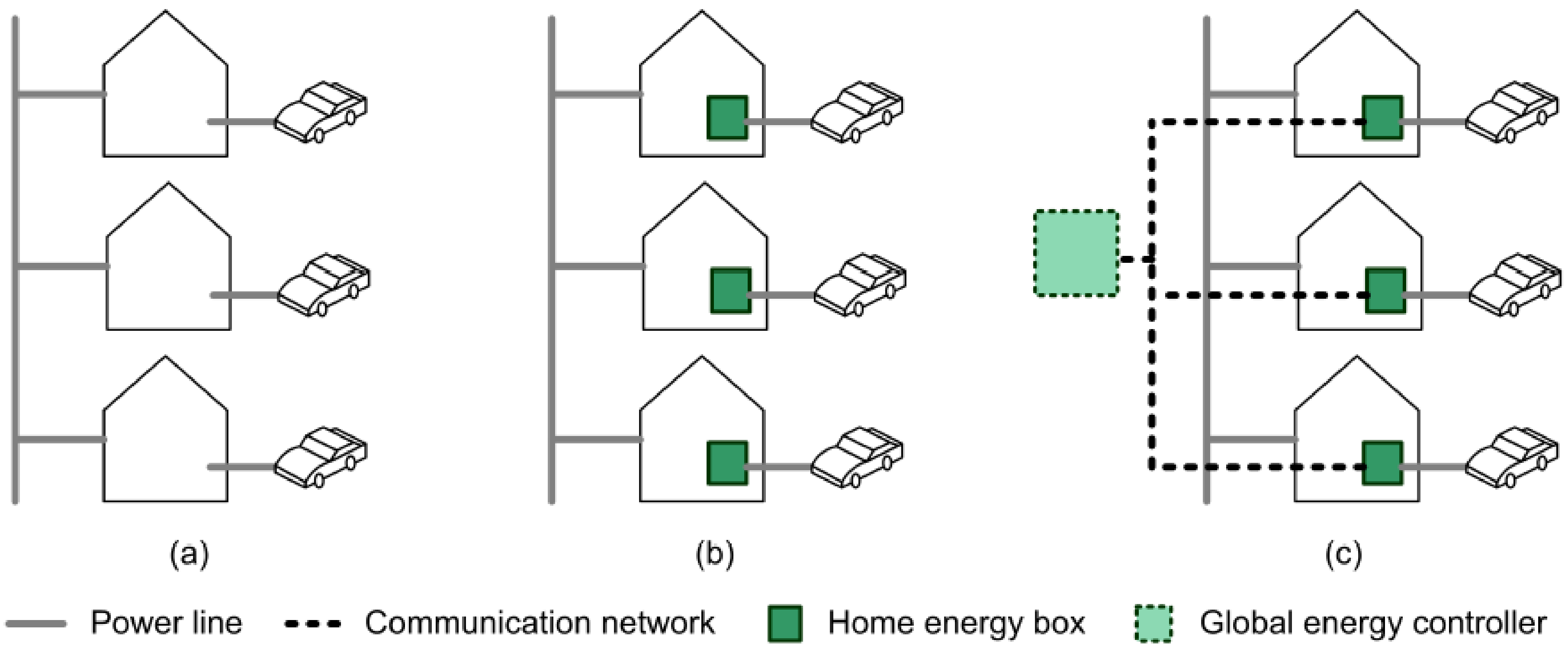

Mets et al., “Optimizing Smart Energy Control Strategies forPlug-In Hybrid Electric Vehicle Charging,” 2010.

Analysis of different strategies to V2H

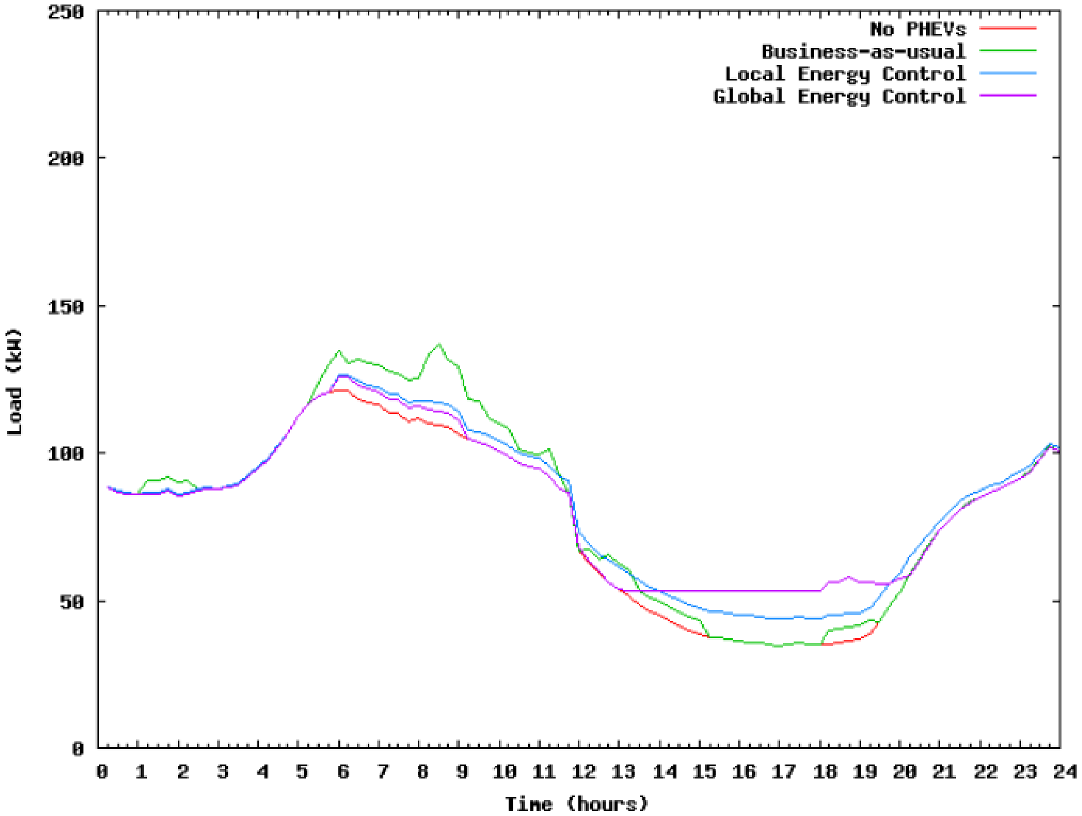

(a) 10% PHEV penetration

Mets et al., “Optimizing Smart Energy Control Strategies forPlug-In Hybrid Electric Vehicle Charging,” 2010.

Analysis of different strategies to V2H

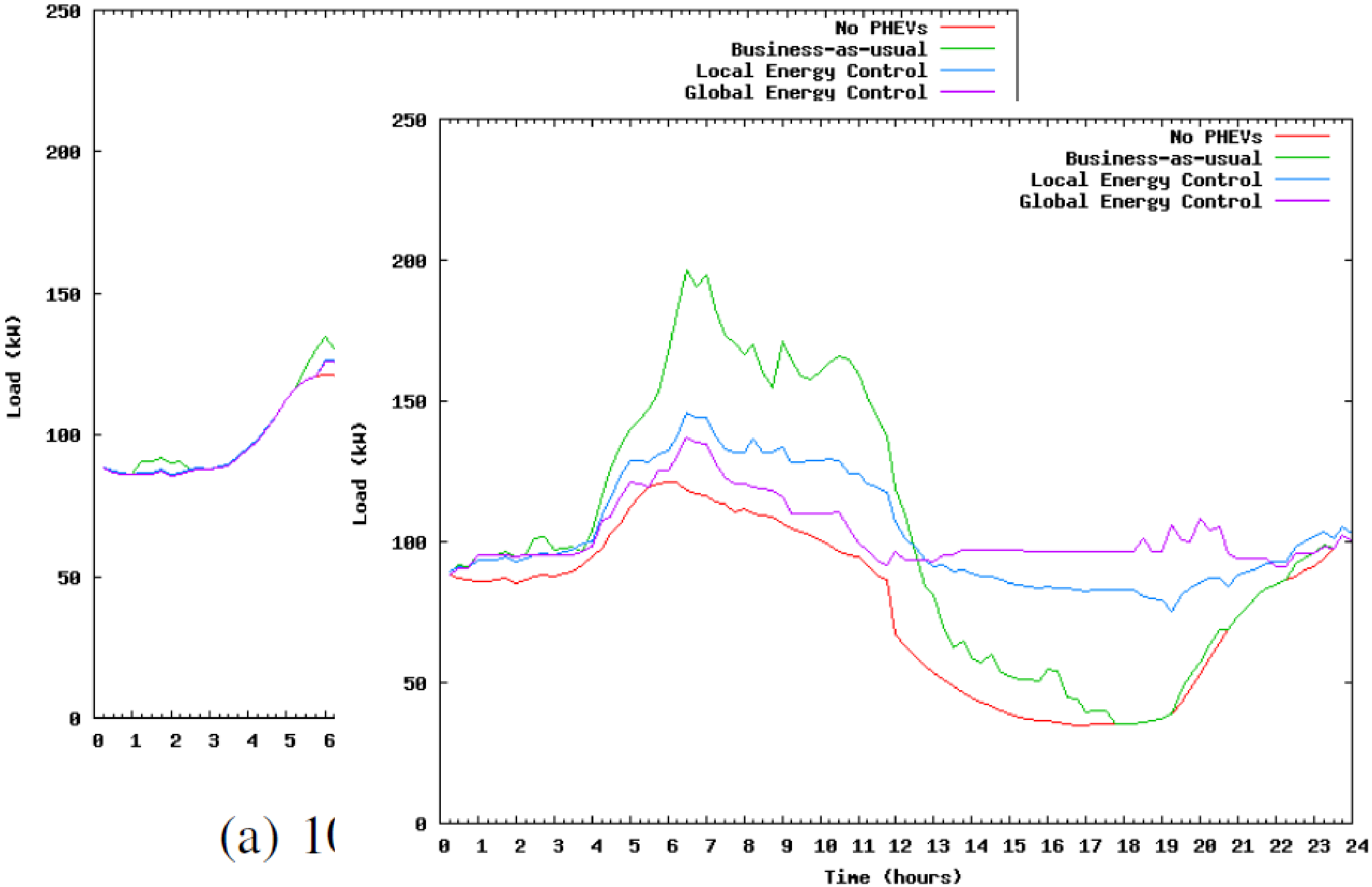

(a) 1(

(b) 30% PHEV penetration

Mets et al., "Optimizing Smart Energy Control Strategies forPlug-In Hybrid Electric Vehicle Charging," 2010.

Analysis of different strategies to V2H

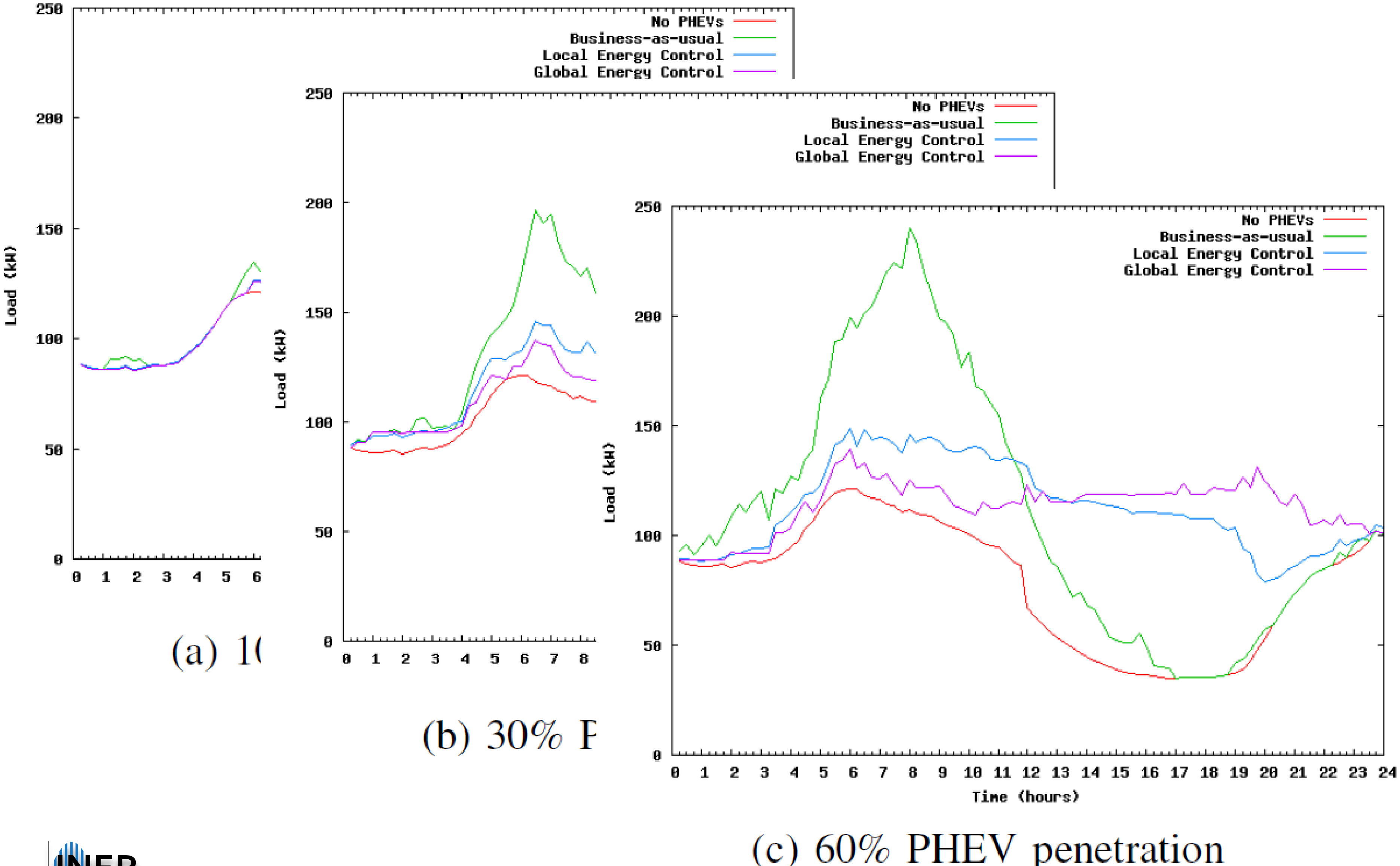

Mets et al., “Optimizing Smart Energy Control Strategies forPlug-In Hybrid Electric Vehicle Charging,” 2010.

Power Electronics for EV Charging Systems

- USA (SAE J1772 Definition)

Level 1 Charging
- Single-Phase AC Connection
- On-Board Charger
- 120 VAC, 16 A → 1.92 kW

Level 2 Charging
- Single-Phase AC Connection
- On-Board Charger
- 204 – 240 VAC, ≤ 80 A → 19.2 kW

Level 3 Charging
- DC Connection
- Three-Phase Off-Board Charger
- 300 – 600 V_{DC}, ≤ 80 A → 240 kW

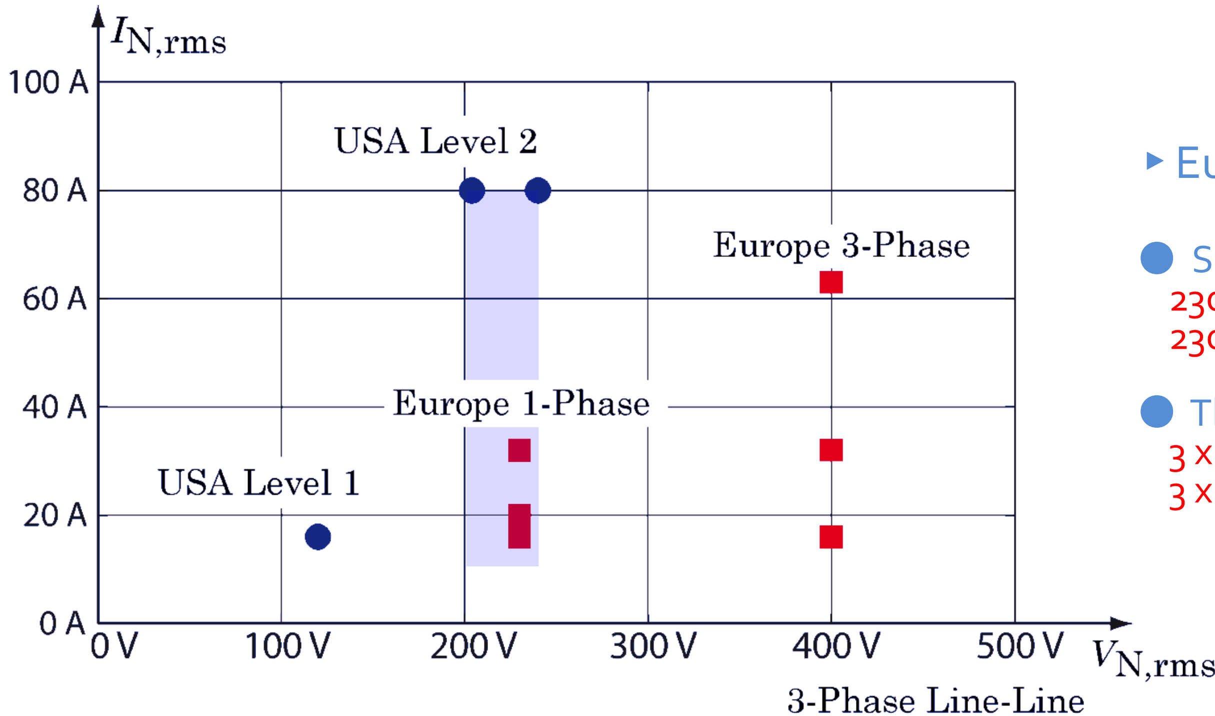

- Europe On-Board Charger:
  - Single-Phase AC Connection
    230 VAC, 16 / 32 A → 3.68 / 7.4 kW
    230 VAC, 20 A → 4.6 kW
  - Three-Phase AC Connection
    3 x 400 VAC, 16 / 32 A → 11 / 22 kW
    3 x 400 VAC, 63 A → 44 kW

Power Electronics for EV Charging Systems

Basic Requirements

- Wide Voltage Range – Voltage Adaption
- Output Current Control
- Mains Sinusoidal Current Shaping
- Isolation of Mains and Battery (?)

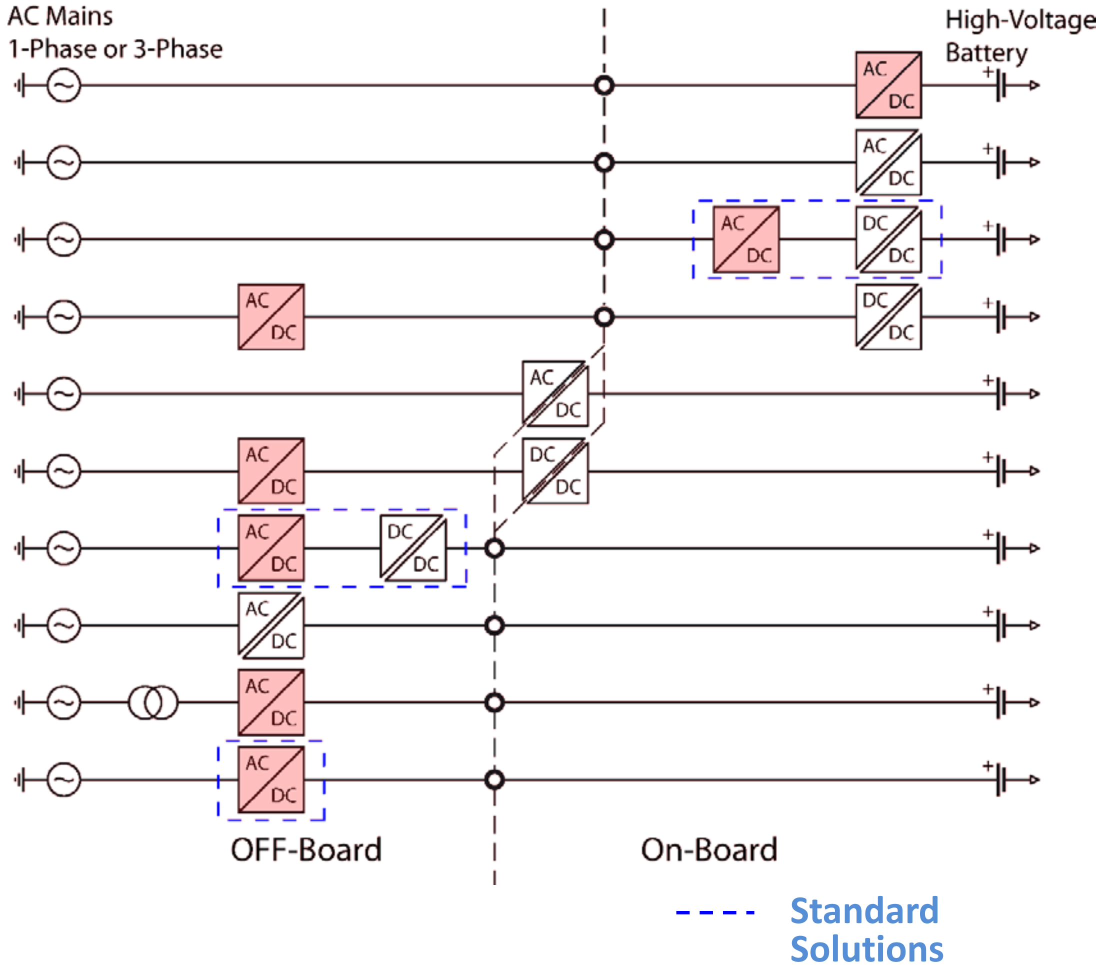

Basic Topologies

- Non-Isolated

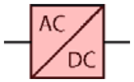

- Isolated Single-Stage

- Non- or Isolated Two-Stage

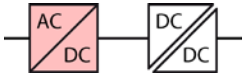

INEP

Power Electronics for EV Charging Systems

Basic Requirements

- Wide Voltage Range – Voltage Adaption
- Output Current Control
- Mains Sinusoidal Current Shaping
- Isolation of Mains and Battery (?)

Basic Topologies

- Non-Isolated

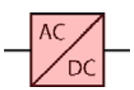

- Isolated Single-Stage

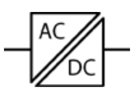

- Non- or Isolated Two-Stage

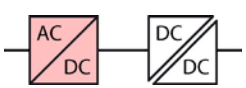

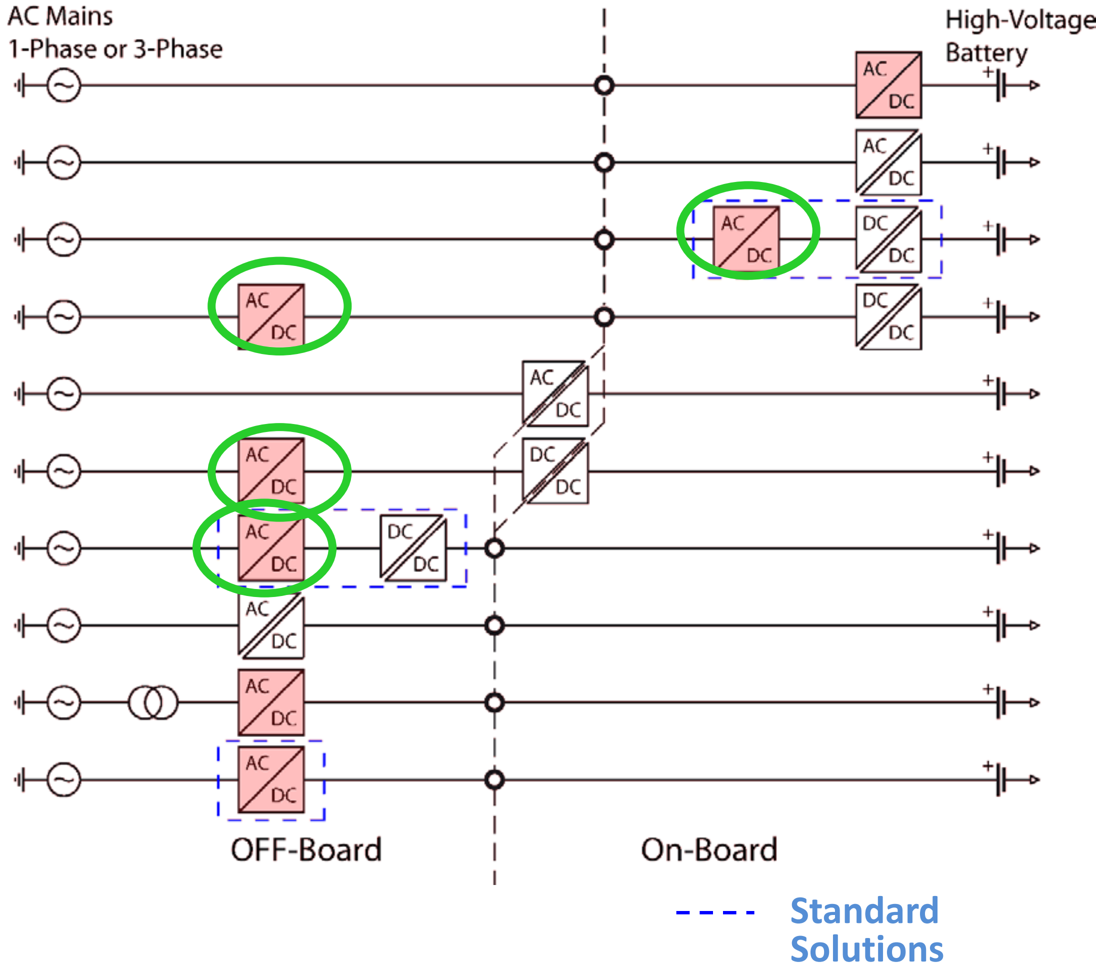

VSRs

VSR

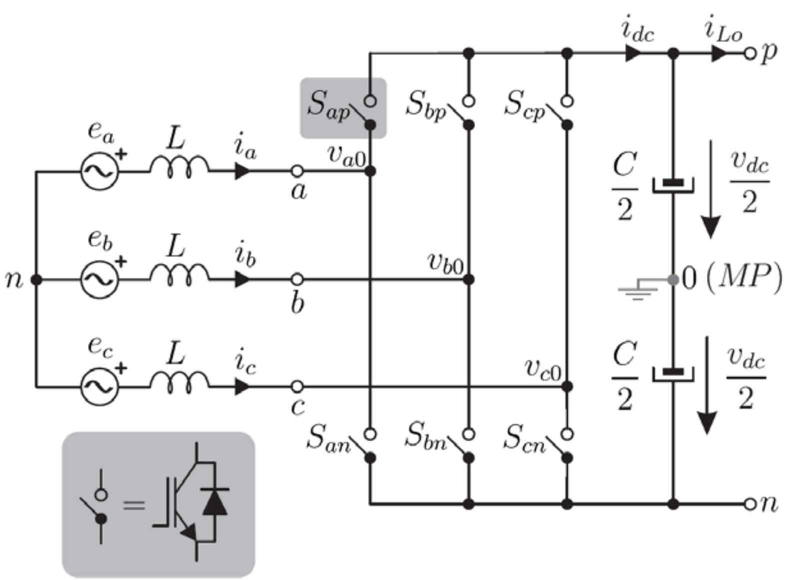

Delta-Switch VSR

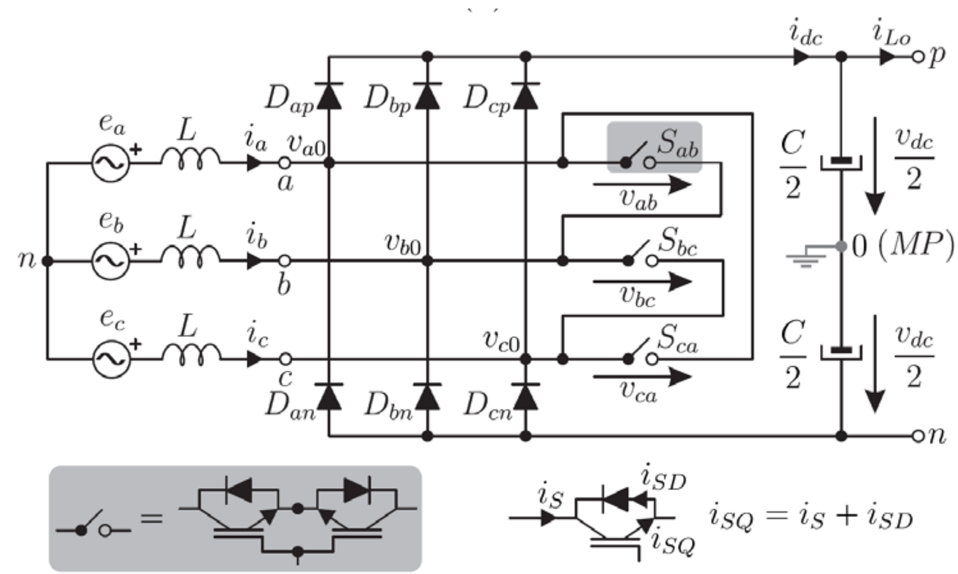

Topology

- This topology was proposed and firstly operated in:

[6] J. W. Kolar, H. Ertl, and F. C. Zach, "Realization considerations for unidirectional three-phase pwm rectifier system with low effects on the mains," in *6th Conf. Power Electron. and Motion Control (PEMC)*, Budapest, Hungary, 1990.

[7] R.-J. Tu and C.-L. Chen, "A new space-vector-modulated control for a unidirectional three-phase switch-mode rectifier," *IEEE Trans. Ind. Electron.*, vol. 45, no. 2, pp. 256–262, 1998.

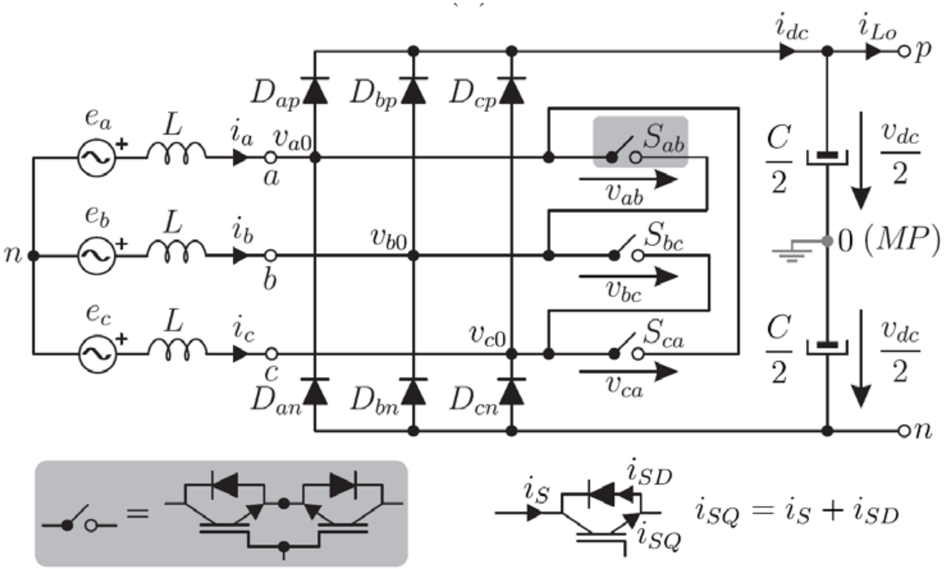

Capabilities

- Reference [1] cites it as the most well suited rectifier for industrial applications where a 2-level boost type 3-phase rectifier is required

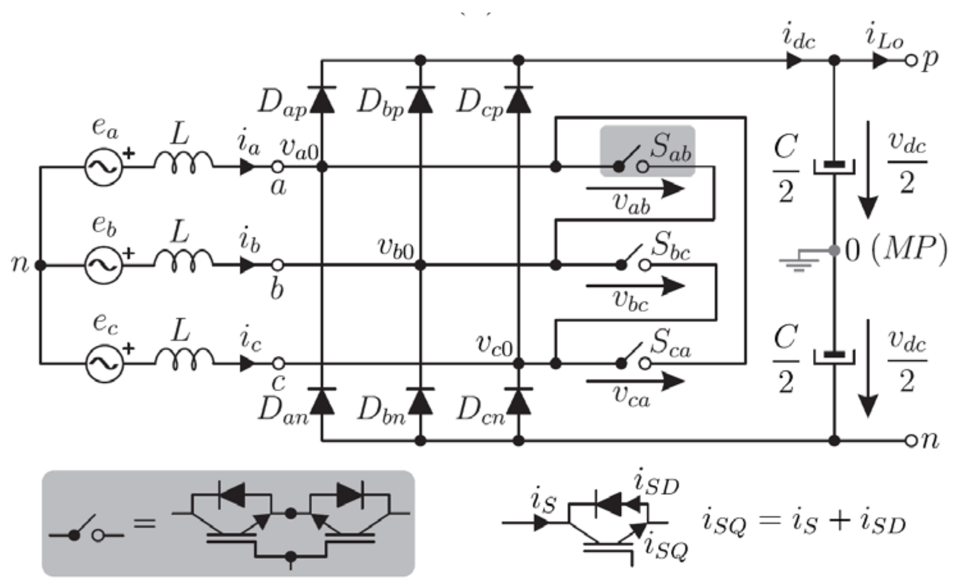

[1] J. W. Kolar and T. Friedli, "The essence of three-phase pfc rectifier systems - part i," *IEEE Trans. Power Electron.*, vol. 28, no. 1, pp. 176–198, 2013.

Applications

- [3-4] WECS applications
- [5] Aircraft application of the Delta-Switch Rectifier

[3] S. K. T. Miller and J. Sun, “Comparative study of three-phase pwm rectifiers for wind energy conversion,” in *21th Annu. IEEE Applied Power Electron. Conf. and Expo. (APEC)*, Dallas, TX, 2006, pp. 937–943.

[4] D. A. F. Collier, V. Maryama, and M. L. Heldwein, “Low conduction losses pwm rectifier for high efficiency wind power micro-generation,” in *Proc. of the Int. Exhibition Conf. Power Electron., Intelligent Motion and Power Quality (PCIM-Asia)*, Shanghai, China, 2011.

[5] M. Hartmann, J. Miniboeck, H. Ertl, and J. W. Kolar, “A three-phase delta switch rectifier for use in modern aircraft,” *IEEE Trans. Ind. Electron.*, vol. PP, no. 99, p. 1, 2011.

Space vectors

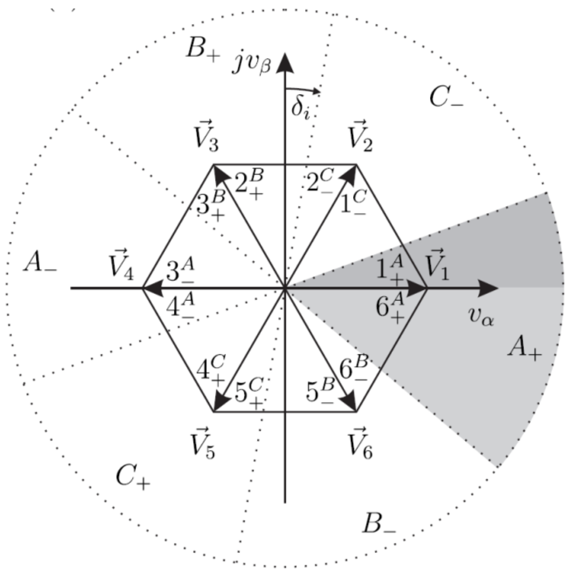

$$\pm\pi/6$$

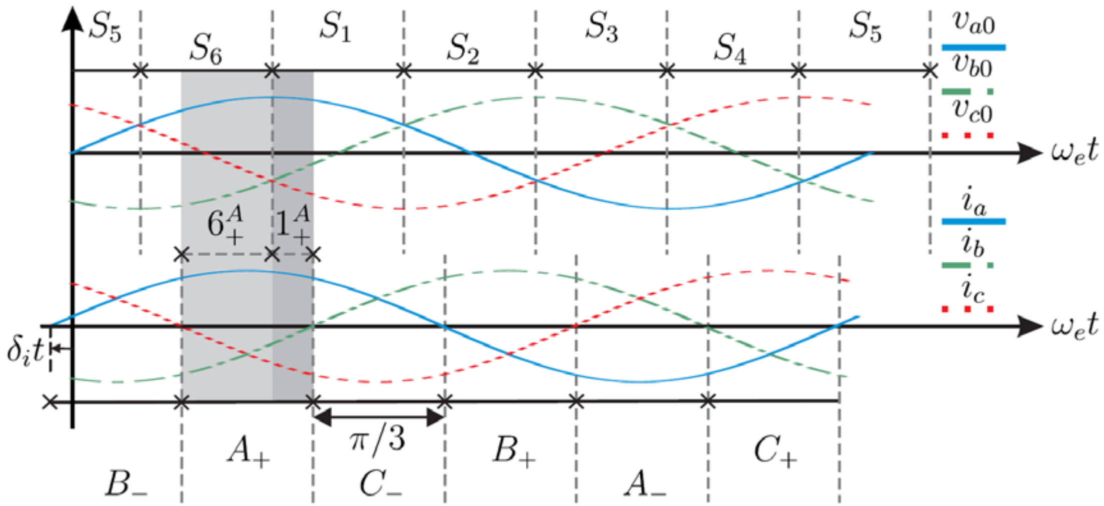

Modulation Strategies

- [5] SVM I: minimizes switching actions
- [4] SVM II: minimizes conduction losses

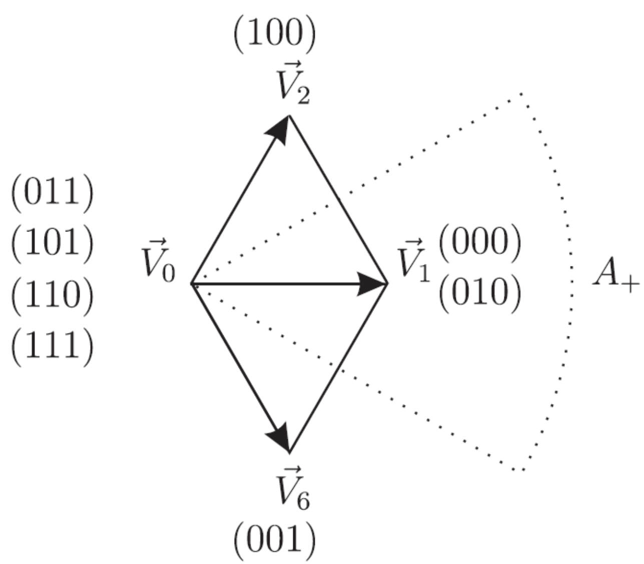

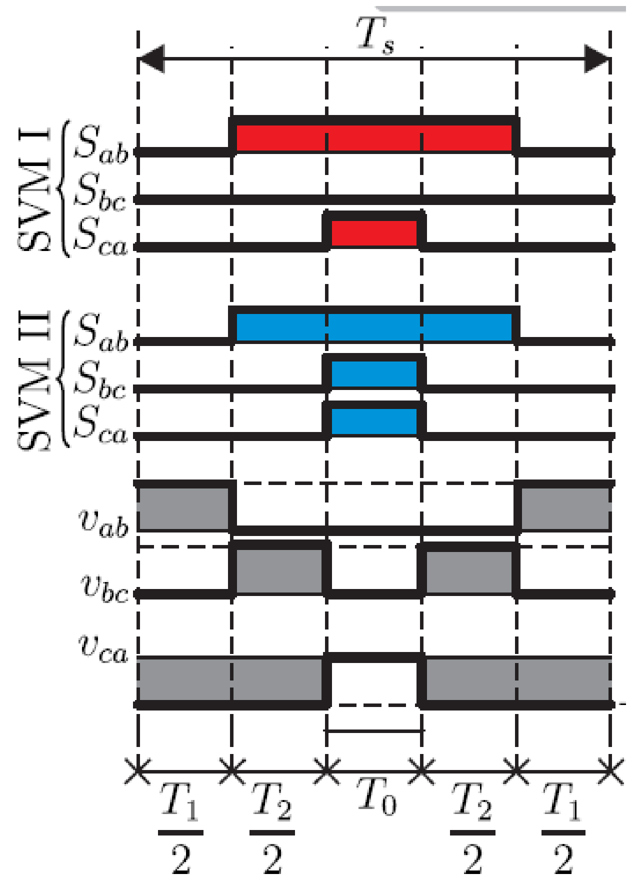

[4] D. A. F. Collier, V. Maryama, and M. L. Heldwein, "Low conduction losses pwm rectifier for high efficiency wind power micro-generation," in *Proc. of the Int. Exhibition Conf. Power Electron., Intelligent Motion and Power Quality (PCIM-Asia)*, Shanghai, China, 2011.

[5] M. Hartmann, J. Miniboeck, H. Ertl, and J. W. Kolar, "A three-phase delta switch rectifier for use in modern aircraft," *IEEE Trans. Ind. Electron.*, vol. PP, no. 99, p. 1, 2011.

Suboptimal Modulation Strategies

- Derived from the optimal strategies and application dependent
- Avoid current sector identification as in [11]

[11] S. K. T. Miller, "Analysis of three-phase rectifiers with ac-side switches and interleaved three-phase voltage-source converters," Ph.D. dissertation, Faculty of Rensselaer Polytechnic Institute, Troy, NY, 2008.

- Improved THD
- Increased losses

Suboptimal Modulation Strategies

- Derived from the optimal strategies and application dependent
- Avoid current sector identification as in [11]

[11] S. K. T. Miller, "Analysis of three-phase rectifiers with ac-side switches and interleaved three-phase voltage-source converters," Ph.D. dissertation, Faculty of Rensselaer Polytechnic Institute, Troy, NY, 2008.

- Improved THD
- Increased losses, **but, hopefully, not too much!**

Novel Suboptimal Modulation Strategies

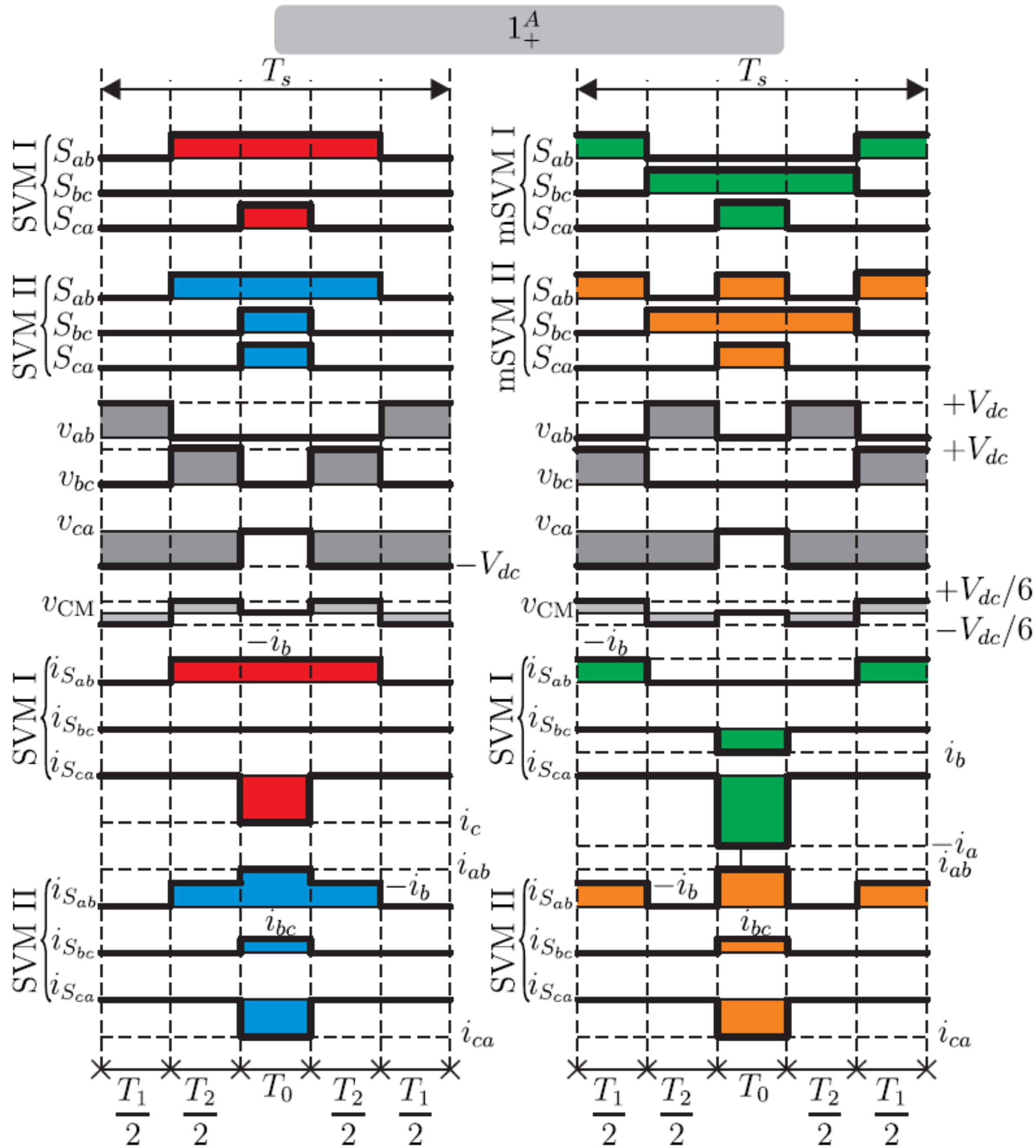

Novel Suboptimal Modulation Strategies

1_{-}^{C}

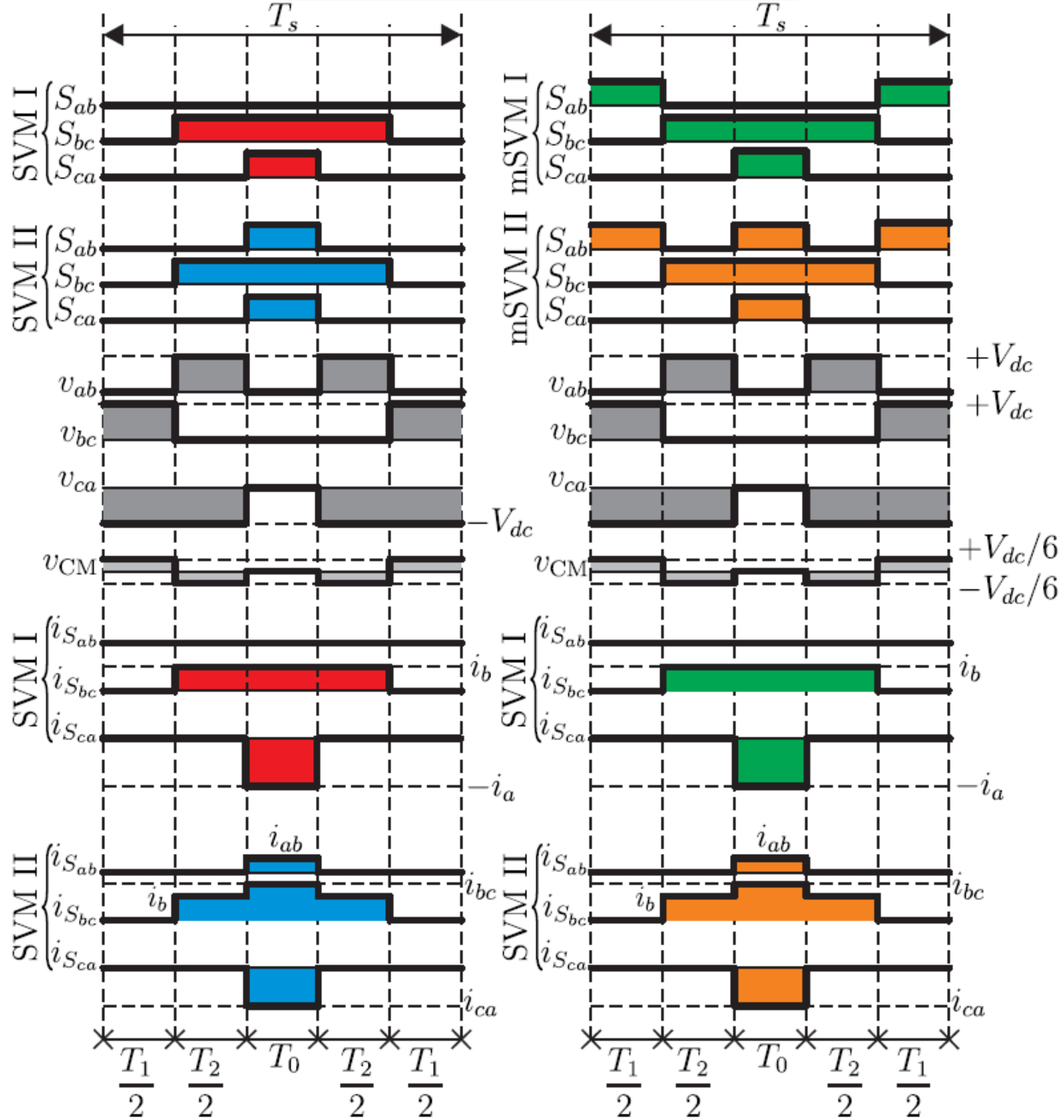

INEP

Carrier-Based Delta-Switch Rectifier Modulation

- Implementation:

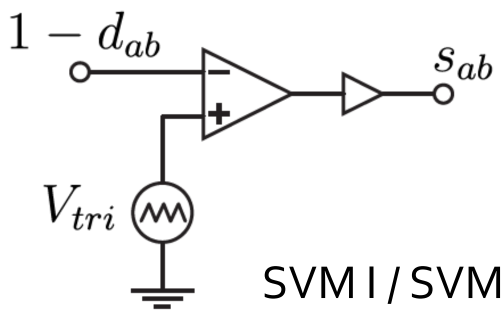

SVM I / SVM II

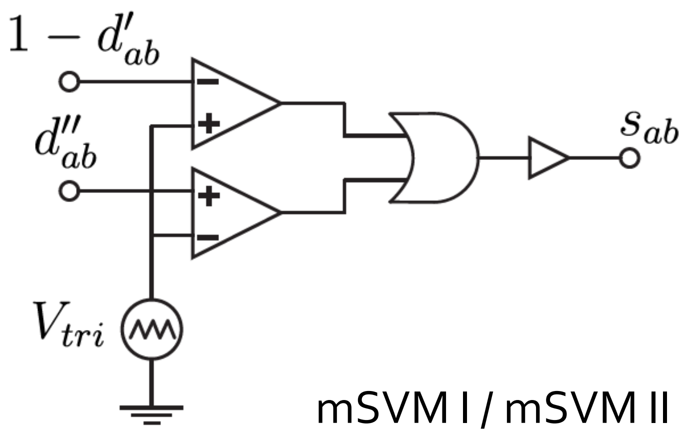

mSVM I / mSVM II

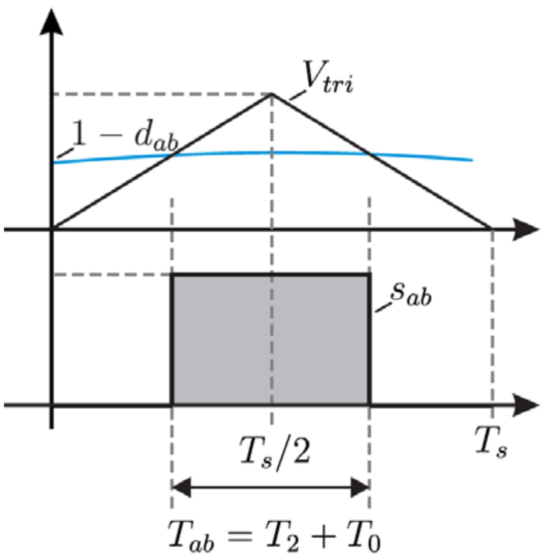

Carrier-Based Delta-Switch Rectifier Modulation

- Implementation:

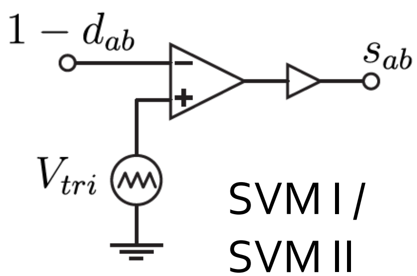

SVM I / SVM II

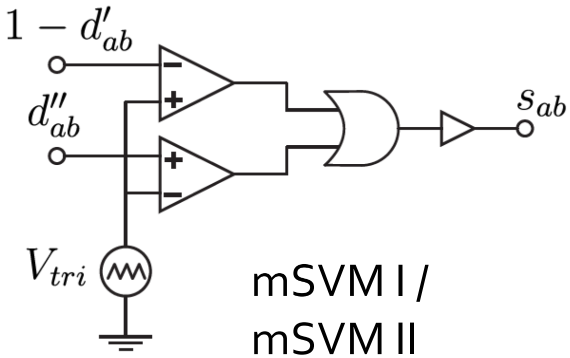

mSVM I / mSVM II

DUTY-CYCLE FUNCTIONS FOR MSVM I AND MSVM II

Voltage Sector	d	Duty-cycle Functions		
		d_{ab}	d_{bc}	d_{ca}
S_1	d'	$0 \vert d'_{ca}$	$1-2\gamma d_\beta$	$1-\kappa d_\alpha-\gamma d_\beta$
	d''	$2\gamma d_\beta$	0	0
S_2	d'	$1+\kappa d_\alpha-\gamma d_\beta$	$1-2\gamma d_\beta$	$0 \vert d'_{bc}$
	d''	0	0	$-\kappa d_\alpha+\gamma d_\beta$
S_3	d'	$1+\kappa d_\alpha-\gamma d_\beta$	$0 \vert d'_{ab}$	$1+\kappa d_\alpha+\gamma d_\beta$
	d''	0	$-\kappa d_\alpha-\gamma d_\beta$	0
S_4	d'	$0 \vert d'_{ca}$	$1+2\gamma d_\beta$	$1+\kappa d_\alpha+\gamma d_\beta$
	d''	$-2\gamma d_\beta$	0	0
S_5	d'	$1-\kappa d_\alpha+\gamma d_\beta$	$1+2\gamma d_\beta$	$0 \vert d'_{bc}$
	d''	0	0	$\kappa d_\alpha-\gamma d_\beta$
S_6	d'	$1-\kappa d_\alpha+\gamma d_\beta$	$0 \vert d'_{ab}$	$1-\kappa d_\alpha-\gamma d_\beta$
	d''	0	$\kappa d_\alpha+\gamma d_\beta$	0

Carrier-Based Delta-Switch Rectifier Modulation

- M=0.75
- δ_i=0

SVM I & SVM II

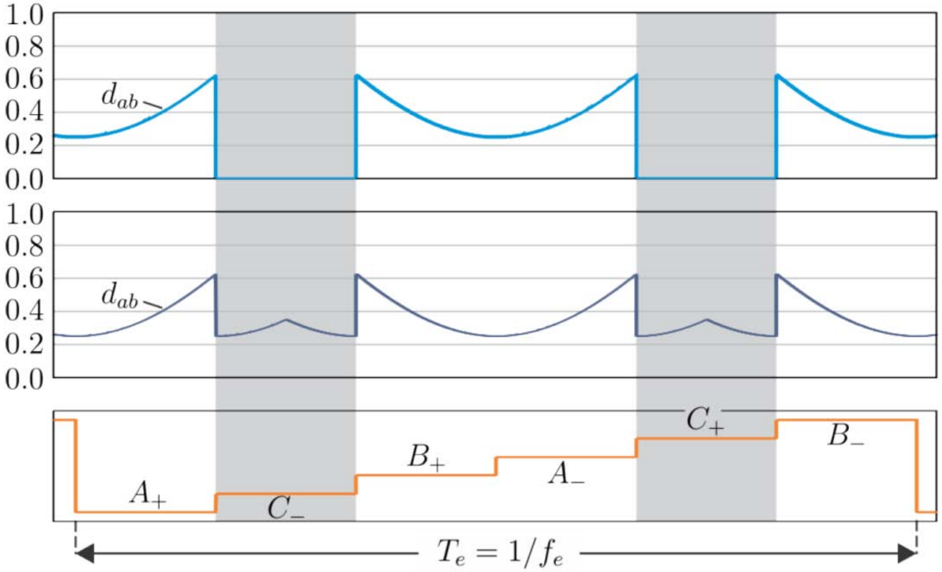

mSVM I & mSVM II

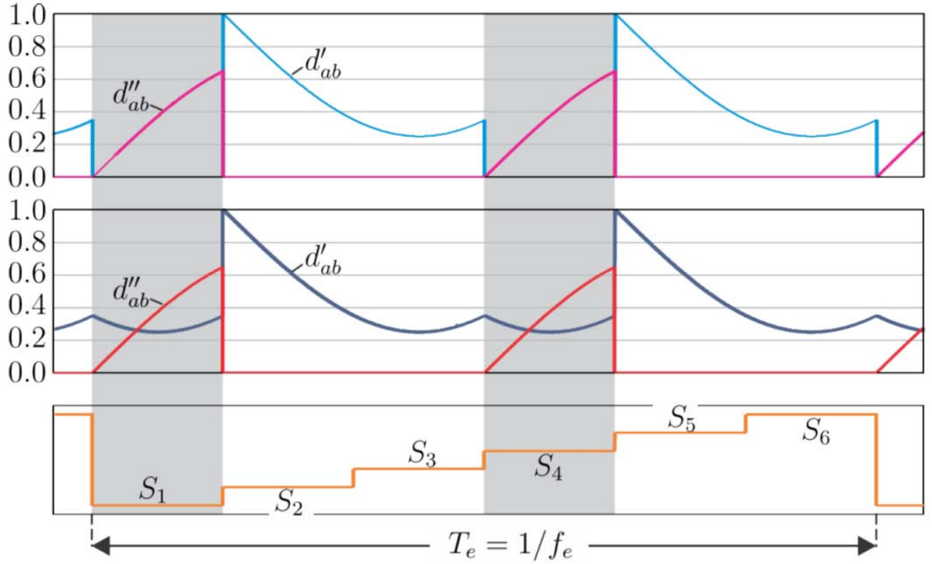

Carrier-Based Delta-Switch Rectifier Modulation

- Analytical losses calculation

DUTY-CYCLE FUNCTIONS FOR SVM I AND SVM II

Current Sector	Duty-cycle Functions		
	d_{ab}	d_{bc}	d_{ca}
A_+	$1-\kappa d_\alpha+\gamma d_\beta$	$0\vert\min(d_{ab},d_{ca})$	$1-\kappa d_\alpha-\gamma d_\beta$
C_-	$0\vert\min(d_{bc},d_{ca})$	$1-2\gamma d_\beta$	$1-\kappa d_\alpha-\gamma d_\beta$
B_+	$1+\kappa d_\alpha-\gamma d_\beta$	$1-2\gamma d_\beta$	$0\vert\min(d_{ab},d_{bc})$

$\kappa = 3/2$

$\gamma = \sqrt{3}/2$

INEP

Delta-Switch Rectifier Currents

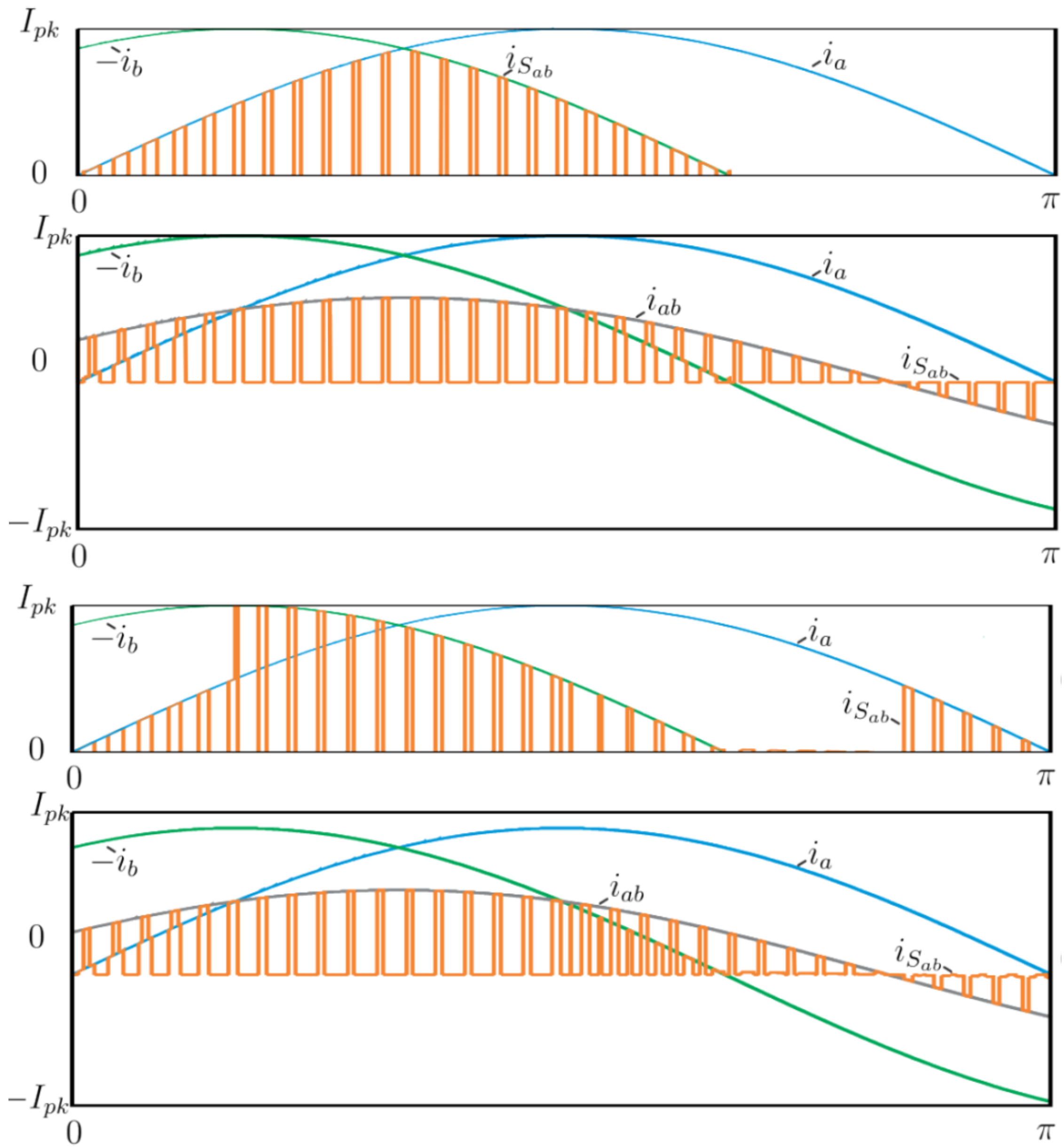

SVM I

SVM II

mSVM I

mSVM II

Delta-Switch Rectifier Current Efforts

- Current efforts

	$I_{D,avg}$	$I_{pk}\frac{M}{2\sqrt{3}}\cos(\delta_i)$	(5)
	$I_{D,rms}$	$I_{pk}\sqrt{\frac{M}{12\pi}\left[3+2\cos(2\delta_i)+2\sqrt{3}\cos(\delta_i)\right]}$	(6)
SVM I	$I_{SQ,avg}$	$I_{pk}\left[\frac{1}{2\pi}-\frac{M}{4\sqrt{3}}\cos(\delta_i)\right]$	(7)
	$I_{SQ,rms}$	$I_{pk}\sqrt{\frac{1}{6}-\frac{\sqrt{3}}{8\pi}-\frac{M}{2\pi\sqrt{3}}\cos(\delta_i)}$	(8)

Delta-Switch Rectifier Current Efforts

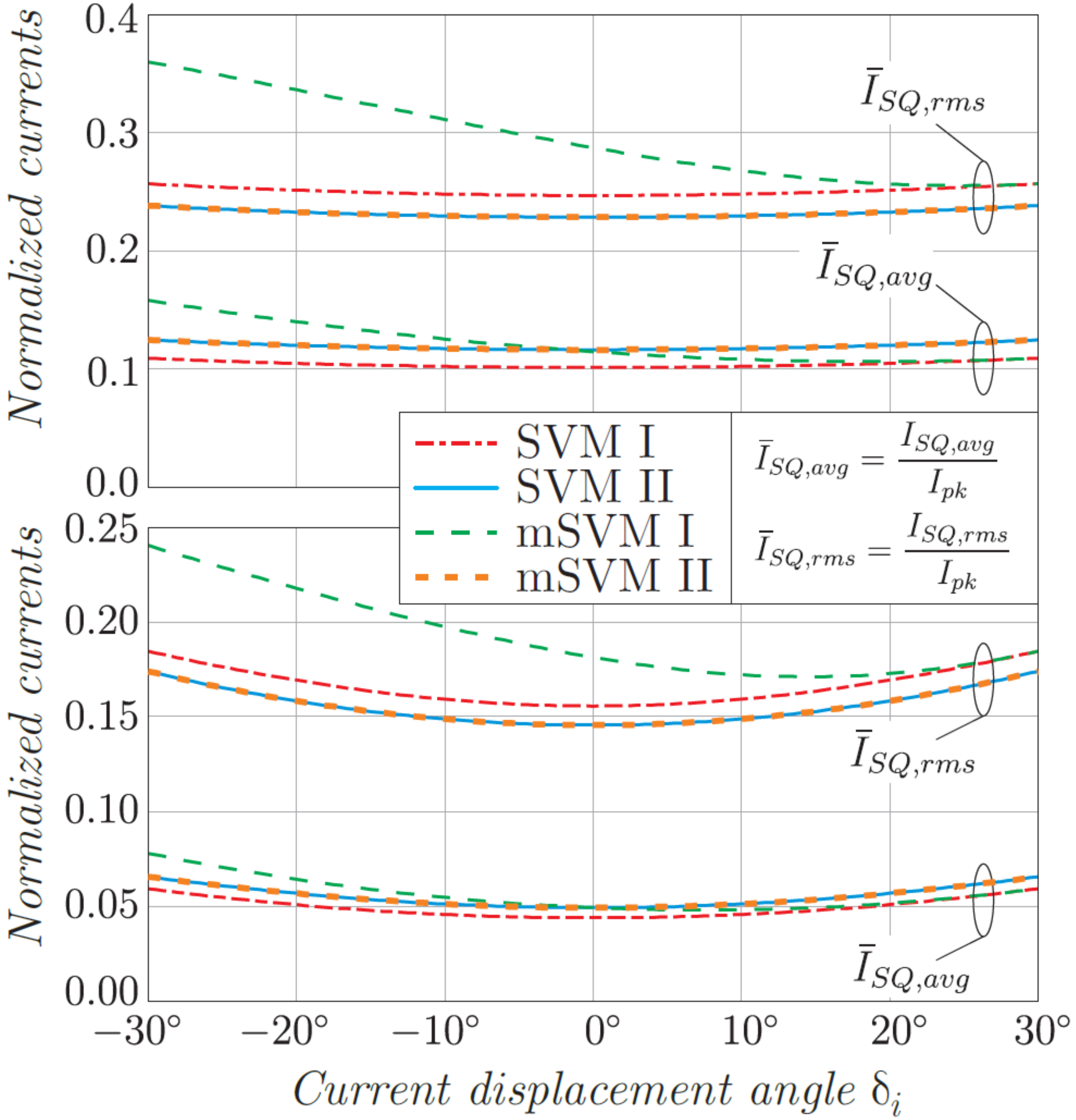

M = 0.4

M = 0.8

Experimental Results

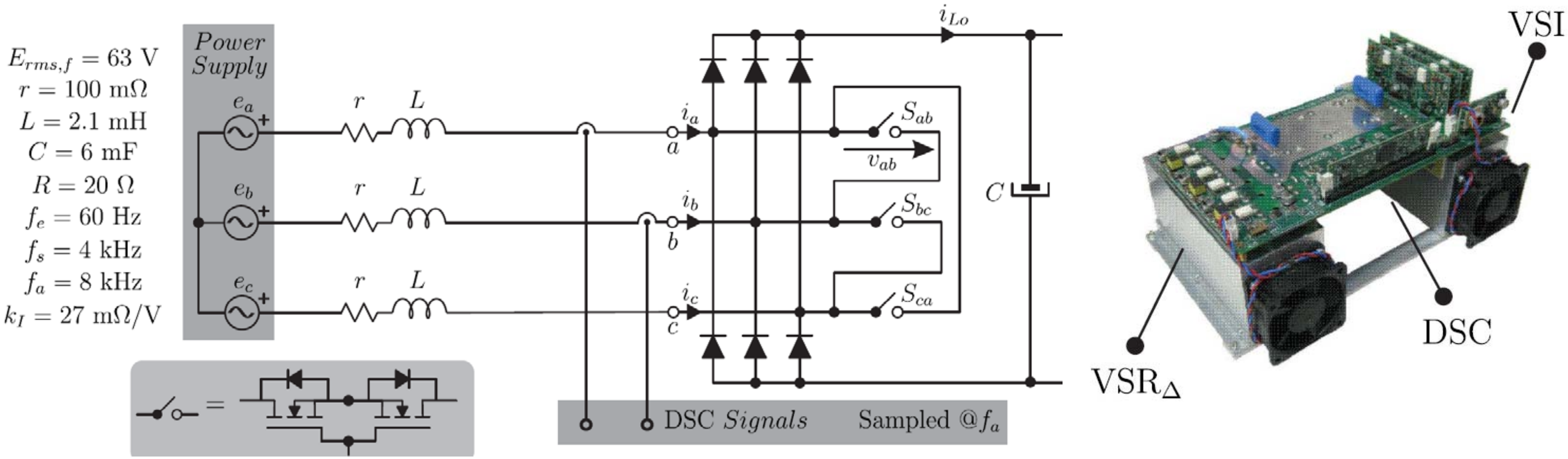

- Employed current control strategy (equivalent to ZADC) in [16]

[16] D. A. F. Collier, M. S. Ortmann, and M. L. Heldwein, "Current self-control applied to sensorless permanent magnet synchronous generators," in *Proc. of the XXth Int. Conf. Electrical Machines (ICEM)*, Marseille, France, 2012.

Experimental Results

SVM I – Current THD 3.16 %

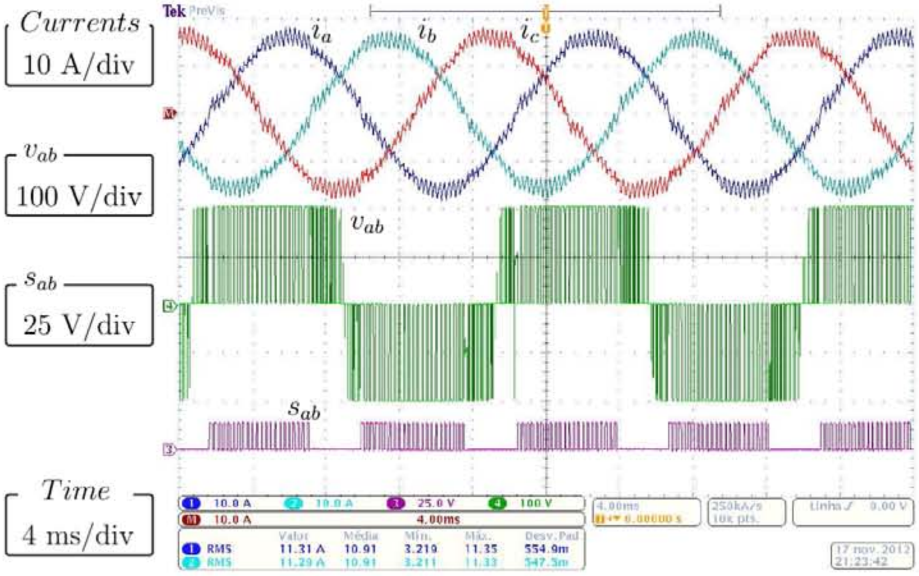

(a)

SVM II – Current THD 3.23 %

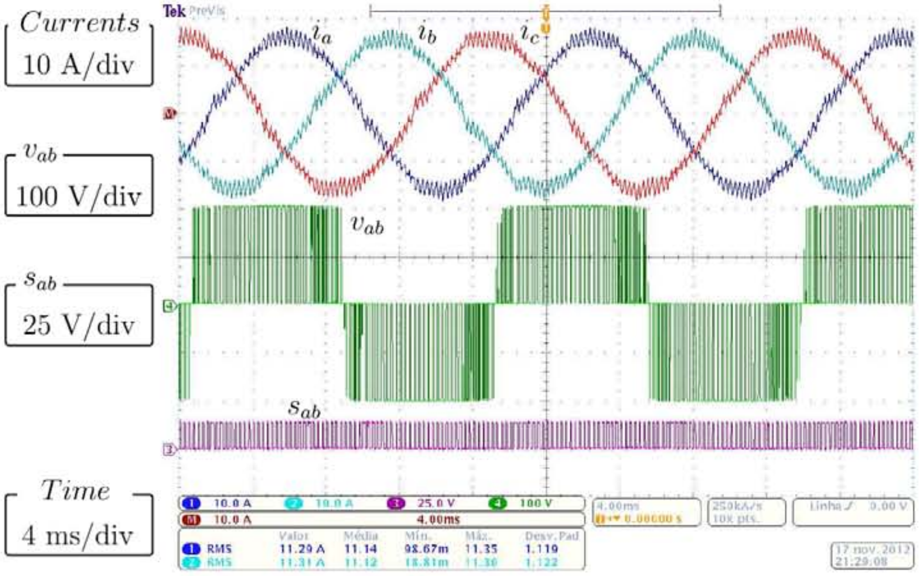

(b)

Experimental Results

mSVM I – Current THD 3.84 %

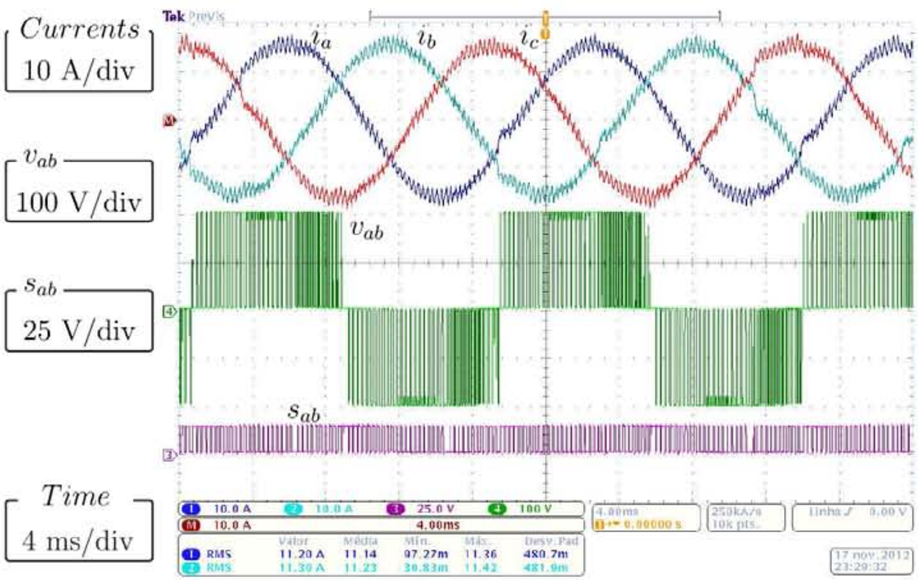

(c)

mSVM II – Current THD 1.54 %

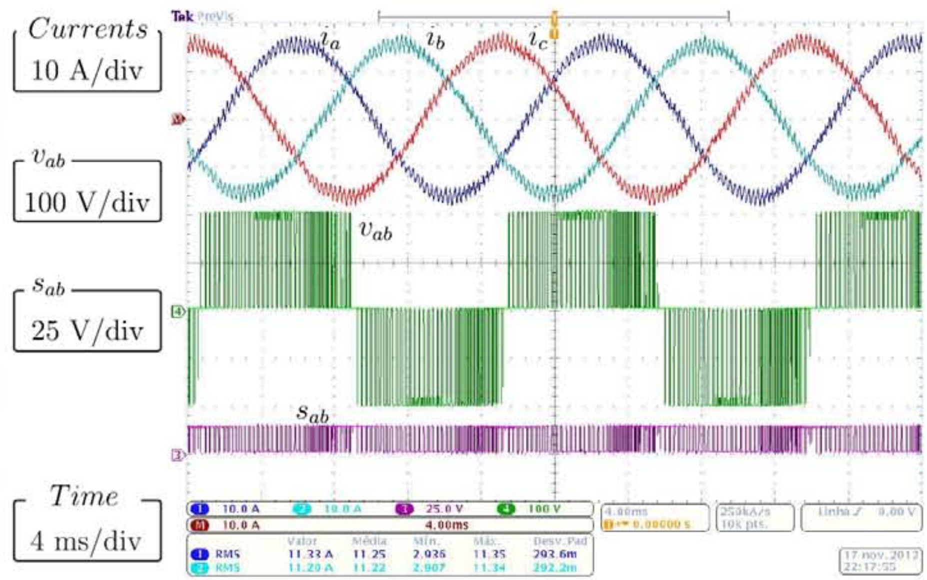

(d)

Experimental Results

- Results @ 200 V (dc) / 2 kW

THD AND RMS MEASUREMENTS

Measurement	SVM I	SVM II	mSVM I	mSVM II
$I_{a,\mathrm{rms}}$	11.39 A	11.35 A	11.28 A	11.34 A
THD_{i_a}	3.16 %	3.23 %	3.84 %	1.54 %
$V_{ab,\mathrm{rms}}$	106.26 V	106.42 V	106.36 V	105.95 V
$\mathrm{THD}_{v_{ab}}$	7.50 %	8.23 %	9.10 %	3.31 %

Multi-state switching cells based 3-phase rectifiers

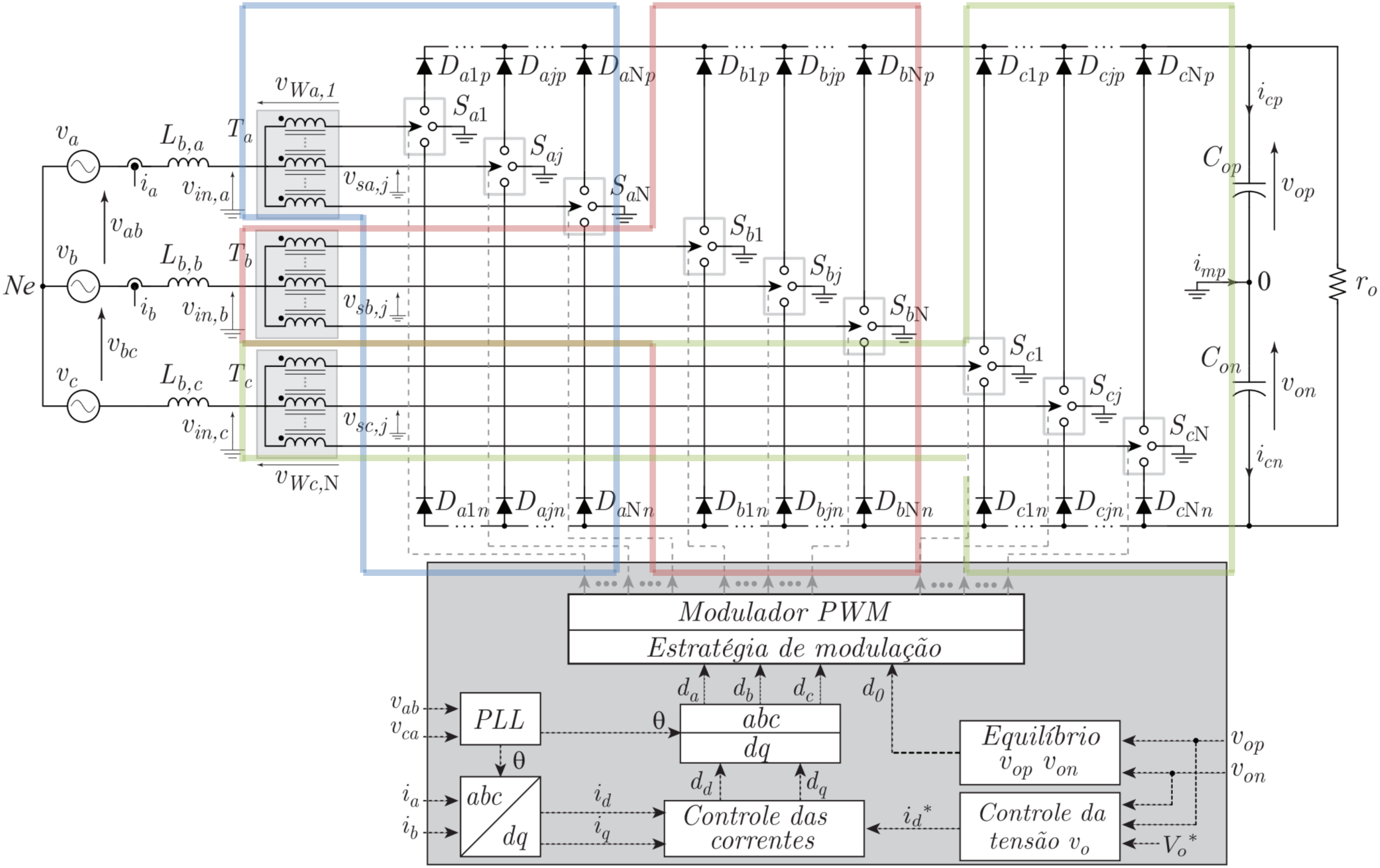

MLMSR

- Space vector analysis
  - Leg voltage:

$$v_{in,k} = \mathrm{sign}(i_k)\,\frac{V_o}{2}\left(1 - \frac{1}{N}\sum_{j=1}^{N} s_{kj}\right)$$

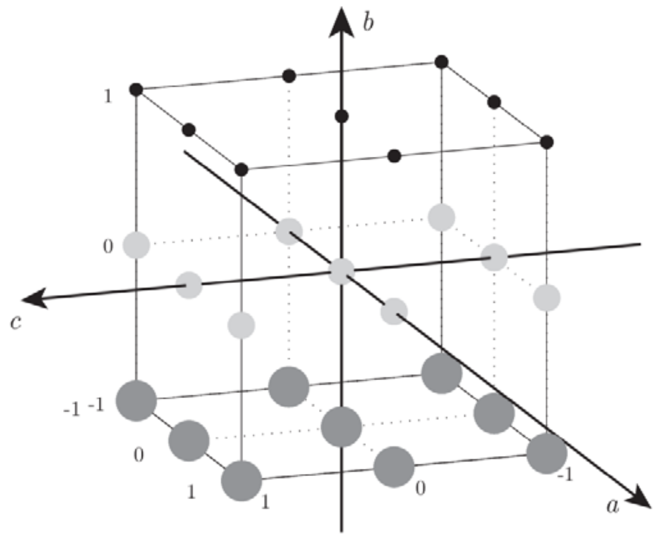

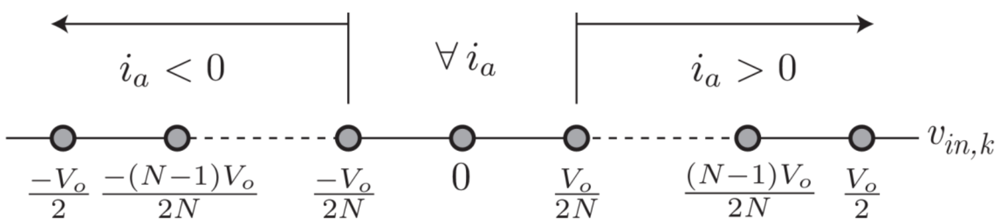

$\mathbb{R}^3 \rightarrow \mathbb{R}^2$

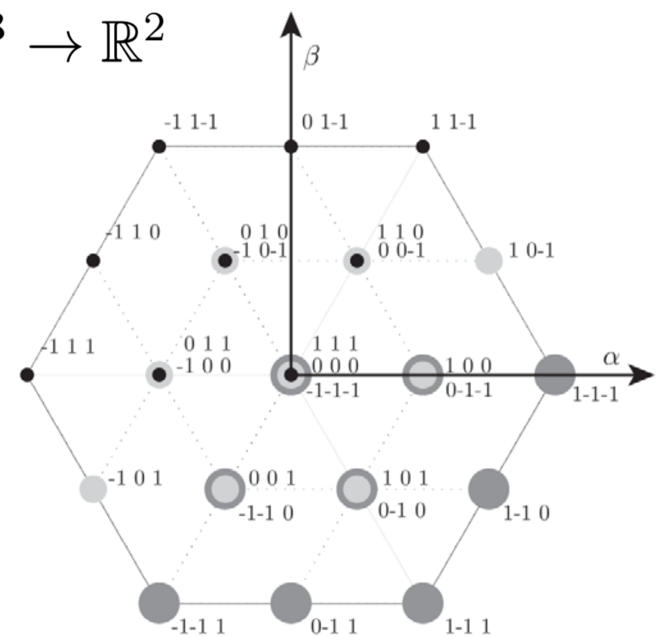

MLMSR

- N=4, 217 vectors in αβ;

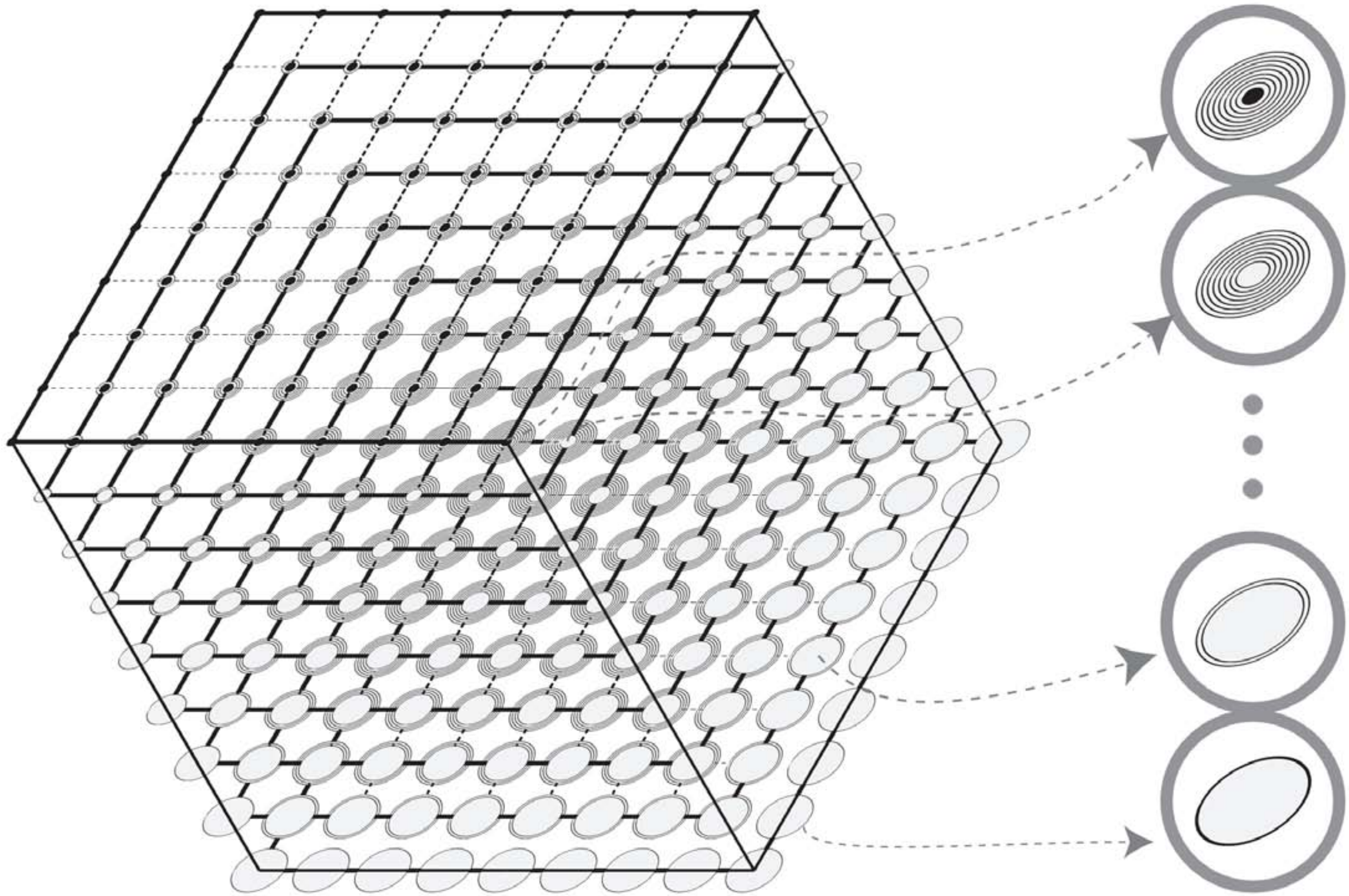

MLMSR

- Input voltages space
  - Current direction enforces restrictions
    - 8 unit sub-cubes

- Example for: $i_a > 0,\ i_b < 0 \text{ e } i_c < 0$

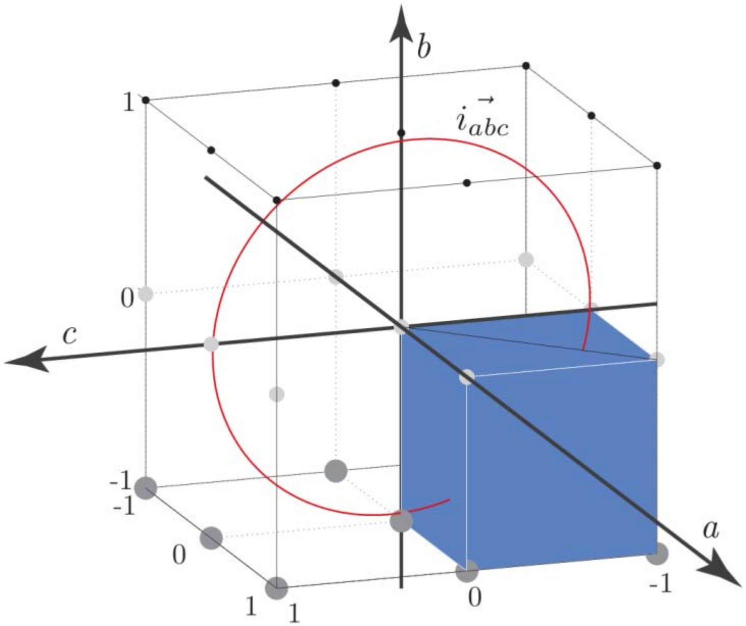

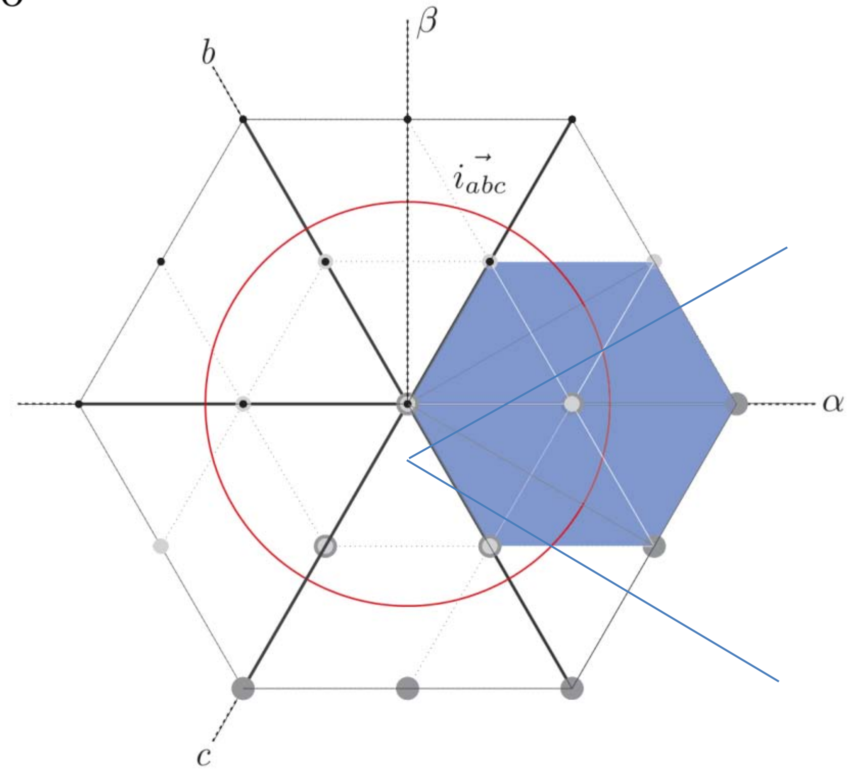

Control oriented models

- Current control:

$$\vec{v}_{abc} = \mathbf{L} \cdot \frac{d}{dt}\vec{i}_{abc} + \vec{v}_{in,abc} - \vec{v}_{Ne,0}$$

$$\begin{cases} L_b \frac{d}{dt} i_d = \sqrt{\frac{2}{3}}\hat{V}_g - \frac{V_o}{2} m_{d,x} + L_b \omega_g i_q \\ L_b \frac{d}{dt} i_q = \frac{V_o}{2} m_{q,x} - L_b \omega_g i_d \\ \frac{V_o}{2} m_{0,x} = -\sqrt{3} v_{Ne,0} \end{cases}$$

- Output voltage control:

$$v_d i_d = \frac{1}{2} C_o \frac{d{v_o}^2}{dt} + \frac{{v_o}^2}{R_o}$$

$$G_{vo}(s) = \frac{\tilde{v}_o}{\tilde{i}_d} = \frac{V_d}{2V_o} \frac{R_o}{s\frac{R_o C_o}{2} + 1}$$

- Partial dc-link voltage balance control:

$$\langle i_{mp} \rangle = -m_{0,\delta v} \left[|i_a| + |i_b| + |i_c| \right]$$

$$\frac{\delta_{vmp}}{m_{0,\delta v}} = -\frac{3\hat{I}_{in}}{sC_{opn}\pi}$$

MLMSR Control strategy

- Similar to 2-level VSR control
- Zero-axis signal controls the dc-offset to balance the dc-link

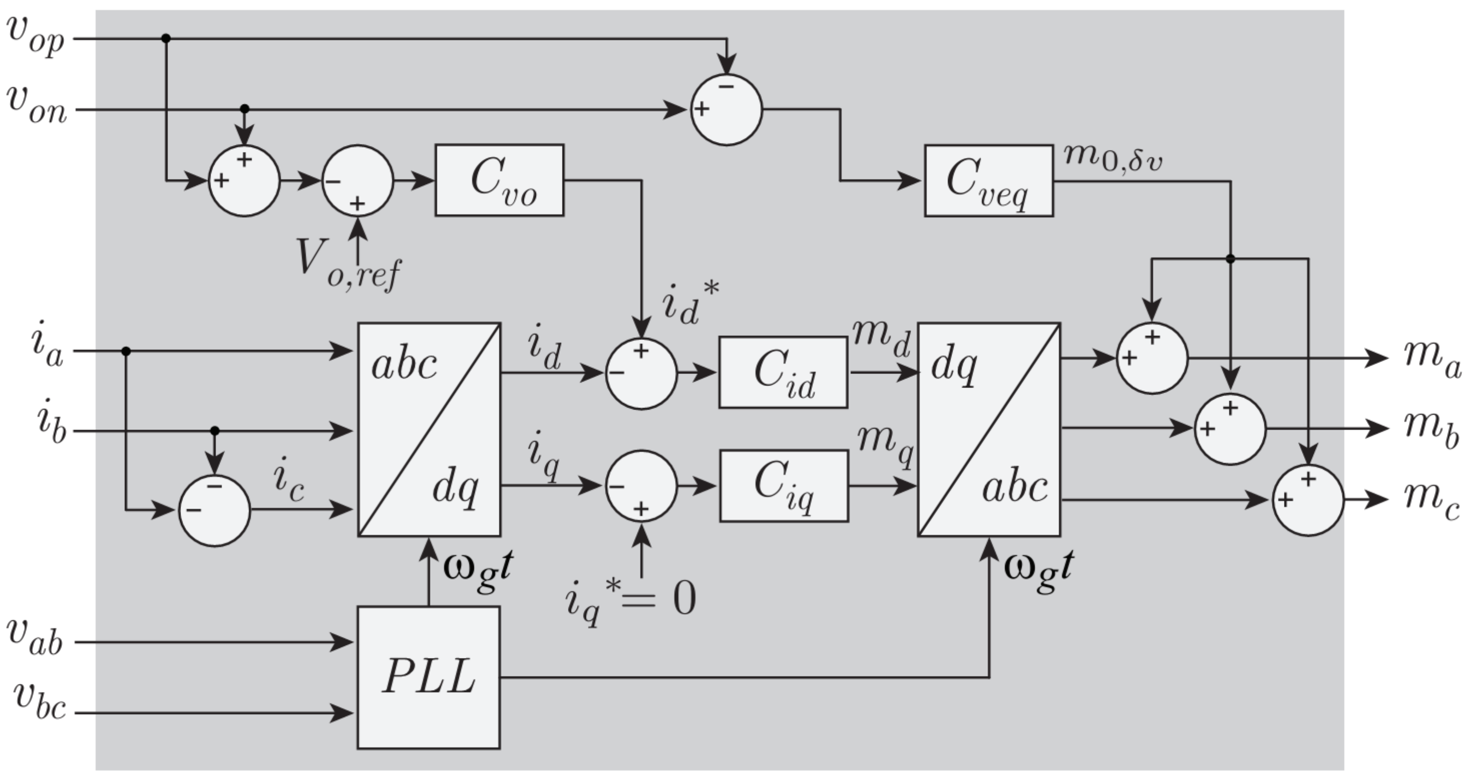

MLMSR modulation

- Space vector
  - Highly flexible
  - Computacionally demanding
  - Freedom: redundancies

- Carrier based
  - Simple
  - Near SVM perfomance is possible
  - Freedom: zero-axis signal

M. S. Ortmann, S. A. Mussa, e M. L. Heldwein, Evaluation of carrier-based PWM strategies for multi-state switching cells-based multilevel three-phase rectifiers, em 2011 Brazilian Power Electro-nics Conference (COBEP), pp. 903-910.

MLMSR carrier-based modulation

$$\begin{cases} m_a = M\text{sen}\left(\omega_g t\right) \\ m_b = M\text{sen}\left(\omega_g t - \frac{2\pi}{3}\right) \\ m_c = M\text{sen}\left(\omega_g t + \frac{2\pi}{3}\right) \end{cases}$$

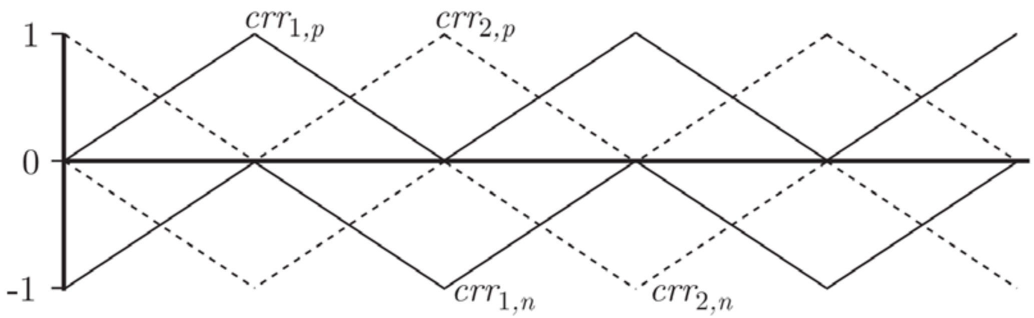

N=2

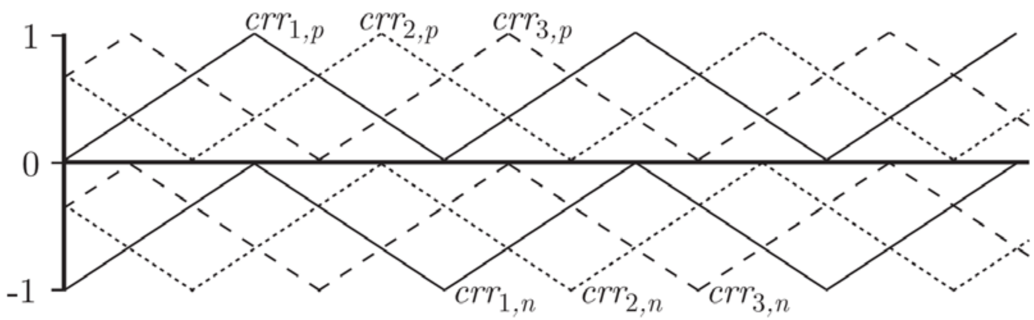

N=3

MLMSR carrier-based modulation

- SPWM
  - Simpler
  - $M \leq 1{,}15$
  - z = 0

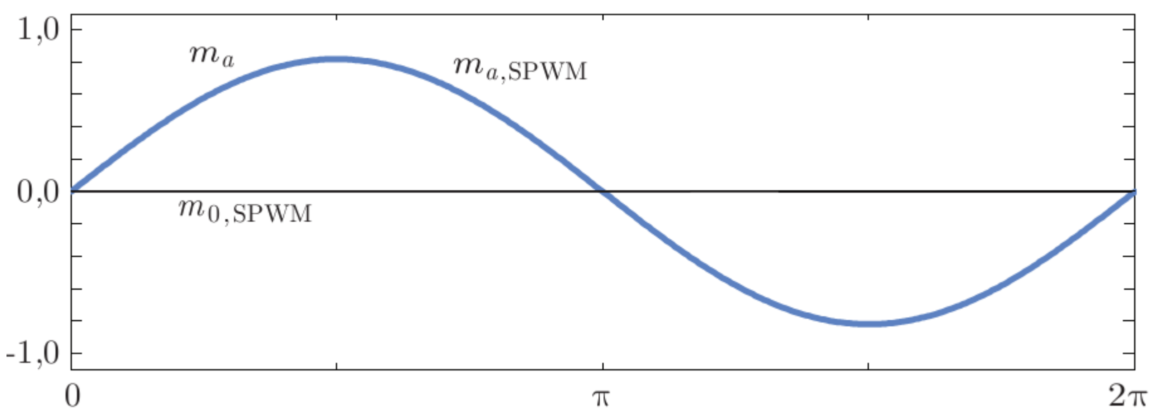

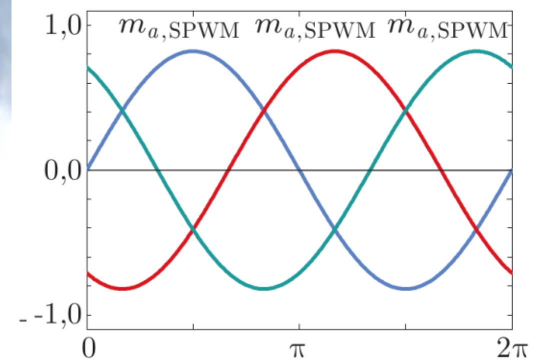

(a)

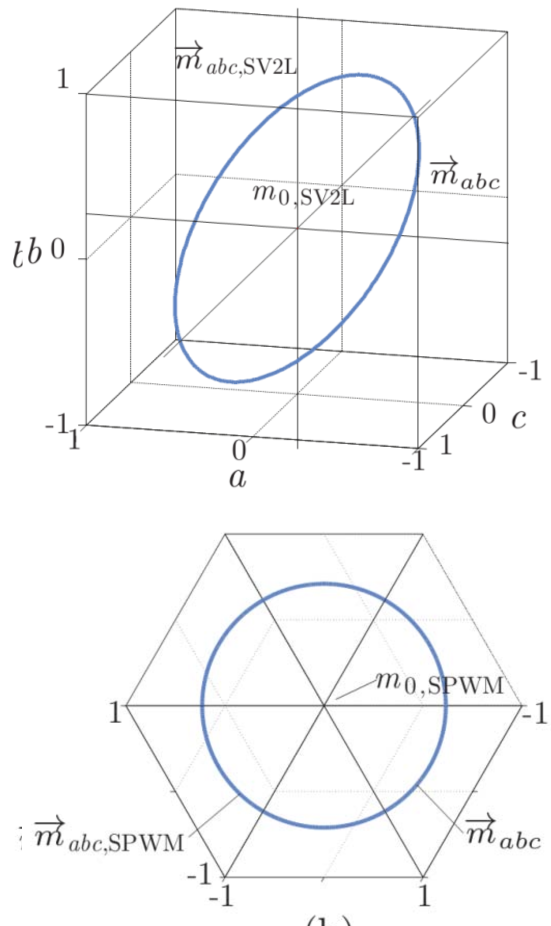

(b)

MLMSR carrier-based modulation

- SV2L
  - 2-level SVM equivalent
  - $M \leq 1{,}15$

$$m_{0,\mathrm{SV2L}} = -\tfrac{1}{2}\left[\max\left(m_a, m_b, m_c\right) - \min\left(m_a, m_b, m_c\right)\right]$$

$$m_{k,\mathrm{SV2L}} = m_k + m_{0,\mathrm{SV2L}}$$

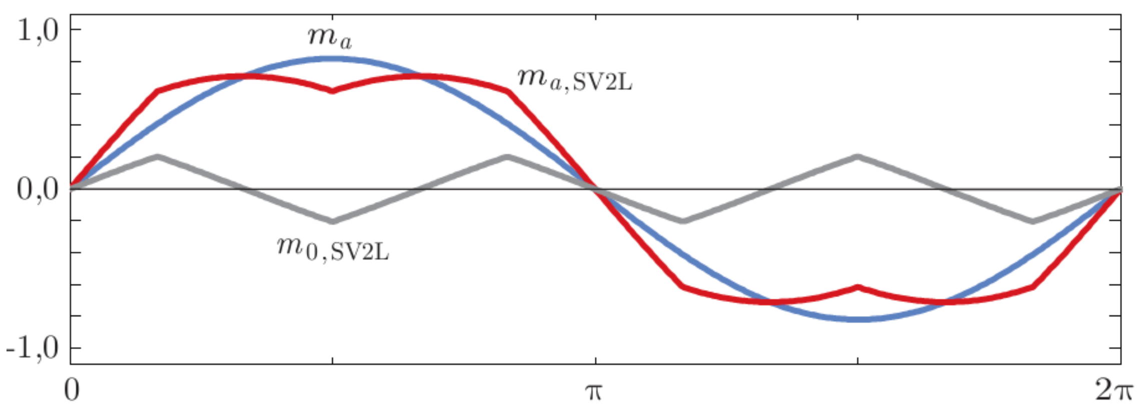

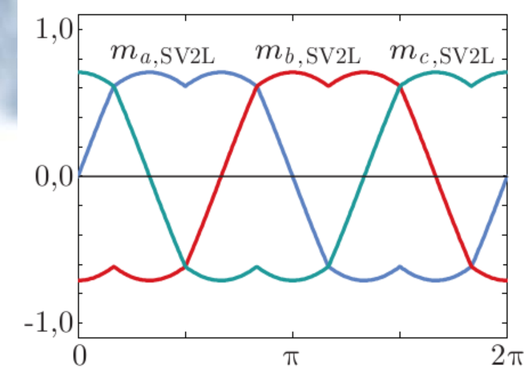

(a)

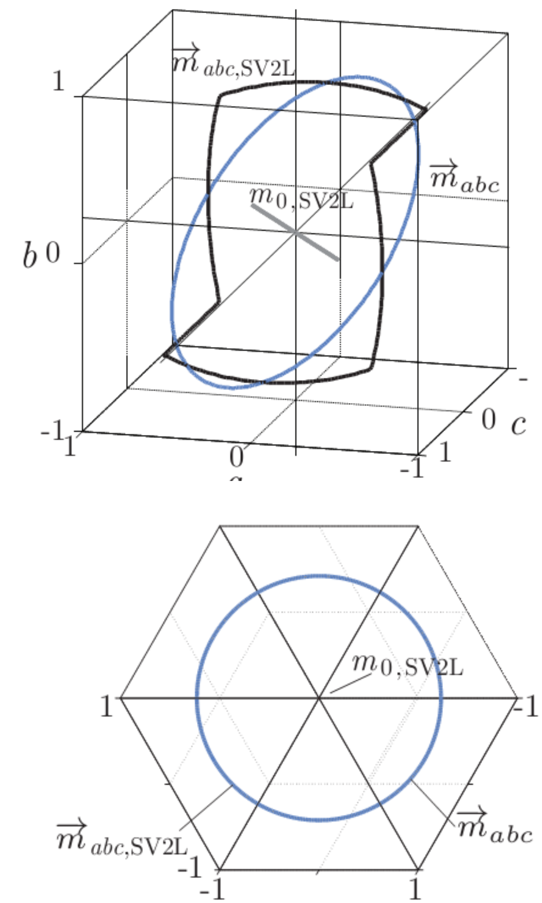

(b)

MLMSR carrier-based modulation

- DPWM
  - Reduced switching losses
  - $M \leq 1{,}15$

$$m_{0,\mathrm{DPWM}} = \frac{\mathrm{sign}(m'_{\max})}{2} - m'_{\max},$$

$$m'_{\max} = \begin{cases} m'_a & \text{se} \quad |m'_a| = \max(|m'_a|, |m'_b|, |m'_c|) \\ m'_b & \text{se} \quad |m'_b| = \max(|m'_a|, |m'_b|, |m'_c|) \\ m'_c & \text{se} \quad |m'_c| = \max(|m'_a|, |m'_b|, |m'_c|) \end{cases}$$

$$m'_a = (m_a + 1) \bmod (1) - 1/2$$
$$m'_b = (m_b + 1) \bmod (1) - 1/2$$
$$m'_c = (m_c + 1) \bmod (1) - 1/2$$

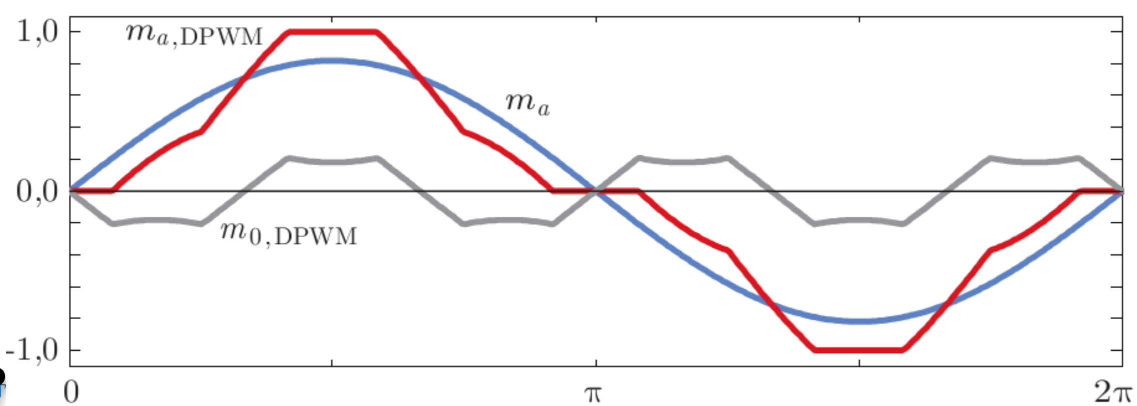

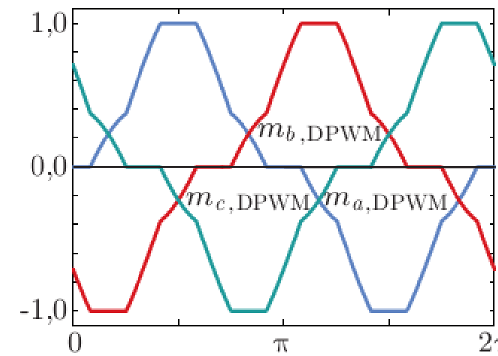

(a)

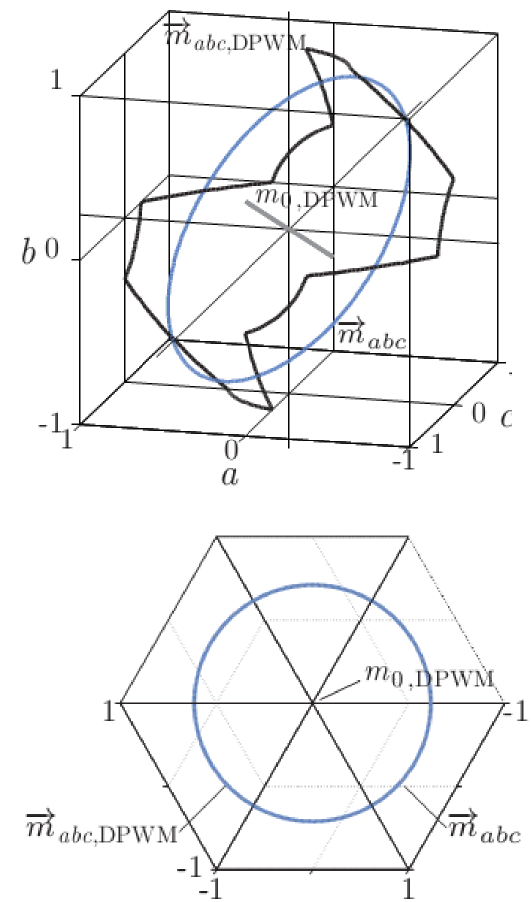

(b)

MLMSR carrier-based modulation

- STHI
  - Minimizes dc-link LF oscillations
  - $M \leq 1{,}15$

$$m_{0,\mathrm{STHI}} = \frac{M}{4}\sin\left(3\omega_g t\right)$$

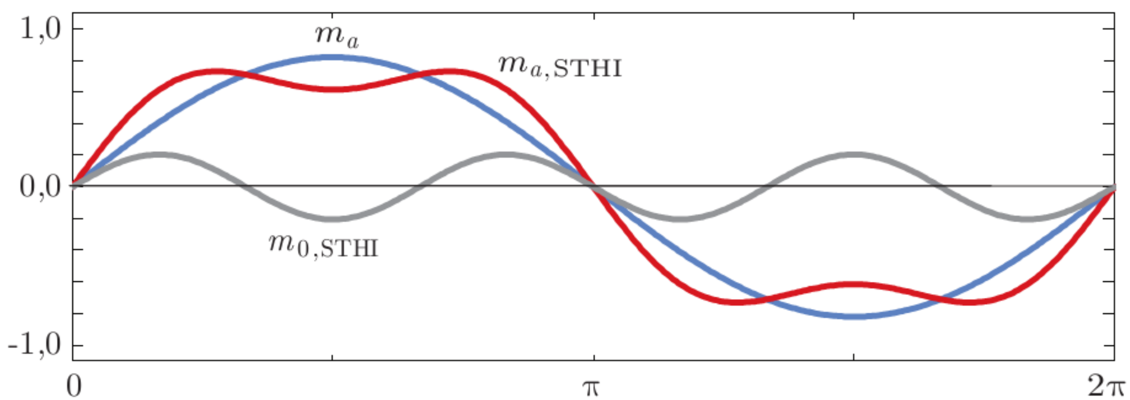

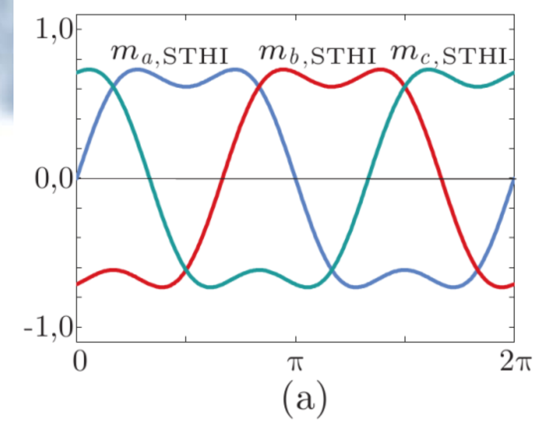

(a)

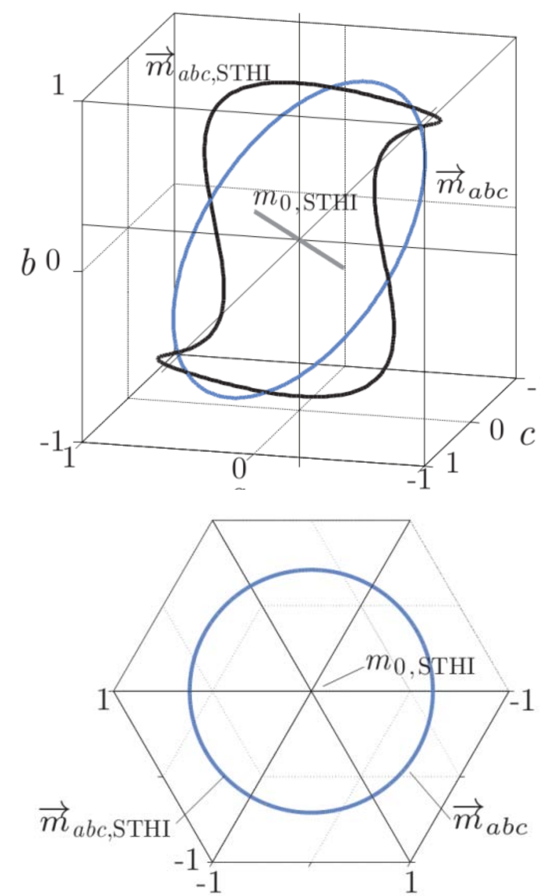

(b)

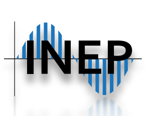

INEP

MLMSR carrier-based modulation comparison

- Input current ripple

$$\begin{cases} v_{Lb,a}^{hf} = -(v_{in,a} - <v_{in,a}>) + (v_{cm} - <v_{cm}>) \\ v_{Lb,b}^{hf} = -(v_{in,b} - <v_{in,b}>) + (v_{cm} - <v_{cm}>) \\ v_{Lb,c}^{hf} = -(v_{in,c} - <v_{in,c}>) + (v_{cm} - <v_{cm}>) \end{cases}$$

- Common mode voltage

$$v_{cm} = \frac{1}{3}\left(v_{in,a} + v_{in,b} + v_{in,c}\right)$$

- IPT magnetizing voltages

$$v_{Wkj,dm} = L_{Wk,dm}\frac{d}{dt}i_{Wkj,dm}$$

- Mid-point current

$$\langle i_{mp} \rangle = i_a\left[1 - m_a \mathrm{sign}\left(i_a\right)\right] + i_b\left[1 - m_b \mathrm{sign}\left(i_b\right)\right] + i_c\left[1 - m_c \mathrm{sign}\left(i_c\right)\right]$$

MLMSR carrier-based modulation comparison

- N=2 e N=3

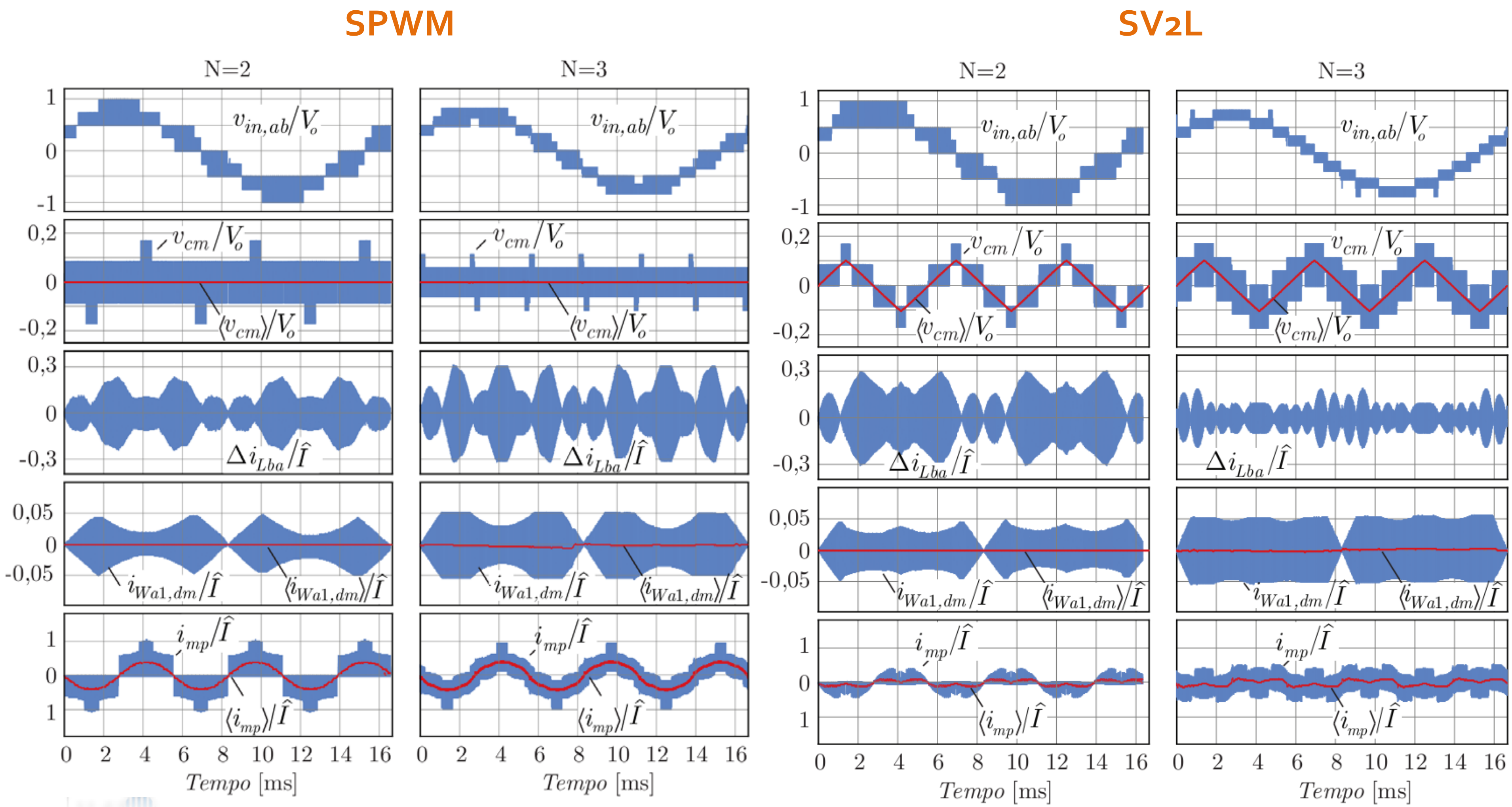

MLMSR carrier-based modulation comparison

- N=2 e N=3

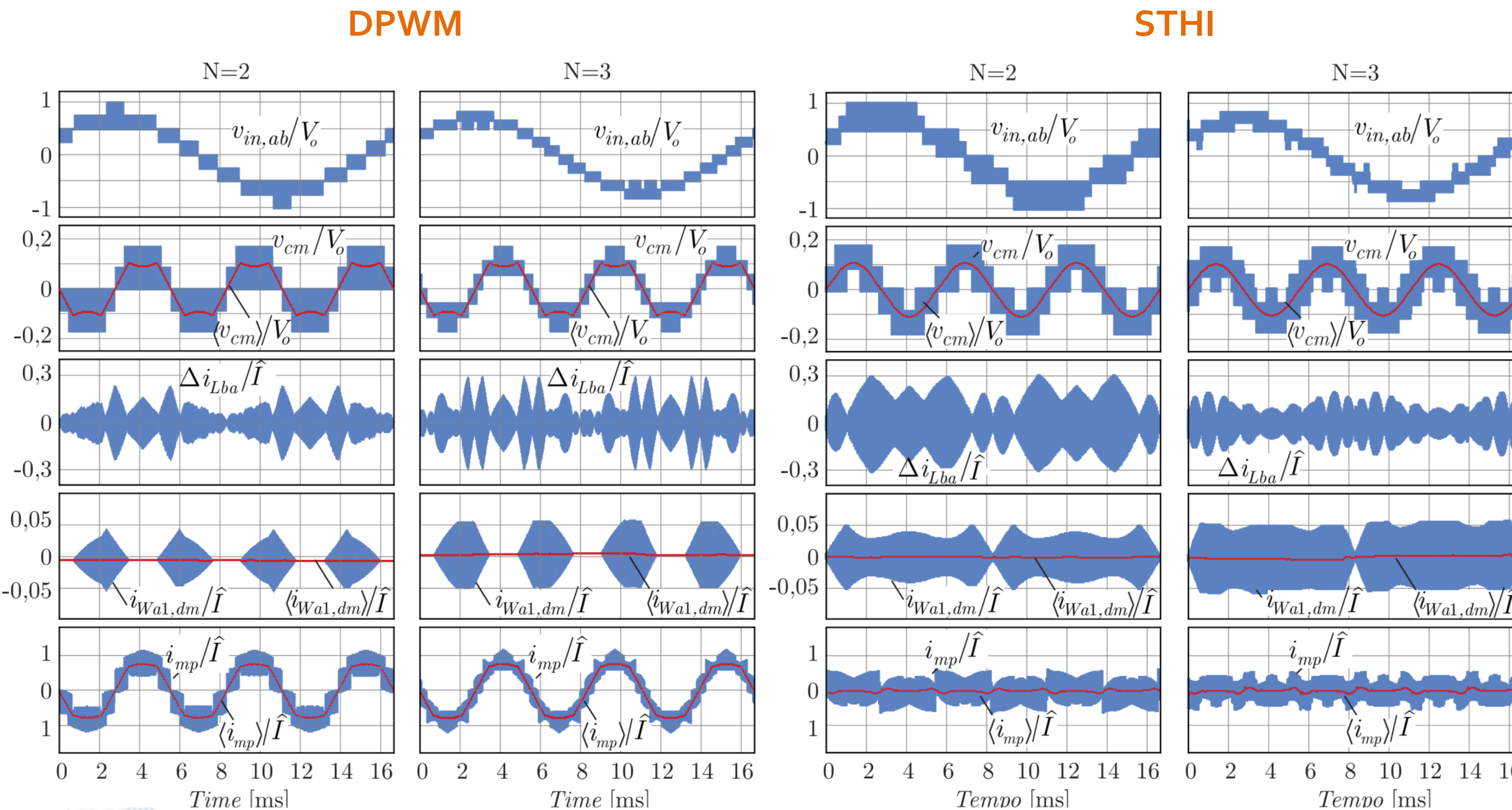

MLMSR carrier-based modulation comparison

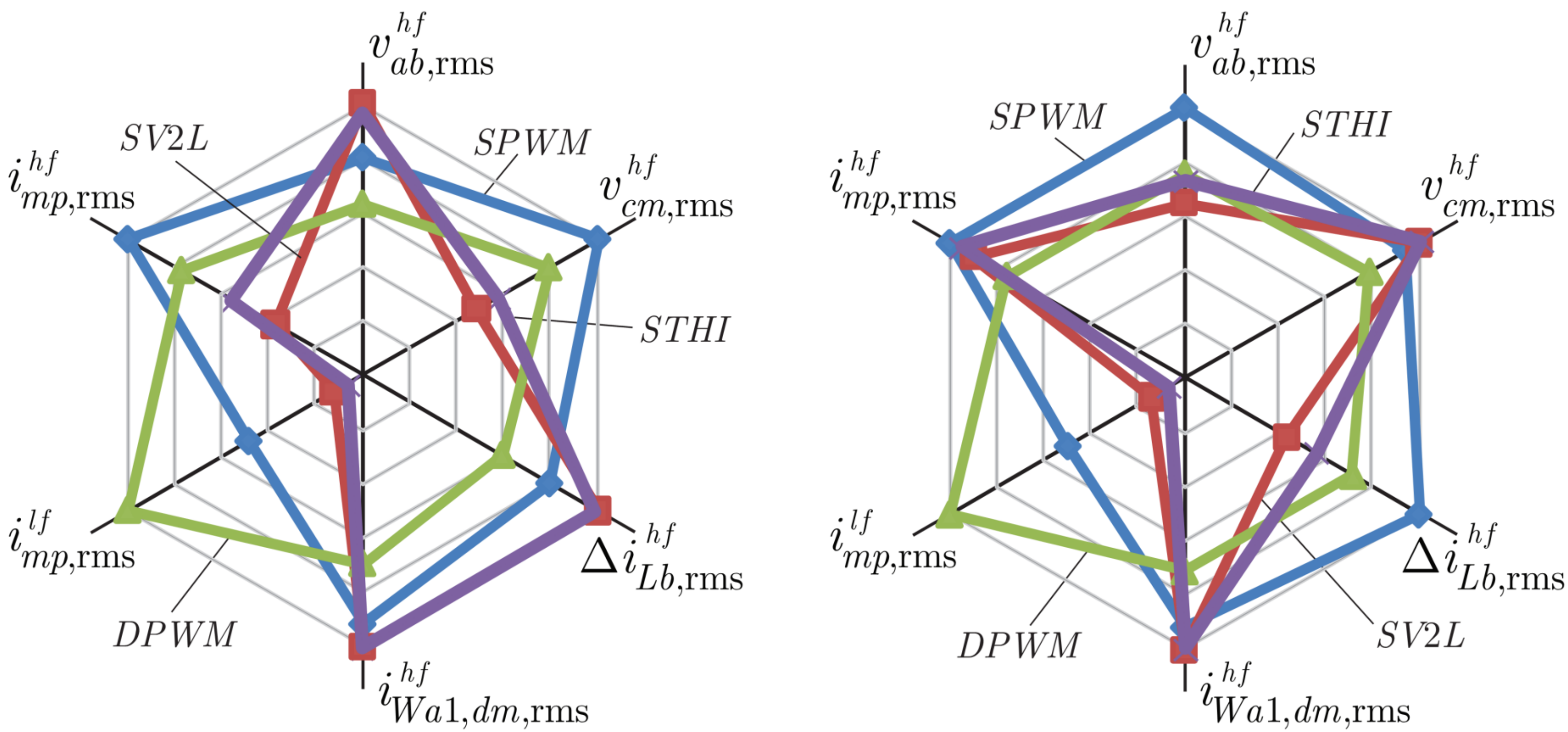

MLMSR example

- PEBBs
- Heatsink-less

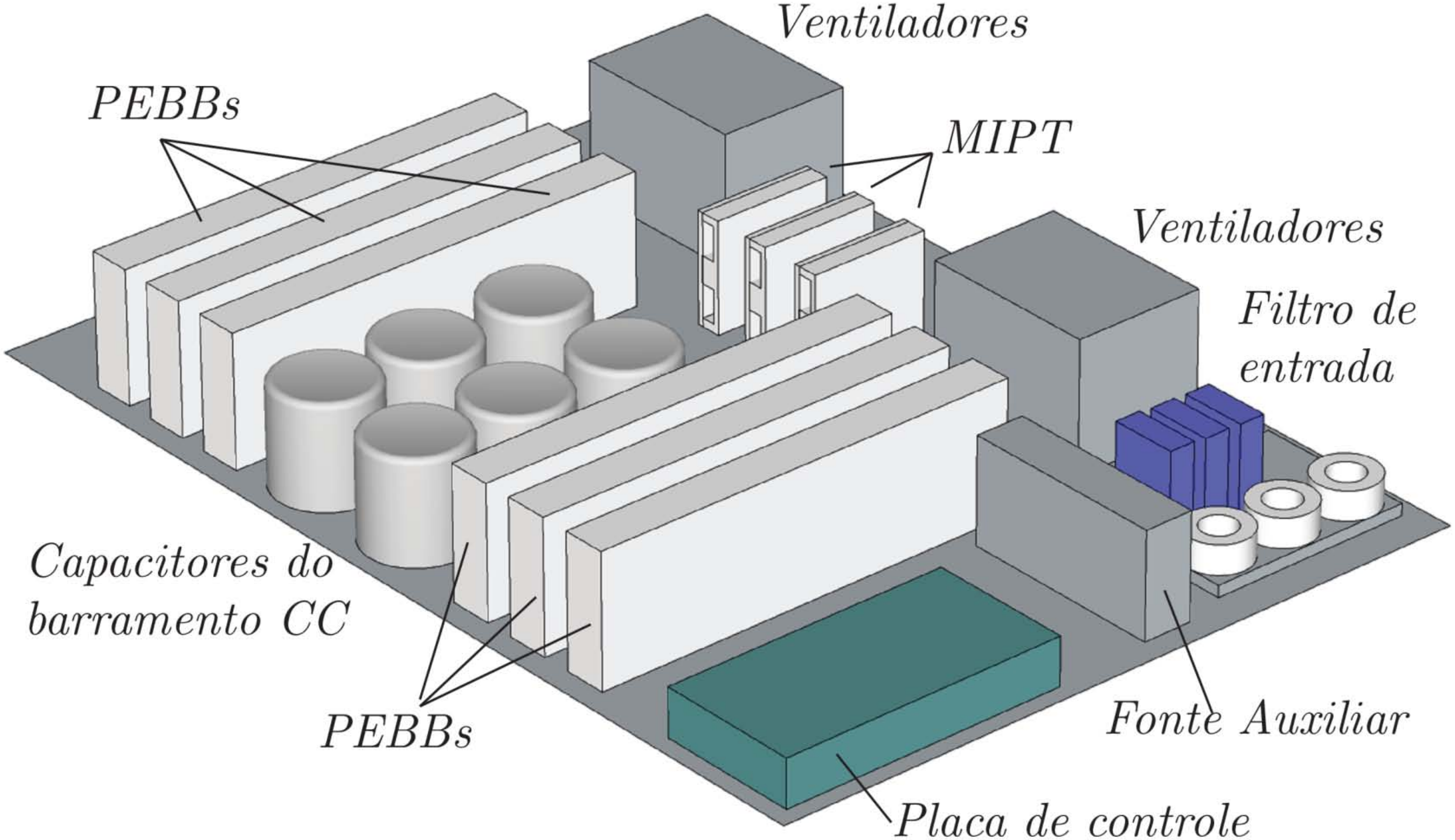

M. S. Ortmann, S. A. Mussa, e M. L. Heldwein, Multilevel Multistate Switching Cells PEBBs as the Basis for the Implementation of Advanced Rectifiers, The Applied Power Electronics Conference and Exposition APEC 2012.

PEBB

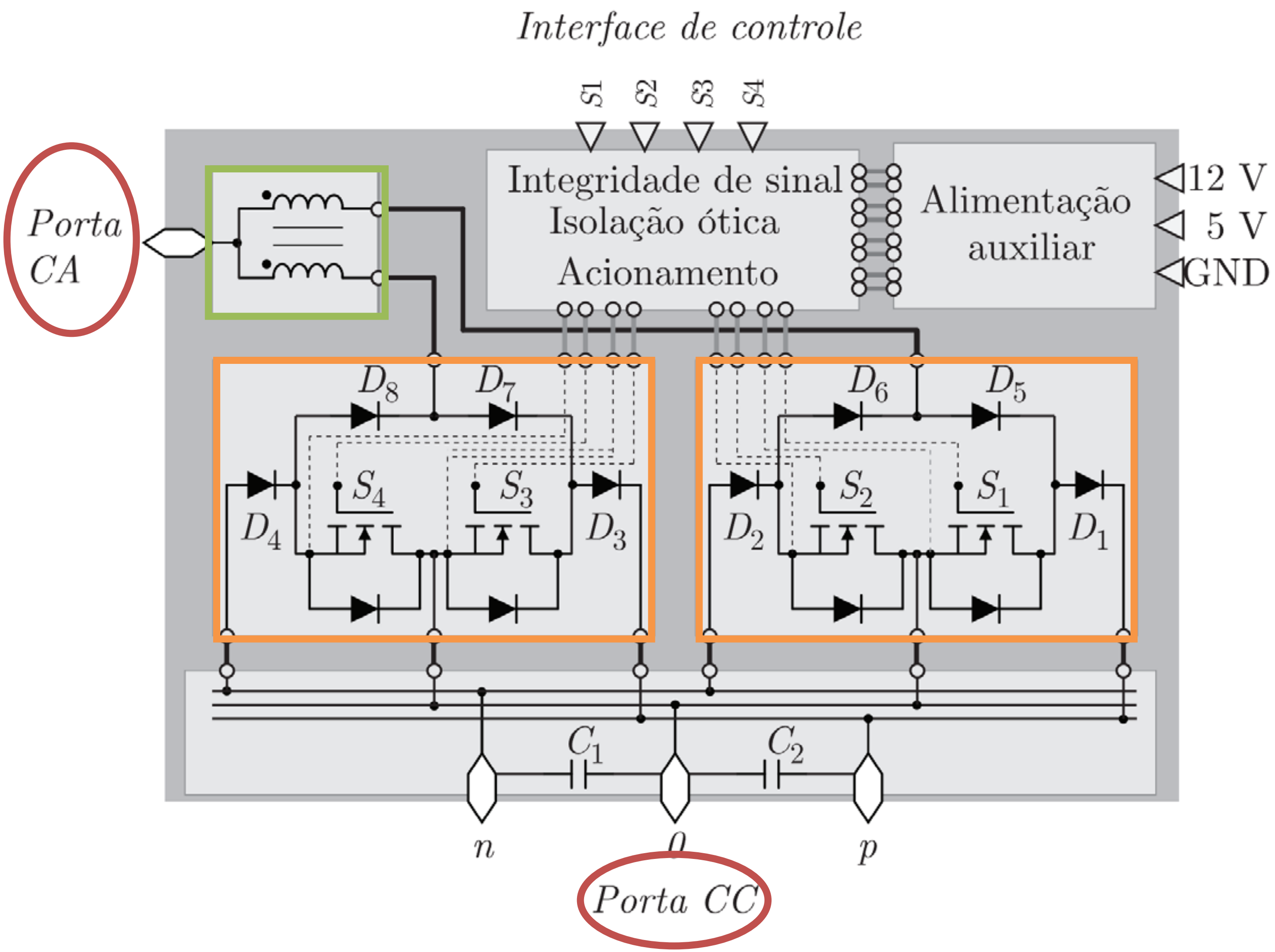

Interface de controle
S1
S2
S3
S4
Porta CA
Integridade de sinal
Isolação ótica
Acionamento
Alimentação auxiliar
12 V
5 V
GND
D_8
D_7
D_6
D_5
S_4
S_3
S_2
S_1
D_4
D_3
D_2
D_1
C_1
C_2
n
0
p
Porta CC

PEBB

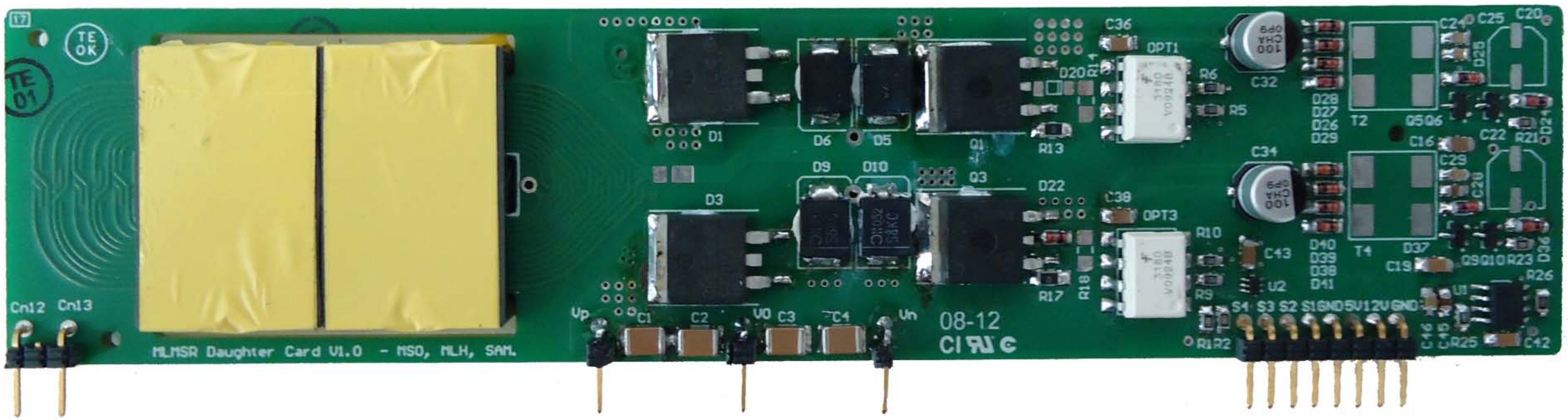

- 6 layers PCB – 180mm x 40,5mm:
- Integrated MIPT
  - 12 turns
  - $J = 1980\ A/cm^2$;
- Power supply:
  - 12V, 5V;

- Digital inputs:
  - S1,S2,S3,S4;
- Mosfets CoolMos 600 V, 20 A;
- Diodes Sic 600V 10 A;
- Diodes Si, 800 V, 8 A;
- Drivers e aux. power;

MLMSR N=4

SPWM

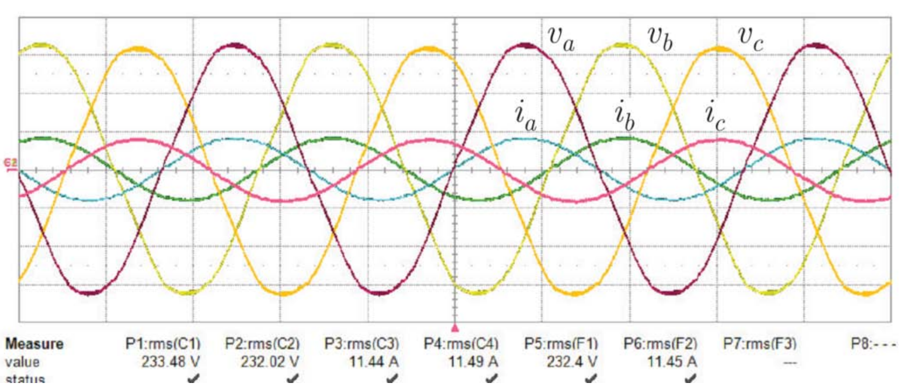

DPWM

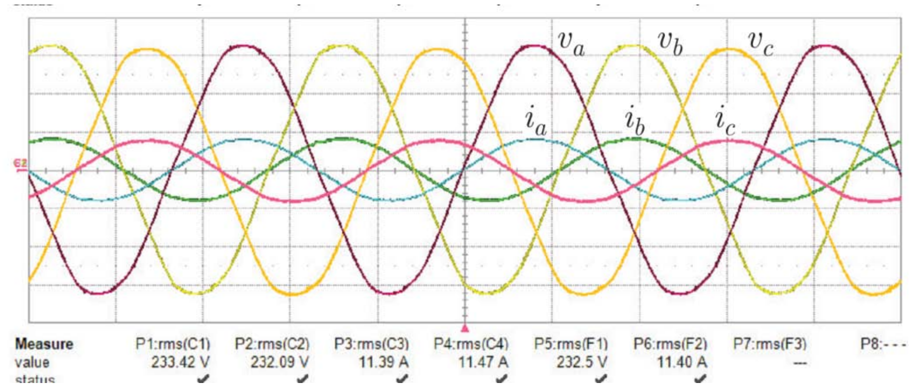

SV2L

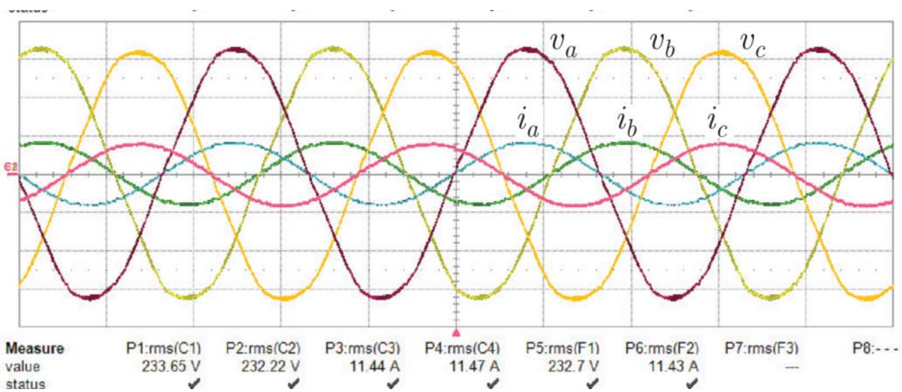

STHI

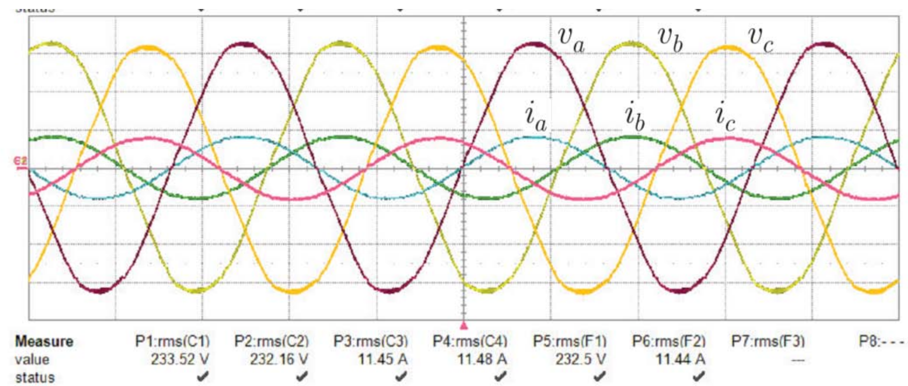

INEP

MLMSR N=4

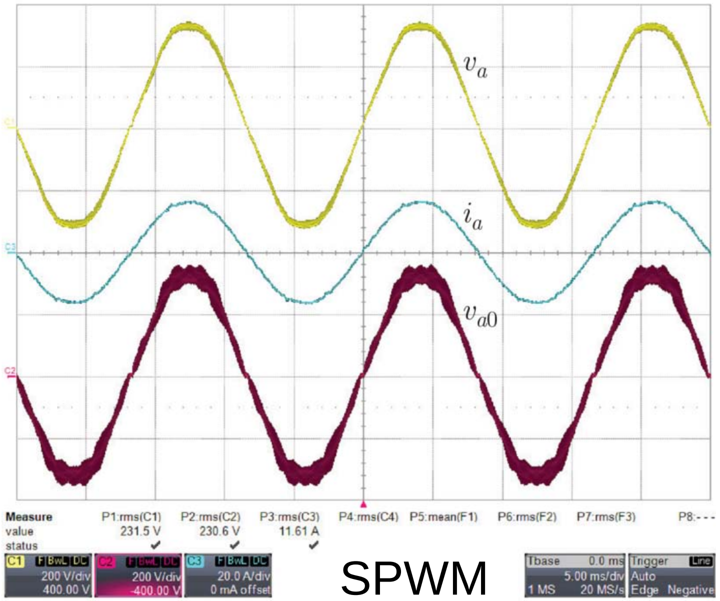

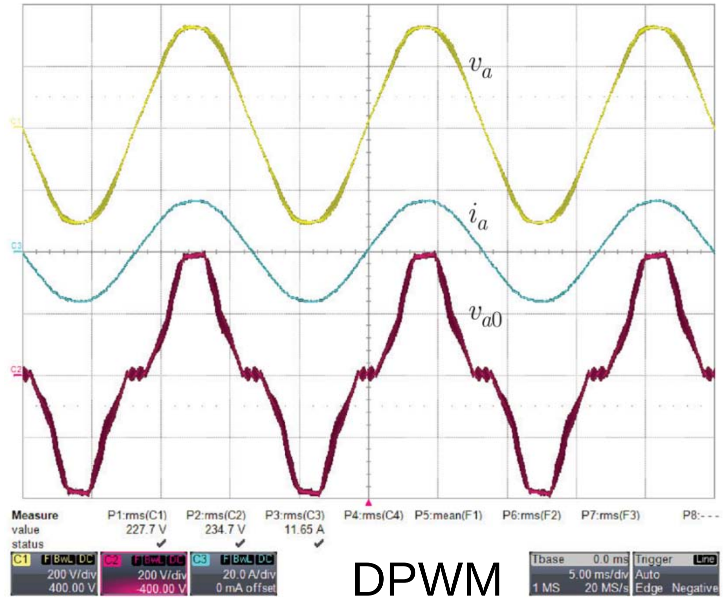

Input voltage

Input current

Converter voltage

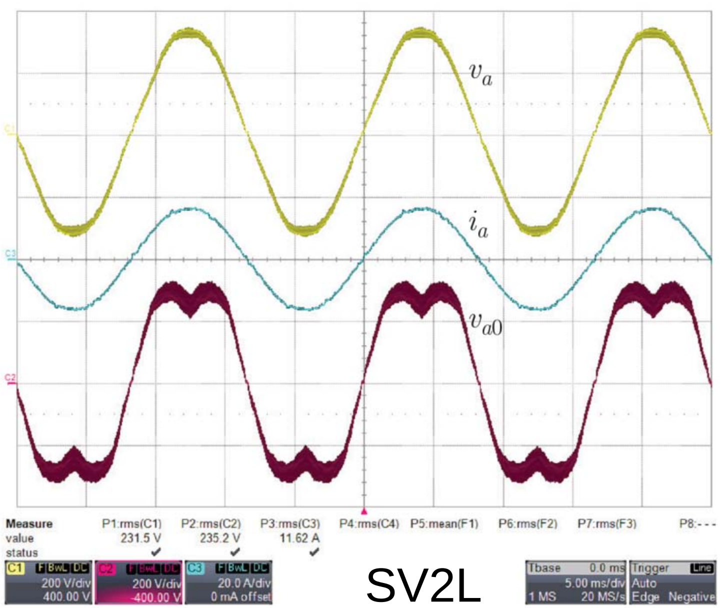

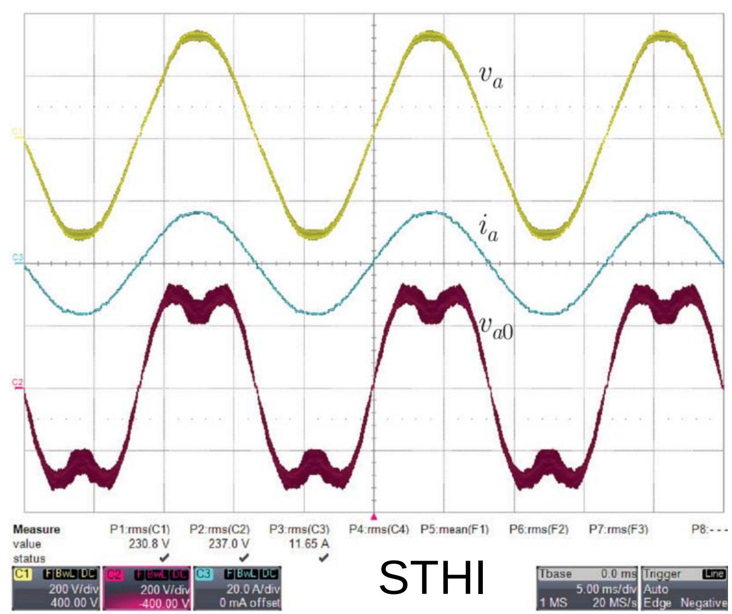

Input voltage

Input current

Converter voltage

MLMSR N=4

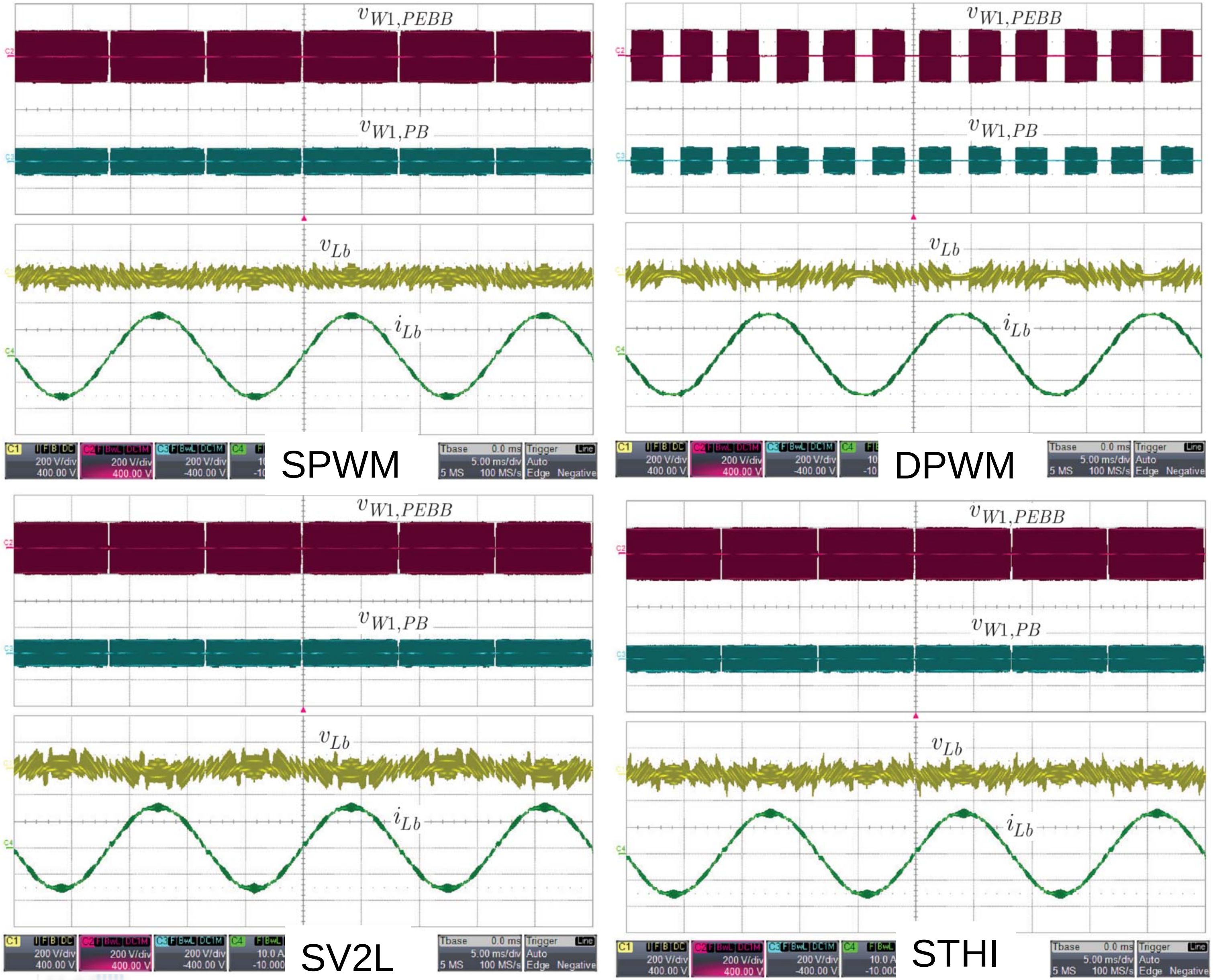

Voltage MITP - PEBB

Voltage MIPT - Base

Inductor voltage

Inductor current

MLMSR N=4

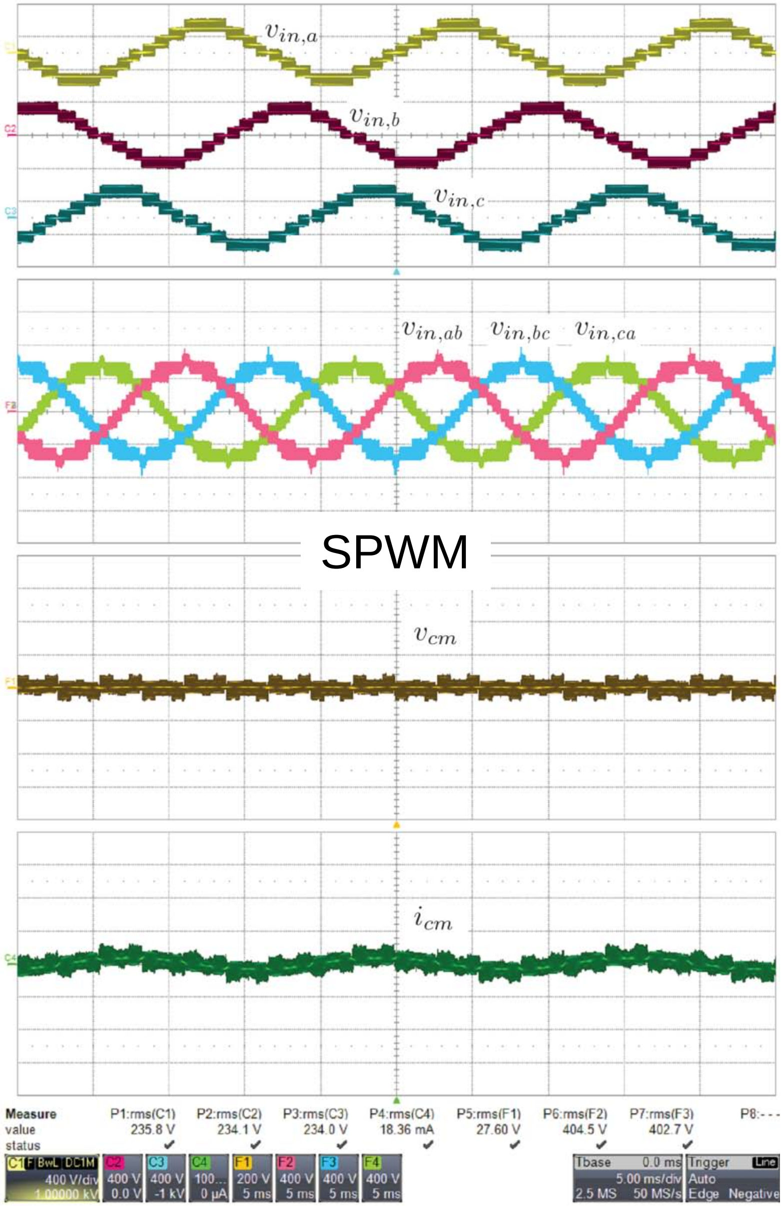

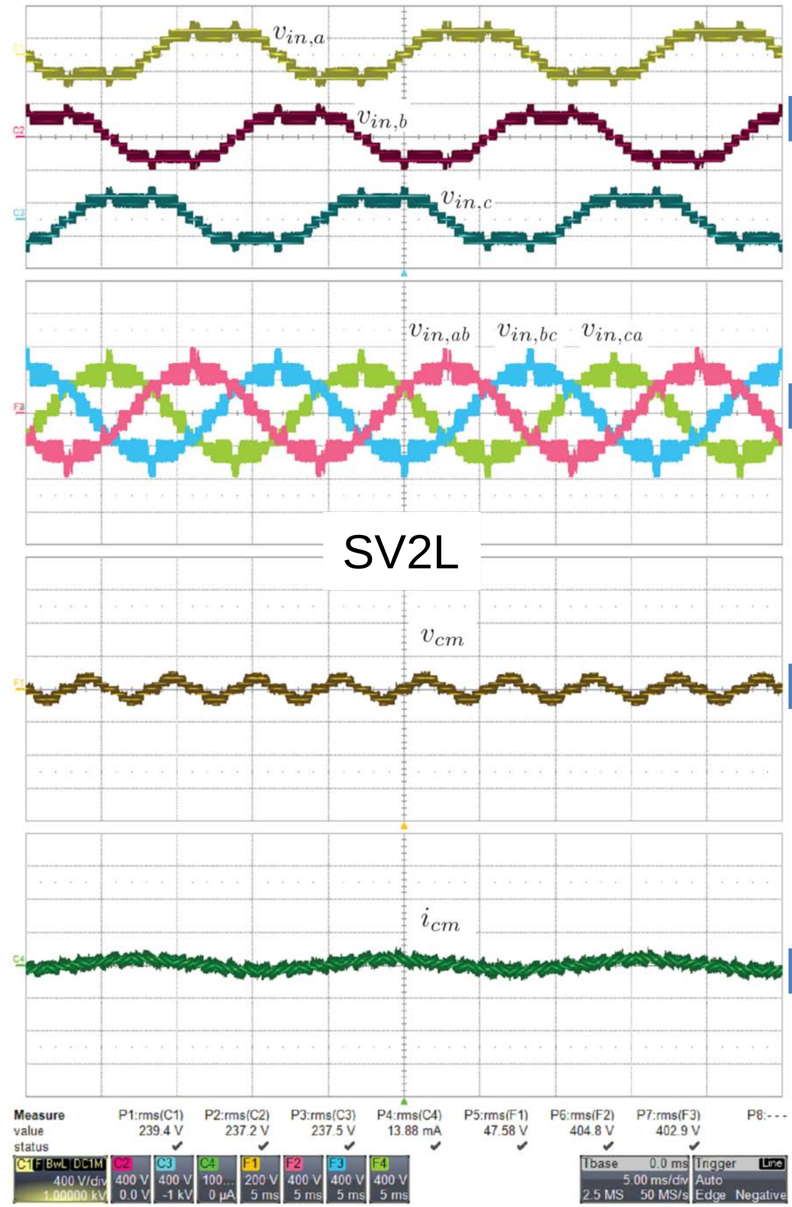

Converter phase voltages

Converter line voltages

Common mode voltage

Common mode current

MLMSR N=4

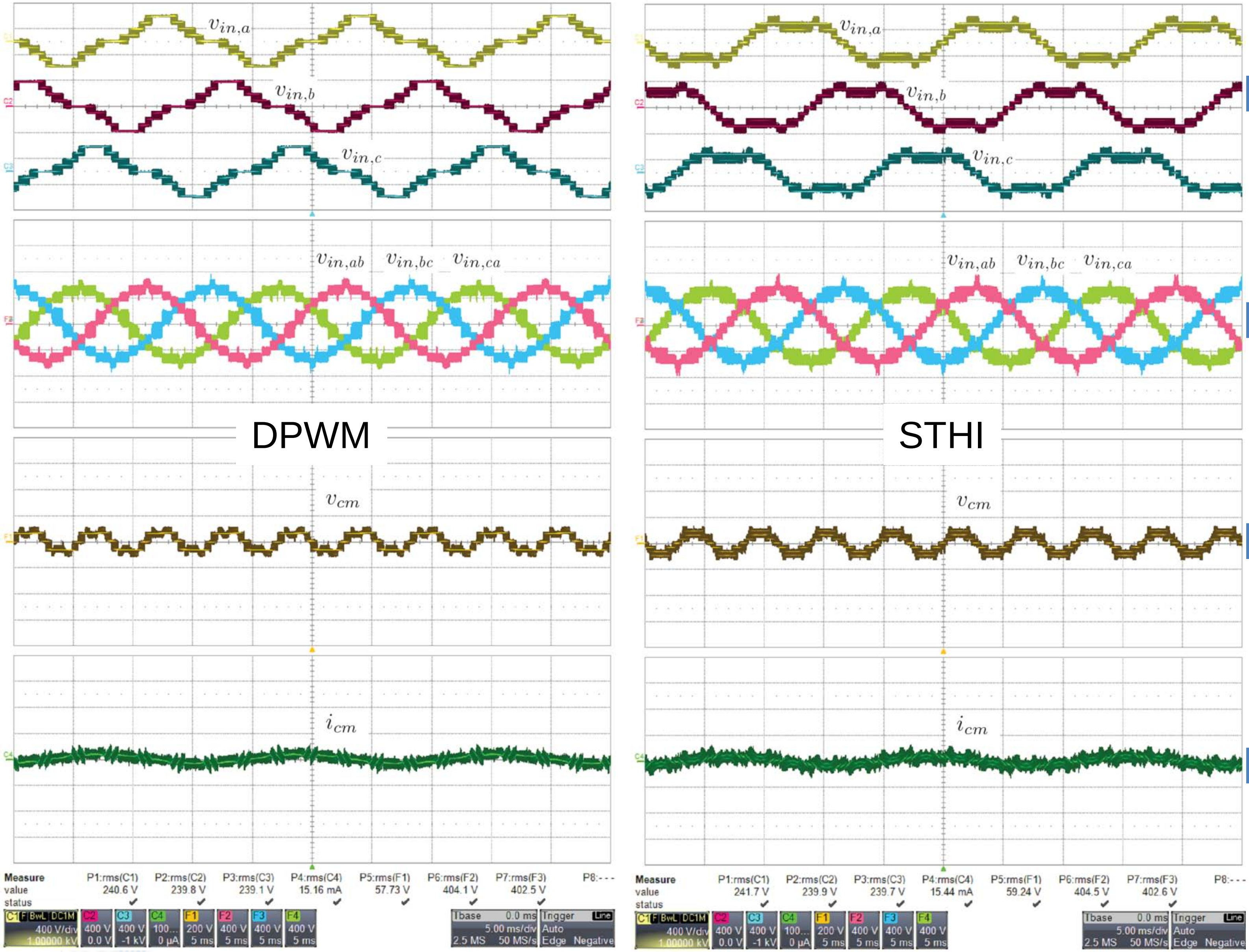

Converter phase voltages

Converter line voltages

Common mode voltage

Common mode current

MLMSR MIPT behavior

- Distribuição das correntes nos enrolamentos dos MIPTS:

$$F_{diW}\% = \frac{\left|I_{W12,\mathrm{RMS}} - \bar{I}_{W,\mathrm{RMS}}\right|}{\bar{I}_{W,\mathrm{RMS}}}$$

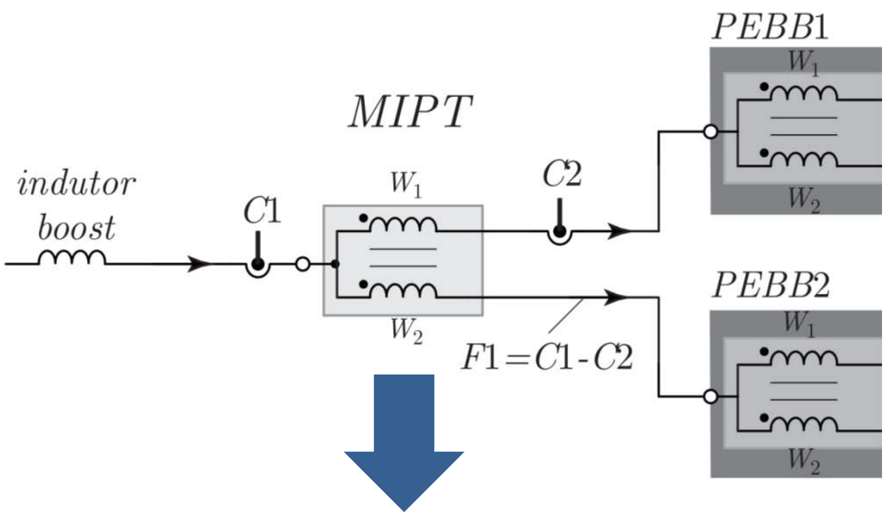

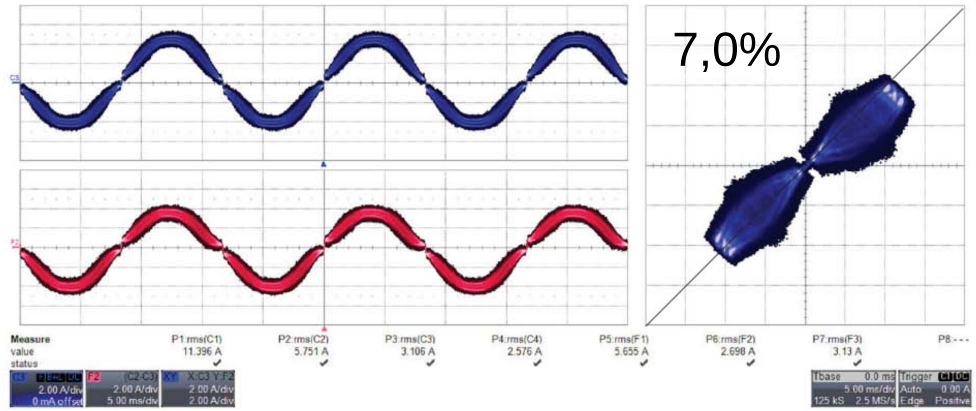

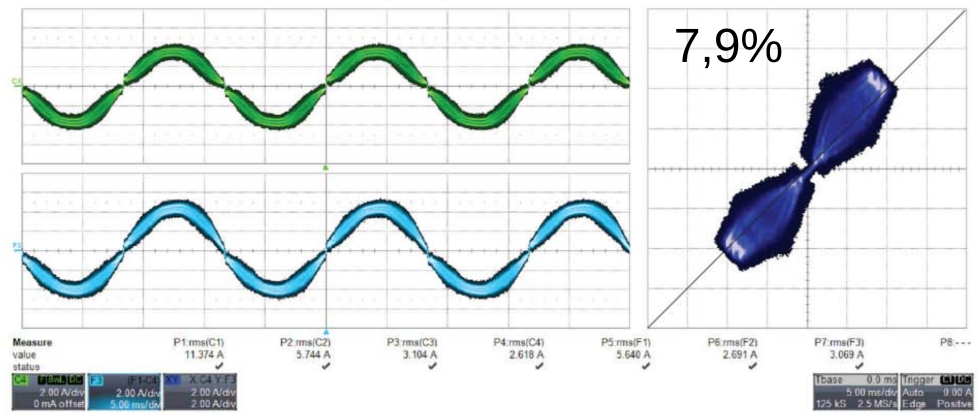

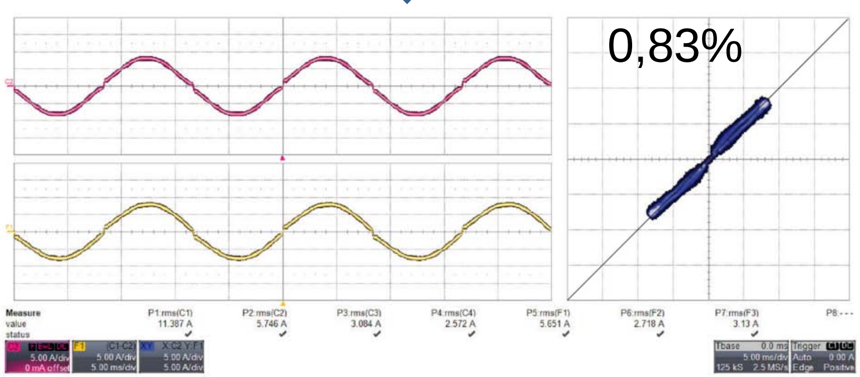

MLMSR N=4

- Transient load step

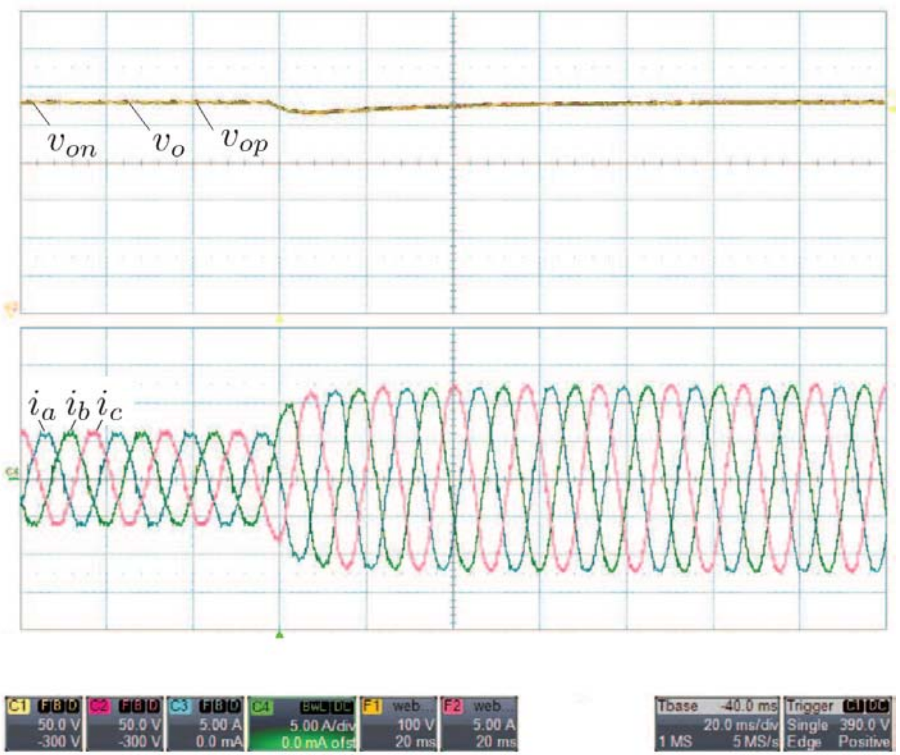

40% to 80% Po

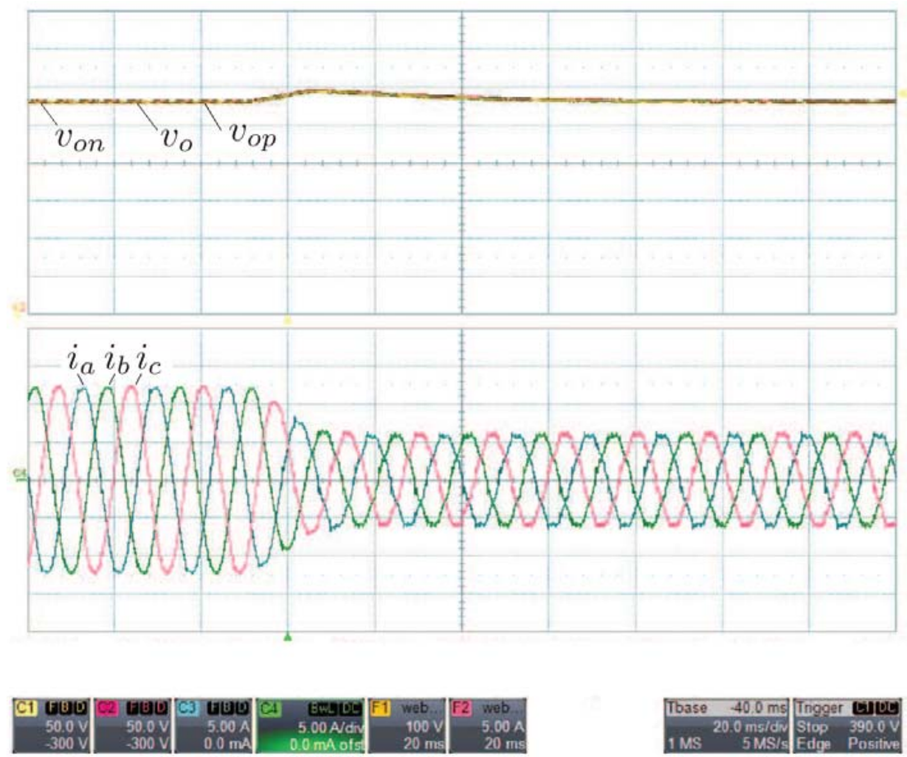

80% to 40% Po

MLMSR N=4

- Dc-link unbalance

Balance control off

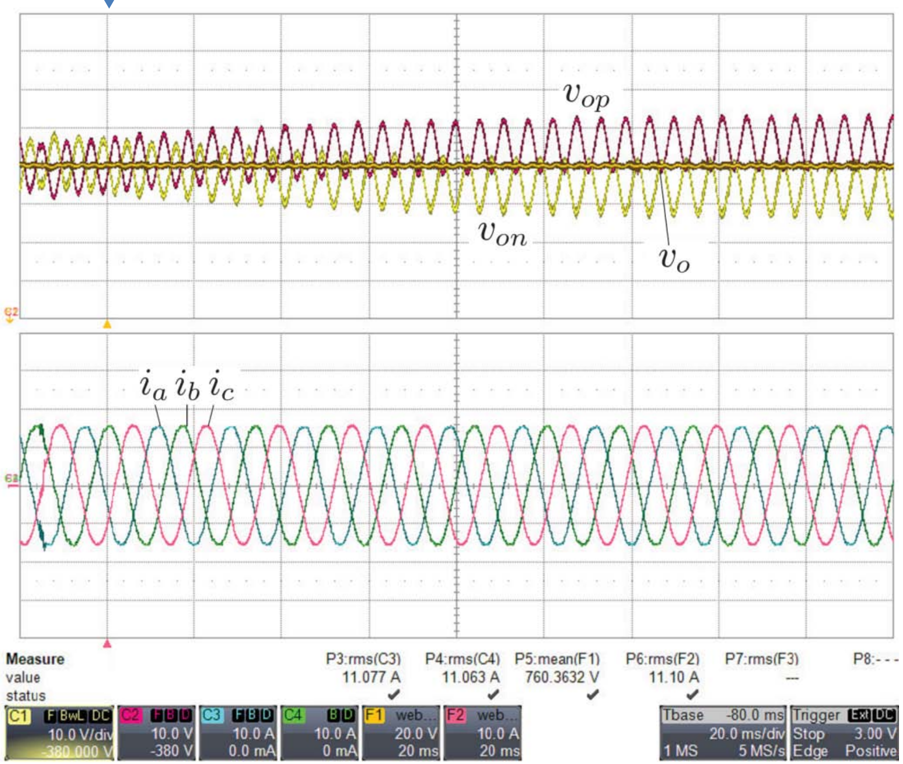

Balance control on

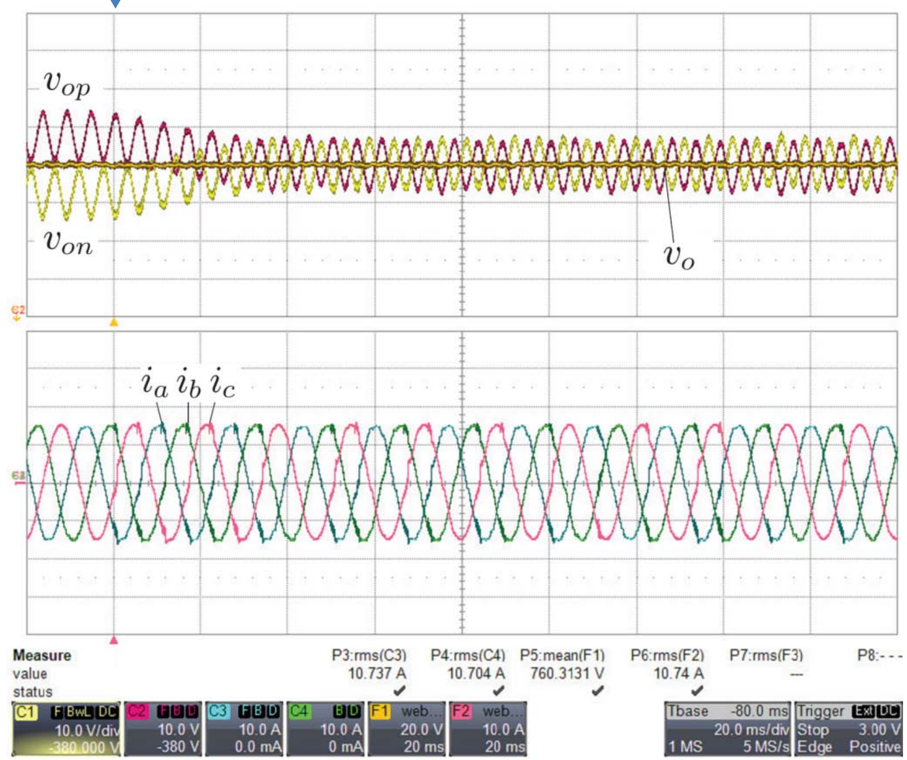

MLMSR N=4

- Efficiency

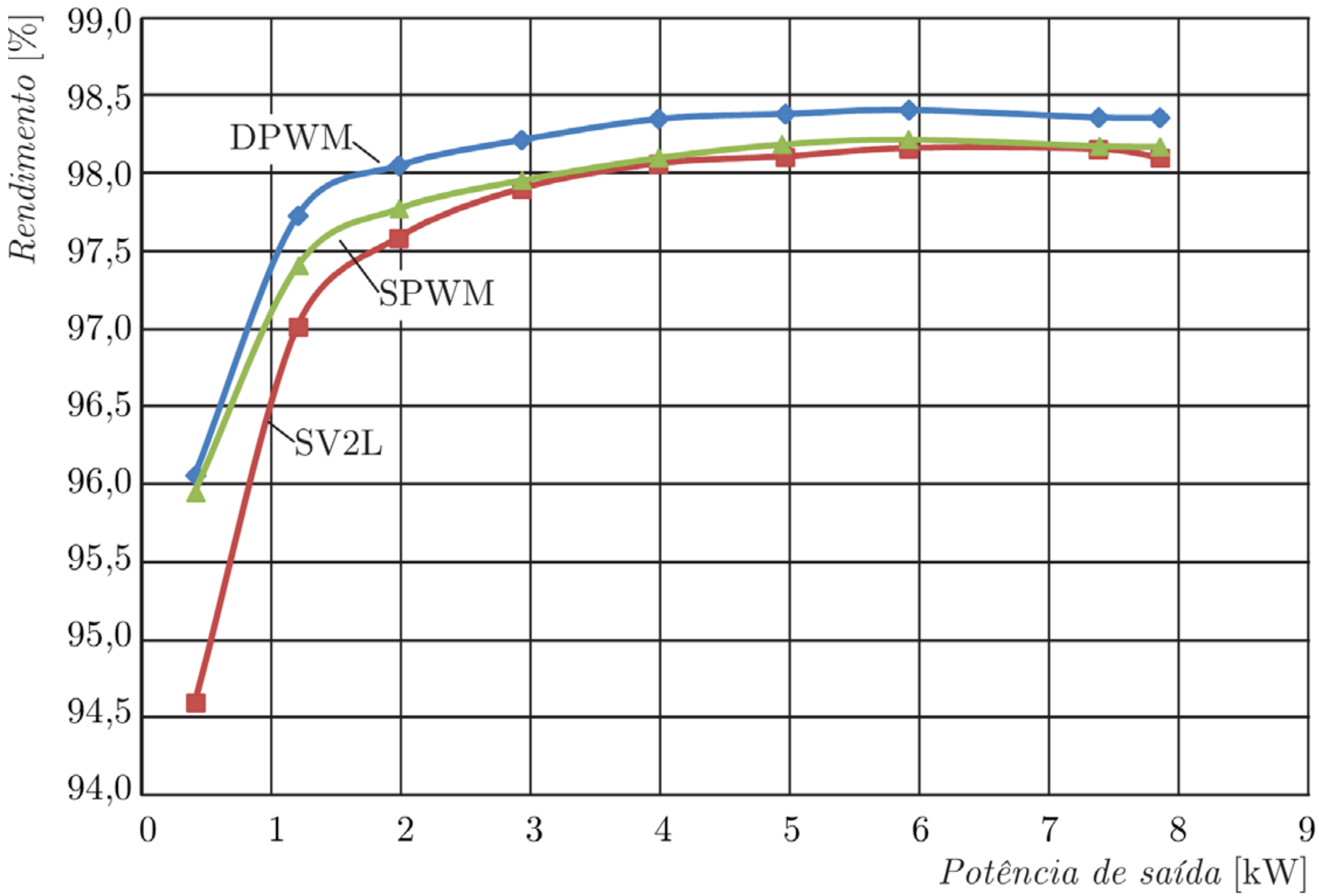

MLMSR N=4

- THDi

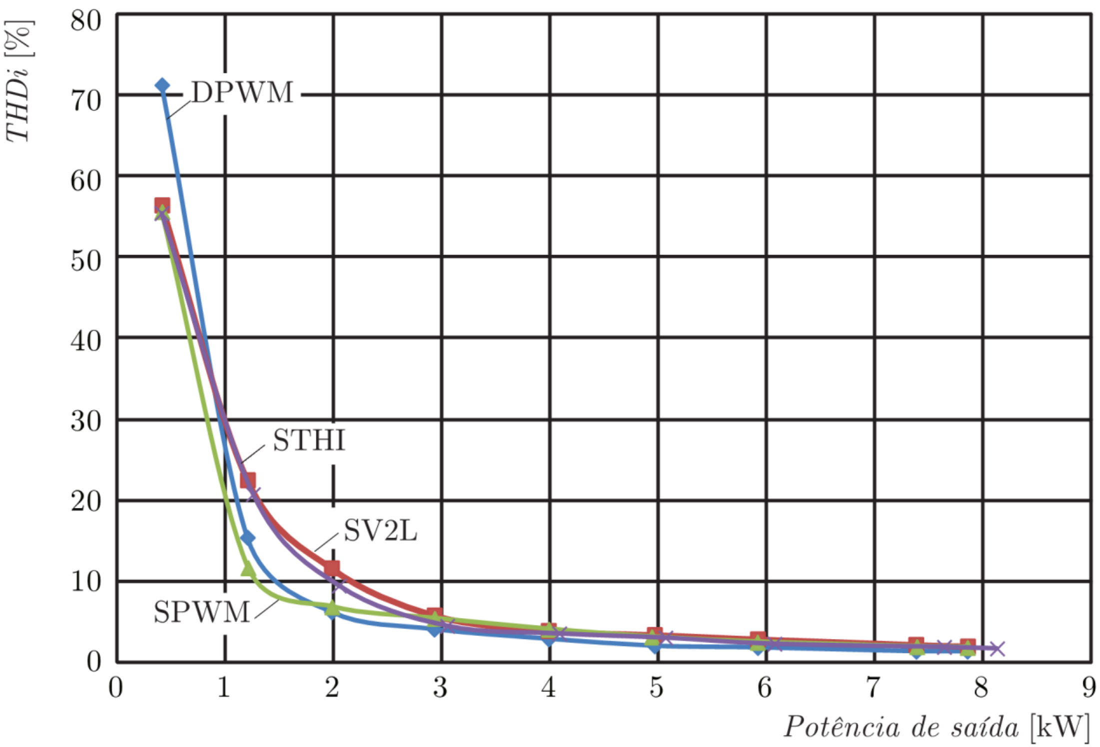

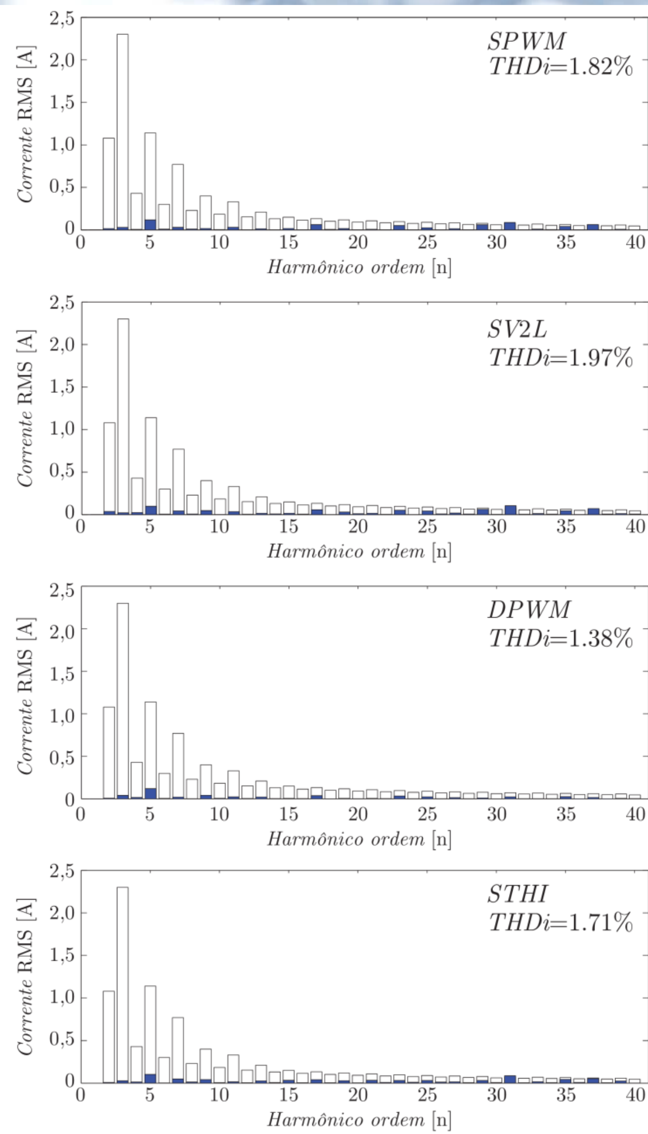

MLMSR N=4

- Comparison

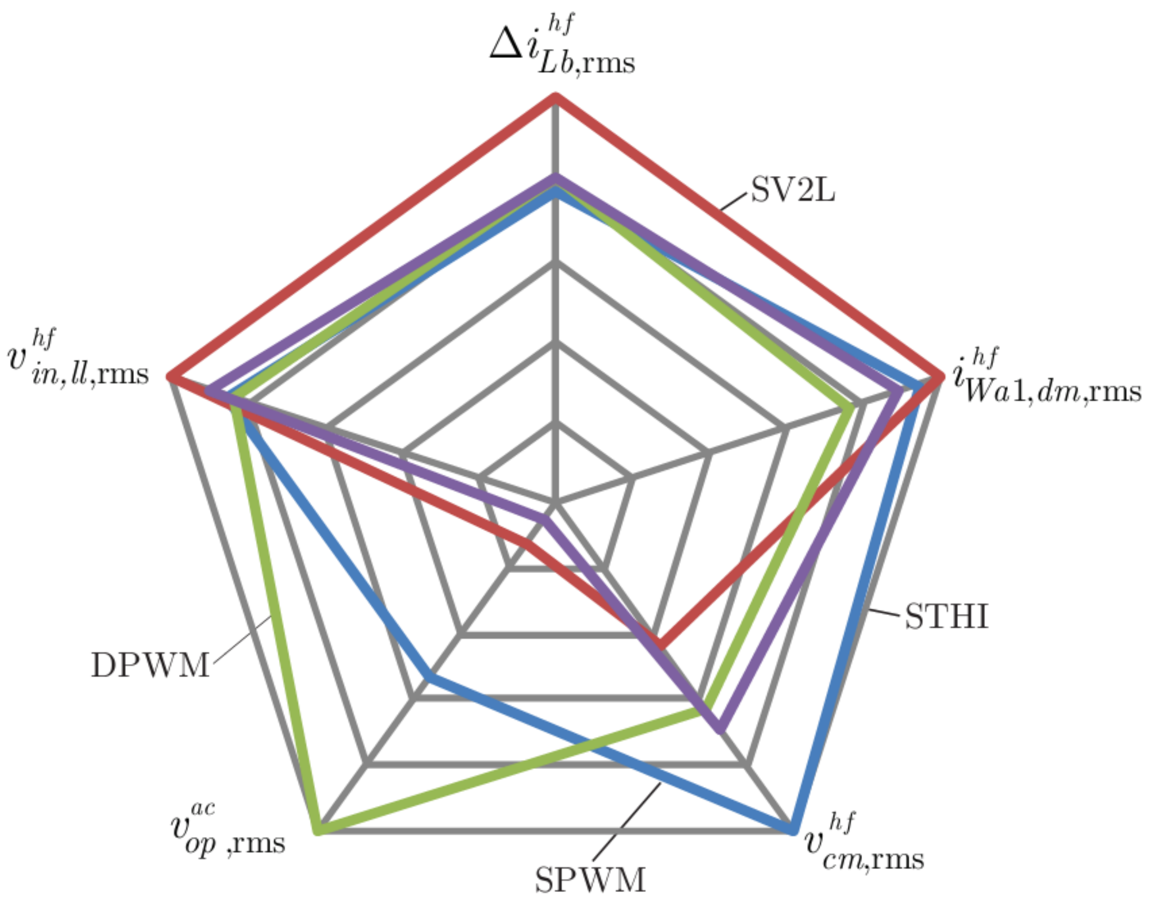

Comparative Evaluation (I)

- **Boost-Type**
  VIENNA / Δ−Switch Rectifier

V_{LL} = 400 V (50 Hz)
P_o = 10 kW
U_o = 720 V
f_s = 72 kHz

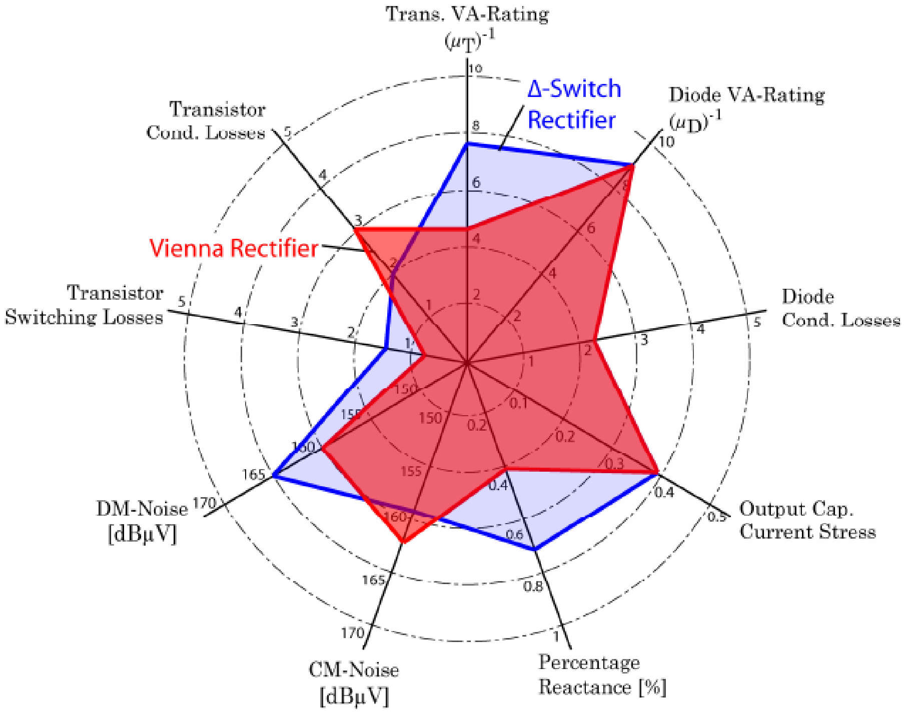

- **Buck-Type**
  SWISS/ 6-Switch Rectifier

V_{LL} = 400 V (50 Hz)
P_o = 10 kW
U_o = 360 V
f_s = 72 kHz

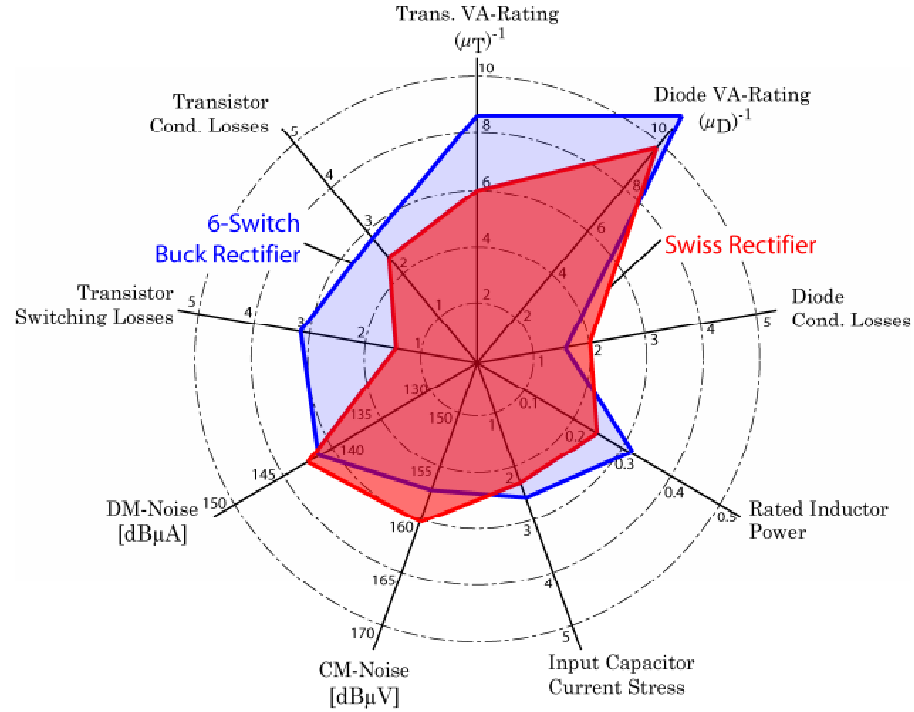

M. Hartmann, T. Friedli and J. W. Kolar
Swiss Federal Institute of Technology (ETH) Zurich

UFSC

Performance Indices

Diodes

$$\text{Diode VA-Rating} = \frac{1}{\mu_D} = \frac{\sum_n V_{D,\max,n} I_{D,\max,n}}{P_o}$$

$$\text{Diode Conduction Losses} = \frac{\sum_n I_{D,avg,n}}{I_o}$$

Transistors

$$\text{Transistor VA-Rating} = \frac{1}{\mu_T} = \frac{\sum_n V_{T,\max,n} I_{T,\max,n}}{P_o}$$

$$\text{Transistor Conduction Losses} = \frac{\sum_n I_{T,rms,n}}{I_o}$$

$$\text{Transistor Sw. Losses Boost} = \frac{\sum_n I_{T,avg,n} V_{T,n}}{P_o}$$

$$\text{Transistor Sw. Losses Buck} = \frac{\sum_n I_{T,n} V_{T,avg,n}}{P_o}$$

Power Passives

$$\text{Percentage Reactance} = \frac{2\pi f_N I_N L_N}{V_N}$$

$$\text{Rated Inductor Power} = \frac{I_L \Delta I_{L,pkpk} L f_s}{P_o}$$

$$\text{Capacitive Current Stress} = \frac{\sum_n I_{C,rms,n}}{I_o}$$

Conducted Noise (DM, CM)

$$V_{Noise} = V_{DM} + V_{CM} \qquad V_{CM} = \frac{V_a + V_b + V_c}{3}$$

$$V_{DM}^2 = V_{DM,tot}^2 - V_{N,rms}^2$$

$$V_{CM}^2 = V_{CM,tot}^2 - V_{CM,LF}^2$$

Dc-dc converters for EV battery chargers

High Efficiency DC-DC Converter for EV Battery Charger Using Hybrid Resonant and PWM Technique

Hongmei Wan

Thesis submitted to the faculty of the Virginia Polytechnic Institute and State University

Power Electronics for EV Charging Systems

Basic Requirements

- Wide Voltage Range – Voltage Adaption
- Output Current Control
- Mains Sinusoidal Current Shaping
- Isolation of Mains and Battery (?)

Basic Topologies

- Non-Isolated
- Isolated Single-Stage
- Non- or Isolated Two-Stage

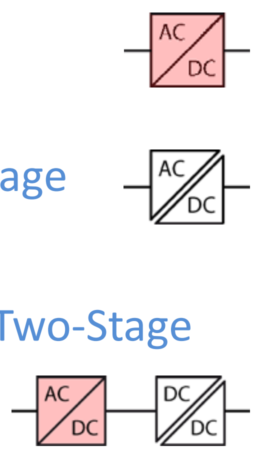

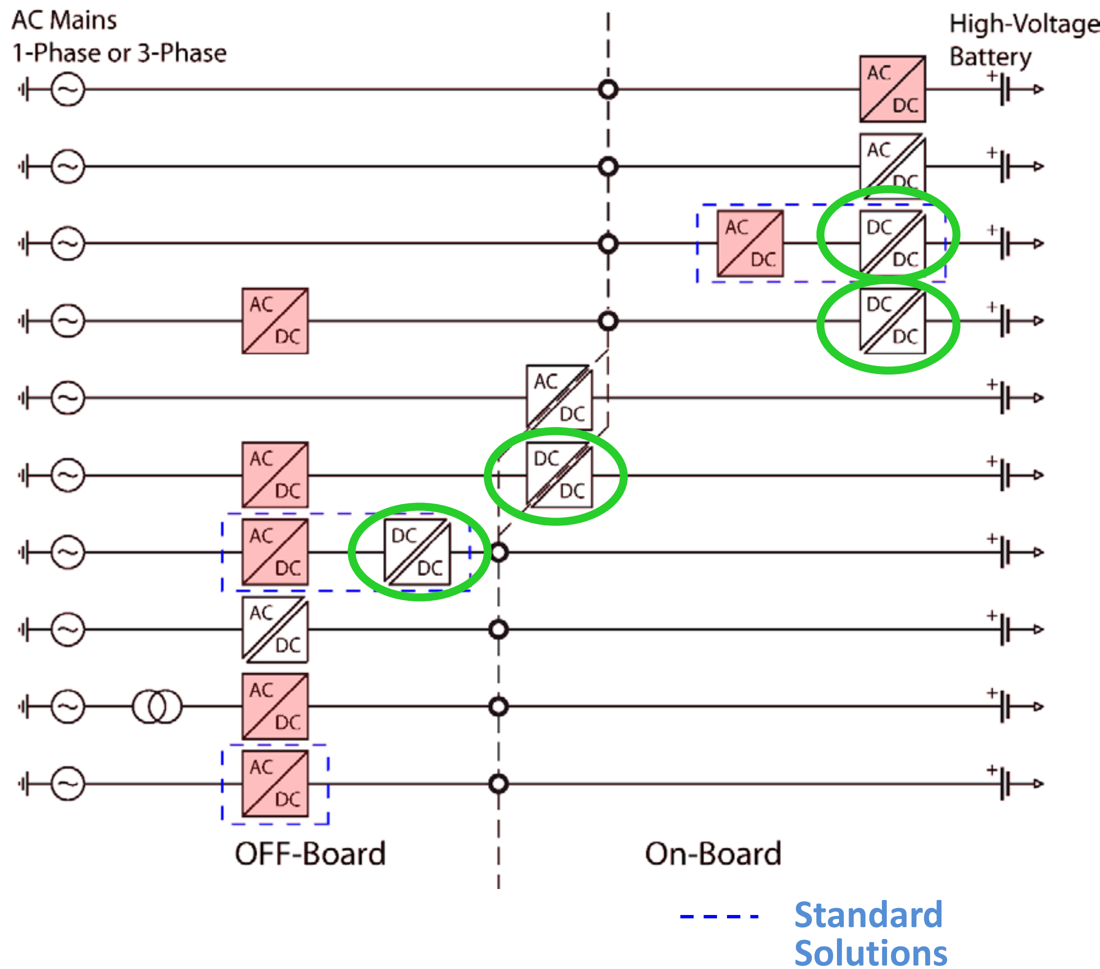

INEP

Insulated dc-dc converters

Table 1.3: Power Supply Topologies from www.ti.com

Type of Converter	FLYBACK	FORWARD	2 SWITCH FORWARD	ACTIVE CLAMP FORWARD
Circuit Configuration	Equations and Waveforms for Discontinuous Mode 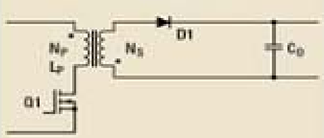	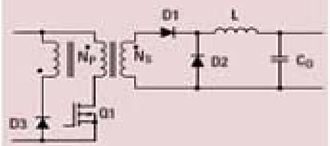	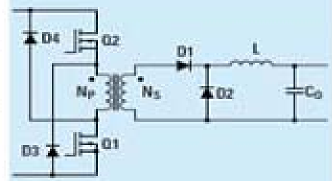	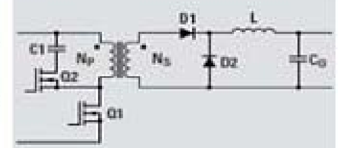
Ideal Transfer Function*	$\frac{V_{OUT}}{V_{IN}} = D \times \sqrt{\frac{T_P \times V_{OUT}}{2 \times I_{OUT} \times L_P}}$	$\frac{V_{OUT}}{V_{IN}} = \left(\frac{N_S}{N_P}\right) \times \left(\frac{t_{ON}}{T_P}\right) = \left(\frac{N_S}{N_P}\right) \times D$	$\frac{V_{OUT}}{V_{IN}} = \left(\frac{N_S}{N_P}\right) \times \left(\frac{t_{ON}}{T_P}\right) = \left(\frac{N_S}{N_P}\right) \times D$	$\frac{V_{OUT}}{V_{IN}} = \left(\frac{N_S}{N_P}\right) \times \left(\frac{t_{ON}}{T_P}\right) = \left(\frac{N_S}{N_P}\right) \times D$
Drain Current*	$I_{Q1}\,(max) = \left(\frac{V_{IN} \times t_{ON}}{L_P}\right)$	$I_{Q1}\,(max) = \left(\frac{N_S}{N_P}\right) \times I_{OUT}$	$I_{Q1}\,(max) = \left(\frac{N_S}{N_P}\right) \times I_{OUT}$	$I_{Q1}\,(max) = \left(\frac{N_S}{N_P}\right) \times I_{OUT}$
Drain Voltage*	$V_{DS} = V_{IN} + V_{OUT} \times \left(\frac{N_P}{N_S}\right)$	$V_{DS} = 2 \times V_{IN}$	$V_{DS} = V_{IN}$	$V_{DS} = V_{IN} \times \left(\frac{1}{1-D}\right)$
Average Diode Current*	$I_{D1} = I_{OUT}$	$I_{D1} = I_{OUT} \times D$	$I_{D1} = I_{OUT} \times D$	$I_{D1} = I_{OUT} \times D$
Diode Reverse Voltage*	$V_{D1} = V_{OUT} + V_{IN} \times \left(\frac{N_S}{N_P}\right)$	$V_{D1} = V_{OUT} + V_{IN} \times \left(\frac{N_S}{N_P}\right)$	$V_{D1} = V_{OUT} + V_{IN} \times \left(\frac{N_S}{N_P}\right)$	$V_{D1} = V_{OUT} + V_{IN} \times \left(\frac{N_S}{N_P}\right) \times \left(\frac{1}{1-D}\right)$
Voltage and Current Waveforms	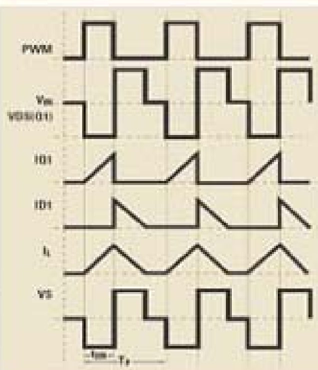	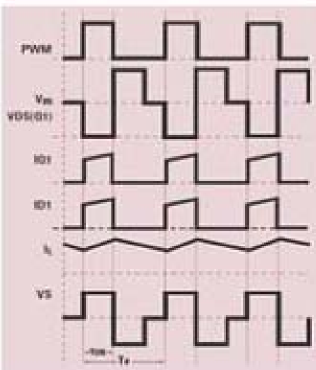	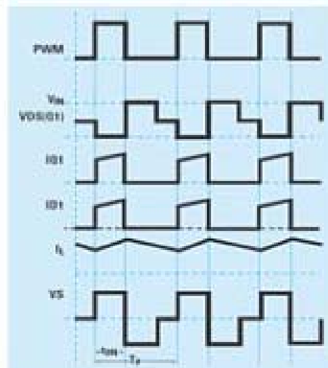	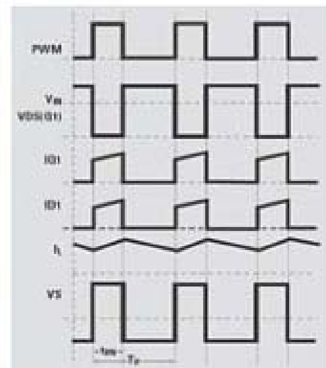

* Excludes ripple current and output diode voltage drop. Continuous conduction mode shown (unless otherwise noted). For

Insulated dc-dc converters

Type of Converter	HALF BRIDGE	PUSH PULL	FULL BRIDGE	PHASE SHIFT ZVT
Circuit Configuration	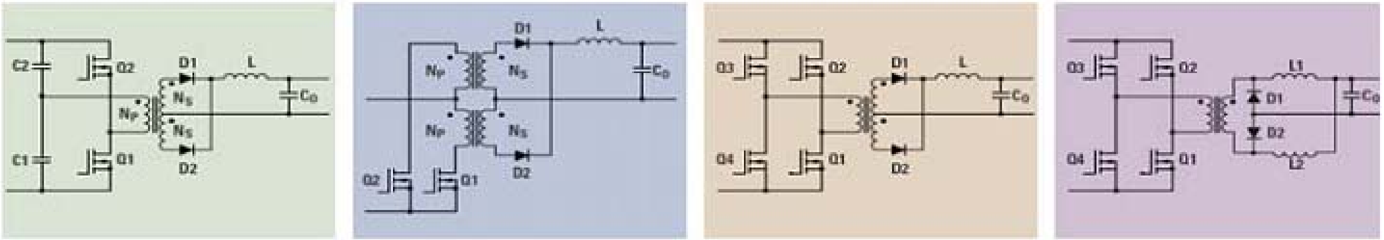			
Ideal Transfer Function*	$\frac{V_{OUT}}{V_{IN}} = \left(\frac{N_S}{N_P}\right) \times \left(\frac{t_{ON}}{T_P}\right) = \left(\frac{N_S}{N_P}\right) \times D$	$\frac{V_{OUT}}{V_{IN}} = 2 \times \left(\frac{N_S}{N_P}\right) \times \left(\frac{t_{ON}}{T_P}\right) = 2 \times \left(\frac{N_S}{N_P}\right) \times D$	$\frac{V_{OUT}}{V_{IN}} = 2 \times \left(\frac{N_S}{N_P}\right) \times \left(\frac{t_{ON}}{T_P}\right) = 2 \times \left(\frac{N_S}{N_P}\right) \times D$	$\frac{V_{OUT}}{V_{IN}} = 2 \times \left(\frac{N_S}{N_P}\right) \times \left(\frac{t_{ON}}{T_P}\right) = 2 \times \left(\frac{N_S}{N_P}\right) \times D$
Drain Current*	$I_{Q1}\ (max) = \left(\frac{N_S}{N_P}\right) \times I_{OUT}$	$I_{Q1}\ (max) = \left(\frac{N_S}{N_P}\right) \times I_{OUT}$	$I_{Q1}\ (max) = \left(\frac{N_S}{N_P}\right) \times I_{OUT}$	$I_{Q1}\ (max) = \left(\frac{N_S}{N_P}\right) \times I_{OUT}$
Drain Voltage*	$V_{DS} = V_{IN}$	$V_{DS} = 2 \times V_{IN}$	$V_{DS} = V_{IN}$	$V_{DS} = V_{IN}$
Average Diode Current*	$I_{D1} = \left(I_{OUT} \times D\right) + \frac{I_{OUT}}{2} \times (1\text{-}2\,D)$	$I_{D1} = \left(I_{OUT} \times D\right) + \frac{I_{OUT}}{2} \times (1\text{-}2\,D)$	$I_{D1} = \left(I_{OUT} \times D\right) + \frac{I_{OUT}}{2} \times (1\text{-}2\,D)$	$I_{D1} = \frac{1}{2} \times I_{OUT}$
Diode Reverse Voltage*	$V_{D1} = V_{IN} \times \left(\frac{N_S}{N_P}\right)$	$V_{D1} = V_{IN} \times \left(\frac{N_S}{N_P}\right) \times 2$	$V_{D1} = V_{IN} \times \left(\frac{N_S}{N_P}\right) \times 2$	$V_{D1} = V_{IN} \times \left(\frac{N_S}{N_P}\right)$
Voltage and Current Waveforms	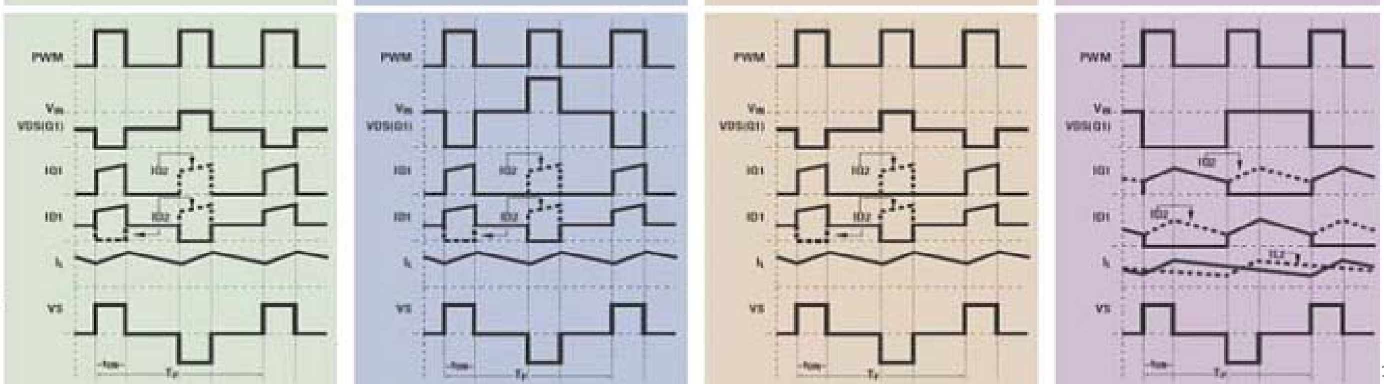			

* Excludes ripple current and output diode voltage drop. Continuous conduction mode shown (unless otherwise noted). For

Insulated resonant dc-dc converters

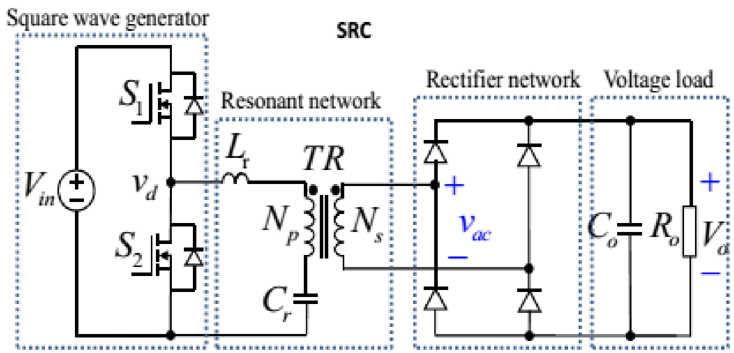

(a) Circuit configuration

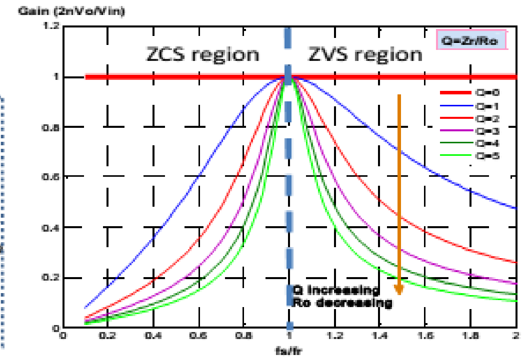

(b) Gain curves

Fig.1.7 Half bridge SRC

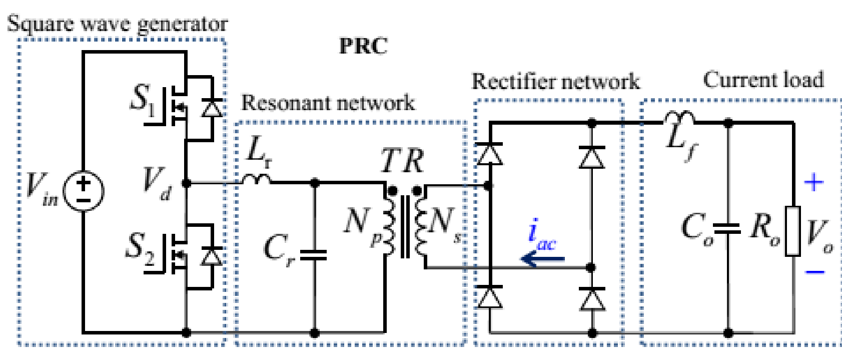

(a) Circuit configuration

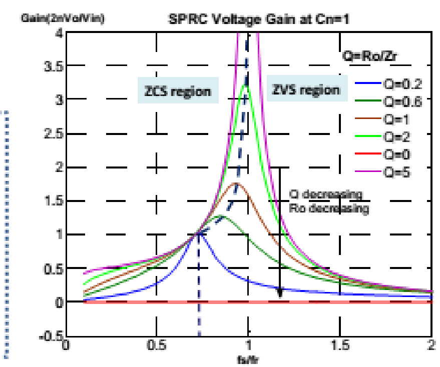

(b) Gain curves

Fig.1.8 Half Bridge PRC

Insulated resonant dc-dc converters

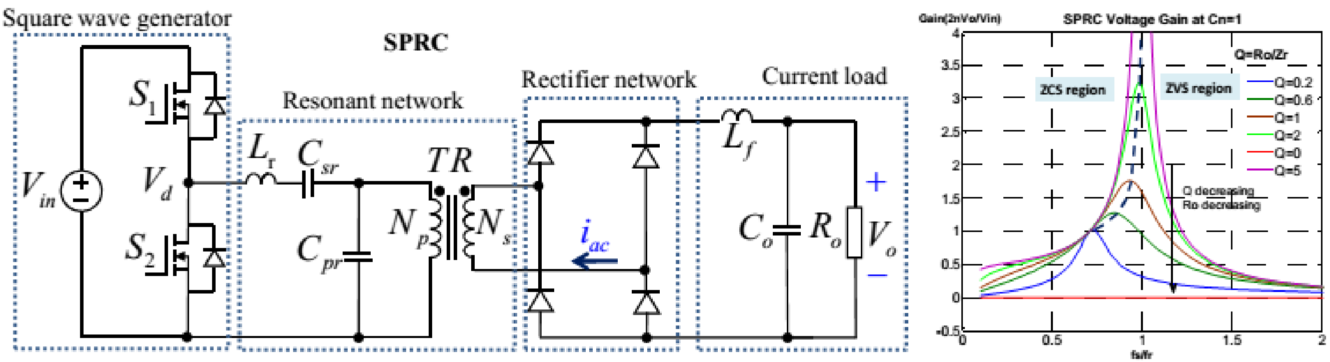

(a) Circuit configuration (b) Gain curves

Fig.1.9 Half Bridge SPRC

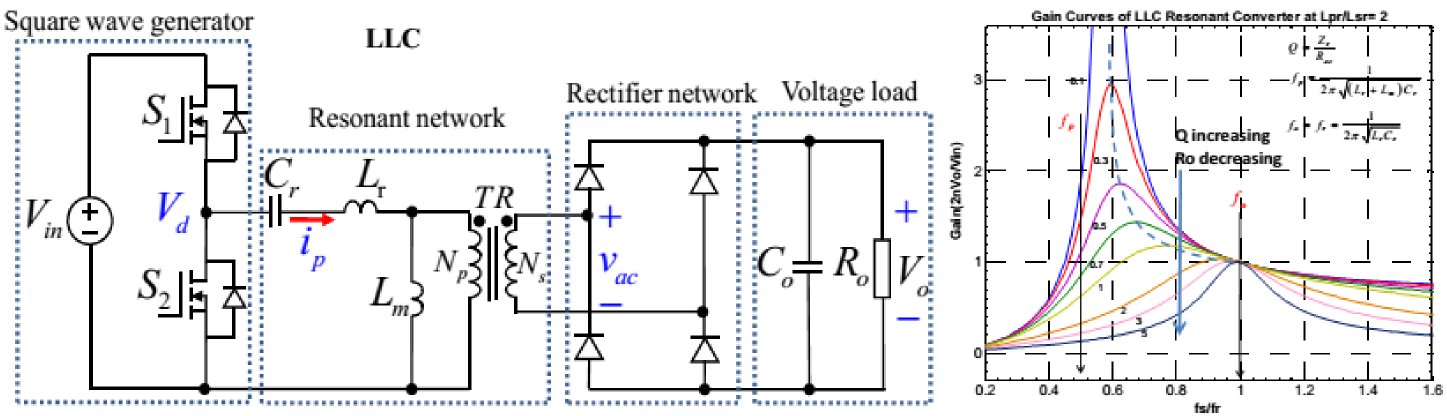

(a) Circuit configuration (b) Gain curves

Fig.1.10 Half Bridge LLC Resonant Converter

Most popular EV topologies

1) A soft-switched full-bridge (FB) DC-DC converter;
2) An asymmetrically controlled zero-voltage switched (ZVS) half-bridge (HB) converter;
3) An active-clamped soft-switched forward converter.

J. Zhang, C.Y. Lin, X. Zhuang, K. Rinne, D. Sable, G. Hua and F.C. Lee, "Design of A 4kw On-Board Battery Charger for Electric Vehicle," Annual VPEC Seminar, September 1995.

W. Andreycak, "Active Clamp and Reset Technique Enhances Forward Converter Performance," in Unitrode Power Supply Design Seminar, 1994.

T. Ninomiya, N. Matsumoto, M. Nakahara, and K. Harada, "Static And Dynamic analysis of Zero-Voltage-Switched Half-Bridge Converter with PWM Control," IEEE PESC, 1991.

INEP

Phase-shifted Full-bridge ZVS

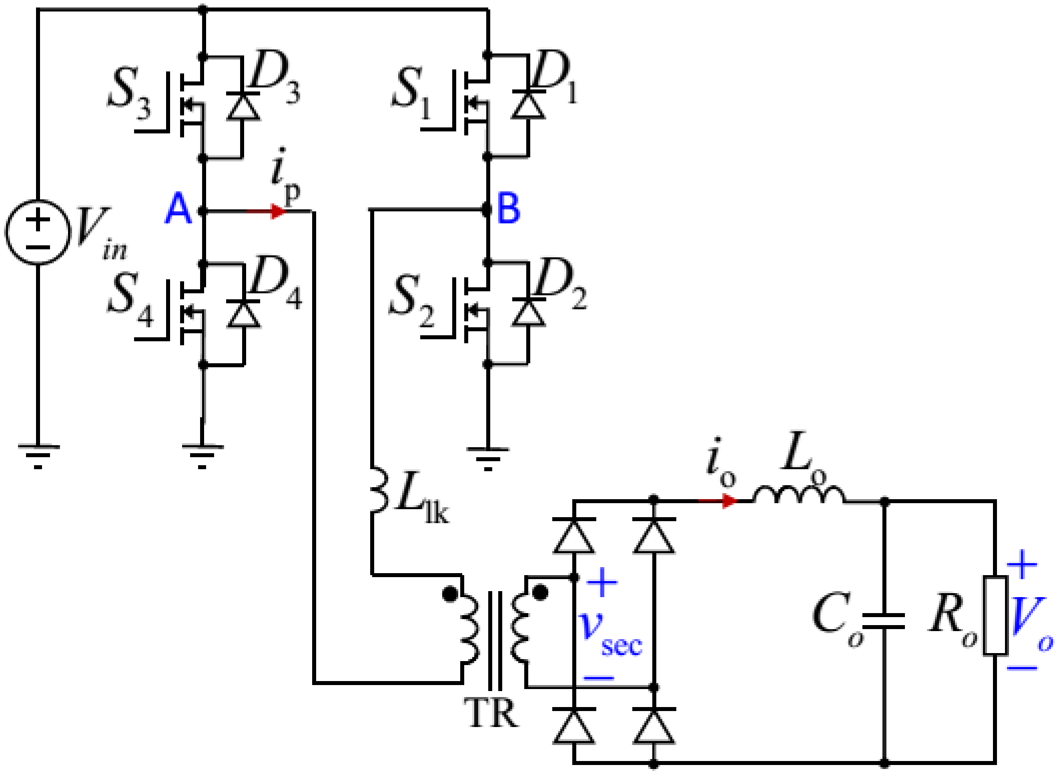

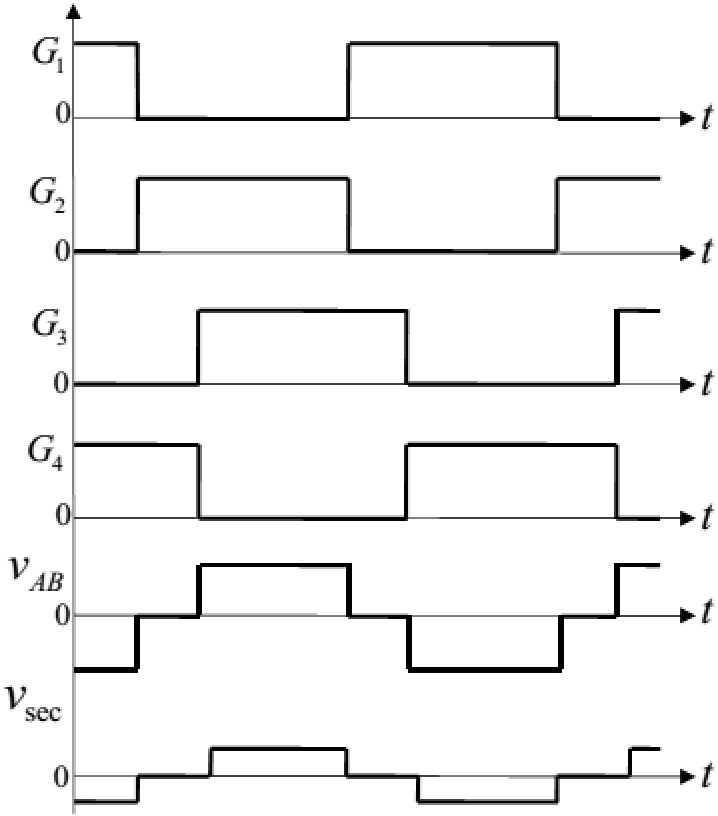

Phase-shifted Full-bridge ZVS

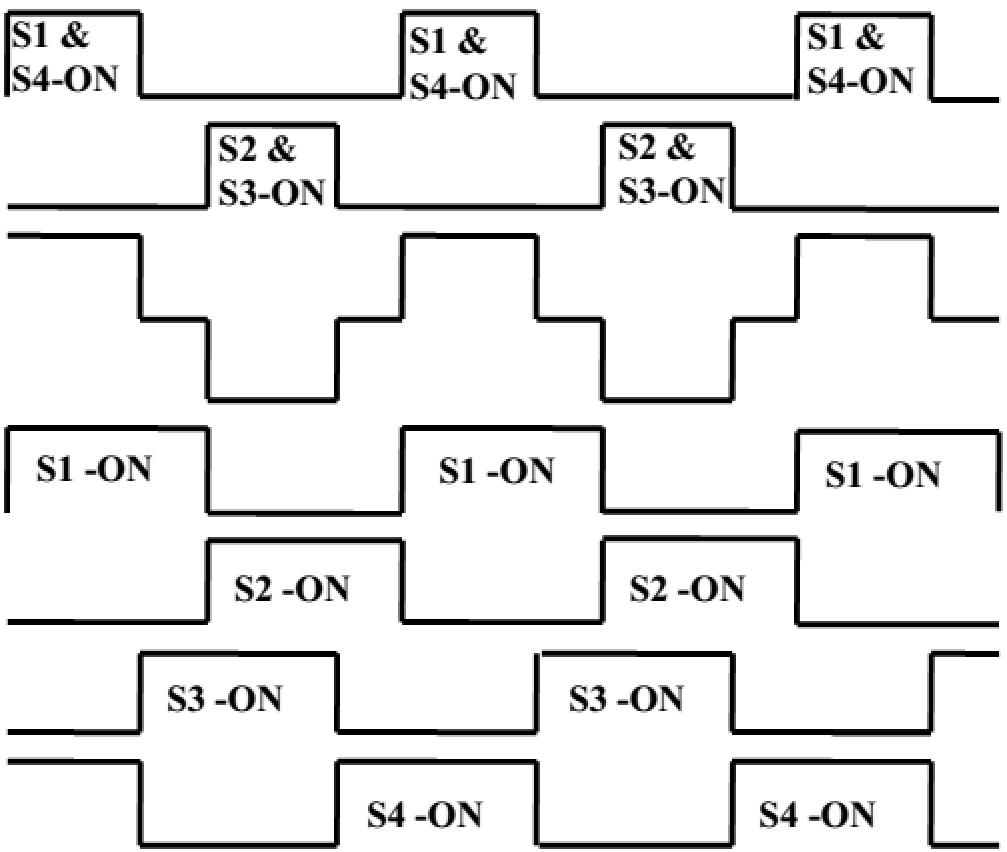

Full bridge topology switching control

Transformer primary winding voltage

Phase shifted FB-ZVS PWM DC/DC converter switching control

Phase-shifted Full-bridge ZVS

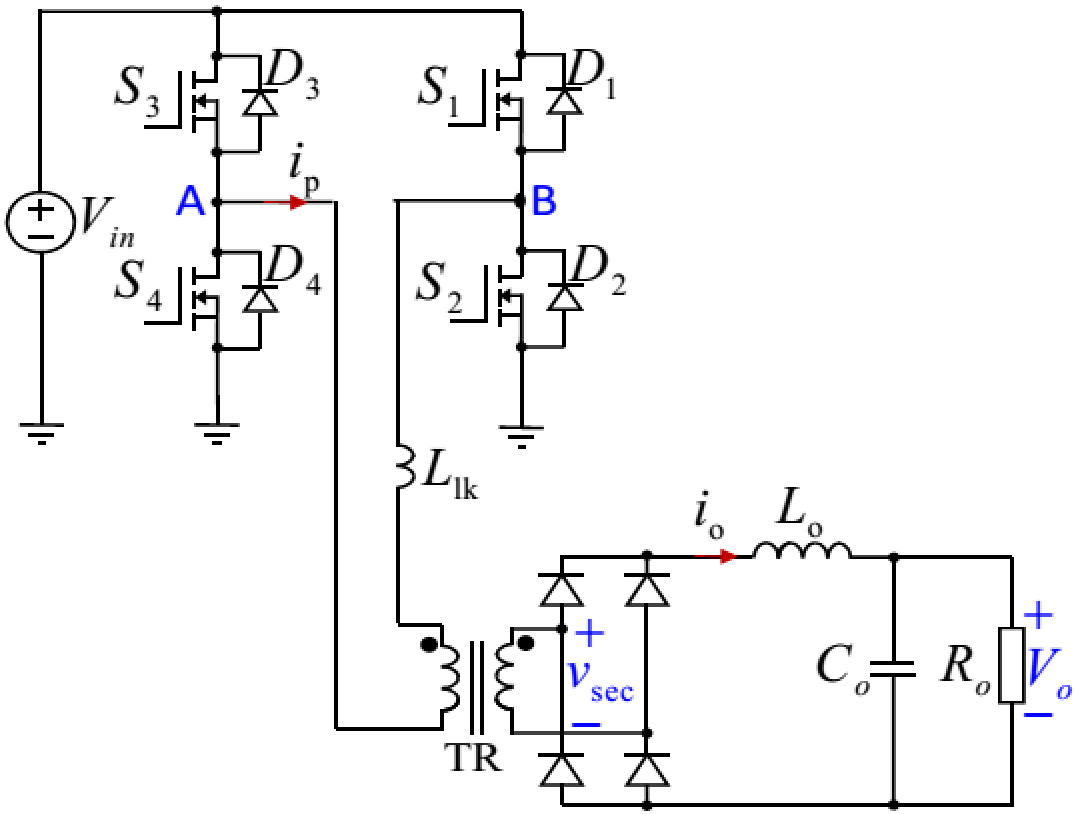

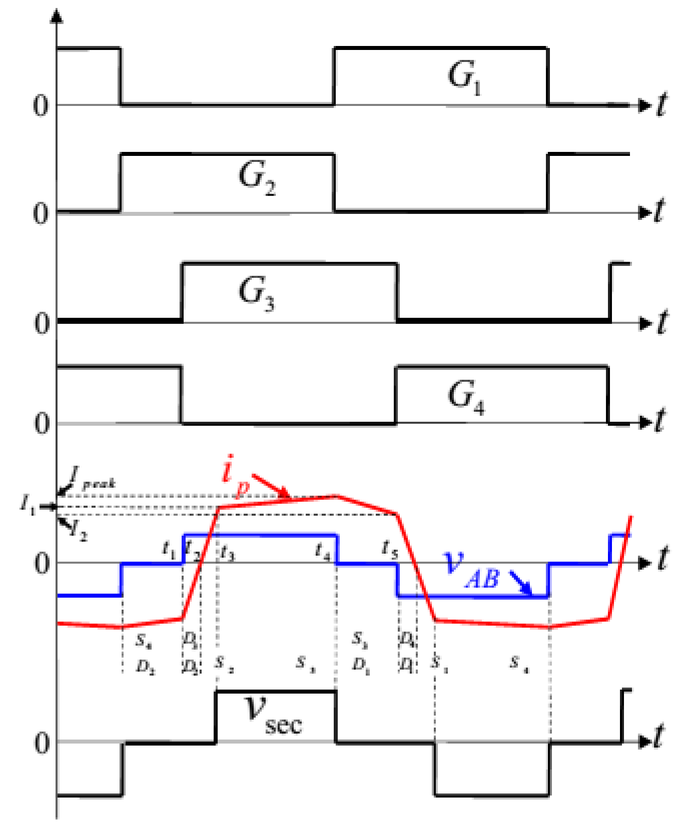

Phase-shifted Full-bridge ZVS

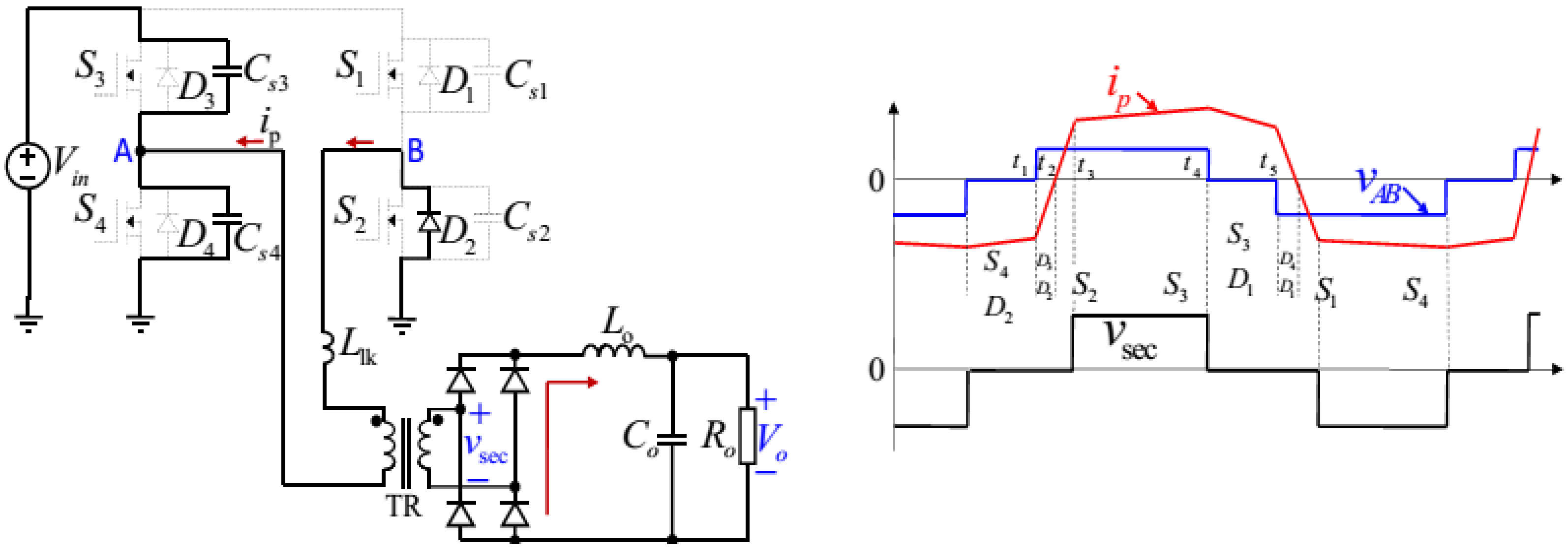

Fig.2.4 Mode1: at time t1

Phase-shifted Full-bridge ZVS

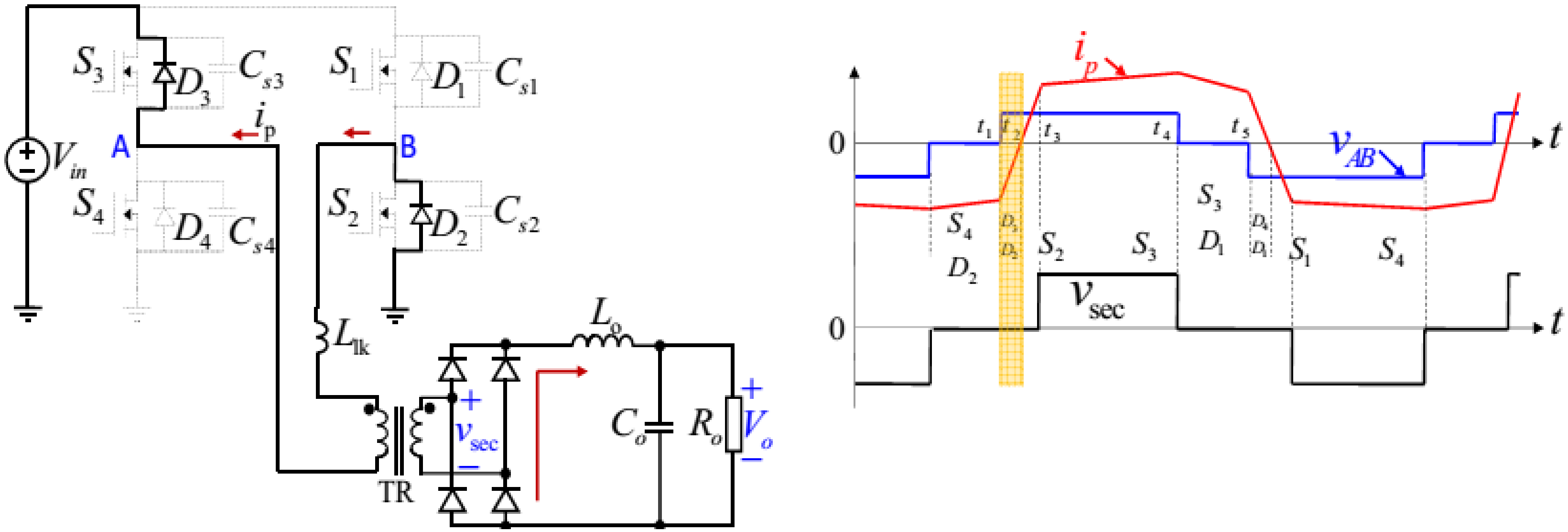

Fig.2.5 Mode2: at interval t_1~t_2

Phase-shifted Full-bridge ZVS

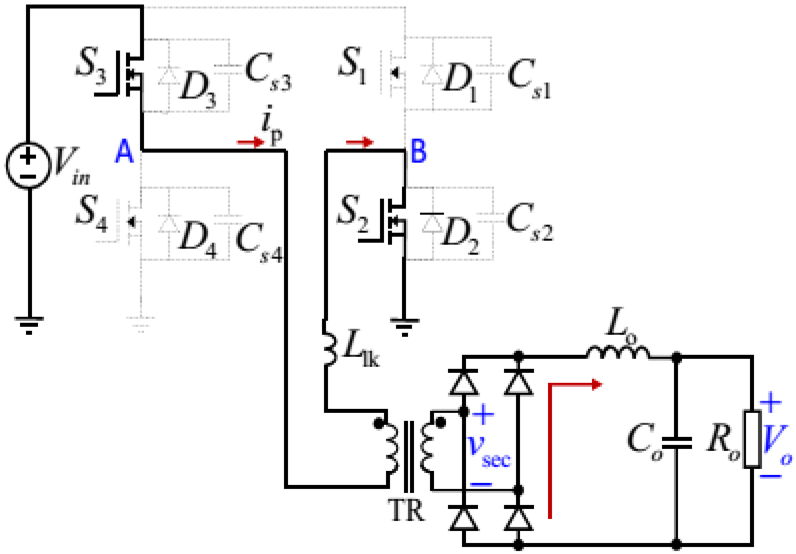

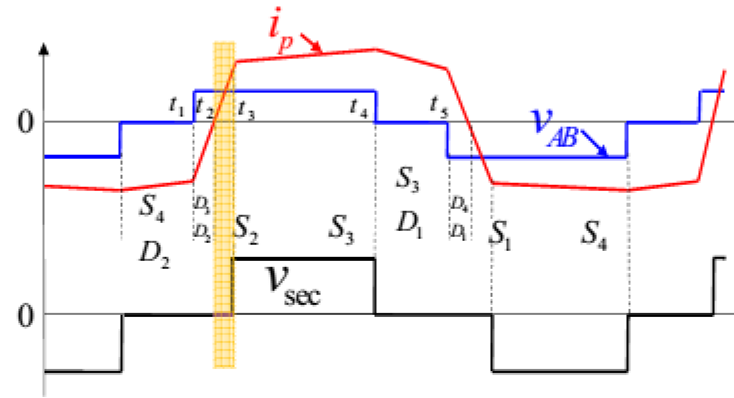

Fig.2.6 Mode3: at interval t2~t3

Phase-shifted Full-bridge ZVS

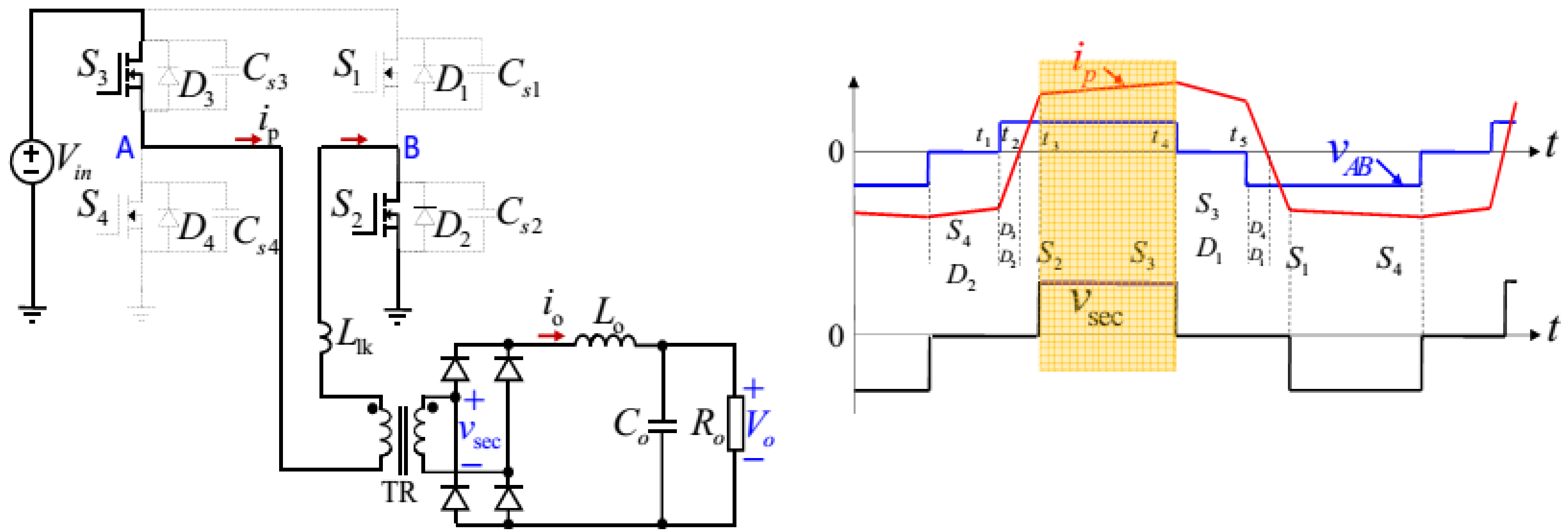

Fig.2.7 Mode4: at interval $t_3 \sim t_4$

Phase-shifted Full-bridge ZVS

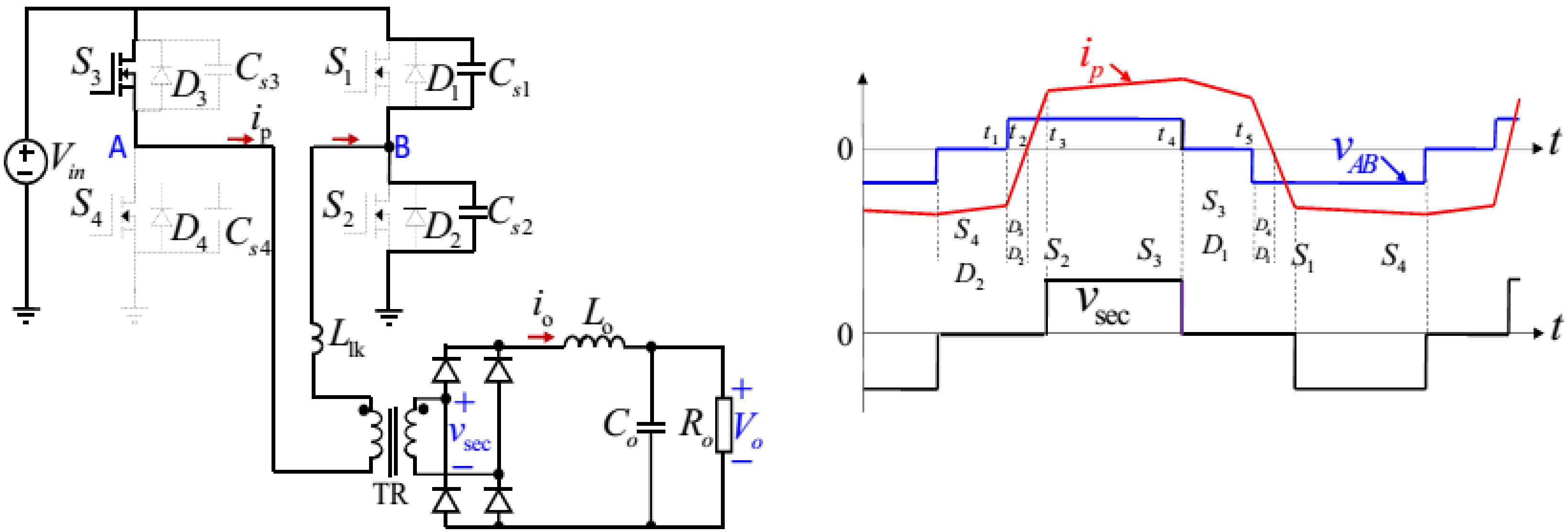

Fig.2.8 Mode5: at time t_4

Phase-shifted Full-bridge ZVS

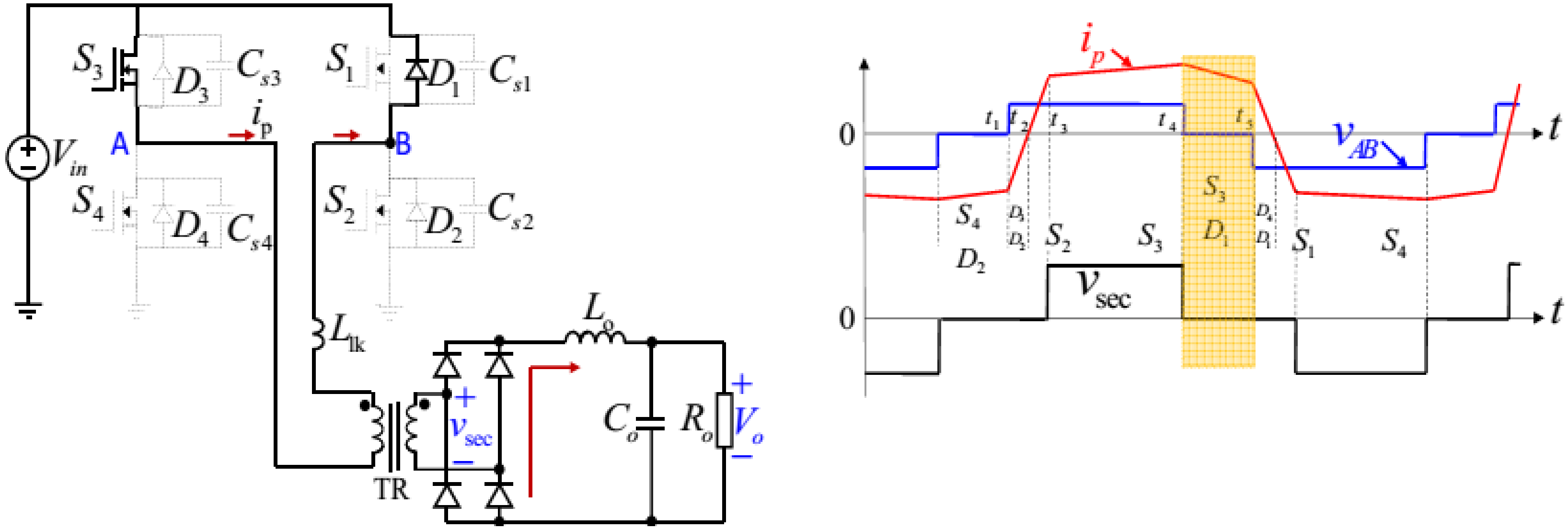

Fig.2.9 Mode6: interval t_4~t_5

ZVS on S_3-S_4 (legging leg)

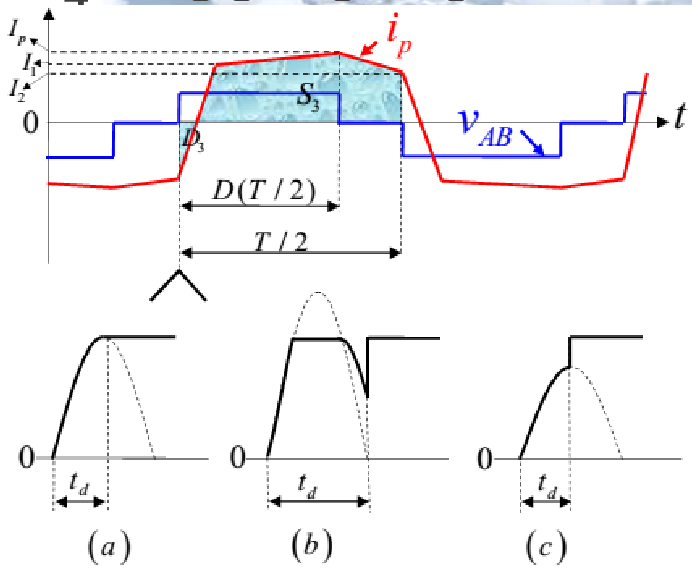

$$I_{ZVS} = \sqrt{\frac{C_{s3} // C_{s4} + C_{tr}}{L_{lk}}} V_{in}$$

$$\omega_r = \frac{1}{\sqrt{L_{lk}\left(C_{s3} // C_{s4}\right)}}$$

$$t_d^{\max} = \frac{1}{4} T = \frac{\pi}{2} \sqrt{L_{lk}\left(C_{s3} // C_{s4} // C_{tr}\right)}$$

Fig.2.10 Detail of the rising edge of the voltage across the switch of lagging leg

where

(a) corresponds to the limit case when the energy in L_{lk} is equal to the energy required to charge the capacitances.

(b) corresponds to the case when the energy in L_{lk} is larger than the energy required to charge/discharge the capacitors. The switch output capacitances are charged/discharged in less than one fourth of the resonant period, and the voltage is clamped to the input voltage.

(c) corresponds to the case when the energy in L_{lk} is not sufficient to charge/discharge the output capacitances, and ZVS is lost.

ZVS on S_1-S_2 (leading leg)

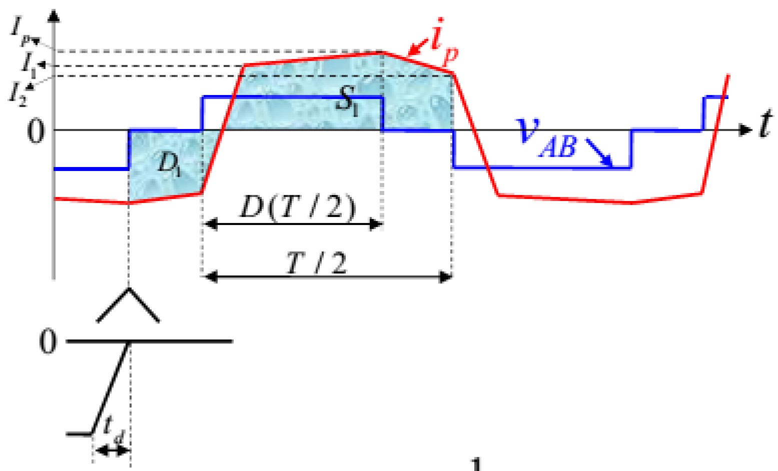

$$I_2 = C_s \frac{dv}{dt}$$

$$dv = V_{in}$$

$$\frac{1}{2}\left(L_{o\_p} + L_{lk}\right) I_2^{\,2} > \frac{1}{2}\left(C_{s1} // C_{s2}\right) V_{in}^{\,2} + \frac{1}{2} C_{tr} V_{in}^{\,2}$$

Phase-shifted Full-bridge ZVS

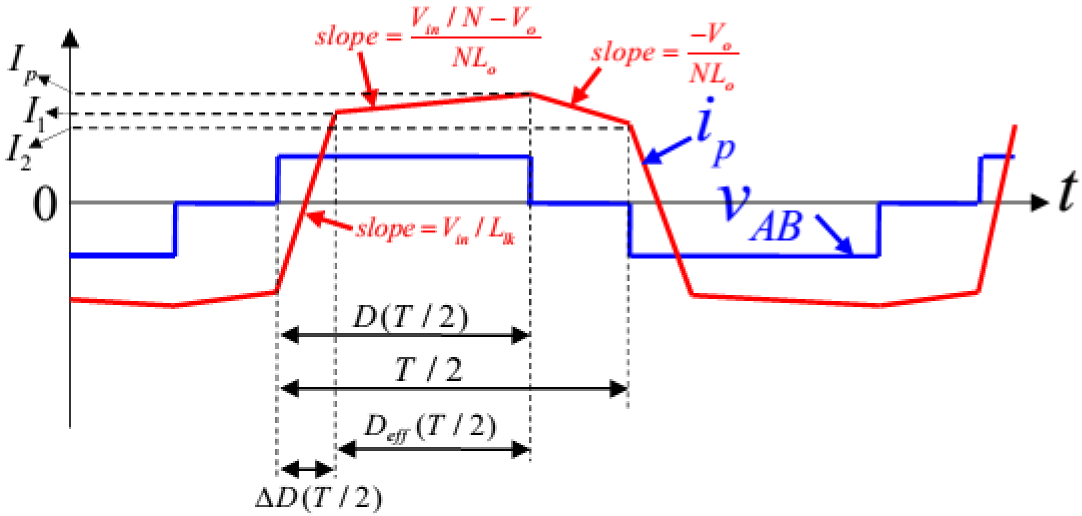

$$
\begin{cases}
D_{\sec} = \dfrac{NV_o}{V_{in}} \\
D_{eff} = D_{\sec} = D_{pri} - \Delta D \\
\Delta D = (I_1 + I_2) / \left(\dfrac{V_{in}}{L_{lk}} \dfrac{T}{2} \right) = D_{\sec} \dfrac{4L_{lk}}{N^2 R_o} f_s
\end{cases}
$$

Phase-shifted Full-bridge ZVS

- Low load ZVS is hard to achieve and depends on L_{lk}
- If L_{lk} is large, duty-cycle is lost
- Maximize N_s/N_p reduces rectifier voltages, but requires higher L_{lk}
- There is circulating current
- ZVS occurs at the primary, but there are oscillations at the secondary (reverse recovery)

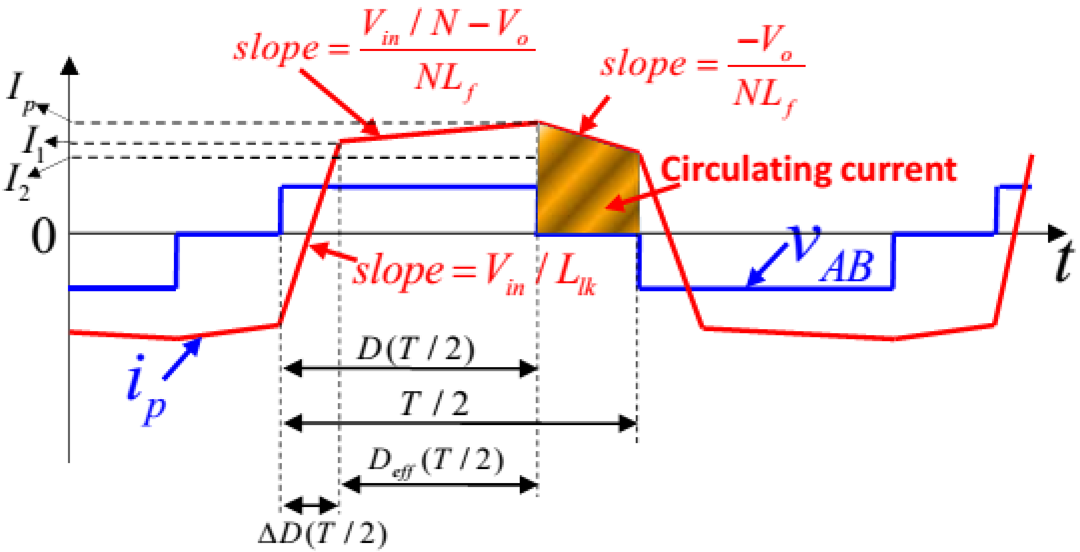

$$I_1 \geq I_{ZVS} = \sqrt{\frac{C_{s3} // C_{s4} + C_{tr}}{L_{lk}}} V_{in}$$

$$\Delta D = D_{sec} \frac{4L_{lk}}{N^2 R_o} f_s$$

LLC resonant converter

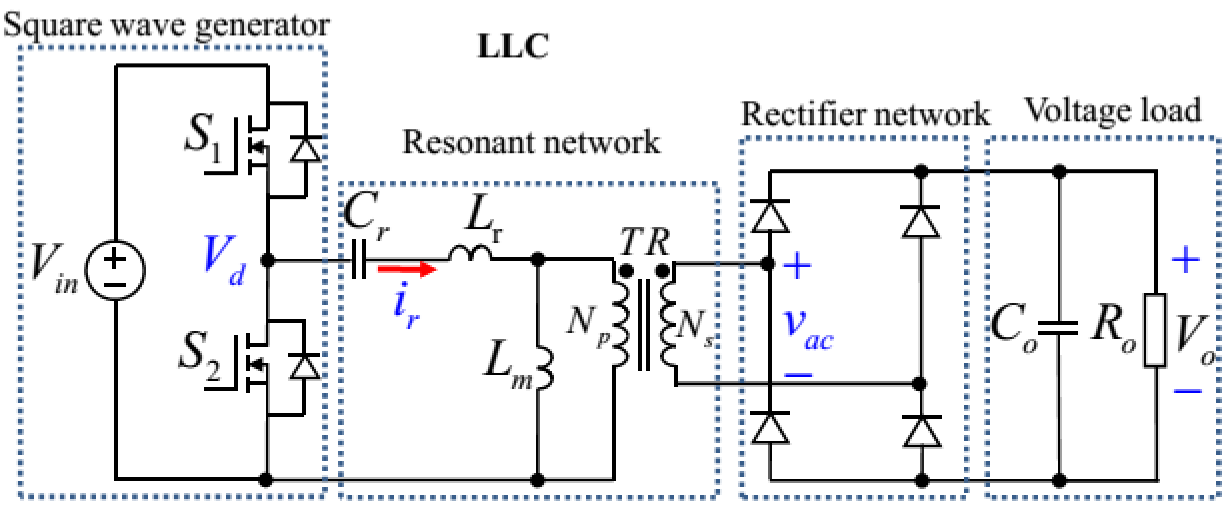

Fig.2.14 Half Bridge LLC Resonant Converter

LLC resonant converter

- Equivalent circuit

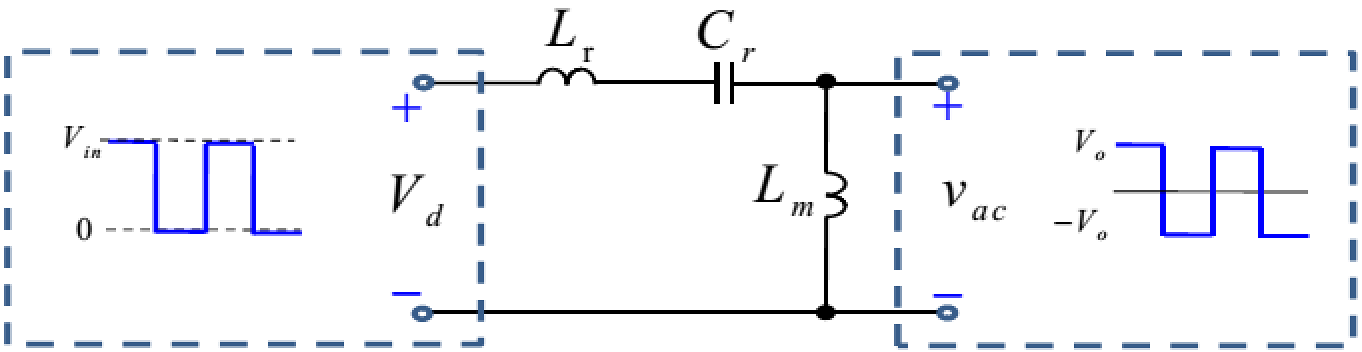

LLC resonant converter

- Primary-side equivalent circuit

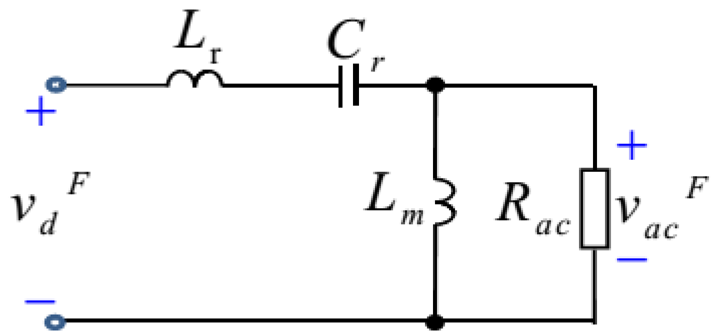

- Secondarry- side equivalent circuit

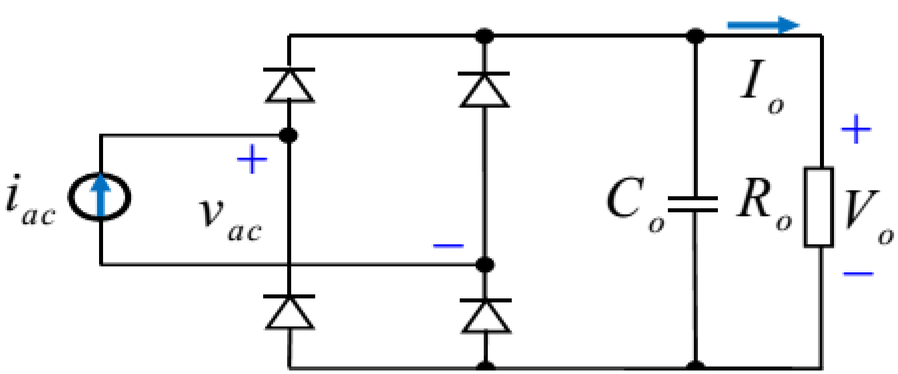

LLC resonant converter

- Primary-side equivalent circuit

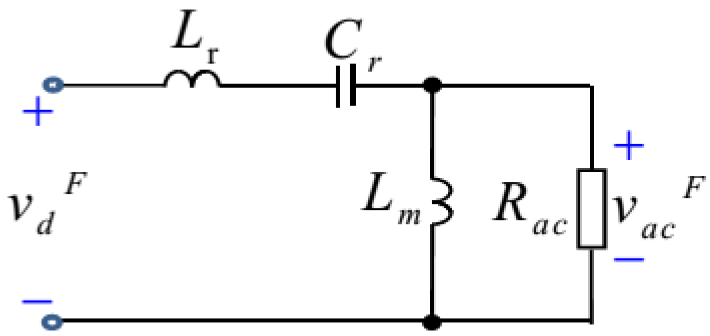

$$R_{ac} = \frac{V_{ac}^F}{i_{ac}} = \frac{8}{\pi^2} R_o$$

$$n = N_p / N_s$$

$$R_{ac} = \frac{V_{ac}^F}{i_{ac}} = \frac{8n^2}{\pi^2} R_o$$

LLC resonant converter

- Dc gain

$$M = \frac{V_o}{V_{in}/2} = \frac{v_{ac,pk}^{\;F}}{v_{d,pk}^{\;F}} = \frac{\frac{4}{\pi}V_o}{\frac{4}{\pi}\frac{V_{in}}{2}} = \left| \frac{\left(\frac{\omega}{\omega_o}\right)^2 (m-1)}{\left(\frac{\omega^2}{\omega_p^{\;2}}-1\right) + j\frac{\omega}{\omega_o}\left(\frac{\omega^2}{\omega_o^{\;2}}-1\right)(m-1)Q} \right|$$

$$L_p = L_m + L_r$$

$$\omega_o = \frac{1}{\sqrt{L_r C_r}}$$

$$m = \frac{L_p}{L_r}$$

$$\omega_p = \frac{1}{\sqrt{L_p C_r}}$$

$$Z_r = \sqrt{\frac{L_r}{C_r}}$$

$$Q = \frac{Z_r}{R_{ac}}$$

INEP

LLC resonant converter

- Gain

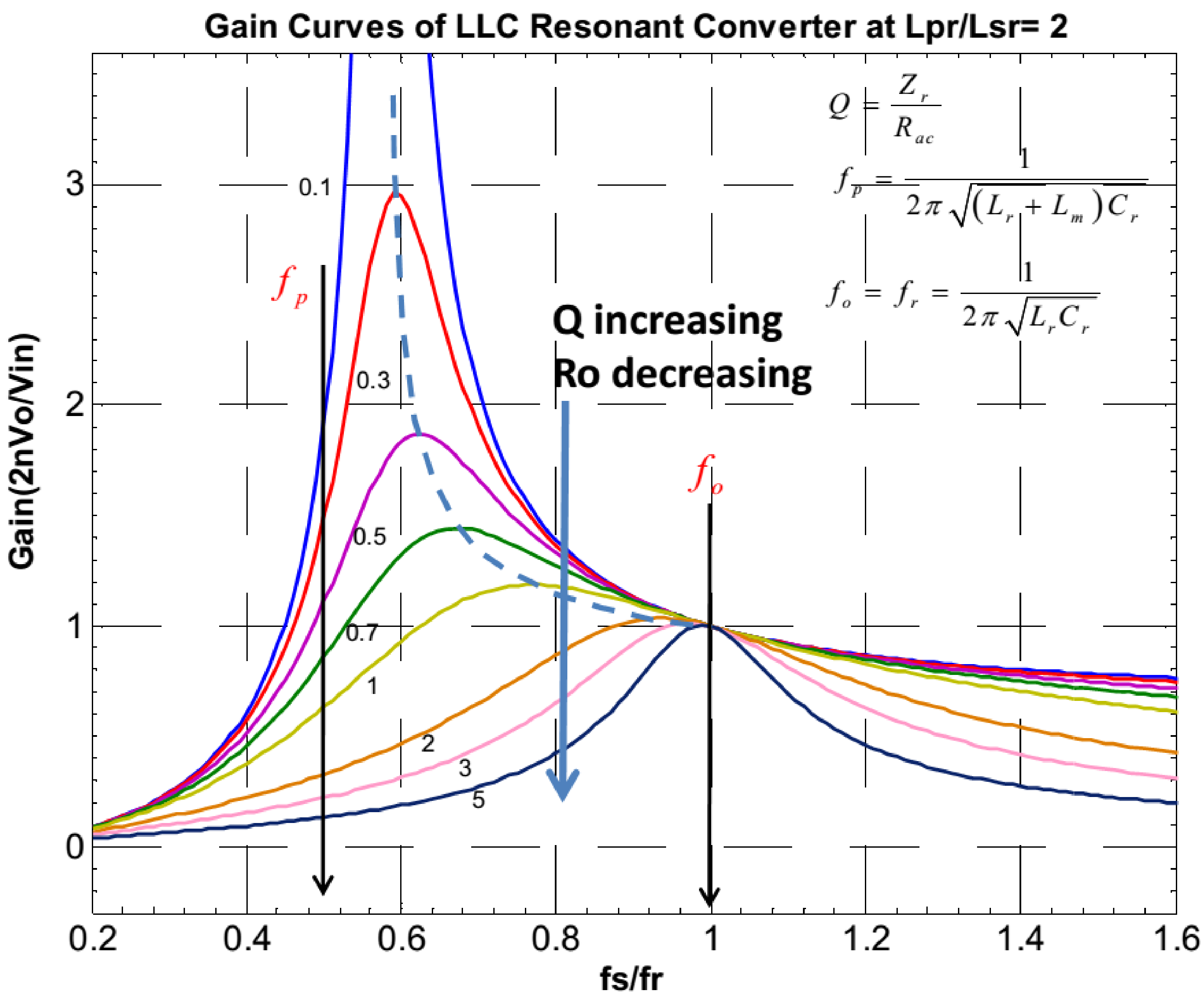

LLC resonant converter

- Gain

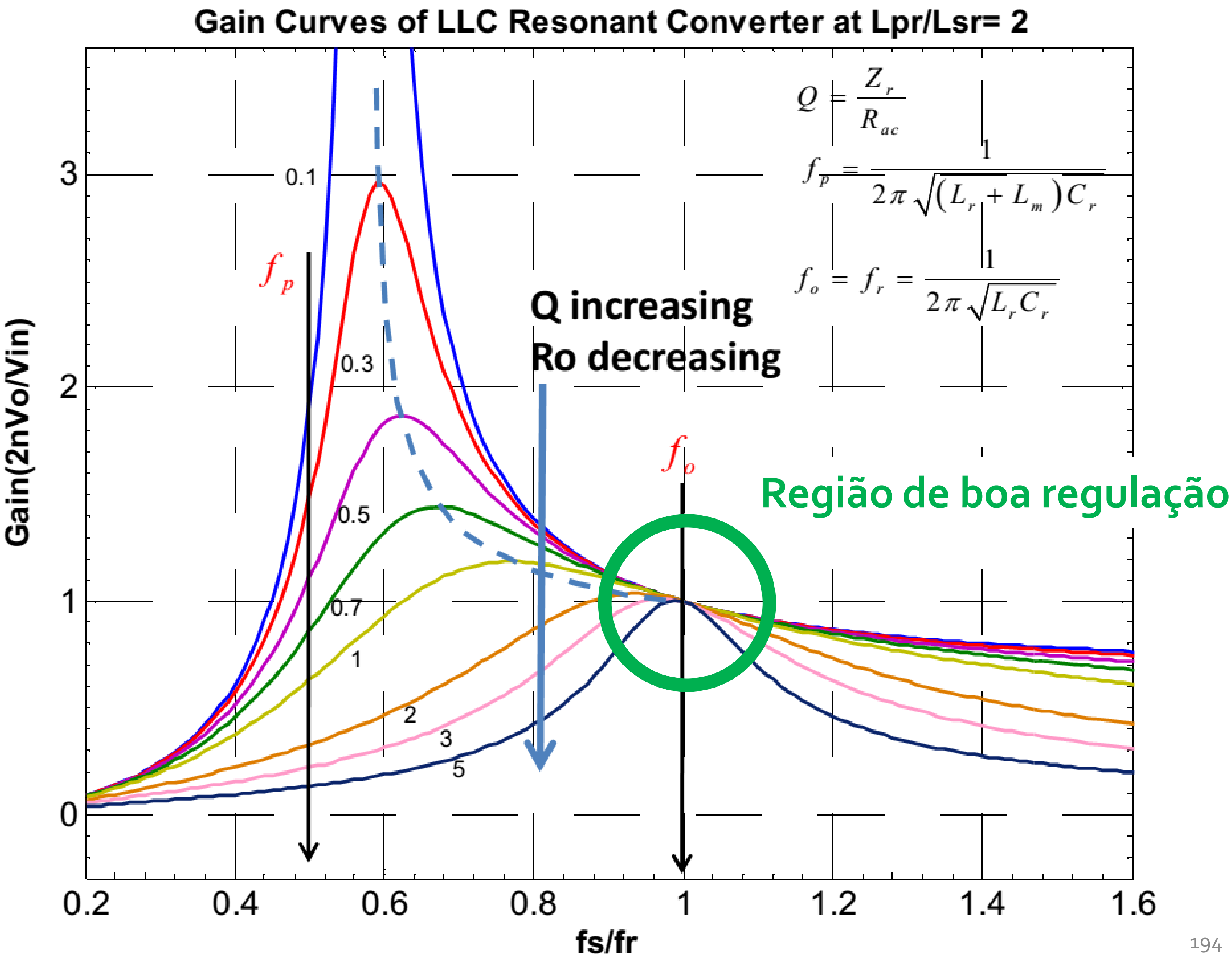

LLC resonant converter

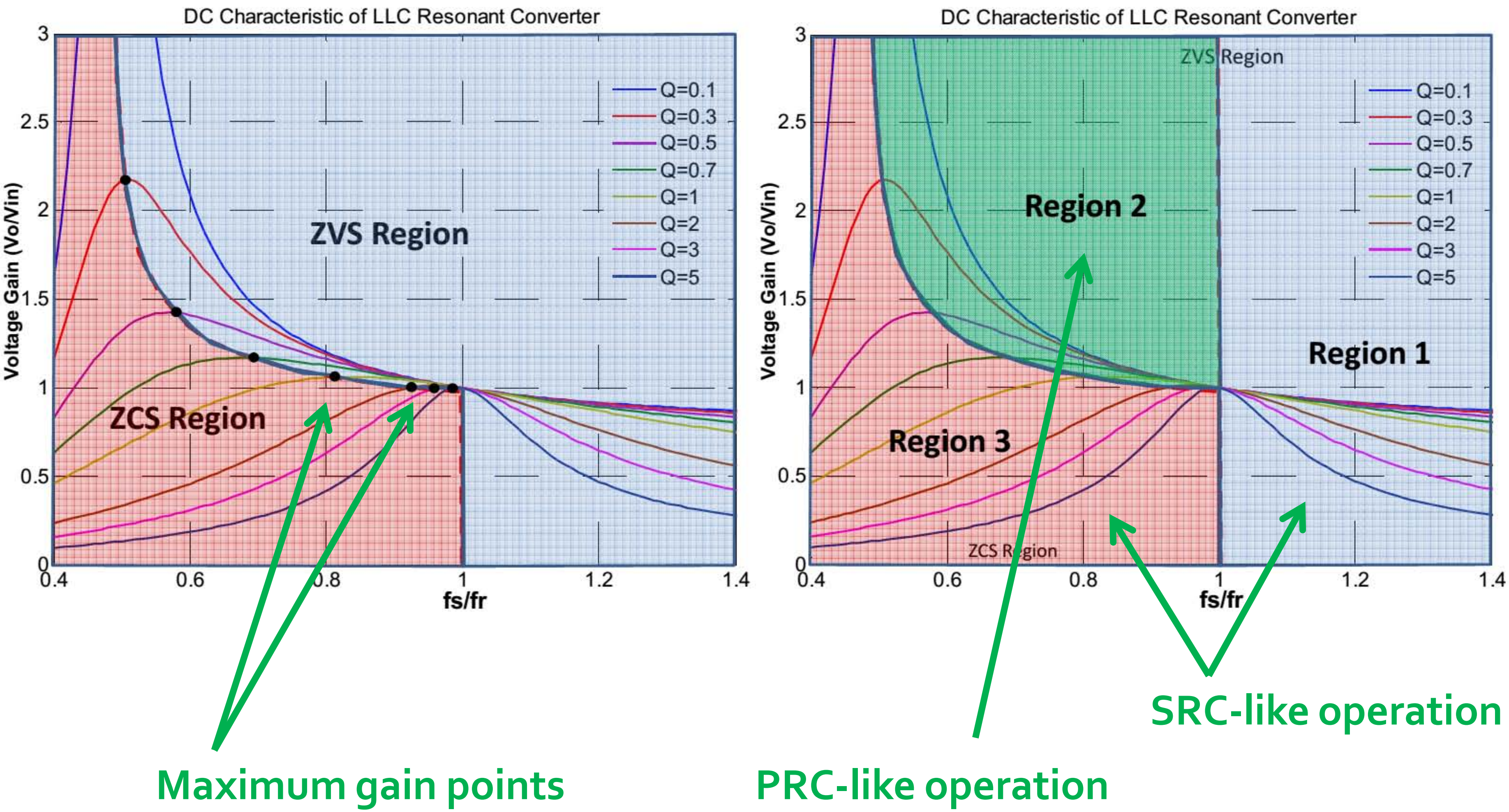

LLC resonant converter

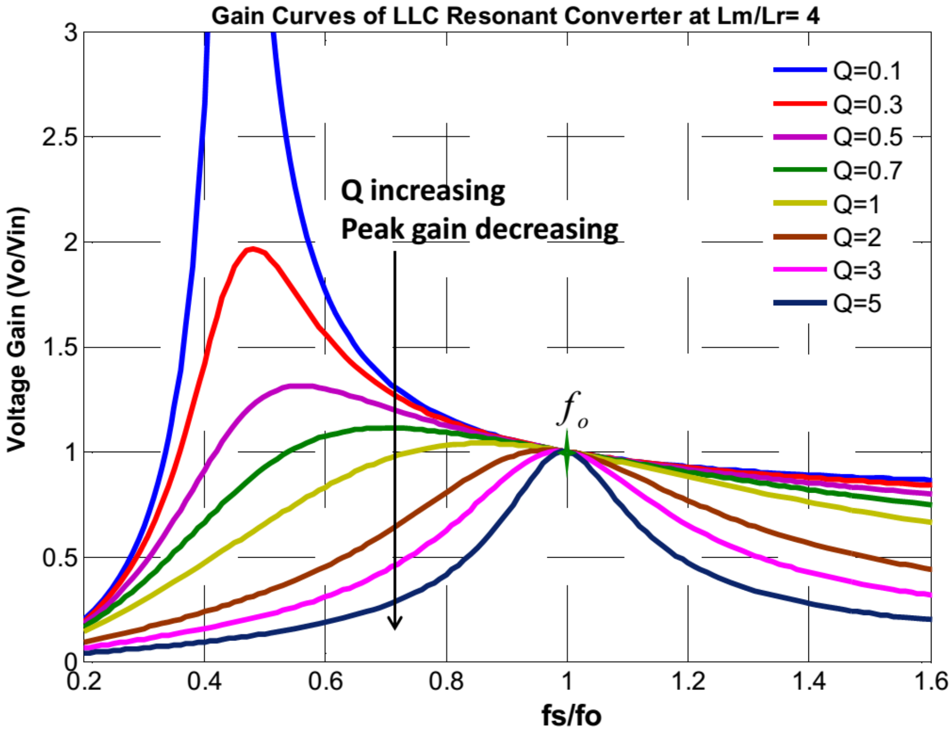

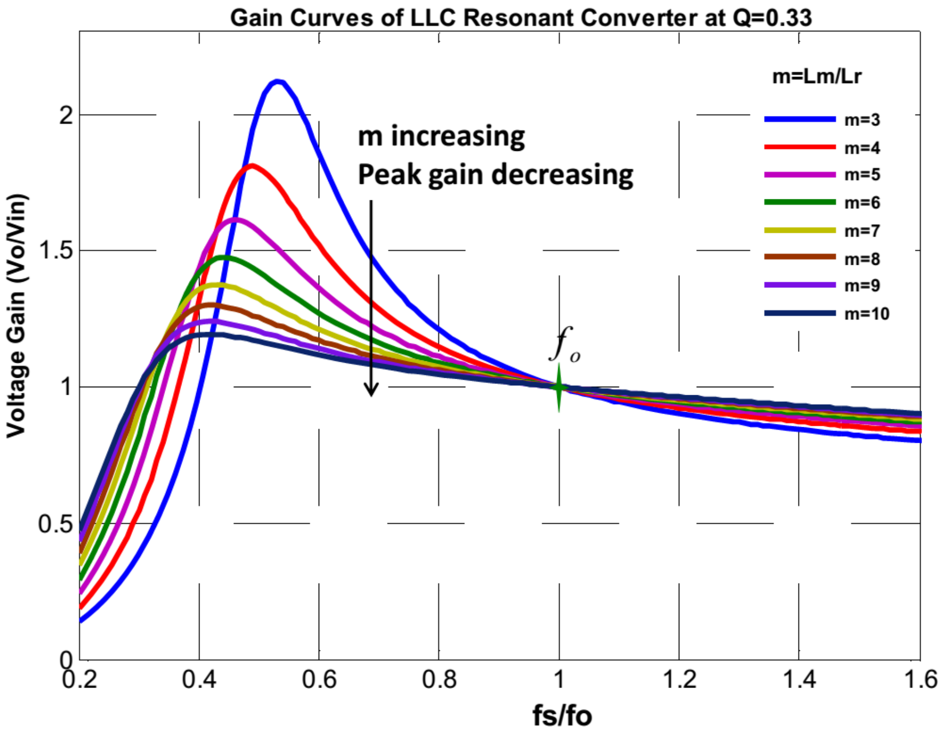

LLC resonant converter

- ZVS operation is preferrable

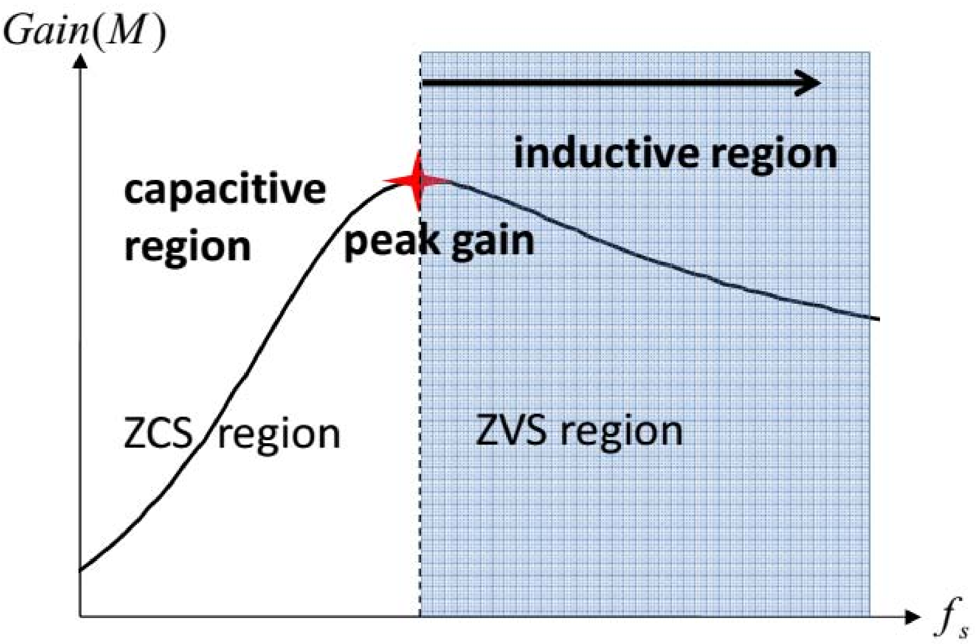

- The MOSFET body-diode suffers reverse recovery at the capacitive region

LLC resonant converter

- Ressonance point operation

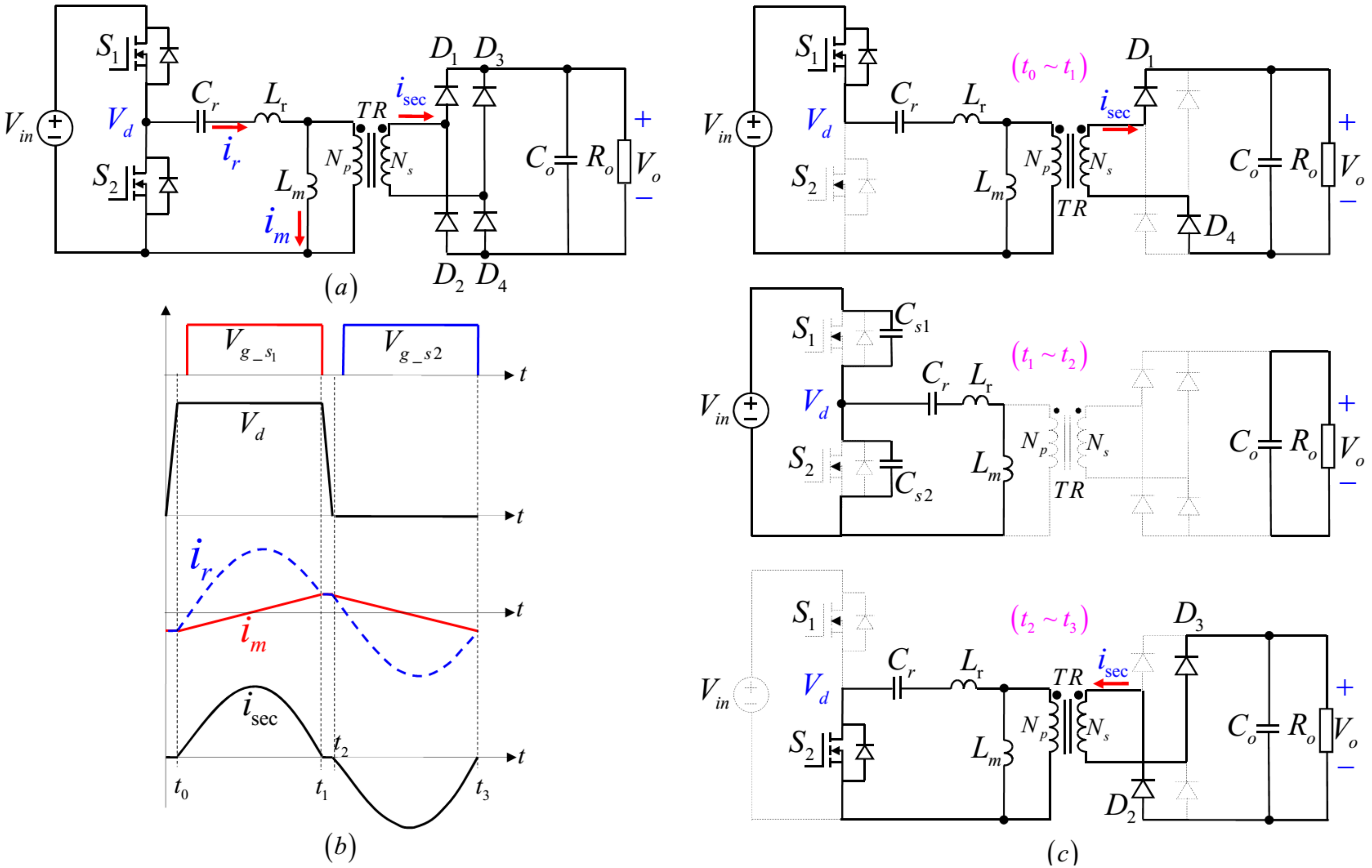

LLC resonant converter

- Below resonance operation

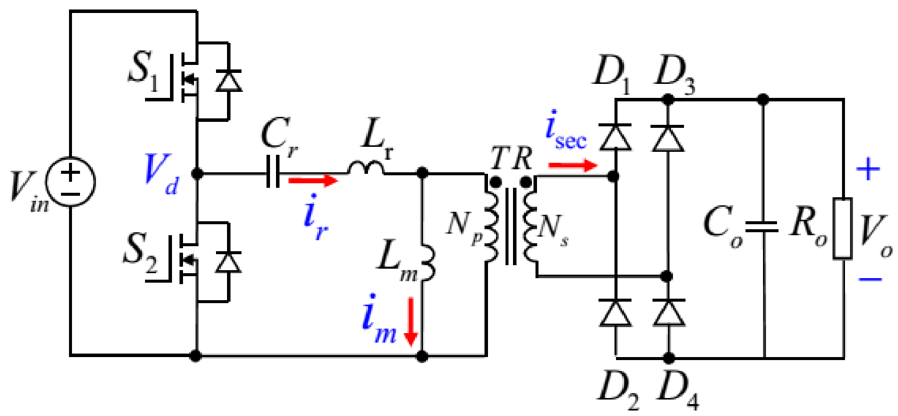

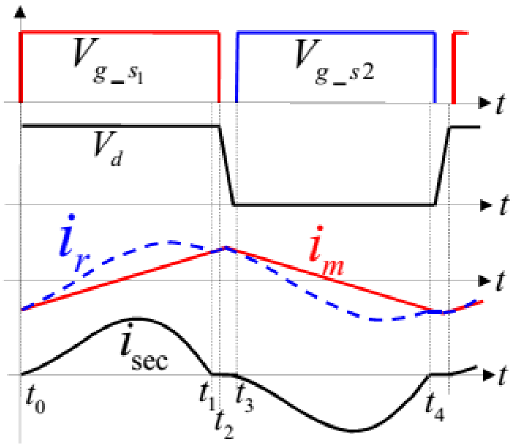

LLC resonant converter

- Below resonance operation

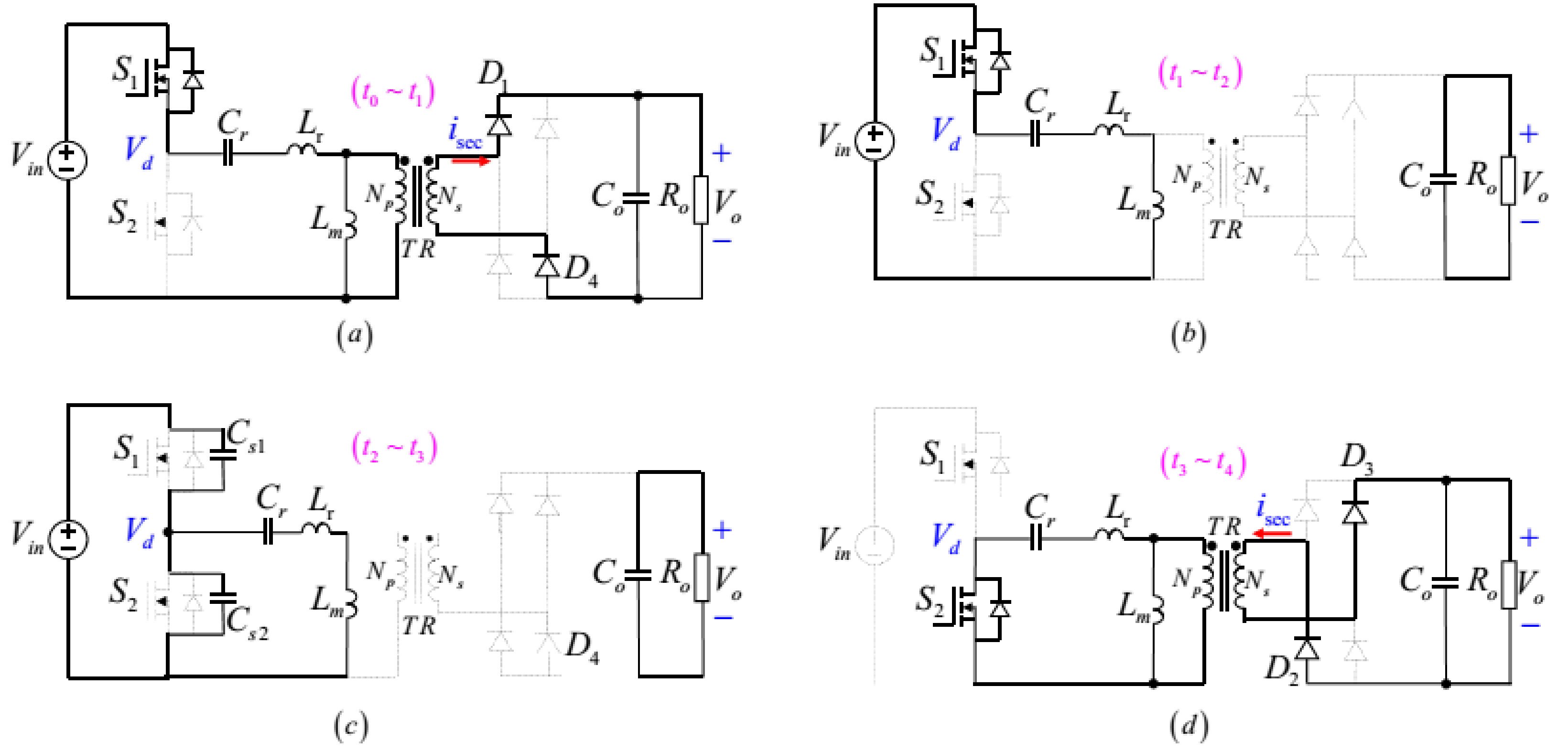

LLC resonant converter

- Above resonance operation

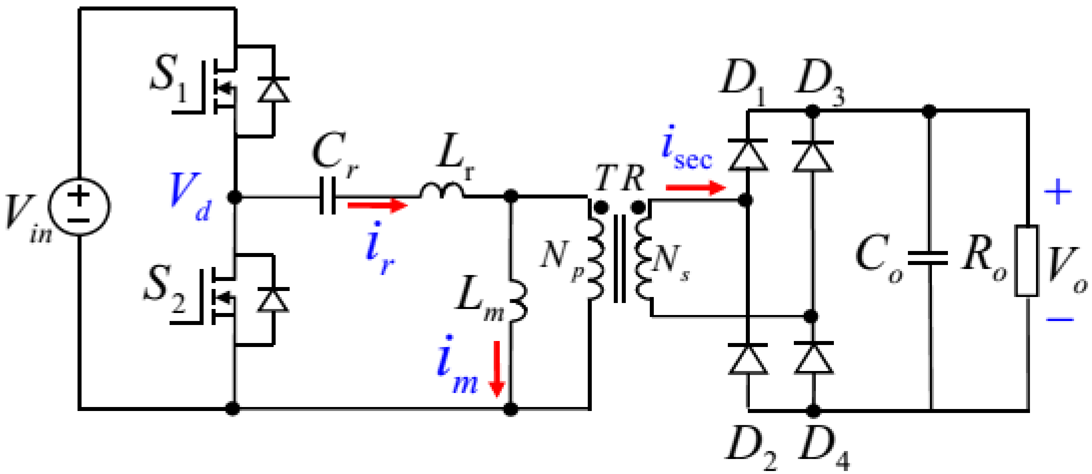

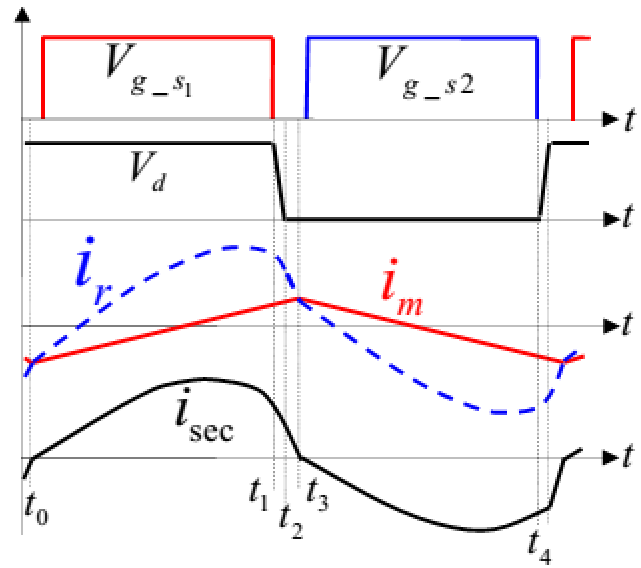

LLC resonant converter

- Above resonance operation

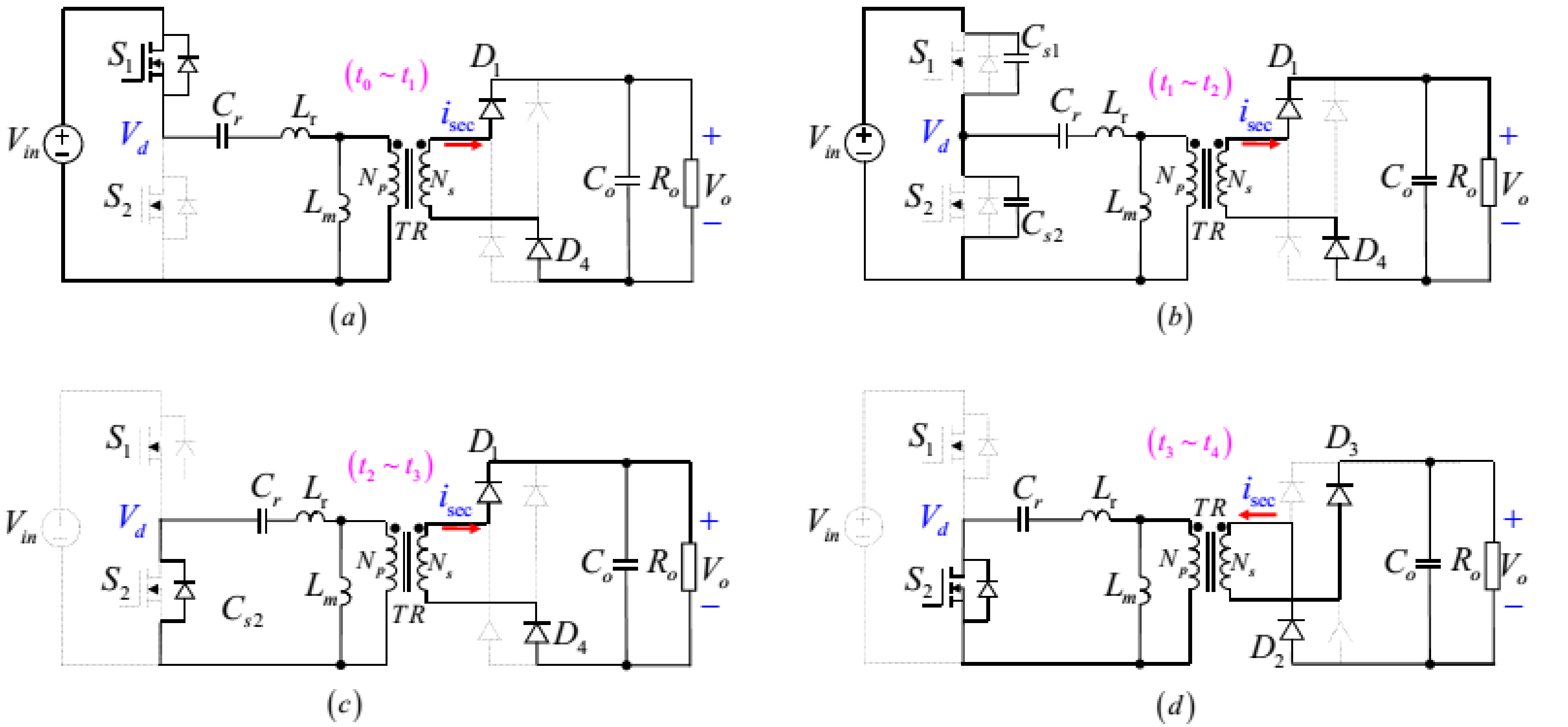

LLC resonant converter

- Below resonance operation leaads to soft-switching at the secondary switches, but circulating current rises
- Increasing ***m*** leads to higher ***fs*** variation
- Reducing ***m*** reduces L_M and increases the circulating current and increases P_{cond} e P_{sw}
- The product $m{\cdot}Q$ is fix when L_M and f_s is fixed
- Reduce ***m*** and increase Q reduces f_s variation, but reduces gain
- L_r and C_r can vary, but low C_r values result in low impedance and higher short-circuit current and, thus, higher f_s

Power flow in an EV

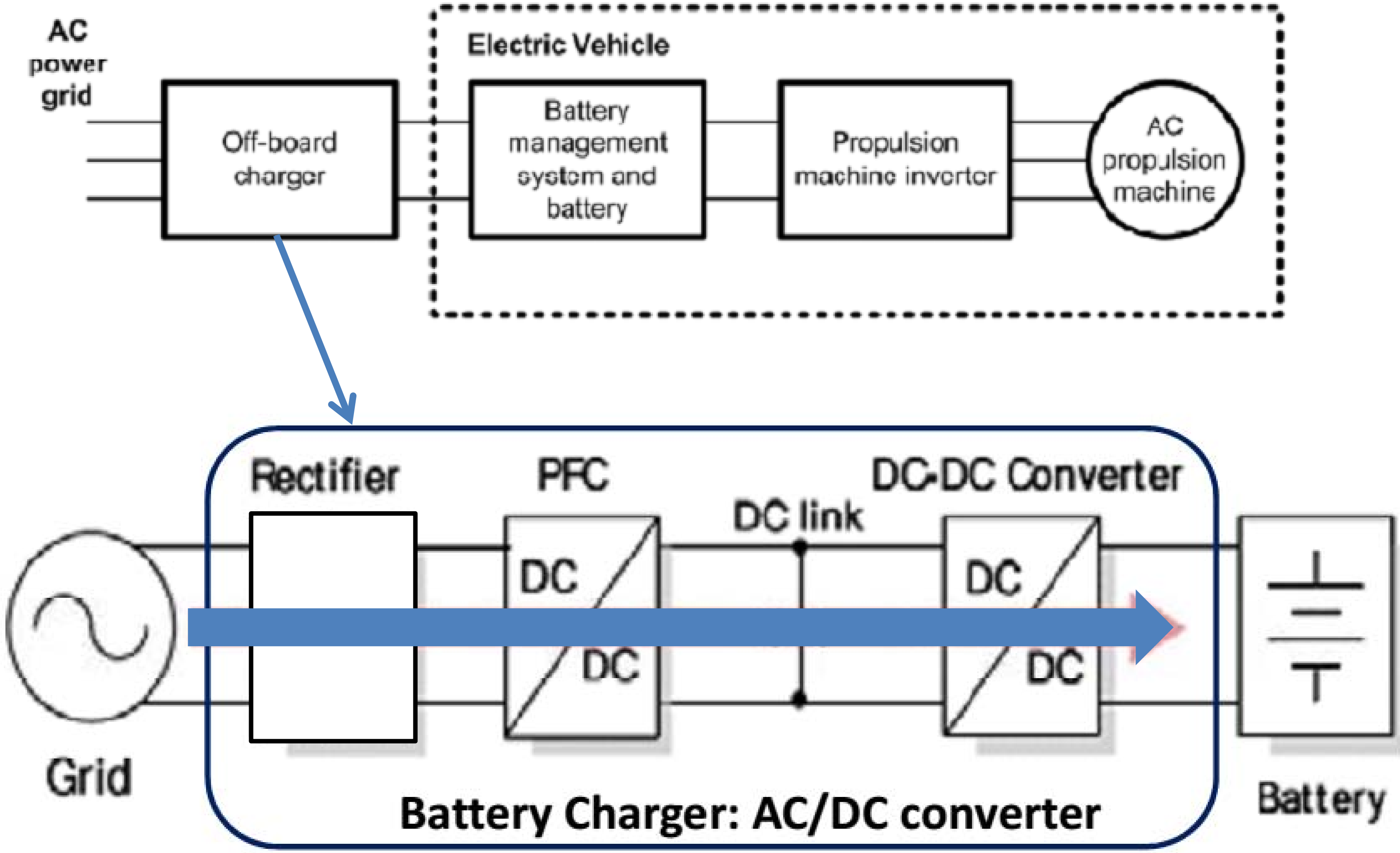

Power flow in an EV

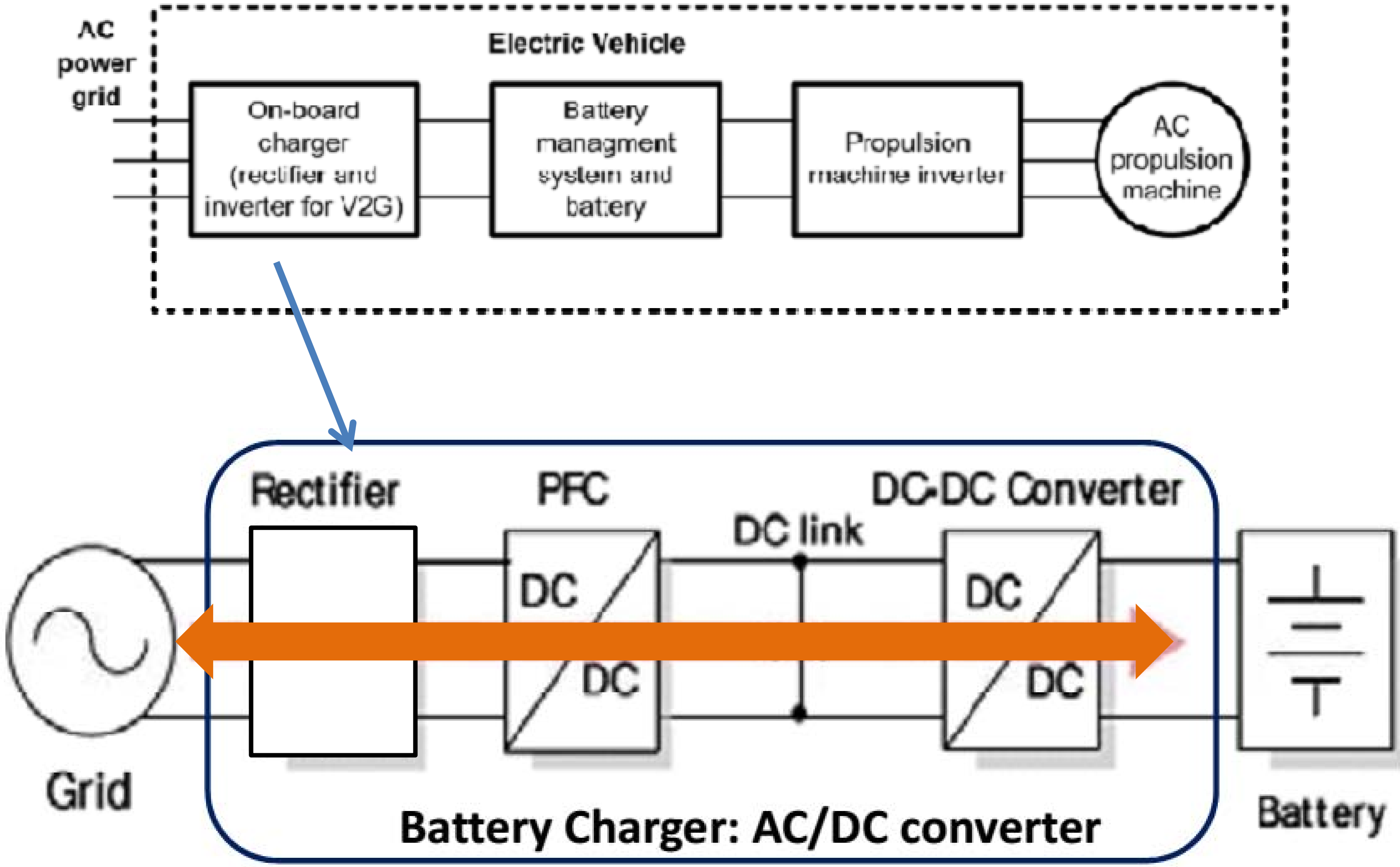

Power Electronics for EV Charging Systems

Basic Requirements

- Wide Voltage Range – Voltage Adaption
- Output Current Control
- Mains Sinusoidal Current Shaping
- Isolation of Mains and Battery (?)

Basic Topologies

- Non-Isolated

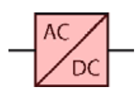

- Isolated Single-Stage

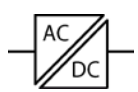

- Non- or Isolated Two-Stage

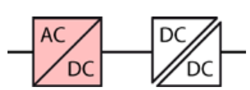

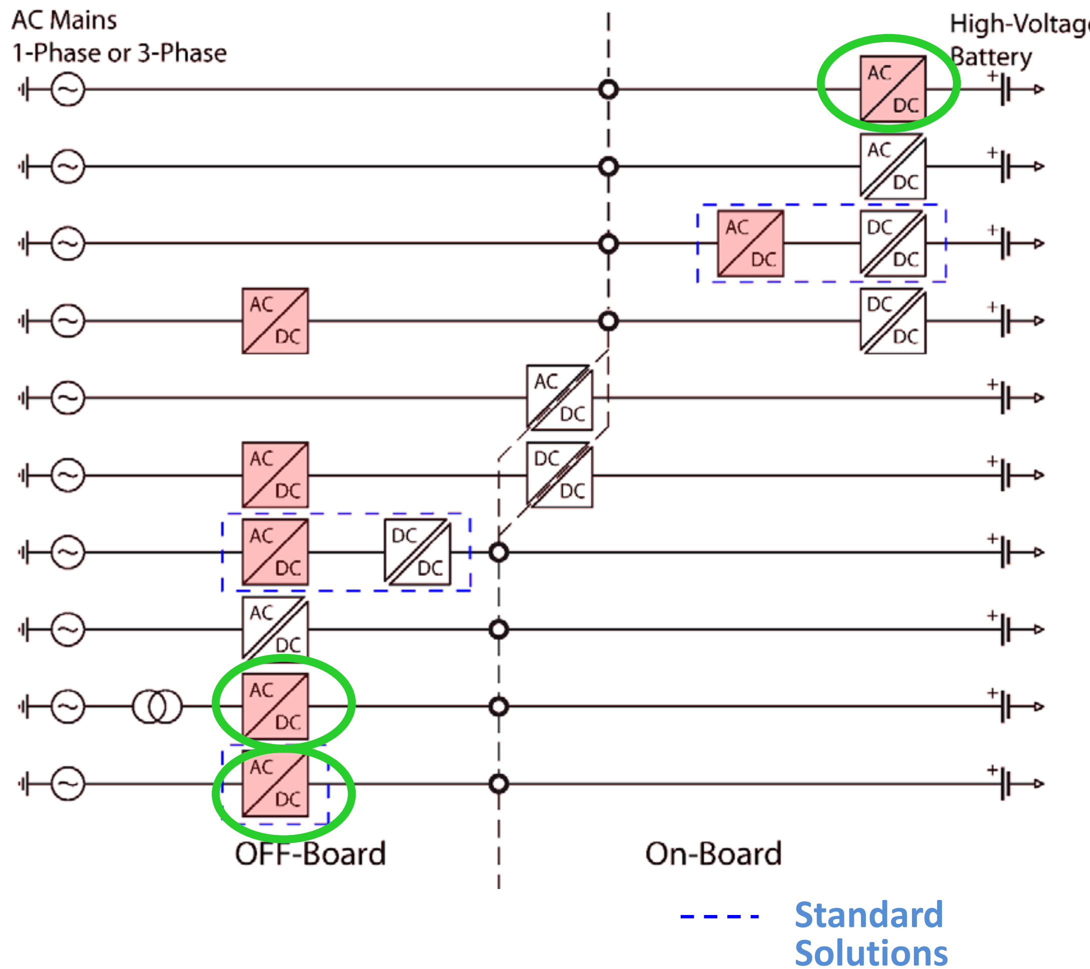

INEP

Operating Range of High Power Factor Grid Interfaces

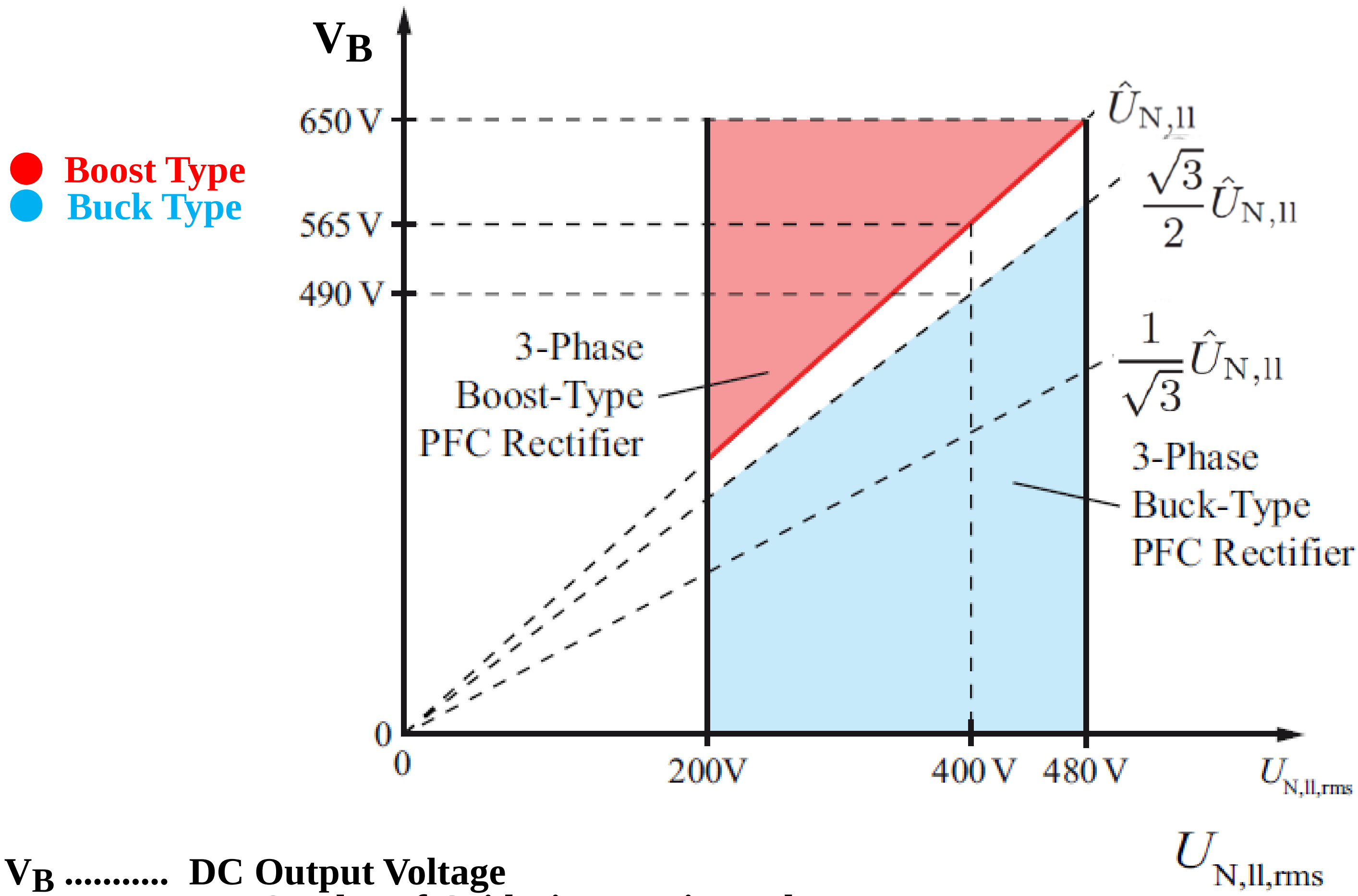

V_B .... DC Output Voltage
$U_{N,ll,rms}$ ... RMS Value of Grid Line-to-Line Voltage

Conventional 3-Ph Current Source AC-DC Systems

Six-Switch Current Source Rectifier:

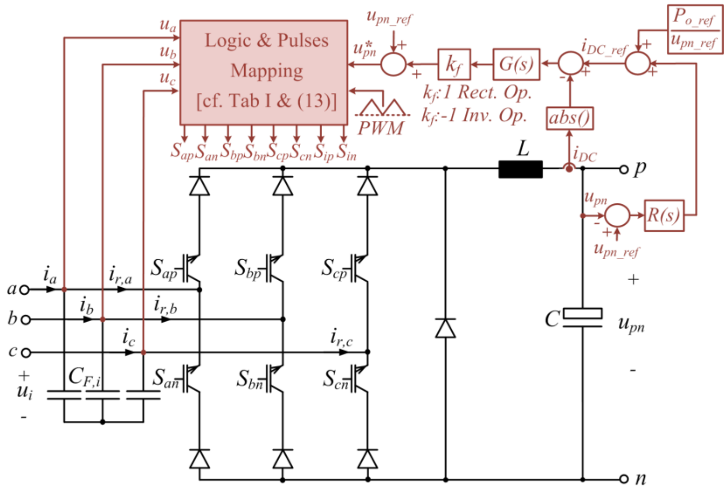

Swiss Rectifier I:

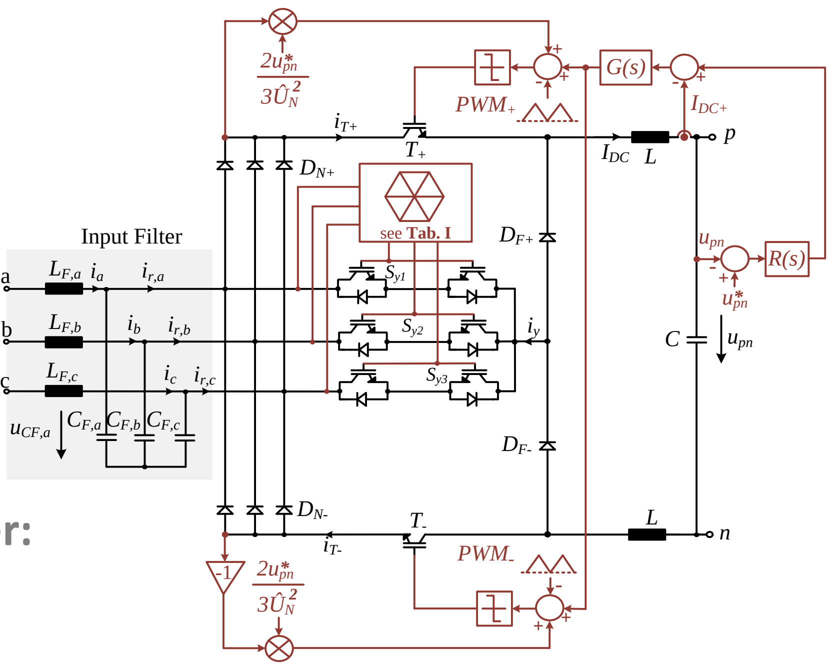

Hybrid 3rd Harmonic Injection Current Source Rectifier:

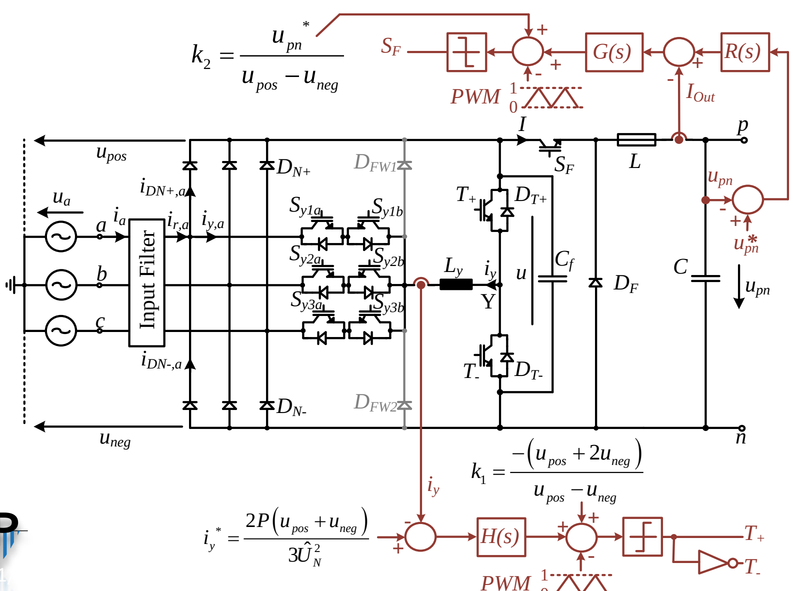

Modular Multilevel Current Source Converters

- Conventional Buck-type PFC Rectifier

(2N+1)-Level Unidirectional Structure:

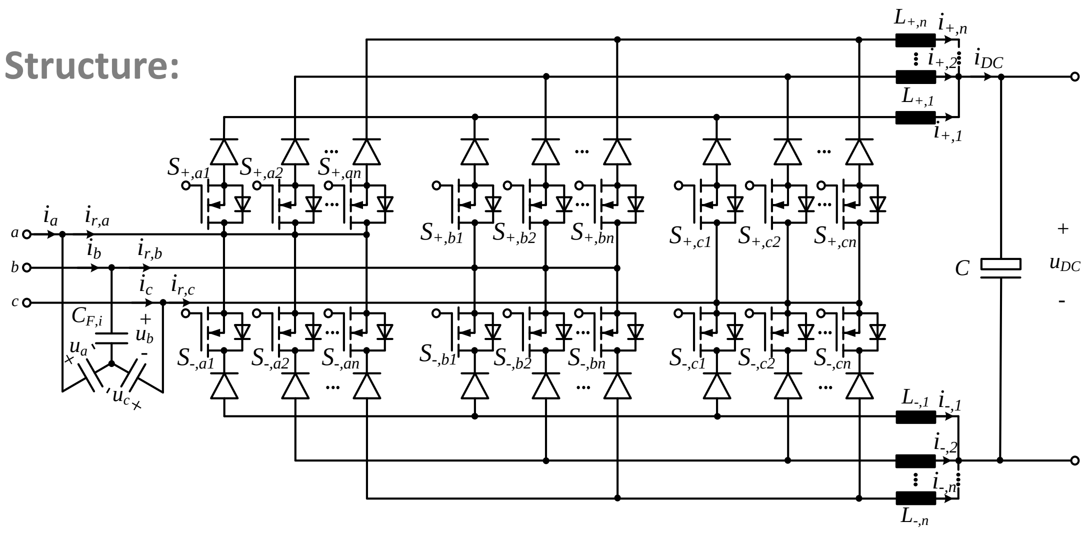

Feedback Control:

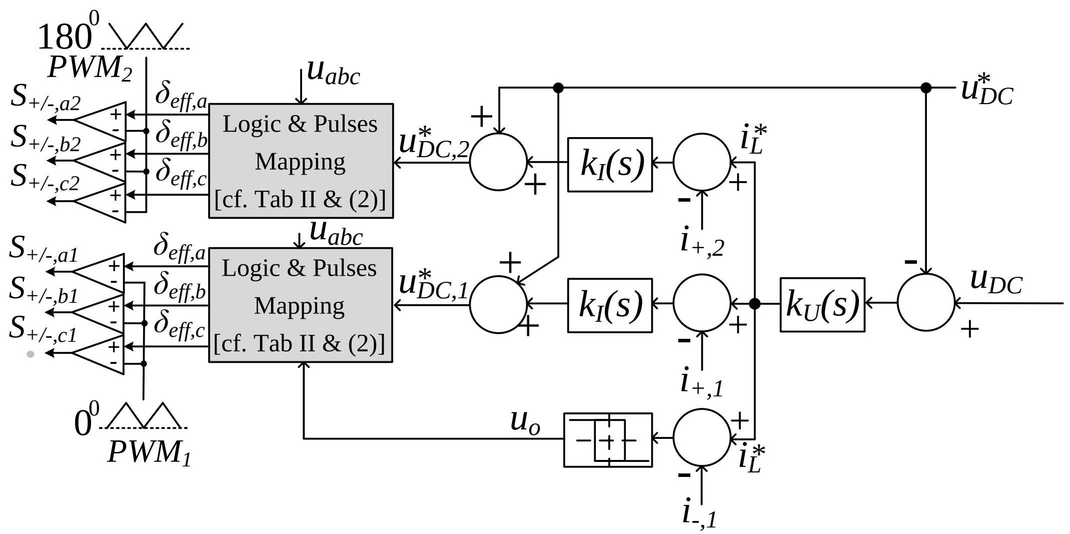

Modular Multilevel Current Source Converters

Conventional 3-Level

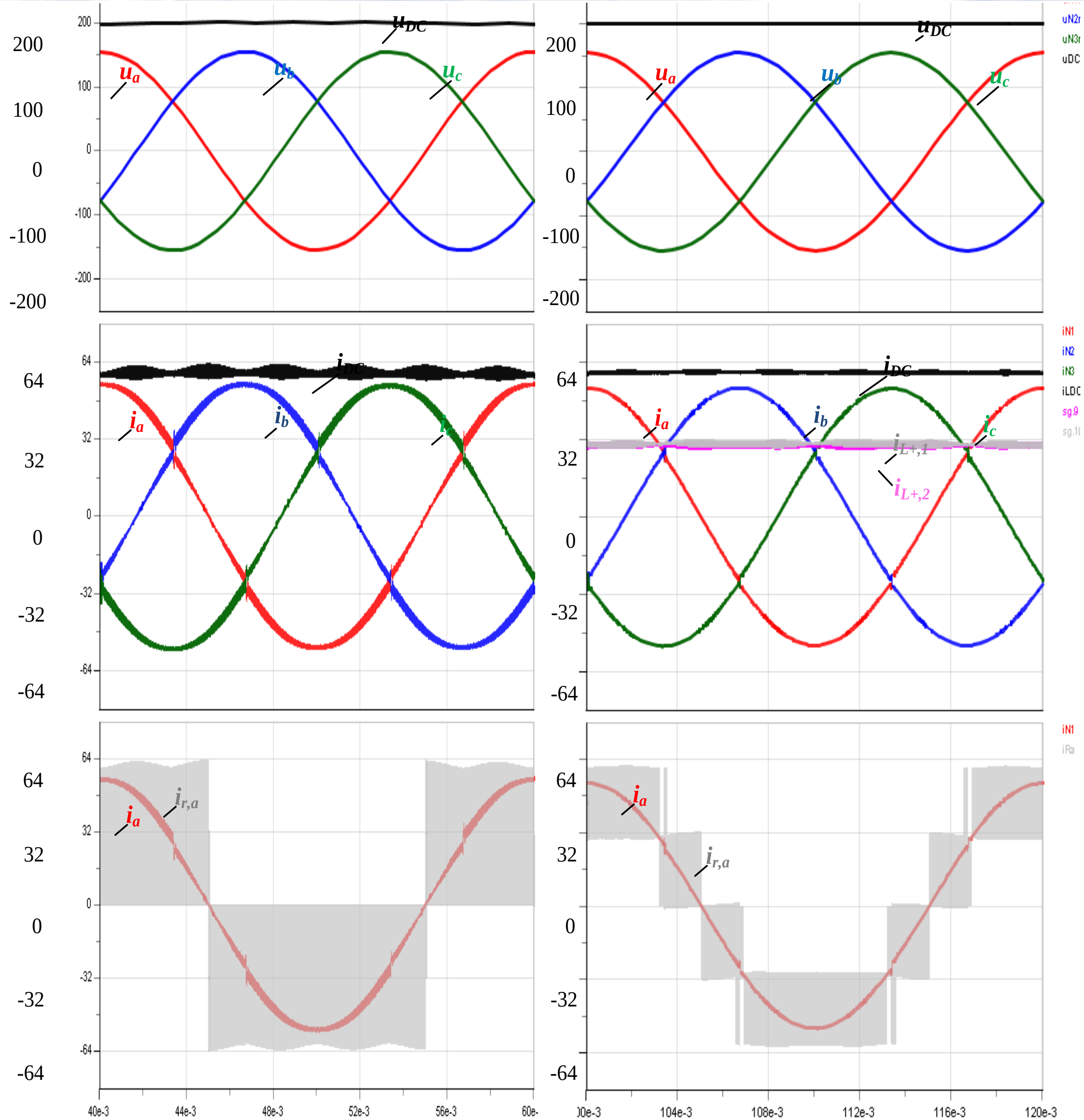

Modular 5-Level

Modular Multilevel Current Source Converters

- Swiss Rectifier (SR) I

(2N+1)-Level Unidirectional Structure:

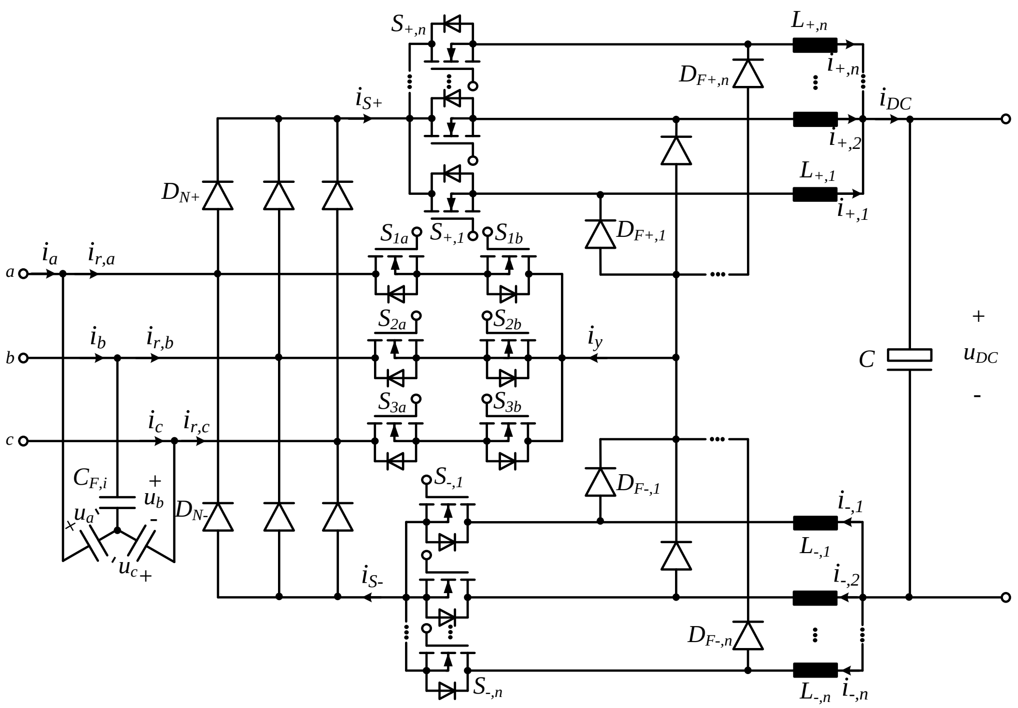

Feedback Control:

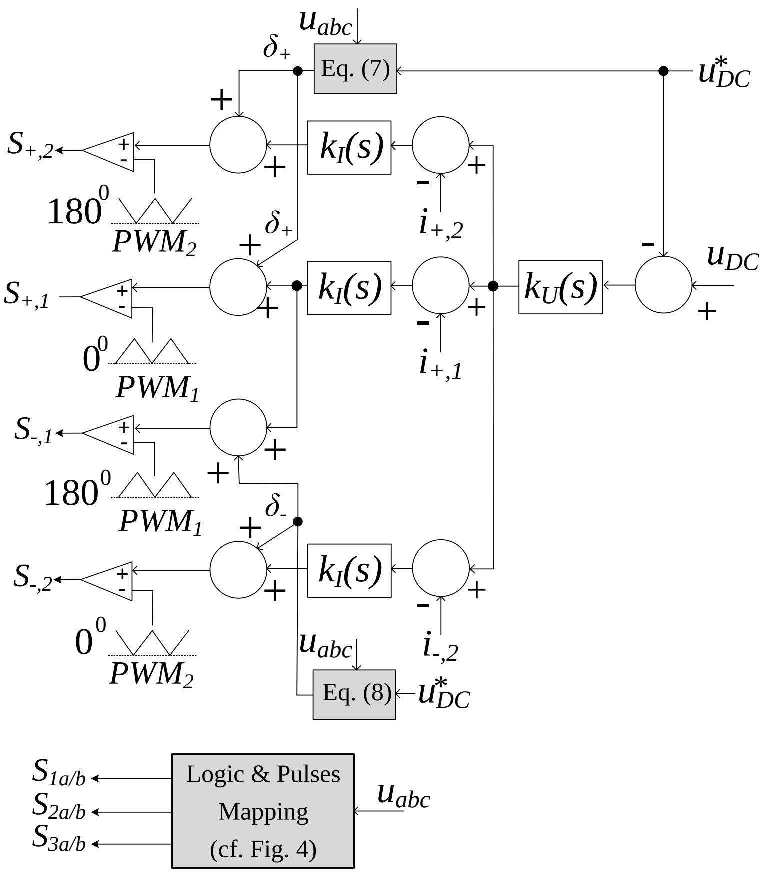

Modular Multilevel Current Source Converters

- Swiss Rectifier (SR) II

(2N+1)-Level Unidirectional Structure:

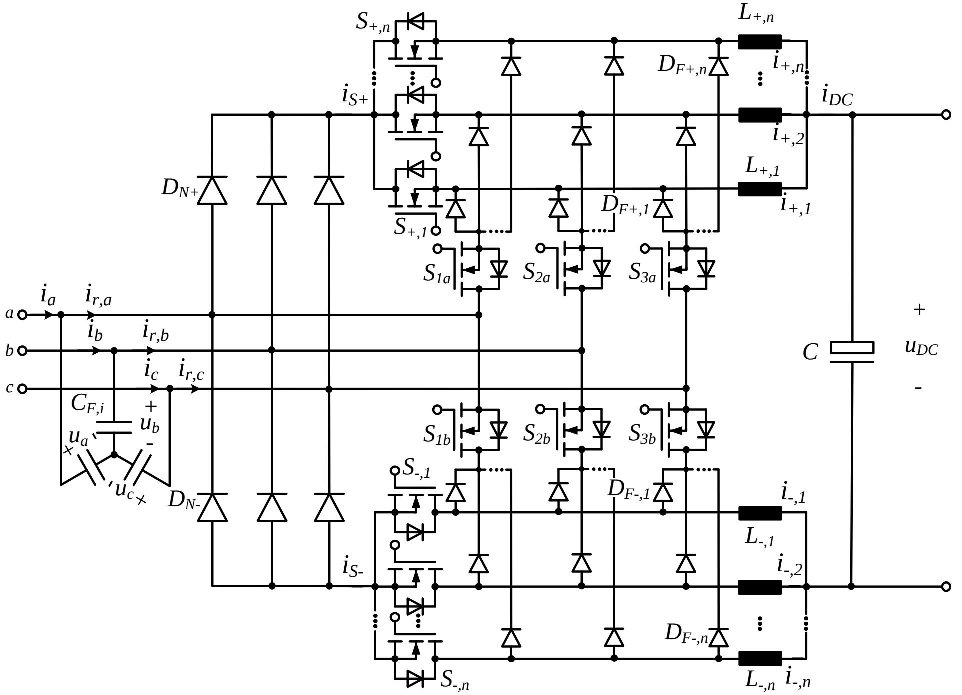

Feedback Control:

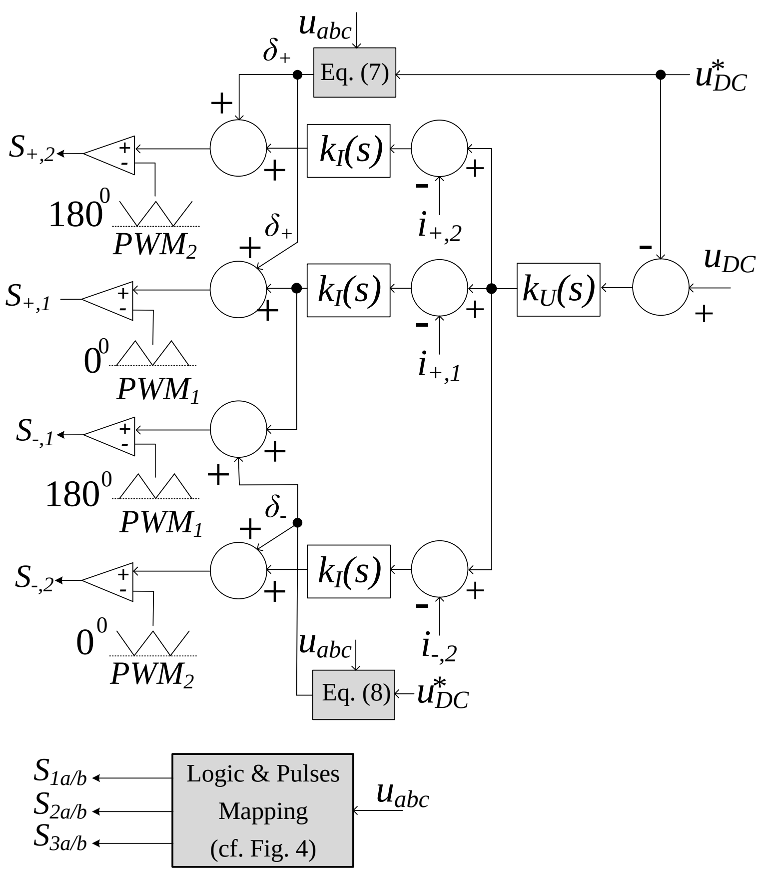

Modular Multilevel Current Source Converters

Conventional 3-Level

Modular 5-Level

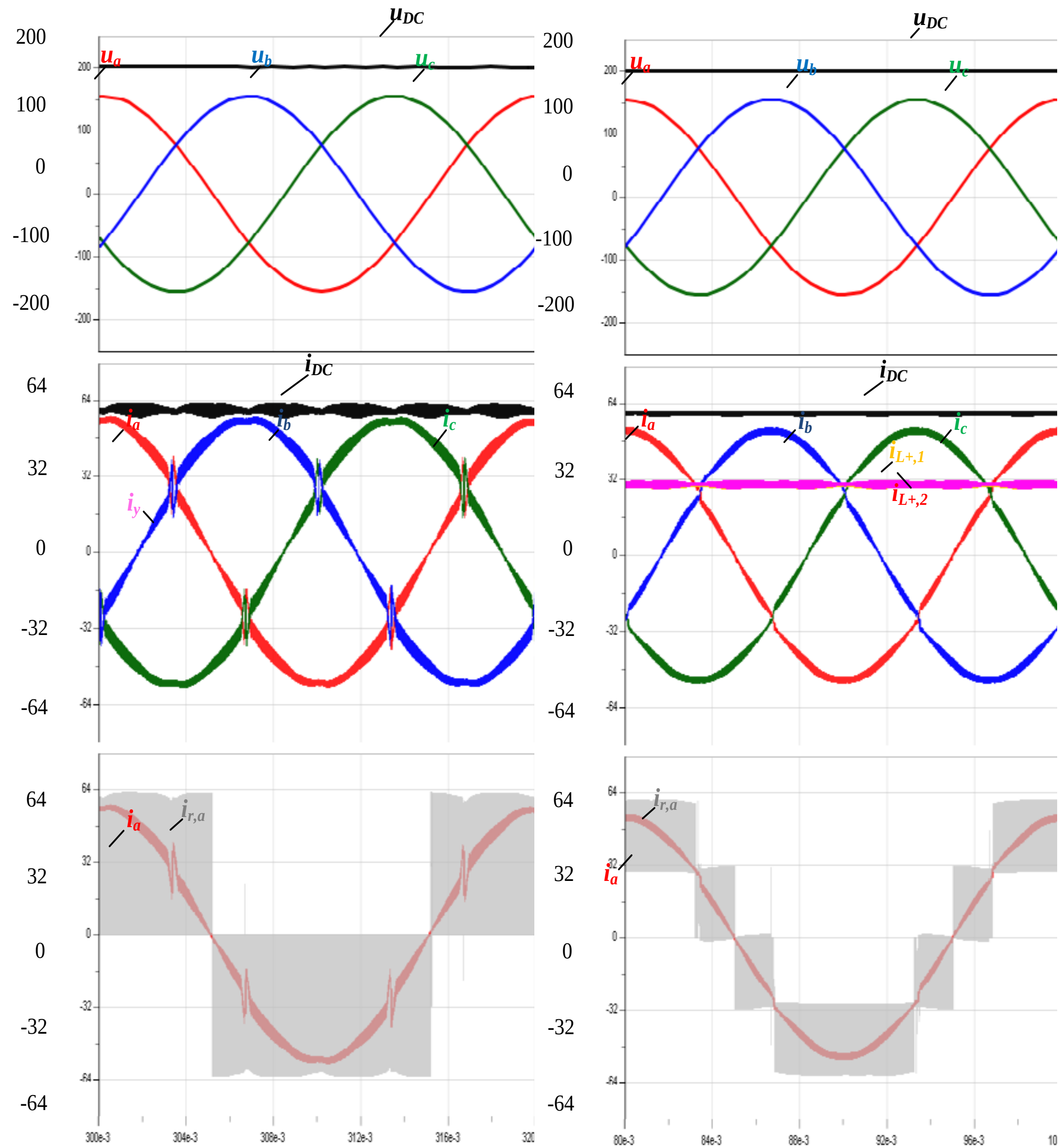

Modular Multilevel Current Source Converters

- Swiss Rectifier (SR) III

(2N+1)-Level Unidir. based on 3-switch:

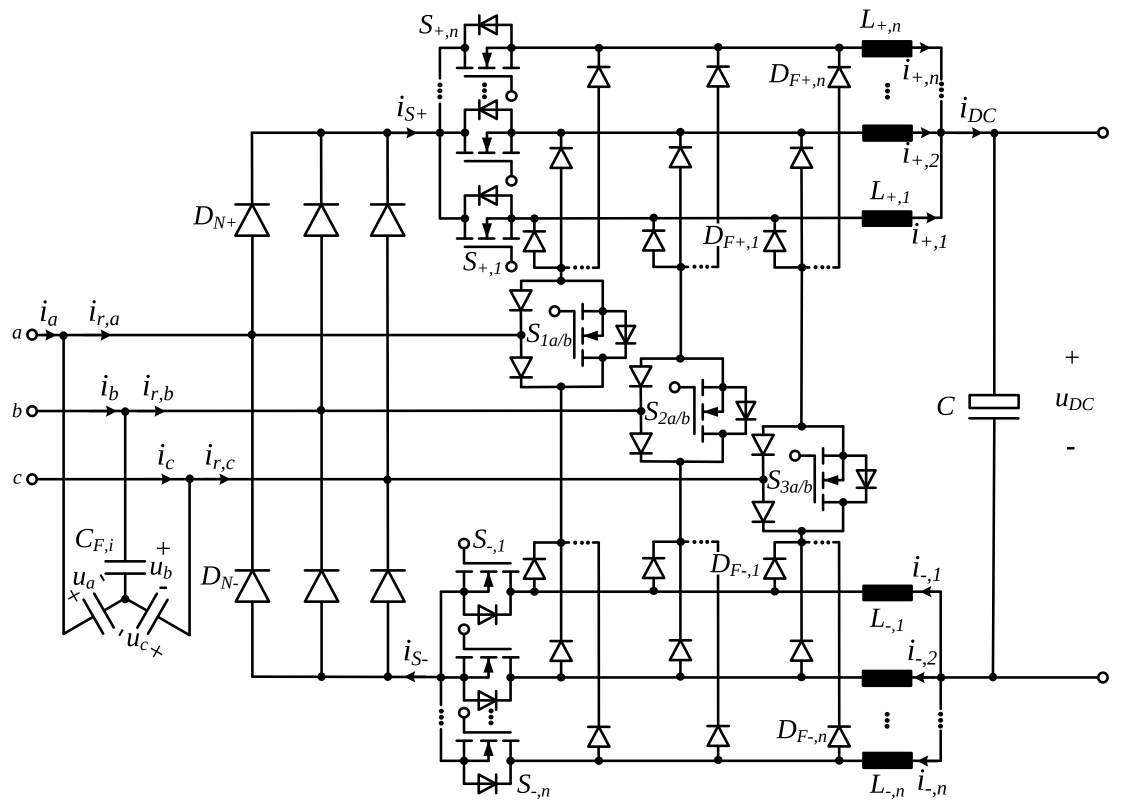

Modular Multilevel Current Source Converters

- Hybrid-Switch Act. 3rd Harm. Inj. Rect.

(2N+1)-Level Structure:

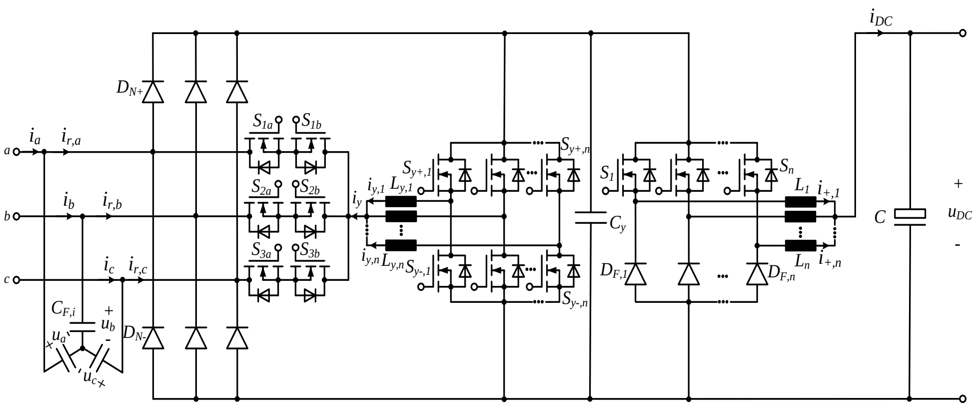

Feedback Control:

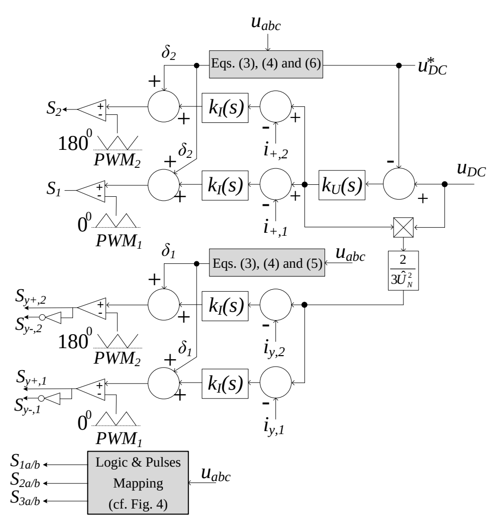

Conventional 3-Level | Modular 5-Level

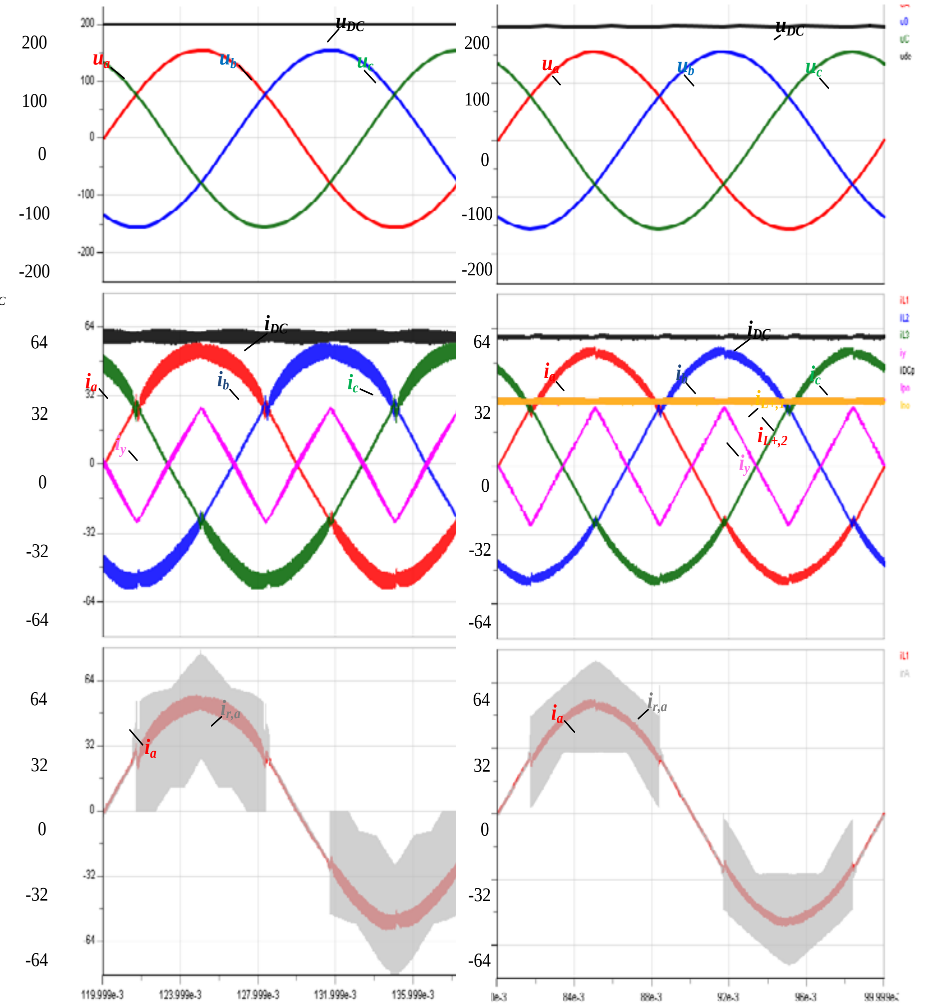

Modular Multilevel Current Source Converters

- Hybrid-Switch Act. 3rd Harm. Inj. Rect. Alternative Implementation

(2N+1)-Level Structure:

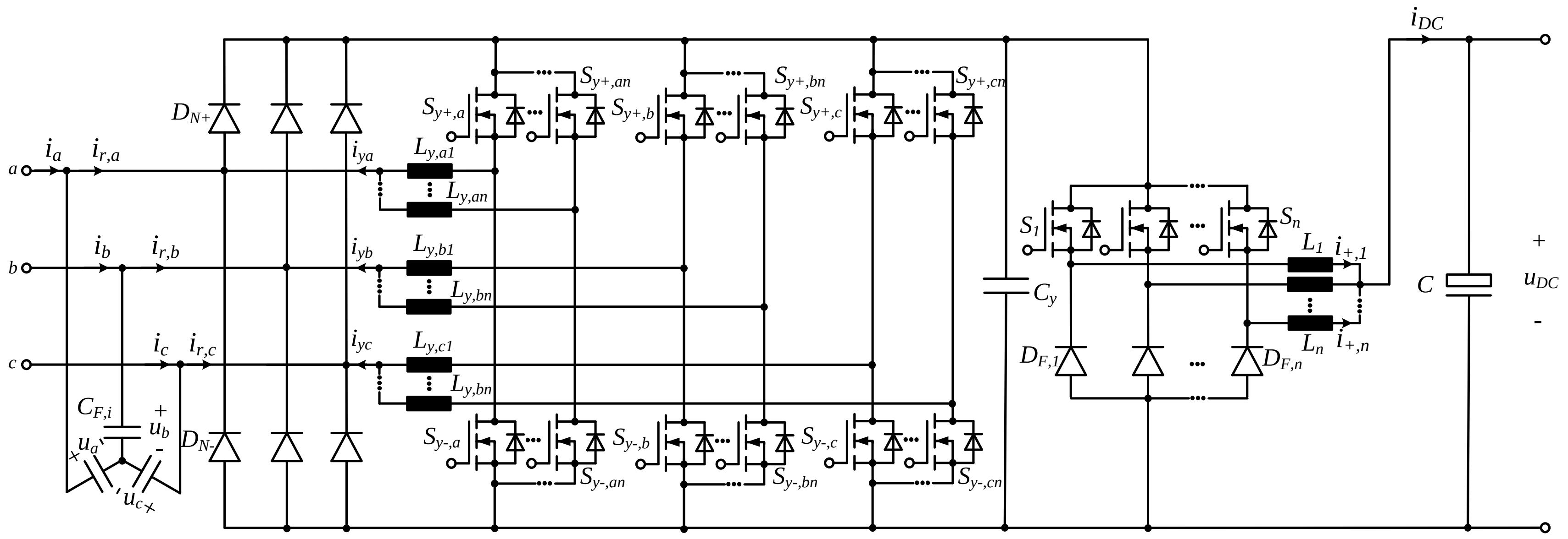

Bidirectional Modular Multilevel Current Source Converters

(2N+1)-Level 6-switch Buck-type Rectifier:

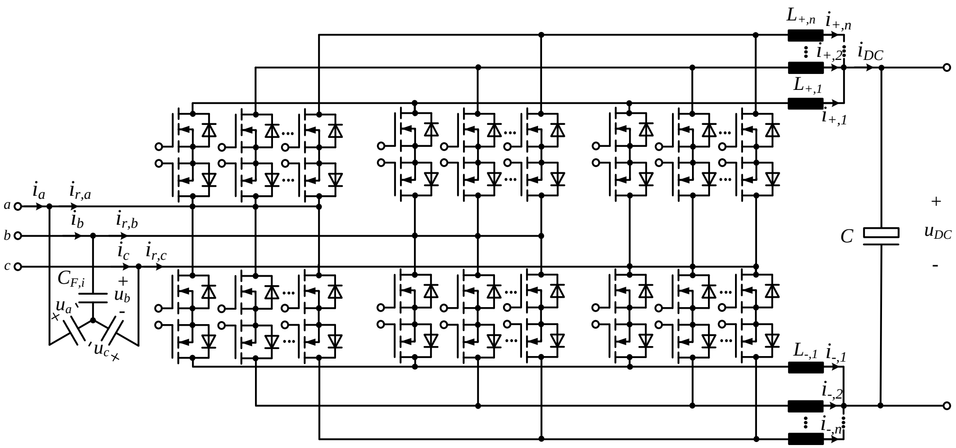

(2N+1)-Level Swiss Rectifier:

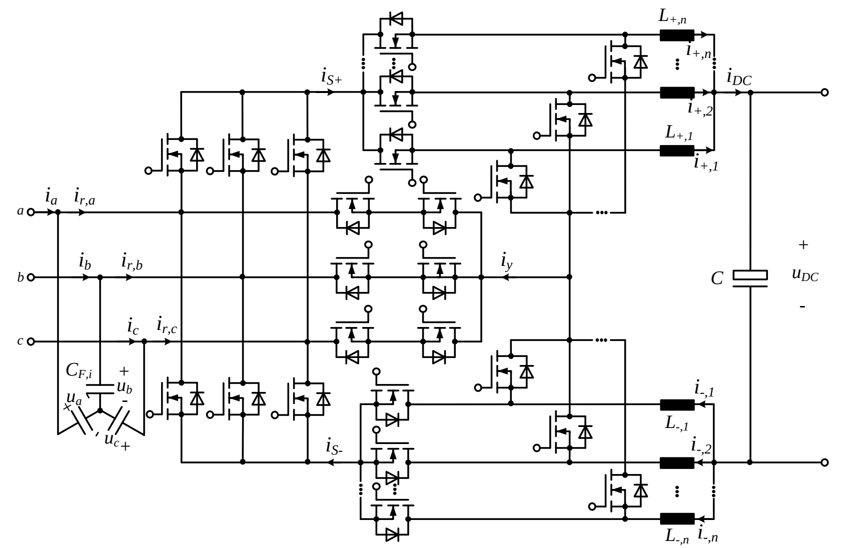

3-Level Structure: **12 Fast Mosfets**

5-Level Structure: **24 Fast Mosfets**

7-Level Structure: **32 Fast Mosfets**

3-Level Structure: **4 Fast + 12 Low Freq. Mosfets**

5-Level Structure: **8 Fast + 12 Low Freq. Mosfets**

7-Level Structure: **12 Fast + 12 Low Freq. Mosfets**

Experimental Results

- 5-Level Current Source Rectifier

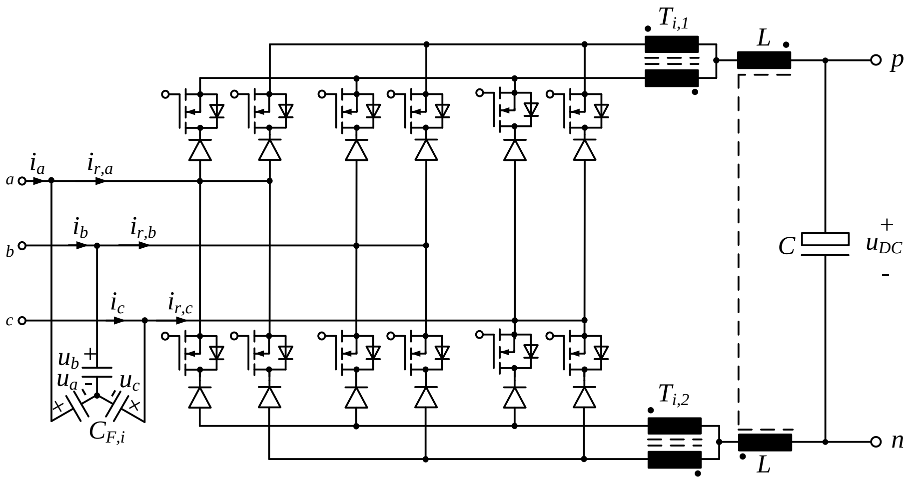

Input phase voltage $u_{a,b,c}$	127 V rms
Mains frequency f_N	60 Hz
Switching frequency f_P	20 kHz
Rated output power P	2.5 kW
Output capacitor C	470 µF
Input capacitor $C_{F,i}$	10 µF
Input inductor $L_{F,i}$	80 µH
DC inductor L	125 µH

Experimental Results

- 5-Level Current Source Rectifier

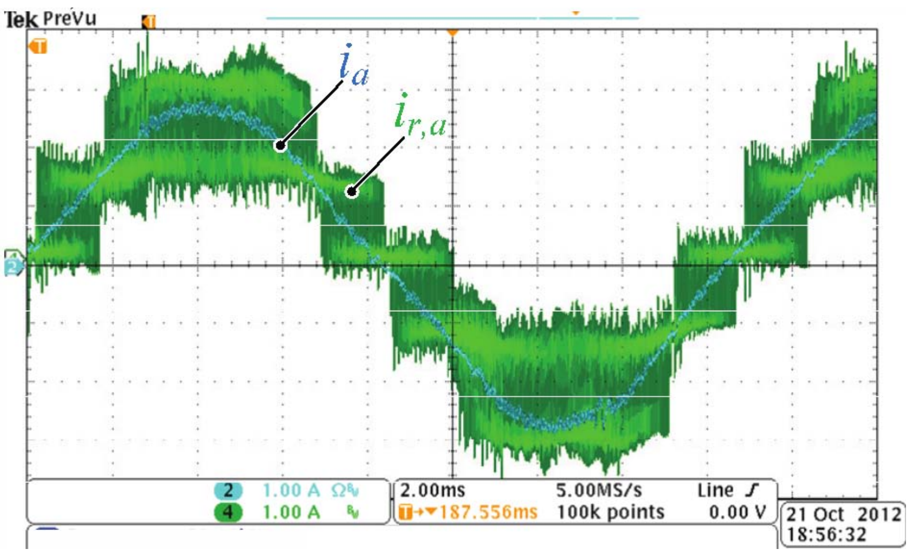

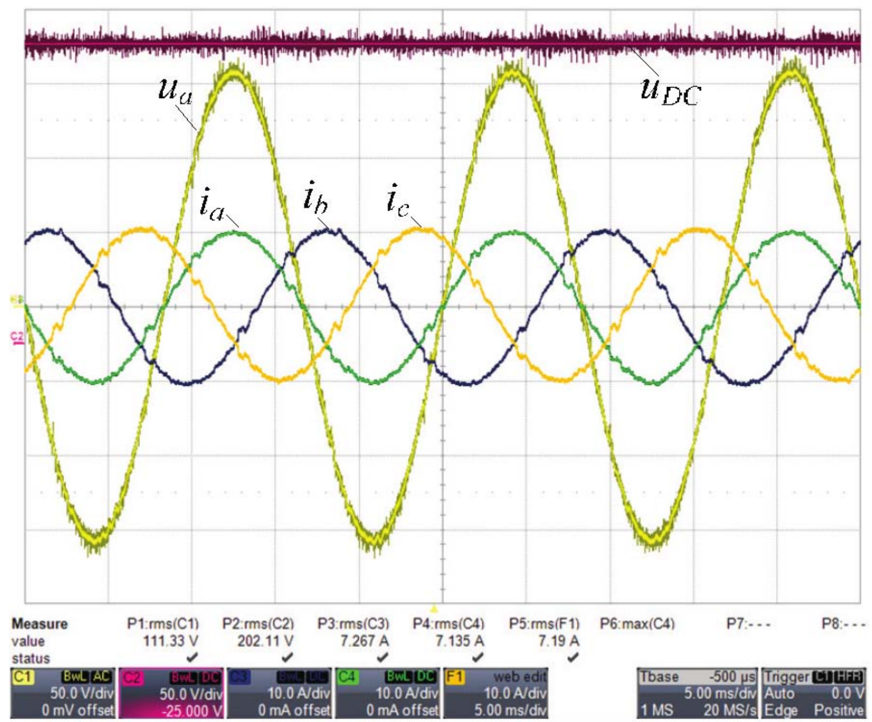

INEP

EV Everywhere: -

A Grand Challenge in Plug-In Electric Vehicles -

Initial Framing Document -

White Paper to Explore -

A Grand Challenge in Plug-In Electric Vehicles -

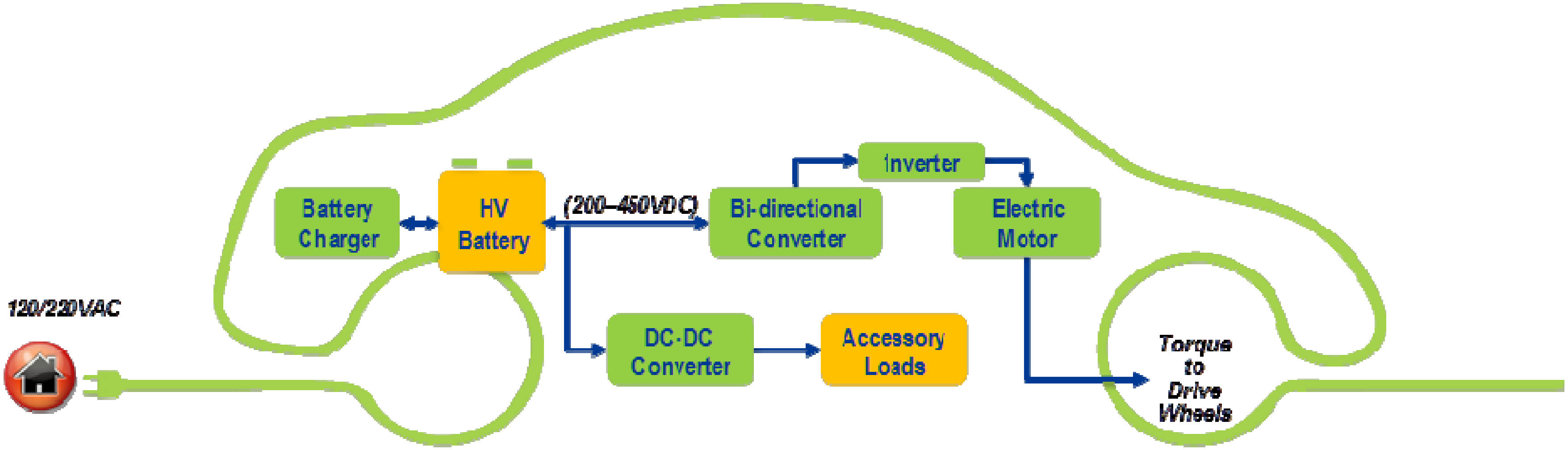
120/220VAC
Battery Charger
HV Battery
(200–450VDC)
Bi-directional Converter
Inverter
Electric Motor
DC-DC Converter
Accessory Loads
Torque to Drive Wheels

Table 1. Batteries and Energy Storage 2022 Targets *(based on EV Everywhere 5-year payback analysis)*

		Current Status	PHEV40	AEV100	AEV300
Battery Cost	$/kWh (usable)	650	190	300	110
Pack Specific Energy	Wh/kg	80-100	150	180	225
Pack Energy Density	Wh/L	200	250	300	425
State-of-Charge Window	%	50	80	90	90

Table 2. Electric Motors and Power Electronics 2022 Targets *(based on EV Everywhere 5-year payback analysis)*

		Current Status	PHEV40	AEV100	AEV300
System Cost	$/kW	20	5	14	4
Motor Specific Power	kW/kg	1.2	1.9	1.3	1.3
Power Electronics Specific Power	kW/kg	10.5	16	12	16.7
System Peak Efficiency	%	90	97	91	98

Table 3. Vehicle Lightweighting 2022 Targets *(based on EV Everywhere 5-year payback analysis)*

		Current Status	PHEV40	AEV100	AEV300
Vehicle Lightweighting	%	n/a	29	3	30
Lightweighting Cost	$/lb-saved	n/a	3.30	3.30	3.30

Table 4. Vehicle Charging Infrastructure 2022 Targets *(based on EV Everywhere 5-year payback analysis)*

		Current Status	PHEV40	AEV100	AEV300
Charger Cost	$/kW	150	35	140	25
Charger Efficiency	%	91	99	91	99

Onboard chargers targets

On-Board Chargers: The on –board charger is essential to *EV Everywhere*. Cost is the most significant challenge. The current status and current technical targets for on-board chargers are shown in Table 8.

Table 8. Current status and current technical targets for on-board chargers

3.3 kW Charger	2010	2015	2022
Cost	$900 - $1,000	$600	$330
Size	6-9 liters	4.0 liters	3.5 liters
Weight	9 -12 kg	4.0 kg	3.5 kg
Efficiency	90 – 92 %`	93%	94%

Inverters targets

Power Electronics - Initially proposed areas of R&D focus include the development of affordable WBG devices, high-temperature capacitors, advanced packaging, high voltage operation, and new circuit topologies. Power electronics based on advanced SiC devices are currently under development and their usage will increase as suppliers mature their manufacturing processes leading to improved device yield and performance specifications. The promise of GaN-on-Si based devices will likely provide substantial performance improvements in terms of efficiency, operating temperature, and reliability relative to Si; however the status of GaN wafer and device technology is in its infancy compared to Si or even even SiC.

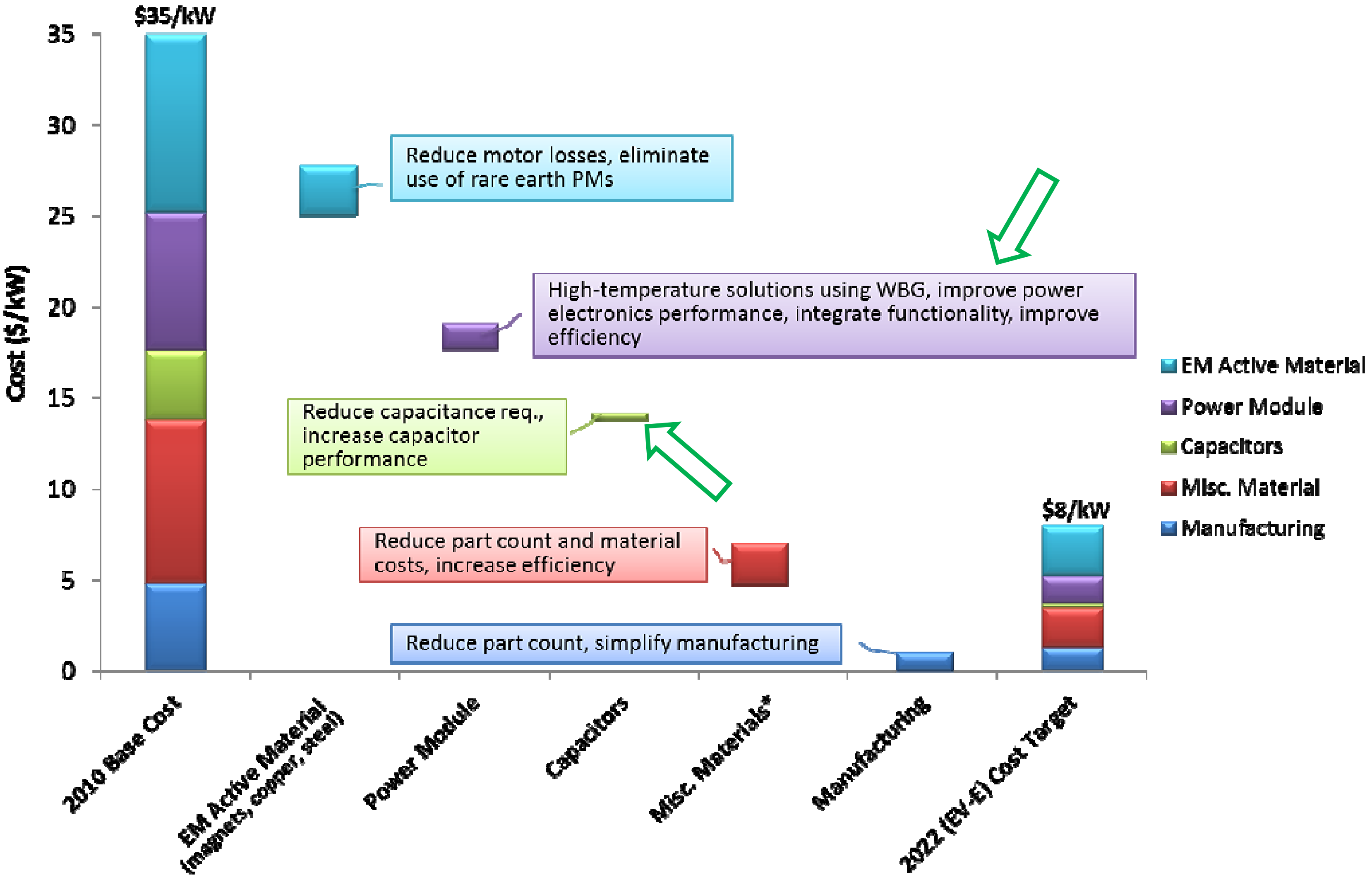

** Misc Materials*

Inverter: cold plate, drive boards, thermal interface material, bus bar, current sensors, housing, control board, etc.

Motor: bearings, housing, sensors, wire varnish and insulation, potting materials, shaft, miscelleneous materials.

V. Additional Requirements

We propose the following other key requirements for the *EV Everywhere* Challenge:

- **Secure Materials Supply at Scale:** Technologies should be based on materials without major supply/availability barriers and risks when deployed at large scale. This is required to meet cost goals, to eliminate foreign material resource dependence, and to ensure large-volume scalability.
- **Safety:** Technologies/solutions should meet all applicable safety and environmental standards and must meet or exceed Federal Motor Vehicle Safety Standards (FMVSS) and SAE–J2929 Battery Safety Standard.
- **Recycling:** Technologies should also be capable of full recycling. Recycling can provide a financial value and thereby contribute to overall affordability and sustainability, can conserve material resources, and can reduce the costs and environmental concerns of vehicle and component disposal at end of life.
- **No Reduction in Grid Reliability:** The charging technologies and charging infrastructures considered must be deployable without compromising the reliability of the electric grid and local distribution networks.

Green charging stations

Table I: Existing Electric Vehicle Charging Stations

Station	SET	Charging Spaces	Installed Power	Cost
UIowa EVCS	224 PV panels[1]	20[2]	57 kW[2]	$950,000[2]
Mitsubishi SPCS[3]	96 PV panels	4	16.8 kW	$130.000[4]
Solar Canopy[5]	15 PV panels	1	3.75 kW	$60,000
Mini E SPCS[6]	24 PV panels	1	5.63 kW	$25,000[7]
Sanya Skypump[8]	1 VAWT	1	4 kW	$30,000

GREEN VILLAGE GREENCAMPUS
Kluyverweg 1
2629 HS Delft
Nederland
http://the-green-campus.com

Master of Science Thesis

Design of a Sustainable Electric Vehicle Charging Station

Bill V. E. Bakolas

Abstract

Electric vehicles only become useful in reducing greenhouse gas emissions, if the electricity used to charge their batteries comes from renewable energy sources. This thesis was conducted within the electric mobility framework of the Green Village, the project put forward to test the Green Campus Concept. The objective was to design a Station that charges electric vehicles, using sustainable energy technologies. To achieve an optimal performance of the selected components, a particular layout architecture was suggested. Additionally, a computer model was developed to simulate the Station operation under variant energy generation and consumption inputs, as established by fitted meteorological data and predicted usage patterns. Simulations were run using the Station model and the corresponding results were analyzed. Finally the economic aspects of the project implementation were examined and conclusions were drawn regarding the commercialization of its conceptual attributes.

Keywords: sustainable energy, electric vehicles, charging station, direct current, renewables, simulation, power flow control

October 2012

TU Delft Delft University of Technology

Faculty of Applied Sciences

Challenge the future

Green charging stations

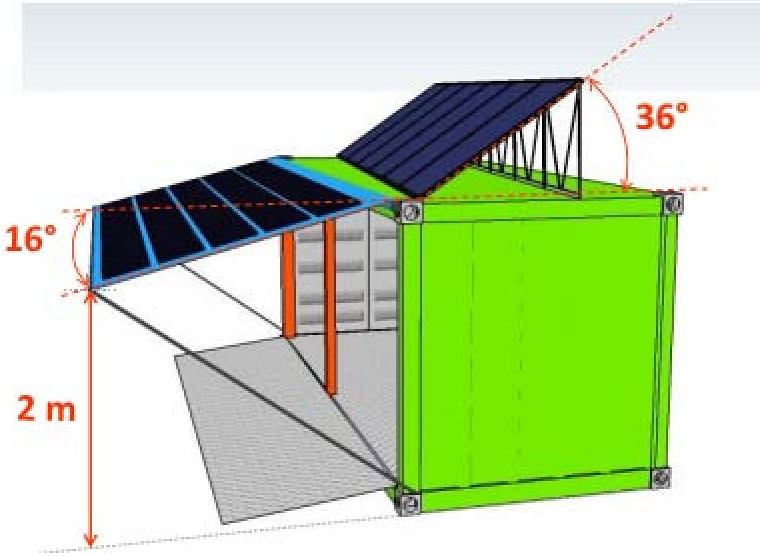

Green charging stations

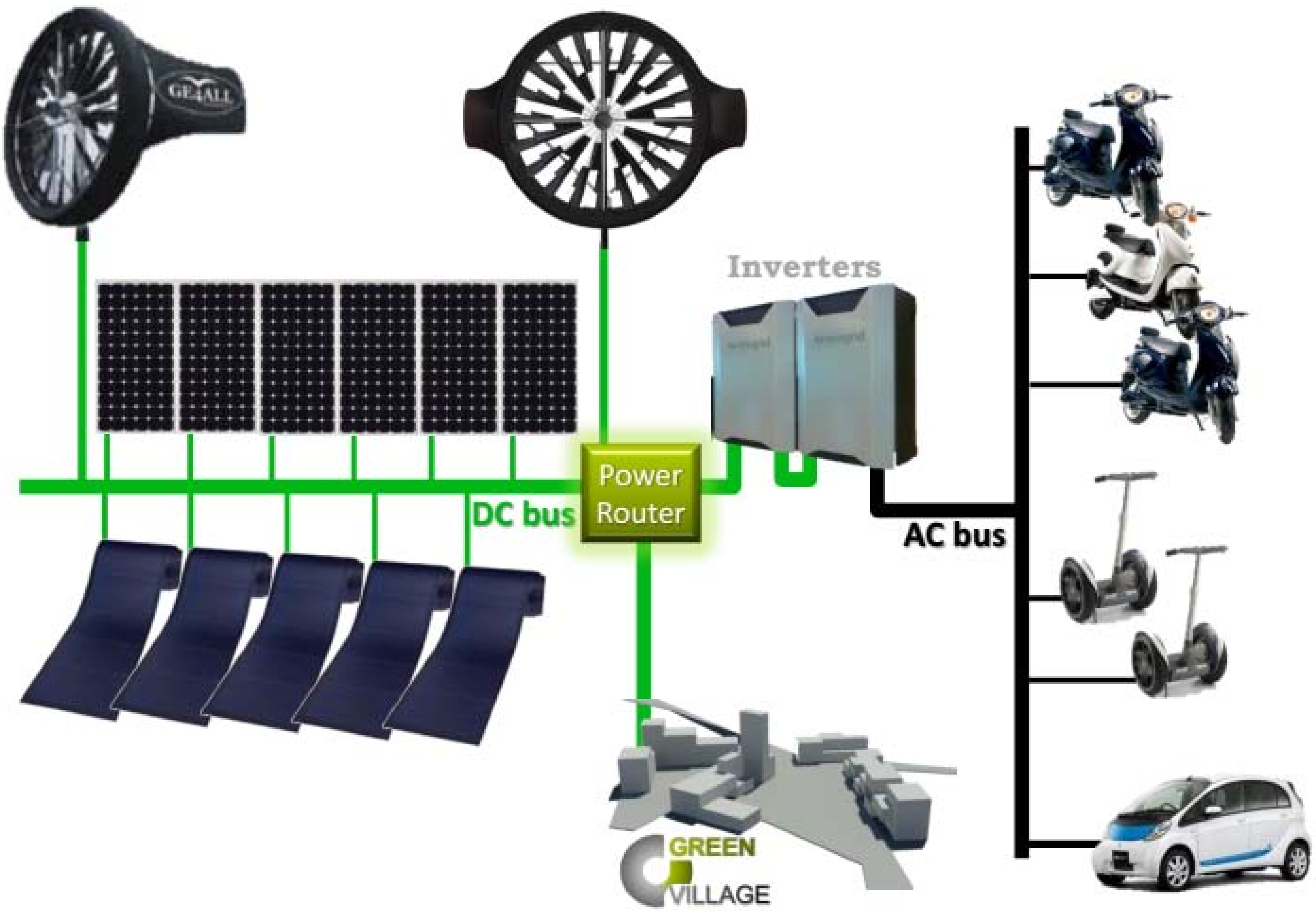

Green charging stations

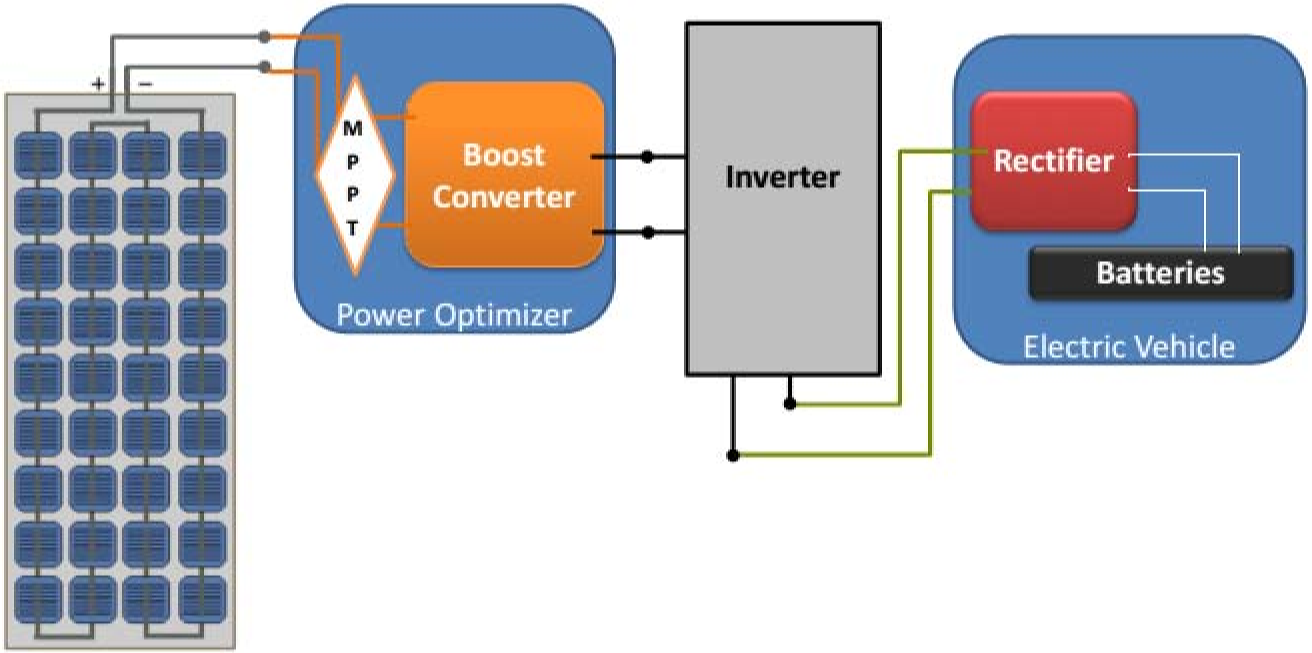

Figure 2.24: Static Model Electric Vehicles

Table III: EV Technical Specifications

Model	Battery		Charging time	Range
	Capacity	Voltage		
Mitsubishi iMiEV[1]	16 kWh	330 V	7 hrs	104 km @ 80 km/h
Peugeot e-Vivacity[2]	2x 1080 kWh	24 V	3 hrs	65 km @ 45 km/h
Segway i2[3]	2x 390 Wh	73.6 V	8-10 hrs	26 km @ 20 km/h

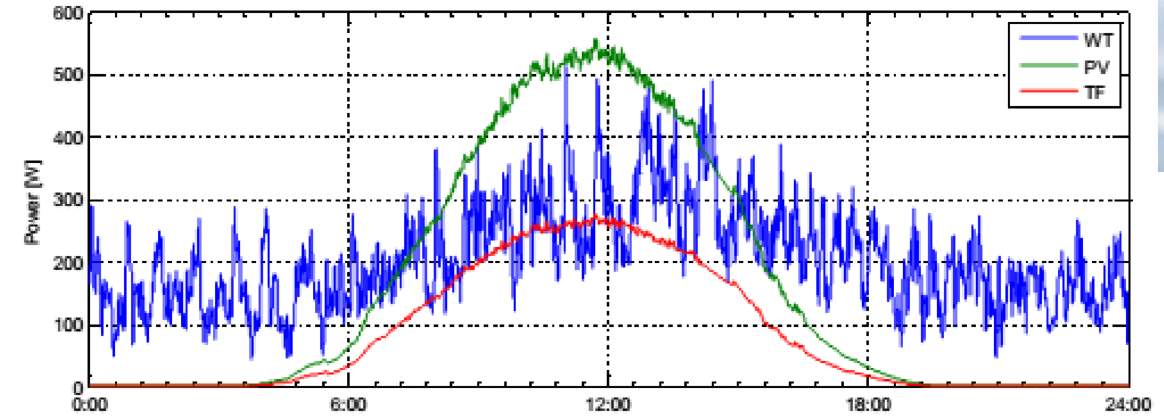

Power [W]
WT
PV
TF
0:00
6:00
12:00
18:00
24:00

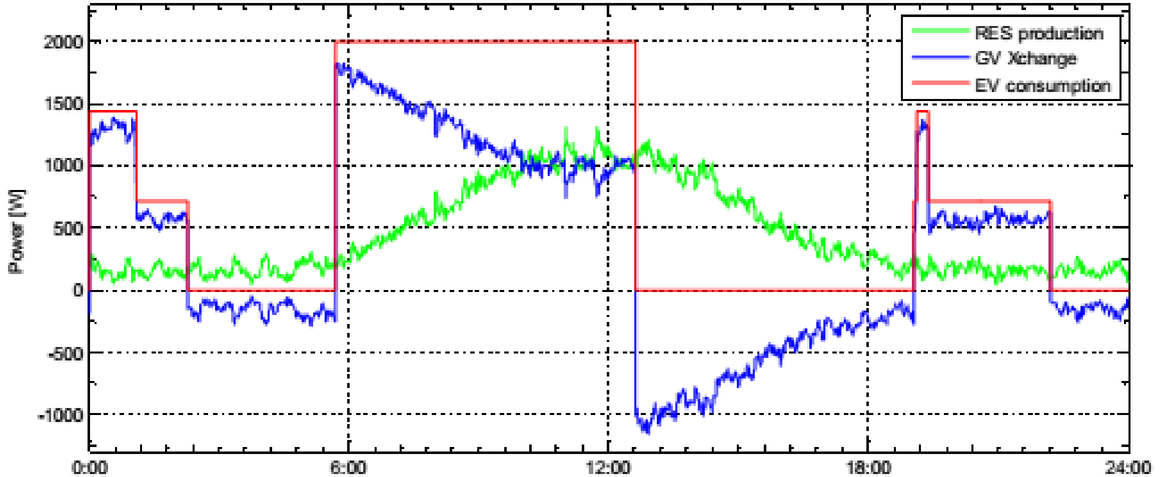

Power [W]
RES production
GV Xchange
EV consumption
0:00
6:00
12:00
18:00
24:00

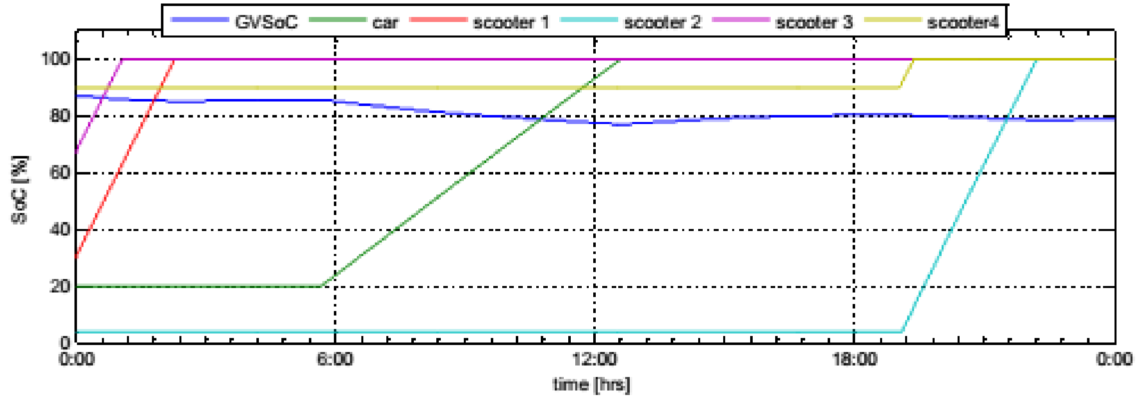

GVSoC
car
scooter 1
scooter 2
scooter 3
scooter4
SoC [%]
time [hrs]

UFSC

Modeling and simulation of electric vehicles (EVs) and design of batteries for Evs

Part 2 – Electric Vehicle Modelling

INEP

Prof. Gierri Waltrich, Dr.

E-mail: gierri.waltrich@ufsc.br

COBEP 2015

NOVEMBER 29th TO DECEMBER 2nd, 2015

SPEC IEEE Power Electronics Society

SOUTHERN POWER ELECTRONICS CONFERENCE

Electric vehicle modelling

- Battery modelling
- Motor modelling
- Vehicle modelling
- Electric vehicle range modelling

Source: Larminie, J.; Lowry, J."Electric Vehicle Technology Explained". John Wiley & Sons Ltd, England,2003.

Battery modelling

Battery modelling

When a current is given out, the voltage will fall; when the battery is being charged, the voltage will rise.

$$V = E - IR$$

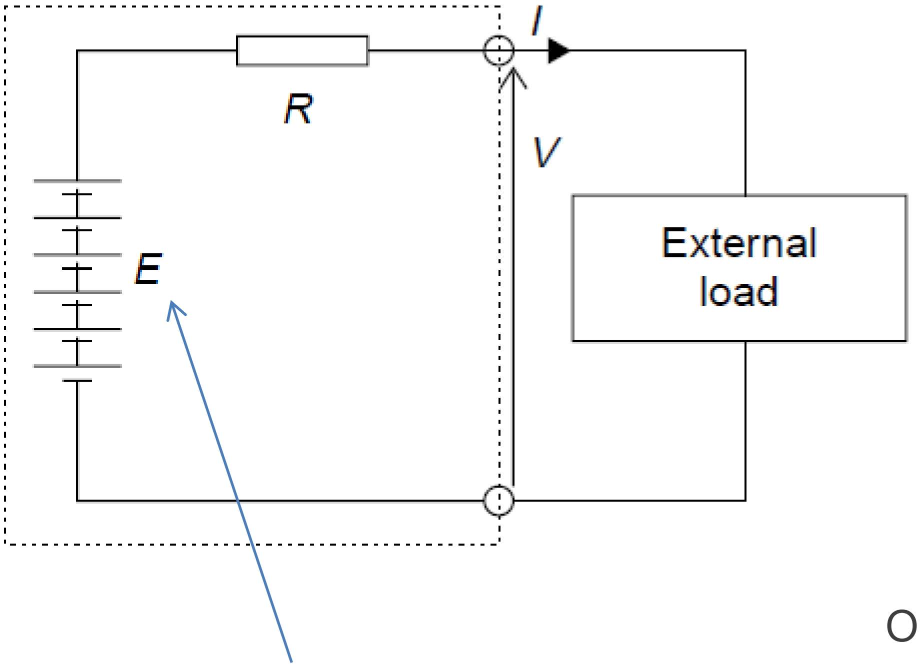

Open circuit voltage

However, the open circuit voltage ***E*** is not in fact constant. The voltage is also **affected by** the '**state of charge**', and other factors such as **temperature**.

Obs.: A good quality 12 V, 25 Amphour lead acid battery will typically have an internal resistance of about 0.005 ohms.

Battery modelling

Capacity is not constant.

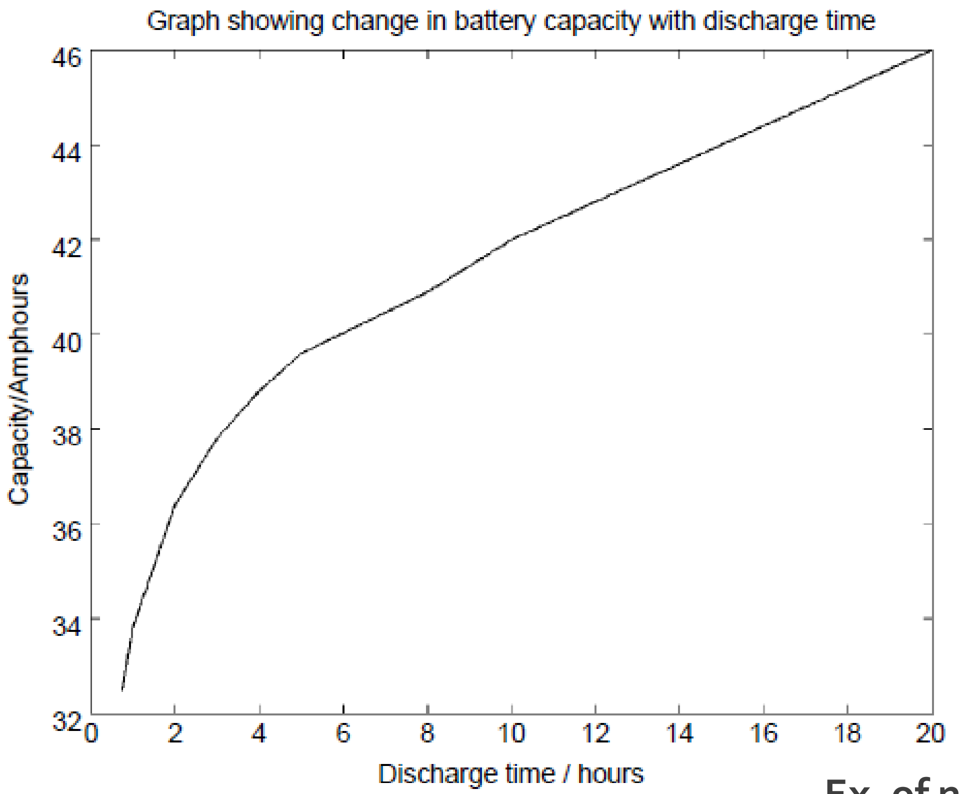

Capacity is affected if the charge is removed more quickly, or more slowly.

Ex. of notation:

C= 42 Ah → 42 A (charge or discharged in one hour)
2C → 84 A (charge or discharged)
0.4C → 16.8 A (charge or discharged)

Battery modelling

UFSC

Kokam™ Global Leader in Power Solution

Cell Specification

Typical Capacity[1]		12.0 Ah
Nominal Voltage		3.7 V
Charge Condition	Max. Current	36.0 A
	Voltage	4.2V ± 0.03 V
Discharge Condition	Continuous Current	60.0 A
	Peak Current	240.0 A
	Cut-off Voltage	2.7 V
Cycle Life [@ 80% DOD] [2]		> 800 Cycles
Operating Temp.	Charge	0 ~ 40 ℃
	Discharge	-20 ~ 60 ℃
Dimension	Thickness (mm)	7.0 ± 0.5
	Width (mm)	206 ± 2.0
	Length (mm)	130 ± 2.0
Weight (g)		354 ± 15

1) Typical Capacity : 0.5C, 4.2~2.7V @25°C
2) Voltage range : 4.15V ~ 3.40V

INEP

Battery modelling

Energy storage

Energy in Watthours = Voltage × Amphours or Energy = V × C

Obs.: Both, V and C, are reduced if the current is increased and the battery is drained quickly.

Specific energy

Specific energy (Wh/kg) is the amount of electrical energy stored for every kilogram of battery mass.

Energy density

Energy density (Wh/m^3) is the amount of electrical energy stored per cubic meter of battery volume.

Specific power

Specific power (W/kg) is the amount of power obtained per kilogram of battery.

INEP

MATLAB: Ragone_plot.m

Battery modelling

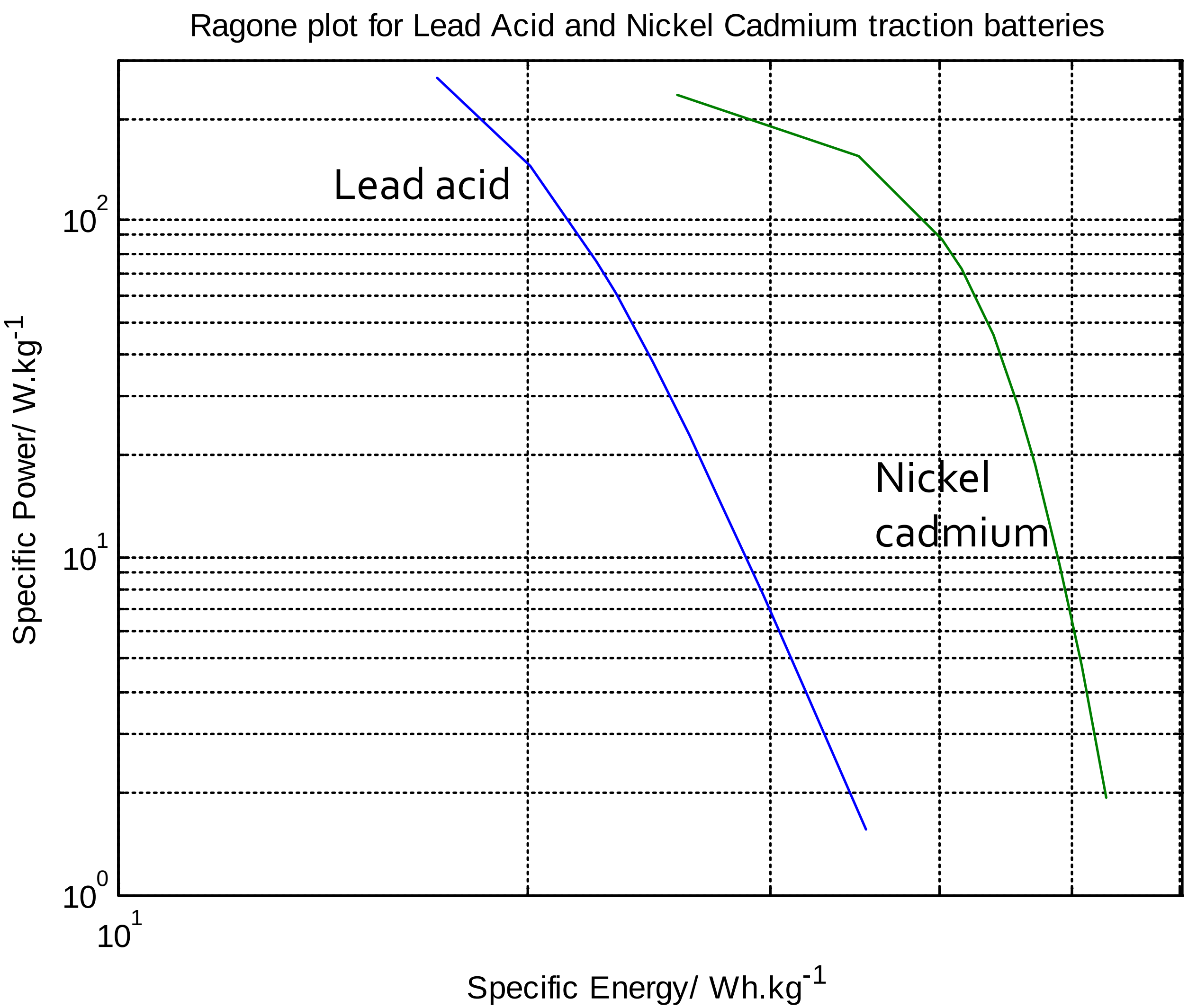

Battery modelling

Batteries types

- **Lead acid** – low cost, low specific energy
- **NiCad** – low cost
- **NiMH** – cadmium free
- **Sodium** – high temperature used in larger systems
- **Li-ion** – high specific power
- **Zinc-air** – high specific energy, negatives electrodes should be replace after it is charged.

Battery	Specific energy $Wh.kg^{-1}$	Energy density $Wh.L^{-1}$	Specific power $W.kg^{-1}$	Current cost
Lead acid	30	75	250	0.5
NiCad	50	80	150	1.5
NiMH	65	150	200	2.0
Zebra	100	150	150	2.0
Li-ion[5]	90	150	300	10
Zinc-air	230	270	105	?

Battery modelling

Equivalent circuit

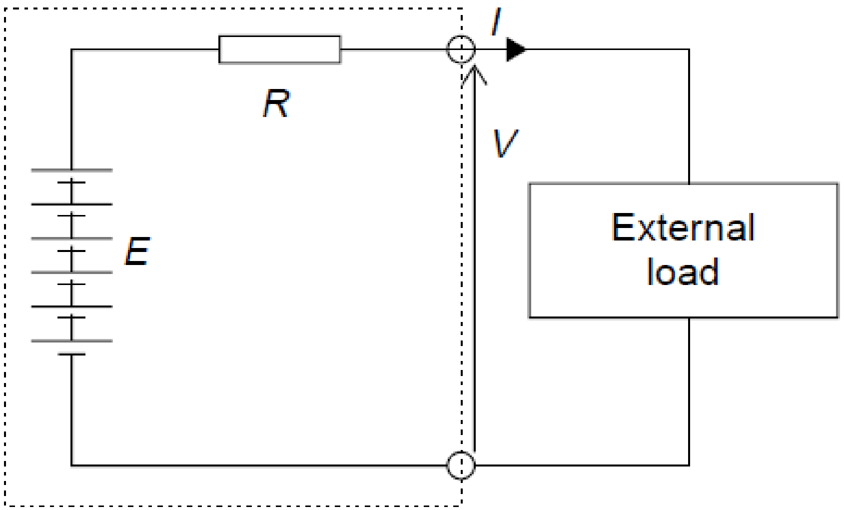

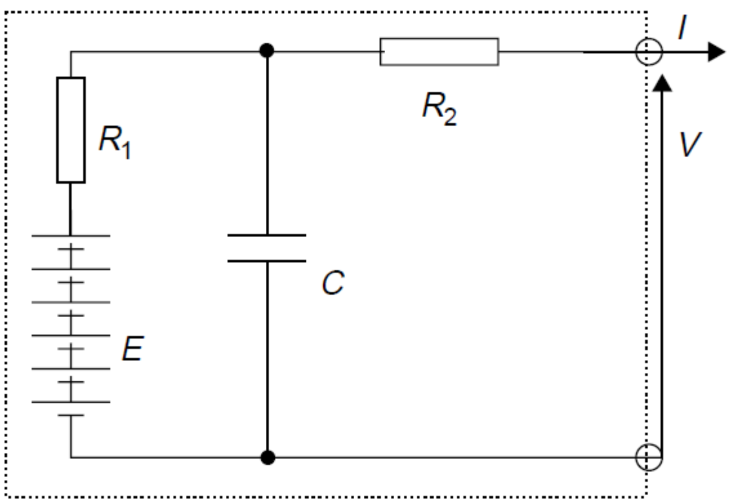

Do not explain the battery dynamics!

This model represents better the dynamic behaviour of a battery.

Battery modelling

Equivalent circuit

Lead acid battery: $E = n \times (2.15 - DoD \times (2.15 - 2.00))$

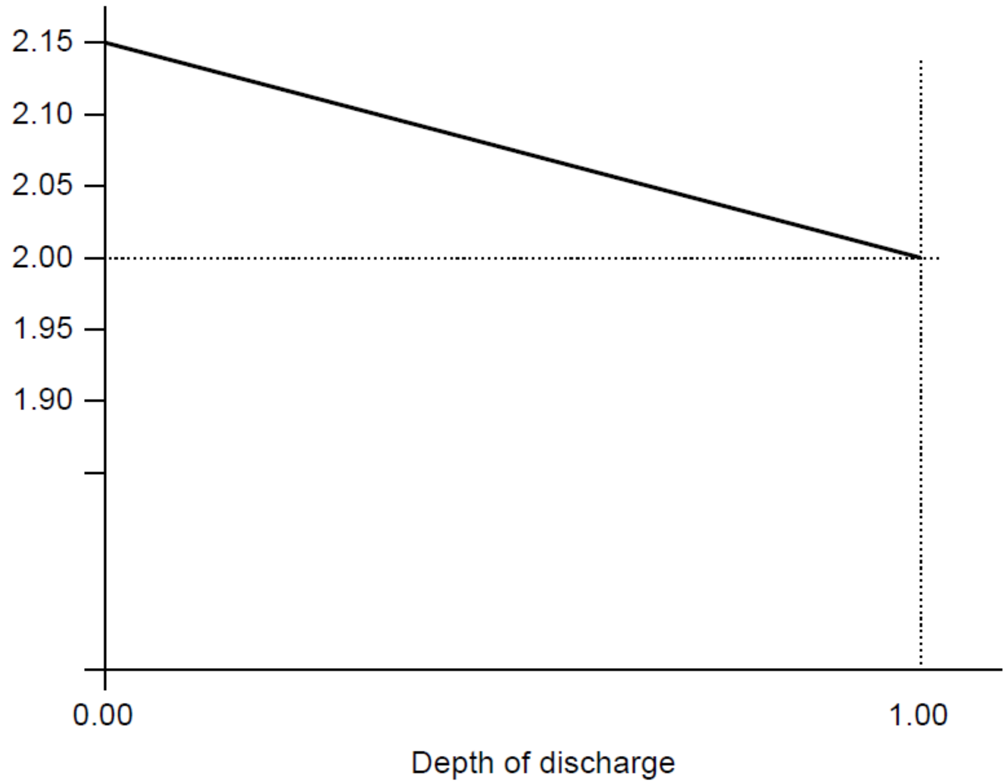

Battery modelling

Equivalent circuit

NiCad battery (obtained by linear regression):

$$E = n \times \begin{pmatrix} -8.2816DoD^7 + 23.5749DoD^6 - 30DoD^5 + 23.7053DoD^4 \\ -12.5877DoD^3 + 4.1315DoD^2 - 0.8658DoD + 1.37 \end{pmatrix}$$

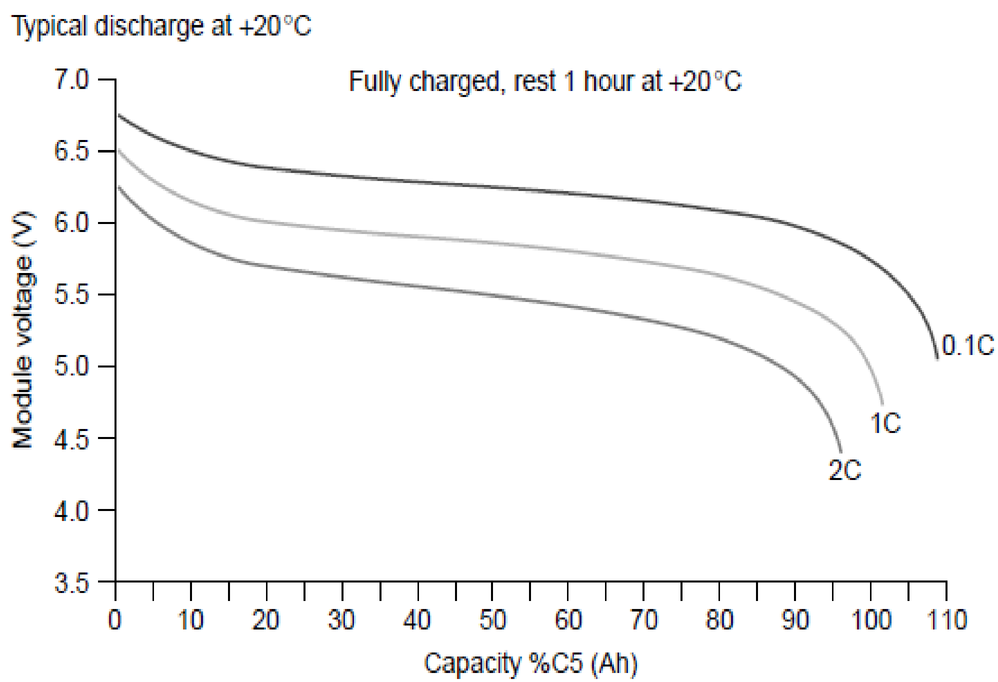

Battery modelling

Equivalent circuit

Battery resistance:

Lead acid resistance:

$$R_{Pb} = n^{o} cells \frac{0.022}{C_{10}} [\Omega]$$

$$C_{10} = capacity\ for\ 10h\ discharge$$

NiCad resistance:

$$R_{NiCad} = n^{o} cells \frac{0.06}{C_{10}} [\Omega]$$

Peukert Model

Drawing 1A for 10 hours does not take the same charge from a battery as running it at 10A for 1 hour, therefore, it is necessary to determine a method to define a capacity of a battery.

The starting point is finding the Peukert capacity:

$$C_P = I^k T$$

C_P is found by the nominal parameters, and k is a constant (typically about 1.2 for a lead acid battery) called Peukert coefficient.

Battery modelling

Peukert Model

Example: Suppose a battery has a nominal capacity of 40 Ah at the 5 h rate. This means that it has a capacity of 40 Ah if discharged at a current of:

$$I = \frac{40}{5} = 8A$$

if k = 1.2 then the Peukert capacity is

$$C_P = 8^{1.2} \times 5 = 60.6Ah$$

now it is possible to find the time that the battery will last at any current I.

$$T = \frac{C_P}{I^k}$$

Battery modelling

Peukert Model

$$C_{predicted} = I \times T$$

$$C_{predicted} = I \times \frac{C_P}{I^k}$$

$$C_{predicted} = C_P I^{(1-k)}$$

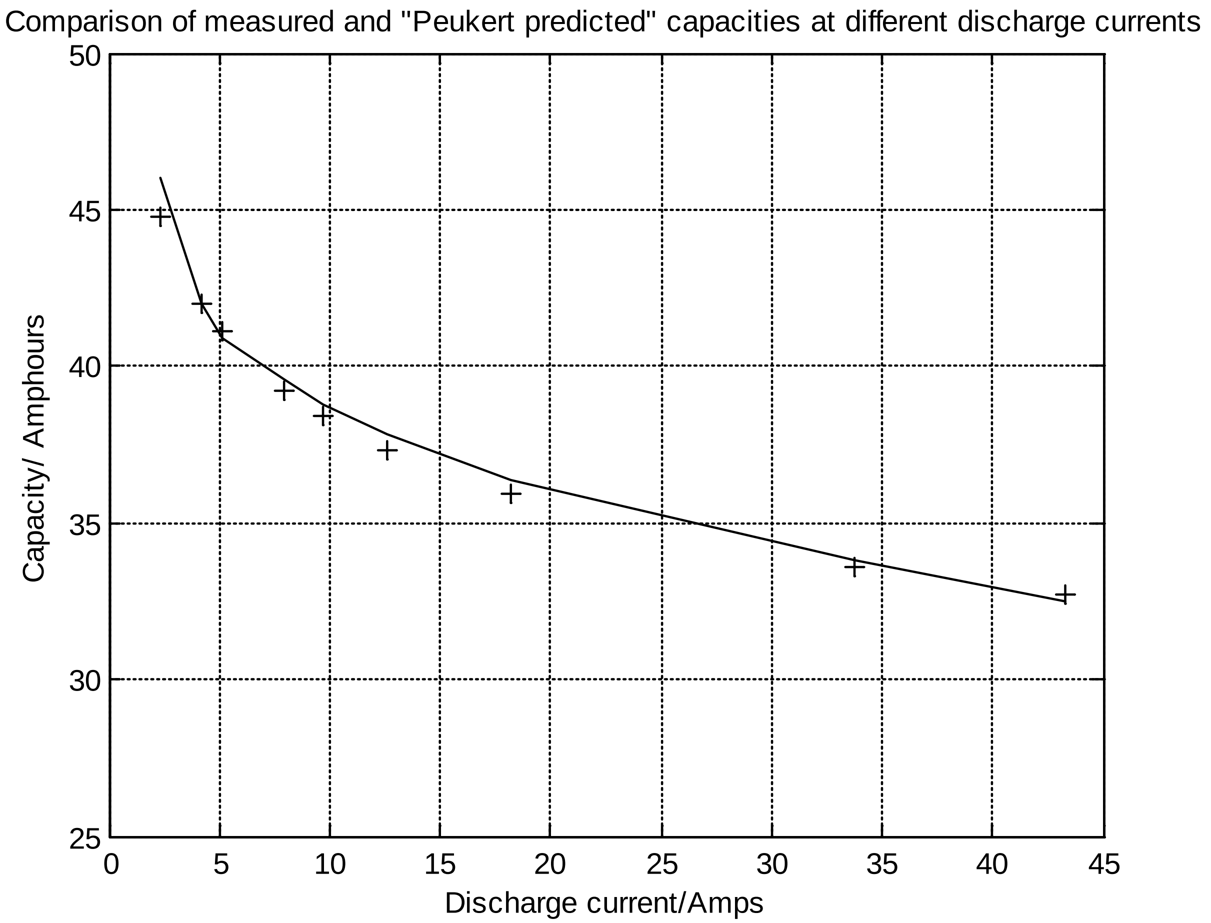

Example

$$I = \frac{C_{10}}{T} = \frac{42Ah}{10h} = 4.2A$$

$$k = 1.107 \text{ (Lead acid)}$$

$$C_P = I^k T$$

$$C_P = 4.2^{1.107} \times 10 = 49Ah$$

$$C_{Predicted} = C_P \times I^{(1-k)} = C_P 49 \times I^{(1-1.107)}$$

MATLAB: Figure_2_14.m

Battery modelling

Time step → δt

Charge removed in one step → $\delta t \times I^k$

Total charge removed the battery → $CR_{n+1} = CR_n + \frac{\delta t \times I^k}{3600}[Ah]$

Total charge supplied for a load → $CS_{n+1} = CS_n + \frac{\delta t \times I}{3600}[Ah]$

Depth-of-discharge → $DoD_n = \frac{CR_n}{C_p}$

Open circuit voltage → $E = n^o cells \times (2.15 - DoD \times 0.15)$

Battery modelling

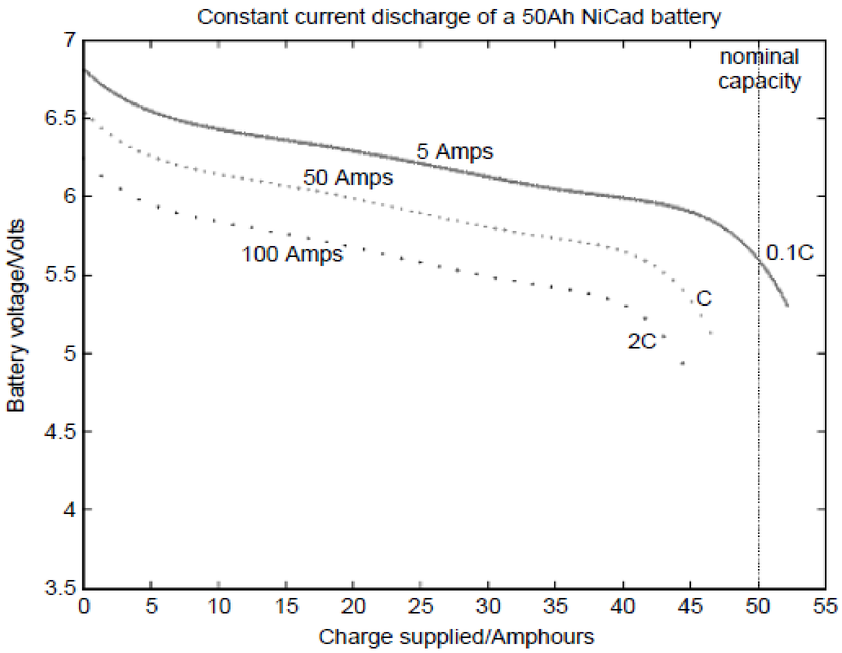

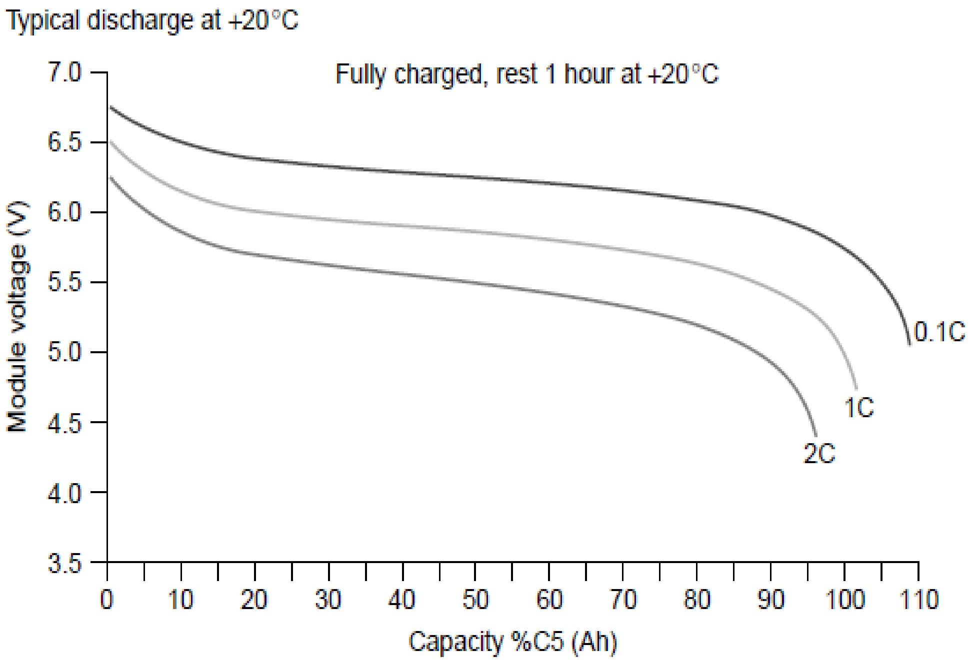

Theoretical results

Experimental results

MATLAB: Figure_2_15.m

Battery modelling

Power supplied for the load → $P = V \times I = (E - IR)I = EI - RI^2$

Current supplied for the load → $I = \dfrac{E - \sqrt{E^2 - 4RP}}{2R}$

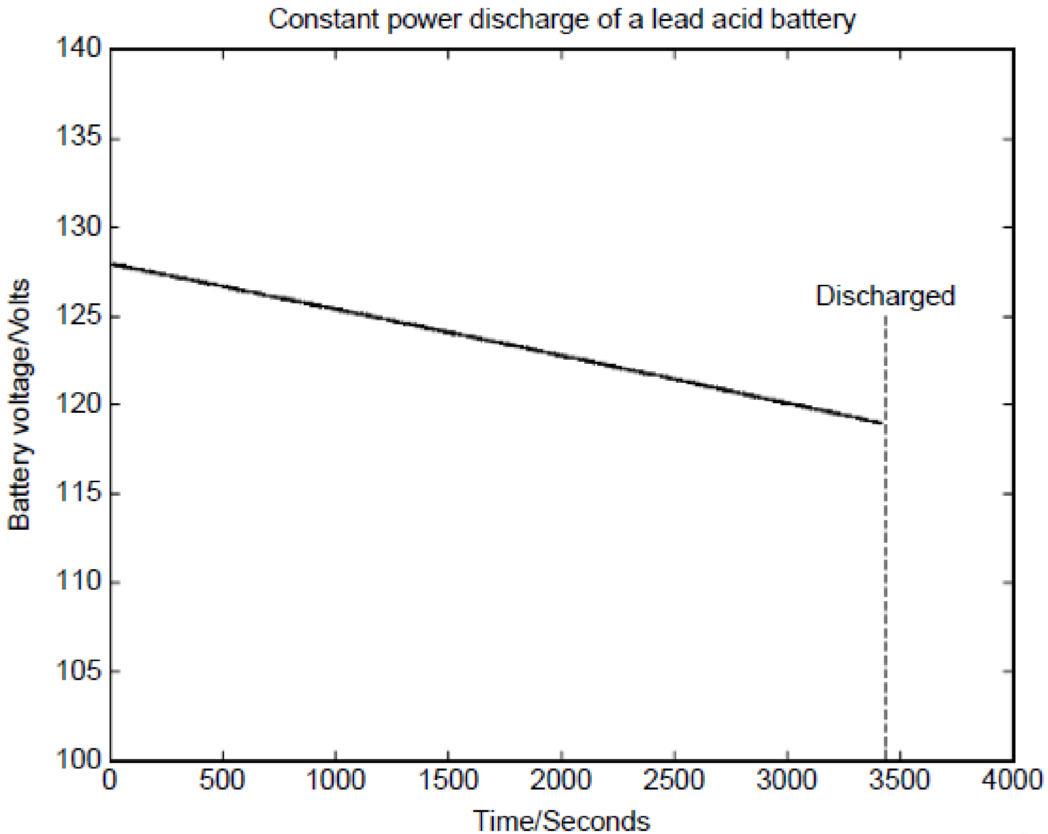

- Graph of constant power discharge of a lead acid battery at 5000 W.
- The nominal ratings of the battery are 120 V (10 batteries), 50 Ah.
- The battery is "dead" if the DoD exceeds 99%

INEP

MATLAB: Figure_2_17.m

Battery modelling

If the battery is being charged:

Terminal voltage → $V = E + IR$

Power drained from the load → $P = V \times I = (E + IR)I = EI + RI^2$

Current drained from the load → $I = \dfrac{-E + \sqrt{E^2 + 4RP}}{2R}$

Charged removed → $CR_{n+1} = CR_n - \dfrac{\delta t \times I^k}{3600}[Ah]$

INEP

Battery modelling

Calculating the Peukert Coefficient

The two different ratings give two different rated currents:

$$I_1 = \frac{C_1}{T_1} \quad \text{and} \quad I_2 = \frac{C_2}{T_2}$$

$$C_P = I_1{}^k \times T_1 \quad \text{and} \quad C_P = I_2{}^k \times T_2$$

$$I_1{}^k T_1 = I_2{}^k T_2$$

$$\left(\frac{I_1}{I_2}\right)^k = \frac{T_2}{T_1}$$

$$k = \frac{\log T_2 - \log T_1}{\log \mathrm{I}_1 - \log \mathrm{I}_2}$$

Battery modelling

Calculating the Peukert Coefficient

Example:

$$I_1 = \frac{C_1}{T_1} = \frac{42}{10} = 4.2A \quad \text{and} \quad I_2 = \frac{33.6}{1} = 33.6A$$

$$k = \frac{\log 1 - \log 10}{\log 4.2 - 33.6} = 1.107$$

INEP

Battery modelling

Approximate battery sizing

The vehicle fuel consumption is normally known.

Diesel car example
Fuel consumption: 18 km/L
Diesel specific energy: 40 kWh/kg
Motor transmission efficiency: 10%

Fuel consumed in a distance of 180 km: 10 L ≈ 11 kg
Energy consumed in 180 km: 40 kWh/kg × 11 kg =440 kWh
Energy delivered in the roads: 440 kWh × 0.1= 44 kWh
Energy required for a electric vehicle:

$$Energy_{EV} = \frac{\text{Energy delivered in the roads}}{\text{efficiency (eletric motor+transmission} \approx 70\%)} = \frac{44kWh}{0.7} = 62.8kWh$$

Battery modelling

Approximate battery sizing

The mass of different types of battery for different distances travelled are shown in Table 2.11, assuming an electric motor/drive efficiency of 70%.

Battery type	Specific energy $Wh.kg^{-1}$	Battery mass kg, 75 km range	Battery mass kg, 150 km range	Battery mass kg, 225 km range	Battery mass kg, 300 km range
Lead acid	30	750	1500	2250	3000
NiMH	65	346	692	1038	1385
Li ion	90	250	500	750	1000
NaNiCl	100	225	450	675	900
Zn-Air	230	98	196	293	391

Motor modelling

Motor modelling

Permanent magnetic DC motor

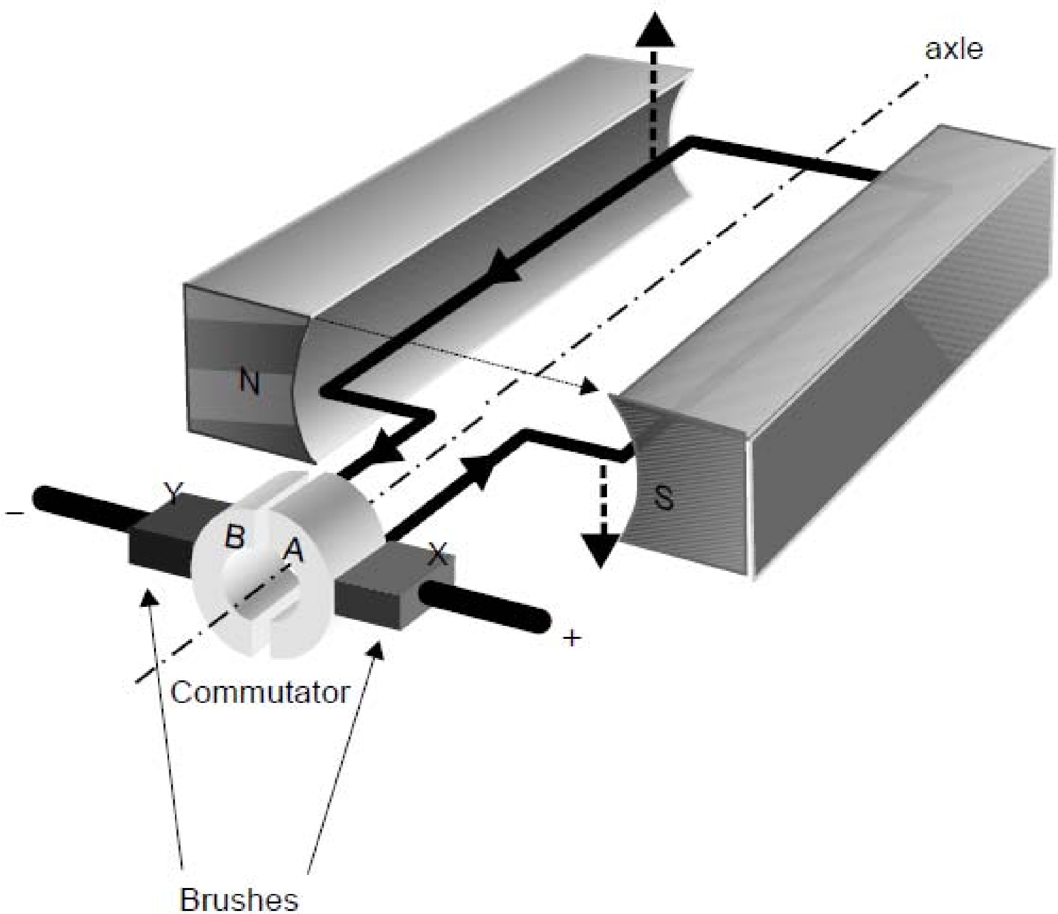

Motor modelling

Permanent magnetic DC motor

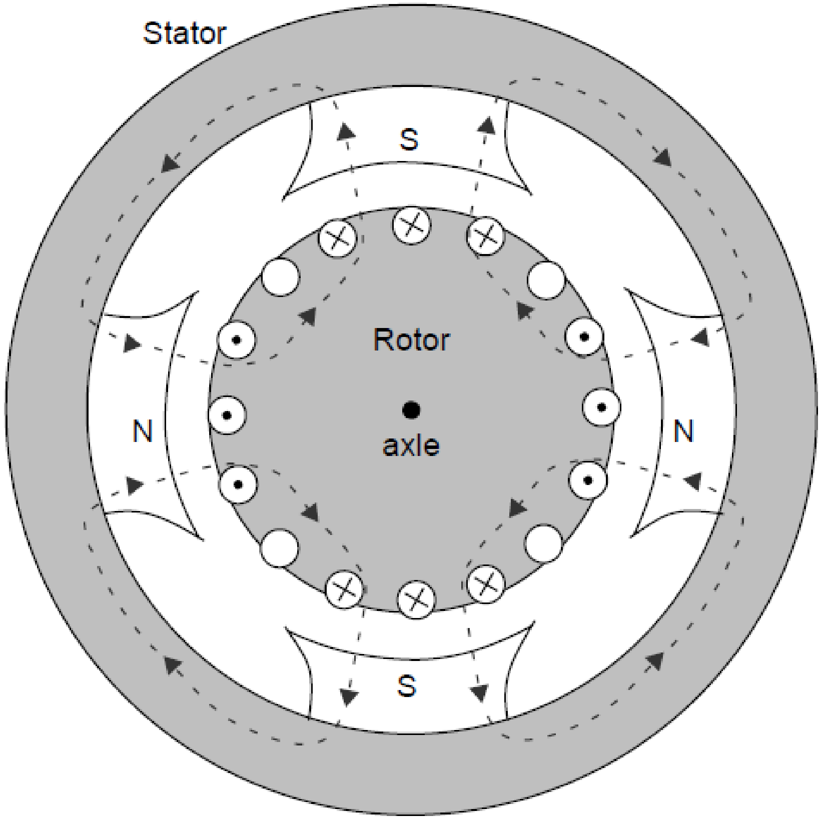

(a)

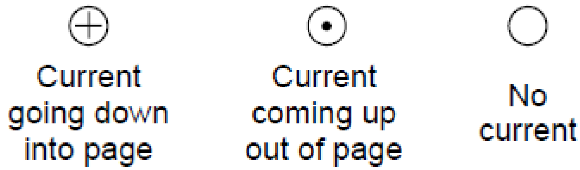

Motor modelling

Permanent magnetic DC motor

Torque:

$$\vec{F} = i\vec{L} \times \vec{B}$$

$$\Phi = BA = B(2Lr)$$

$$\vec{\tau} = \vec{F} \times \vec{r}$$

$$\tau = 2nBILr$$

$$\tau = n\Phi I \quad \text{or}$$

$$\boxed{\tau = K_m \Phi \cdot I}$$

$K_m \propto$ n°polos, n° turns, etc.

Back EMF:

$$E_b = \frac{d\Phi}{dt} = \frac{d(BA)}{dt} = BLv$$

$$v = r\omega$$

$$E_b = 2nBLr\omega$$

$$\boxed{E_b = K_m \Phi \cdot \omega}$$

INEP

Motor modelling

Permanent magnetic DC motor

$$I = \frac{V}{R_a} = \frac{E_s - E_b}{R_a} = \frac{E_s}{R_a} - \frac{K_m \Phi}{R_a}\omega$$

$$\tau = K_m \Phi I = \frac{E_s K_m \Phi}{R_a} - \frac{(K_m \Phi)^2}{R_a}\omega$$

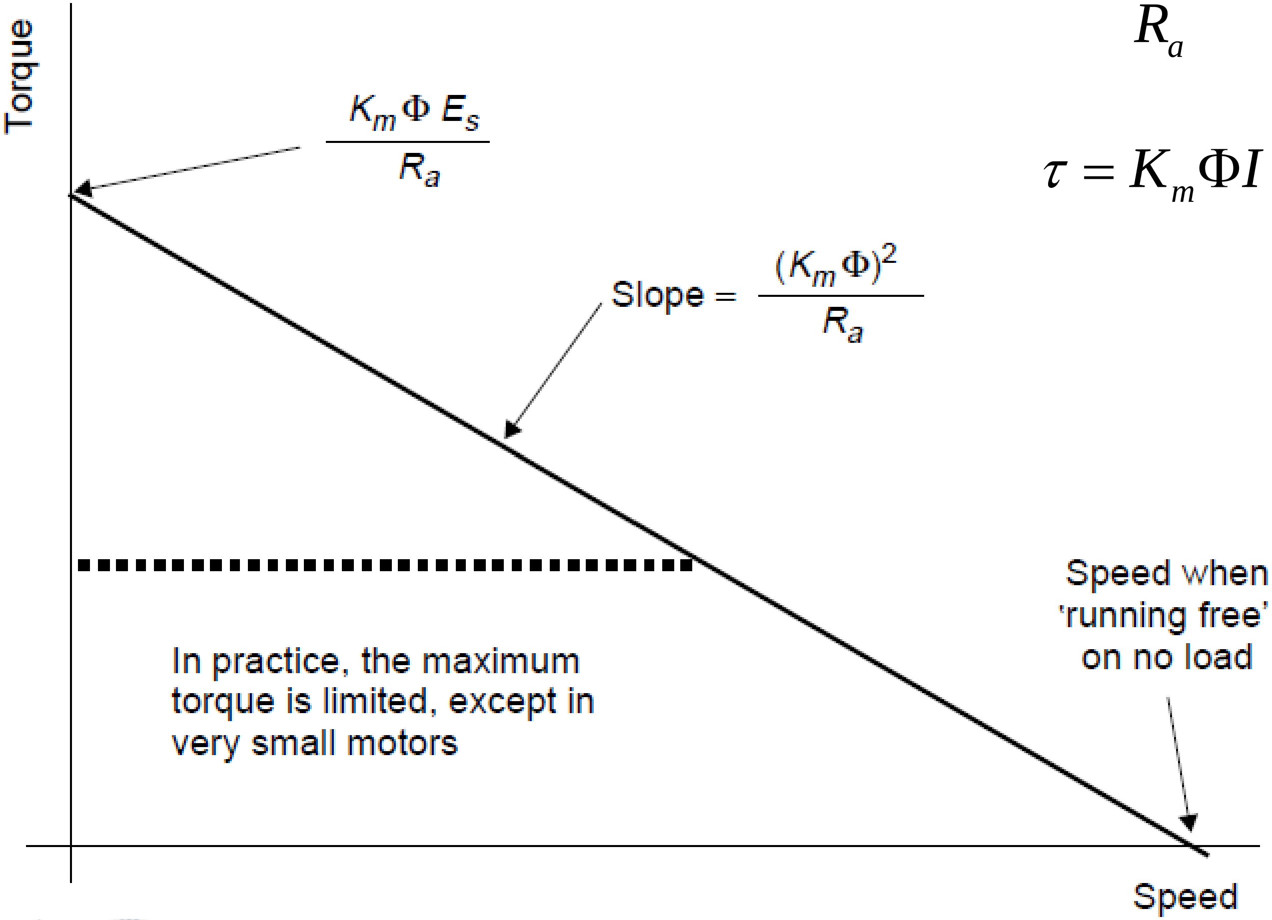

Motor modelling

Permanent magnetic DC motor

For a DC **Lynch motor**:

Motor speed = 70 rpm/V
Armature resistance = 0.016Ω

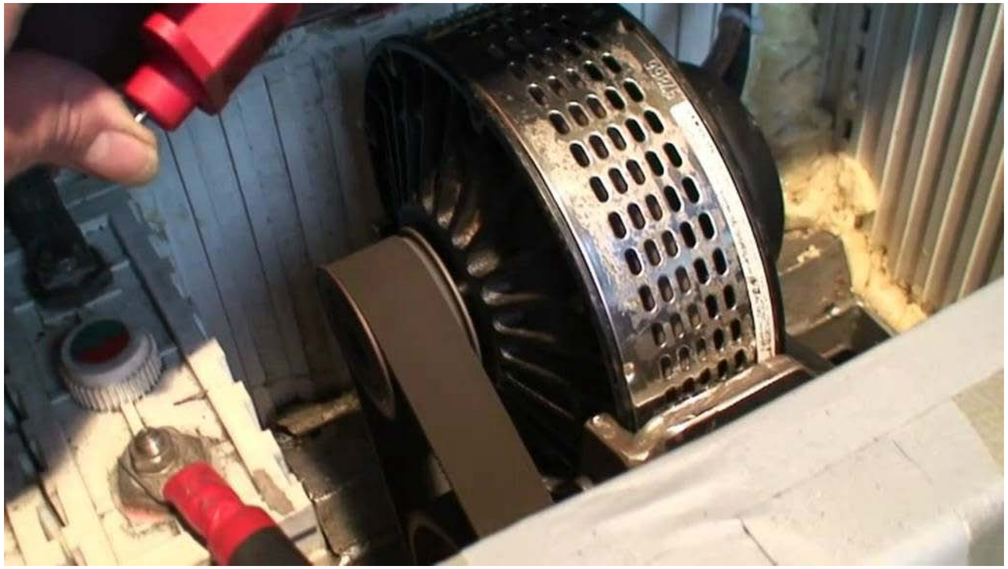

$$\omega = \frac{E}{K_m\Phi}\frac{rad}{s} = \frac{60}{2\pi}\frac{E}{K_m\Phi}RPM$$

$$K_m\Phi = 0.136$$

If the motor is running with 24 V:

$$\tau = K_m\Phi I = \frac{E_s K_m\Phi}{R_a} - \frac{\left(K_m\Phi\right)^2}{R_a}\omega$$

$$\boxed{\tau = 205 - 1.16\omega}$$

Motor modelling

Permanent magnetic DC motor

At zero speed: $\tau = 205 - 1.16\omega = 205 - 1.16(0) = 205 Nm$

At zero speed there is no back EMF, so: $I = \frac{V}{R_a} = \frac{E_s - E_b}{R_a} = \frac{E_s}{R_a} = \frac{24}{0.016} = 1500 A$

The current is too large and should be limited. In this example it will be limited in 250 A. Therefore, the maximum toque is:

$$\tau = K_m \Phi I = 0.136 \times 250 = 34 Nm$$

These values are typical for 5 kW dc motors.

Motor modelling

DC motor efficiency

Copper losses = $k_c \tau^2$ → $P = I^2 R,\ I \alpha \tau$
Iron losses = $k_i \omega$
Friction and windage losses = $k_\omega \omega^3$
Constant losses = C

$$\eta_m = \frac{P_o}{P_i} = \frac{\tau\omega}{\tau\omega + k_c \tau^2 + k_i \omega + k_\varpi \omega^3 + C}$$

MATLAB: motoreff.m

Typical values for the parameters of equation

Parameter	Lynch type PM motor, with brushes, 2–5 kW	100 kW, high speed induction motor
k_c	1.5	0.3
k_i	0.1	0.01
k_w	10^{-5}	5.0×10^{-6}
C	20	600

Motor modelling

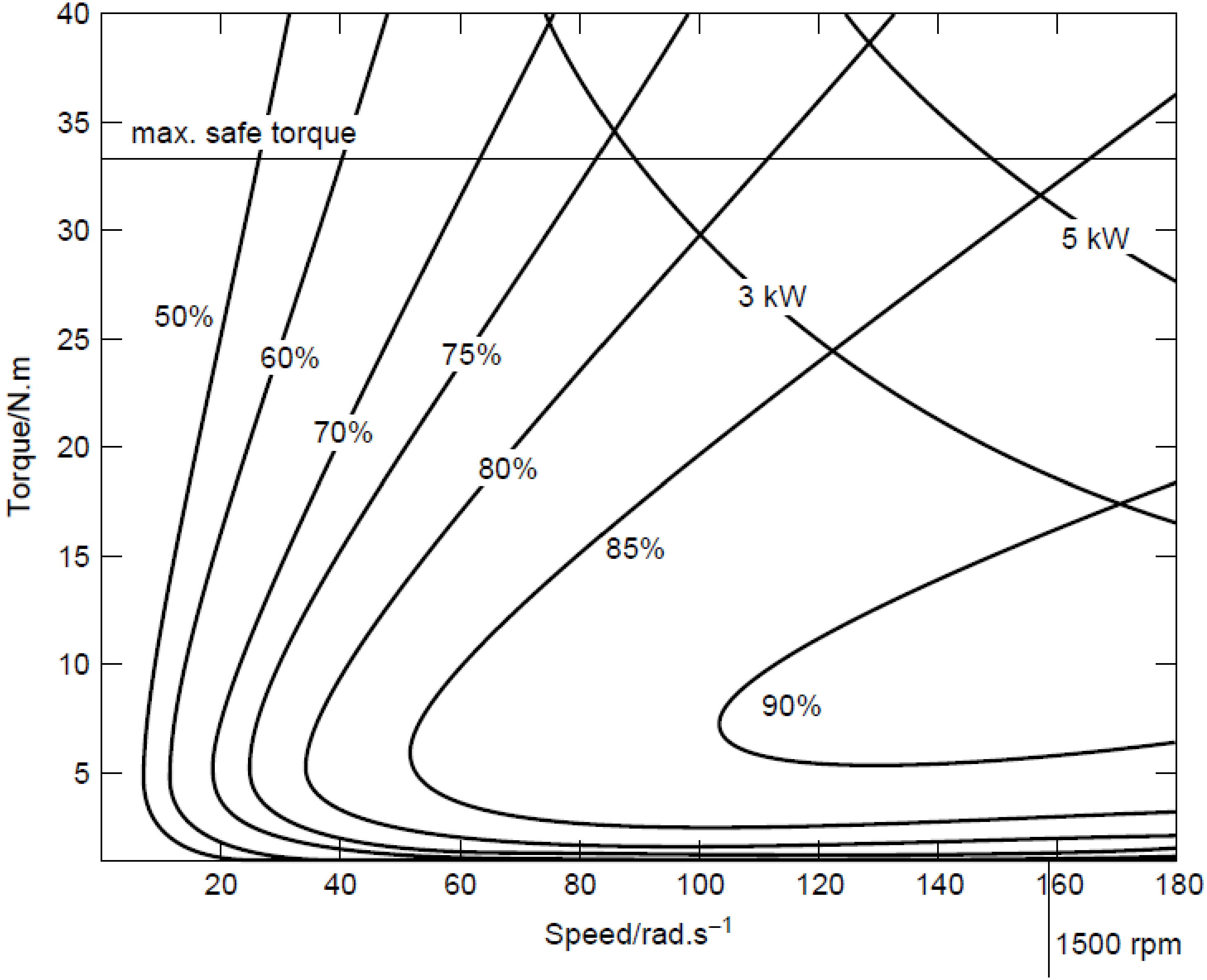

Vehicle modelling

Vehicle modelling

Tractive force

The electric vehicle should:

- overcome the rolling resistance
- overcome the aerodynamic drag
- provide the force needed to overcome the component of the vehicle's weight acting down the slope
- accelerate the vehicle, if the velocity is not constant

Vehicle modelling

Tractive force

Rolling resistance force	$= F_{rr}$
Aerodynamic drag	$= F_{ad}$
Hill climbing force	$= F_{hc}$
Linear acceleration force	$= F_{la}$
Angular acceleration force	$= F_{\omega a}$
Total tractive effort	$= F_{te}$

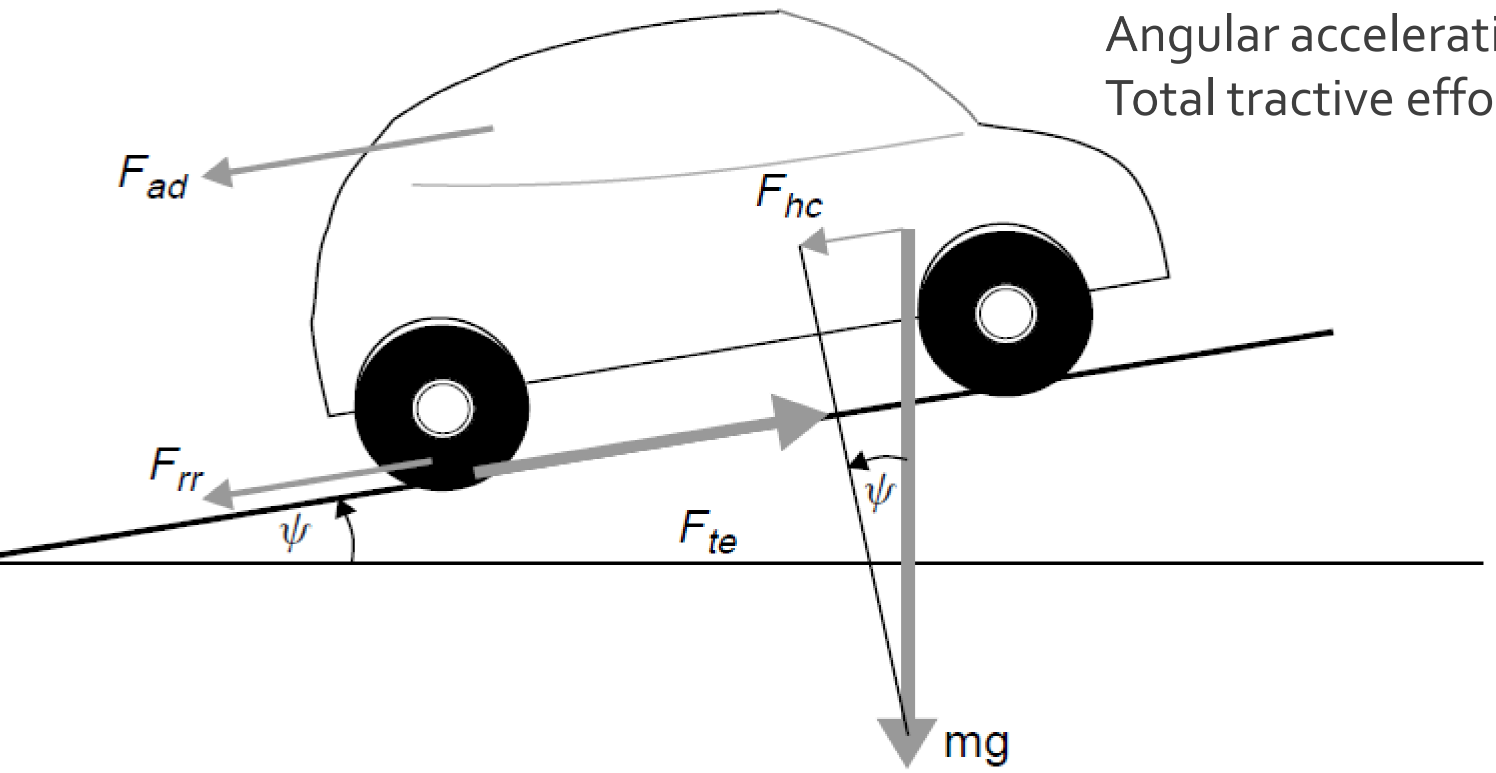

Vehicle modelling

Tractive force

Rolling resistance force → $F_{rr} = \mu_{rr} mg$

Typical values: μ_{rr}= 0.015 for a radial ply tyre
μ_{rr}= 0.005 for tyre developed especially for electric vehicles.

Aerodynamic drag → $F_{ad} = 0.5 \rho A C_d \upsilon^2$

ρ = density of the air
A = frontal area
υ = speed
C_d = drag coefficient

Typical values for C_d:
Conventional cars: C_d=0.3
Electric vehicle: C_d=0.19
Motorcycle and bus: C_d=0.7

Vehicle modelling

Tractive force

Hill climbing force → $F_{hc} = mg\sin(\psi)$

Linear acceleration force → $F_{la} = ma$

Angular acceleration force → due to the rotating parts

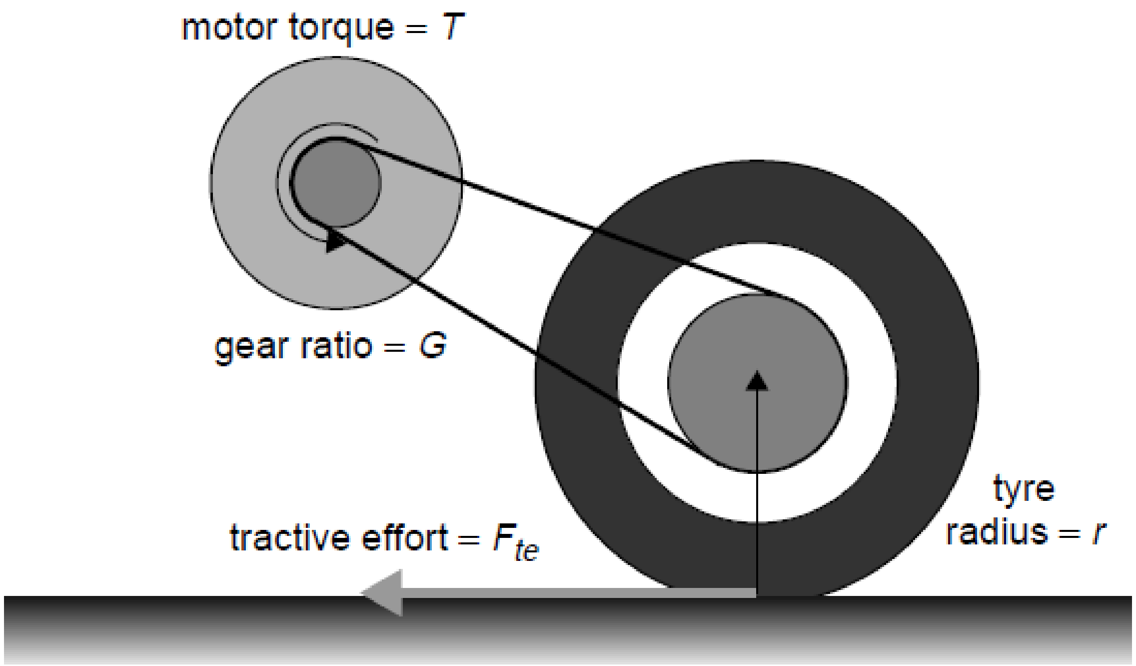

$$\vec{\tau} = \vec{F} \times \vec{r}$$

$$\tau = \frac{F_{te} r}{G}$$

$$F_{te} = \frac{G}{r}\tau$$

Vehicle modelling

Tractive force

Angular speed at the axle → $\omega = \dfrac{v}{r}$

Angular speed at the motor → $\omega = G\dfrac{v}{r}$

Motor angular acceleration → $\dot{\omega} = G\dfrac{a}{r}$

Torque required for this acceleration → $\tau = I\dot{\omega} = IG\dfrac{a}{r}$

Angular acceleration force → $F_{\omega a} = \dfrac{G}{r}T = I\left(\dfrac{G}{r}\right)^2 a$

Vehicle modelling

Tractive force

It will quite often turn out that the moment of inertia of the motor will not be known.

In such cases a reasonable approximation is to simply increase the mass by 5% in F_{la} and to ignore the $F_{\omega a}$ term.

Total tractive force → $$F_{te} = F_{rr} + F_{ad} + F_{hc} + F_{la} + F_{\omega a}$$

We should note that F_{la} and $F_{\omega a}$ will be negative if the vehicle is slowing down, and that F_{hc} will be negative if it is going downhill.

Vehicle modelling

Modelling Vehicle Acceleration

For $\omega < \omega_c$ or $v < (r/G)\,\omega_c$ then $\tau = \tau_{max}$

For $\omega \geq \omega_c$ or $v \geq (r/G)\,\omega_c$ then $\tau = \tau_o - k\omega$

For a vehicle on level ground, and air density of 1.25 kg.m^{-3} :

$$F_{te} = \mu_{rr} mg + 0.625 A C_d v^2 + ma + I \frac{G^2}{\eta_g r^2} a$$

$$F_{te} = \frac{G}{r}\tau \qquad a = \frac{dv}{dt}$$

$$\frac{G}{r}\tau = \mu_{rr} mg + 0.625 A C_d v^2 + \left(m + I \frac{G^2}{\eta_g r^2} \right) \frac{dv}{dt}$$

Vehicle modelling

Modelling the acceleration of an electric scooter:

2013 Peugeot Vivacity E

Vehicle modelling

Modelling the acceleration of an electric scooter:

Characteristics:

- Electric Scooter mass = 115 kg + 70 kg (pilot) = 185 kg
- The moment of inertia of the motor is not known, so *m is increased* by 5%, therefore, Electric Scooter mass = 194 kg
- The drag coefficient (C_d) is estimated as 0.75
- The frontal area of vehicle and rider = 0.6 m^2
- Coefficient of the tire rolling resistance μ_{rr} = 0.007
- The motor ratio belt = 2:1, and wheel diameter= 42 cm, thus, *G* = 2
- Gear system efficiency (η_g) = 98%
- The motor is an 18V **Lynch** type motor
- Motor speed = 70 rpm/V
- Armature resistance = 0.016 Ω

Vehicle modelling

Modelling the acceleration of an electric scooter:

Torque equation:

$$K_m\Phi = \frac{60}{2\pi}\frac{E}{RPM} = \frac{60}{2\pi}\frac{1}{70} = 0.136$$

$$\tau = K_m\Phi I = \frac{E_s K_m\Phi}{R_a} - \frac{\left(K_m\Phi\right)^2}{R_a}\omega = \frac{18\times 0.136}{0.016} - \frac{\left(0.136\right)^2}{0.016}\omega$$

$$\tau = 153 - 1.16\omega$$

The current will be limited in 250A, therefore, the maximum torque is:

$$\tau = K_m\Phi I = 0.136\times 250 = 34Nm$$

INEP

Vehicle modelling

Modelling the acceleration of an electric scooter:

Critical motor speed :

$$34 = 153 - 1.16\omega$$

$$\omega = \frac{153-34}{1.16} = 103\frac{rad}{s}$$

For constant torque:

$$\frac{G}{r}\eta_g\tau = \mu_{rr}mg + 0.625AC_d v^2 + \left(m + I\frac{G^2}{\eta_g r^2}\right)\frac{dv}{dt}$$

$$\frac{2}{0.21}\times 0.98\times 34 = 0.007\times 185\times 9.8 + 0.625\times 0.6\times 0.75v^2 + 194\frac{dv}{dt}$$

$$317 = 12.7 + 0.281v^2 + 194\frac{dv}{dt}$$

$$\frac{dv}{dt} = 1.57 - 0.00145v^2$$

INEP

Vehicle modelling

Permanent magnetic DC motor

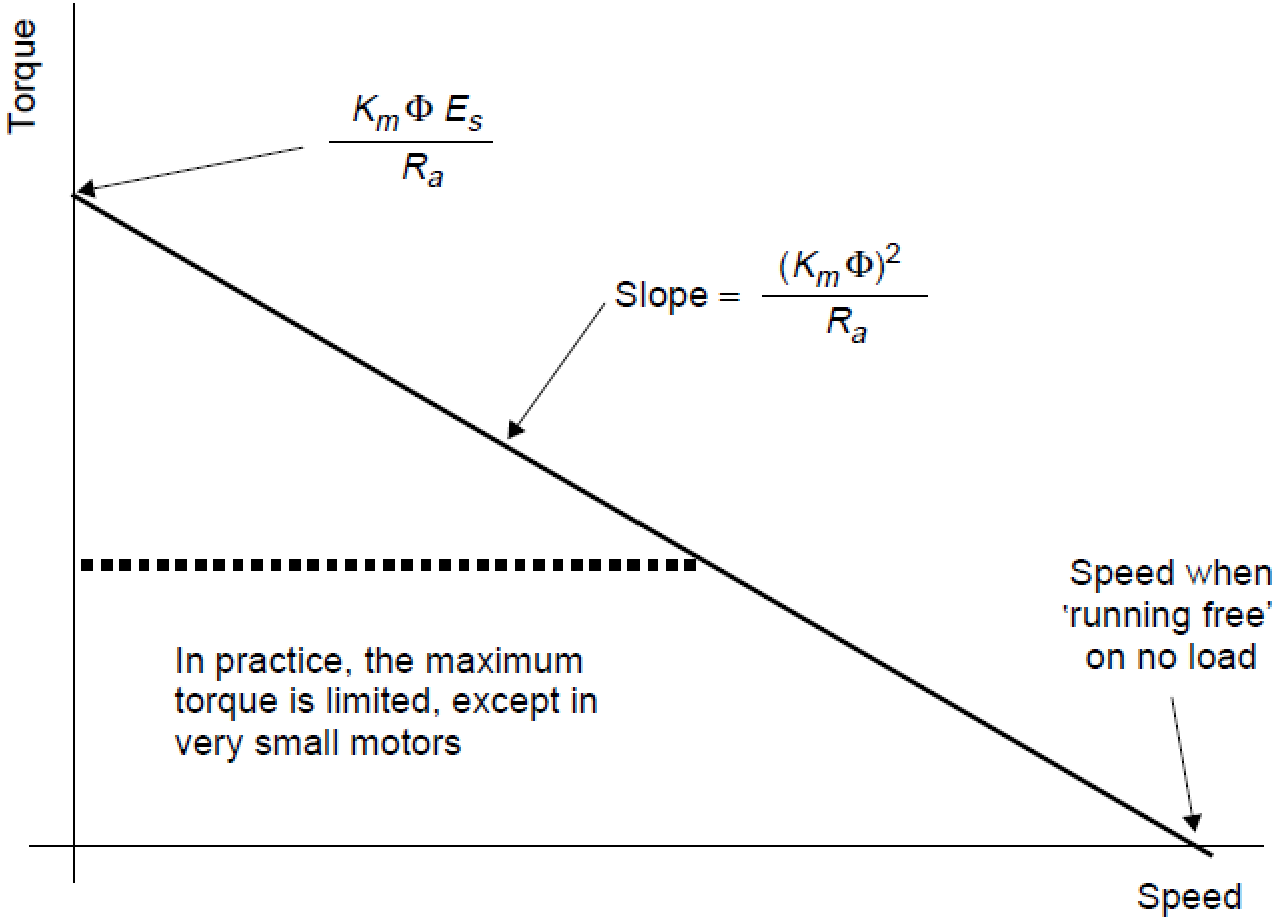

Vehicle modelling

Modelling the acceleration of an electric scooter:

This equation holds until the torque begins to fall when, $\omega = \omega_c$ = 103 rad/s, which corresponds to 103 × 0.21/2 = 10.8 m/s. After this point the torque is governed by :

$$153 - 1.16\omega = \mu_{rr} mg + 0.625 A C_d v^2 + \left(m + I \frac{G^2}{\eta_g r^2} \right) \frac{dv}{dt}$$

$$\frac{2}{0.21} \times 0.98 \times \left(153 - 1.16 \frac{2}{0.21} v \right) = 0.007 \times 185 \times 9.8 + 0.625 \times 0.6 \times 0.75 v^2 + 194 \frac{dv}{dt}$$

$$1428 - 103v = 12.7 + 0.281 v^2 + 194 \frac{dv}{dt}$$

$$\frac{dv}{dt} = 7.3 - 0.53v - 0.00145 v^2$$

Vehicle modelling

Modelling the acceleration of an electric scooter:

The derivative of *v* is simply the difference between consecutive values of *v* divided by the time step given by :

Constant torque:

$$\frac{v_{n+1} - v_n}{\partial t} = 1.57 - 0.00145 v^2$$

$$v_{n+1} = v_n + \partial t \times \left(1.57 - 0.00145 {v_n}^2\right)$$

After critical speed:

$$v_{n+1} = v_n + \partial t \times \left(7.30 - 0.53 v_n - 0.00145 {v_n}^2\right)$$

MATLAB: ScootA.m

INEP

Vehicle modelling

Modelling the acceleration of an electric scooter:

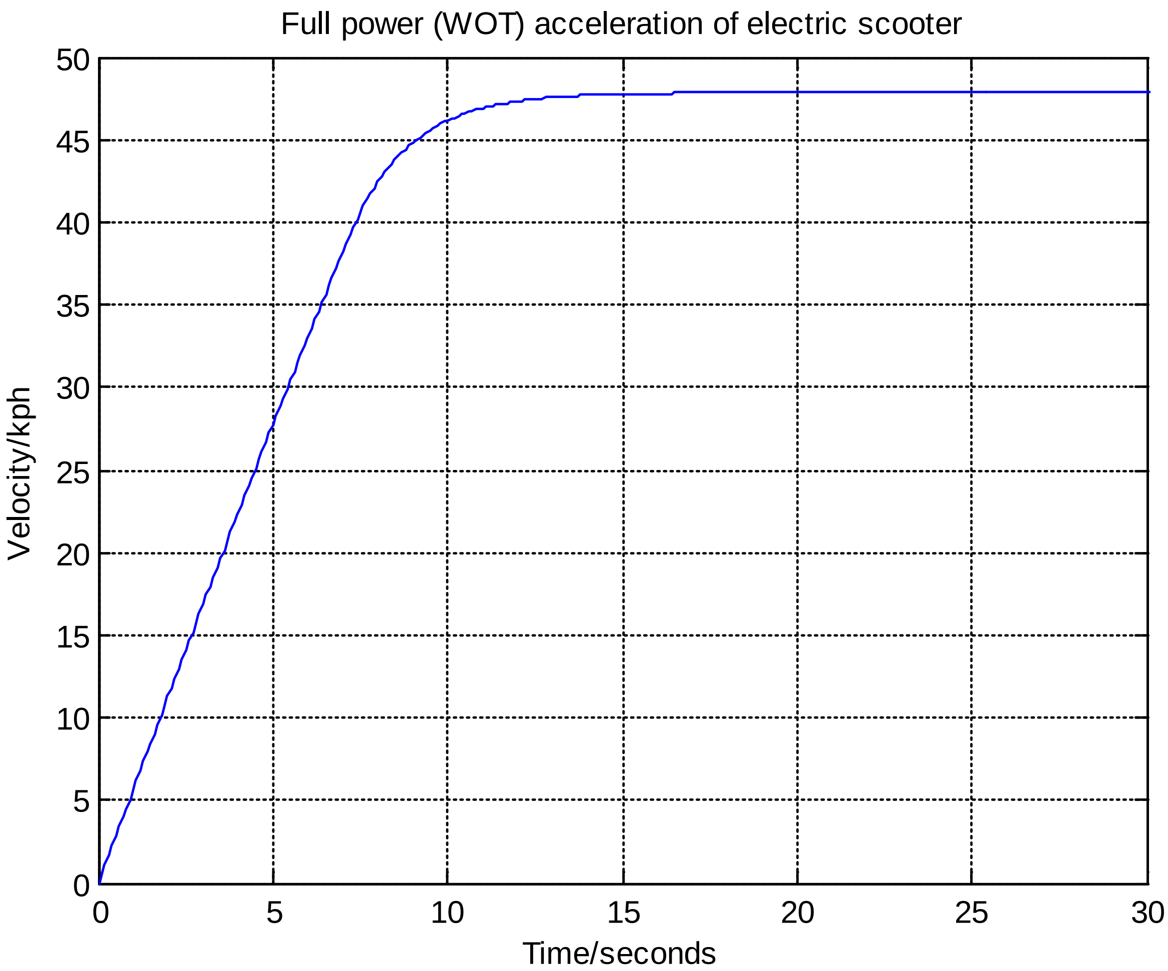

Peugeot electric scooter:
Maximum speed: 45 kph

Vehicle modelling

Modelling the acceleration of an electric scooter:

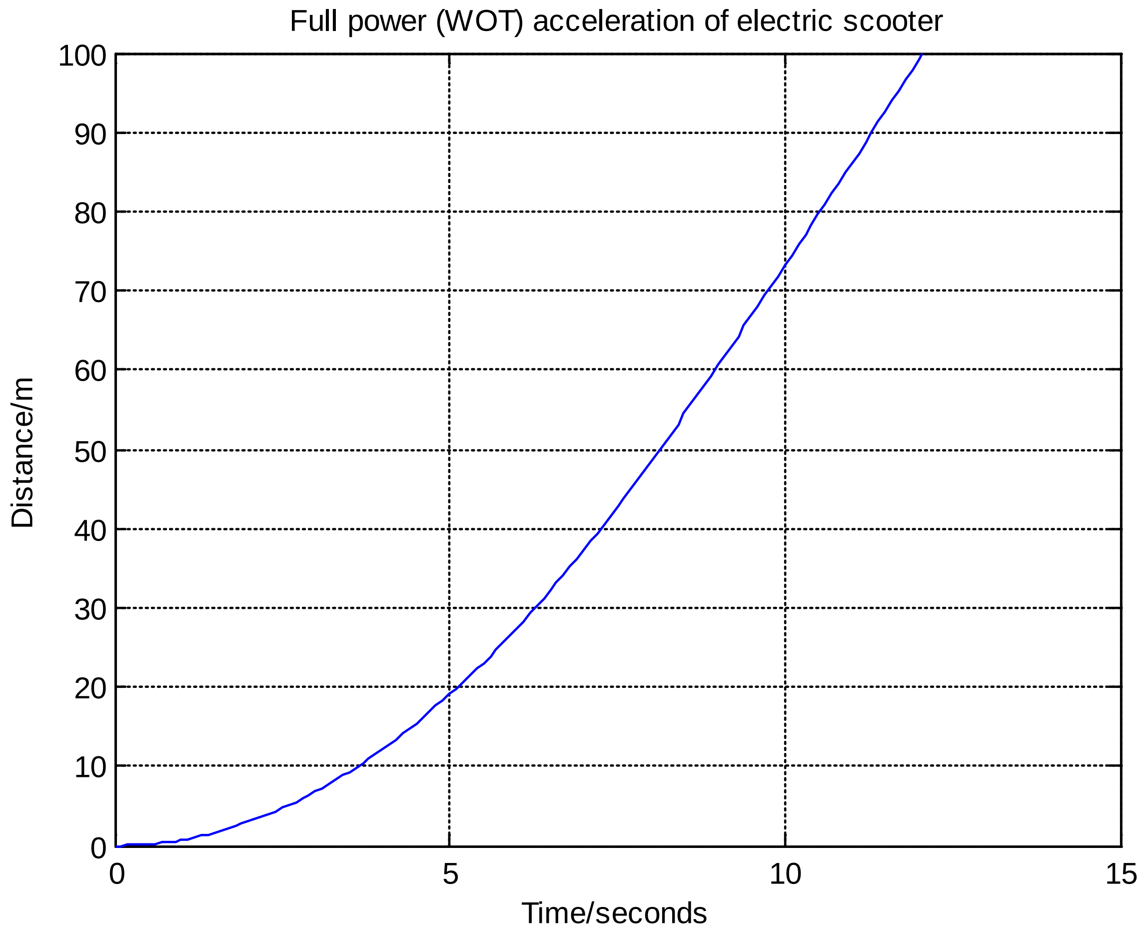

Peugeot electric scooter:

- 10m from standing start time, 3.2 s
- 100m from standing start time, 12 s

Vehicle modelling

Modelling the acceleration of a small car:

GM EV1

Vehicle modelling

Modelling the acceleration of a small car:

Manufacturer	General Motors
Also called	GM EV1, Saturn EV1
Production	1996–1999 (1,117 units) 1997 Model Year: 660 Gen I units 1999 Model Year: 457 Gen II units
Body and chassis	
Class	Electric subcompact car
Body style	2-seat, 2-door coupé
Layout	Transverse front-motor, front-wheel drive
Powertrain	
Electric motor	three-phase Alternating current Induction motor with IGBT power inverter 137 bhp (102 kW) at 7000 rpm 110 lb·ft (149 N·m) at 0–7000 rpm
Transmission	Single-speed reduction integrated with motor and differential
Plug-in charging	6.6 kW Magne Charge inductive converter
Dimensions	
Wheelbase	98.9 in (2,512 mm)
Length	169.7 in (4,310 mm)[1]
Width	69.5 in (1,765 mm)[2]
Height	50.5 in (1,283 mm)
Curb weight	3,086 lb (1,400 kg) with Lead-acid batteries 2,908 lb (1,319 kg) with NiMH batteries
Chronology	
Predecessor	GM Impact (prototype)

Vehicle modelling

Modelling the acceleration of a small car:

Characteristics:

- Vehicle mass = 1400 kg + 140 kg (driver + passenger) = 1540 kg
- The moment of inertia of the motor is not known, so m is increased by 1.3%, therefore, the total vehicle mass = 1560 kg
- An ultra-low drag coefficient (C_d) of 0.19
- The frontal area of vehicle = 1.8 m^2
- Very low Coefficient of rolling resistance μ_{rr} = 0.0048
- Variable frequency induction motors, operating at nearly 12000 rpm (maximum)
- The gear ratio = 11:1, thus, G=11; and tyre radius = 30 cm
- Gear system efficiency (η_g) = 95%
- Motor specification: T_{max} = 140 Nm and ω_c = 733 rad/s note this means $T = T_{max}$ until v = 19.8 m/s (= 71.3 kph)

Vehicle modelling

Modelling the acceleration of a small car:

- Motor specification: T_{max} = 140 Nm and ω_c = 733 rad/s note this means $T = T_{max}$ until v = 19.8 m/s (= 71.3 kph)

For constant torque:

$$\frac{G}{r}\eta_g \tau = \mu_{rr} mg + 0.625 A C_d v^2 + \left(m + I \frac{G^2}{\eta_g r^2} \right) \frac{dv}{dt}$$

$$\frac{11}{0.3} \times 0.95 \times 140 = 72.4 + 0.214 v^2 + 1560 \frac{dv}{dt}$$

$$\frac{dv}{dt} = 3.11 - 0.000137 v^2$$

Vehicle modelling

Modelling the acceleration of a small car:

Above 19.8 m/s the motor operates at a constant 102 kW

$$T = \frac{P}{\omega} = \frac{P}{v\frac{G}{r}} = \frac{102000}{v\frac{11}{0.3}} = \frac{102000}{37 \times v} = \frac{2756}{v}$$

$$\frac{G}{r}\eta_g \frac{2756}{v} = 72.4 + 0.214v^2 + 1560\frac{dv}{dt}$$

$$\frac{96873.4}{v} = 72.4 + 0.214v^2 + 1560\frac{dv}{dt}$$

$$\frac{dv}{dt} = \frac{62.1}{v} - 0.046 - 0.000137v^2$$

INEP

Vehicle modelling

Modelling the acceleration of a small car:

The derivative of v is simply the difference between consecutive values of v divided by the time step given by :

Constant torque: $$v_{n+1} = v_n + \partial t\left(3.11 - 0.000137 v_n^{\ 2}\right)$$

After critical speed: $$v_{n+1} = v_n + \partial t\left(\frac{62.1}{v_n} - 0.046 - 0.000137 v_n^{\ 2}\right)$$

MATLAB: GMEV1.m

INEP

Vehicle modelling

Modelling the acceleration of a small car:

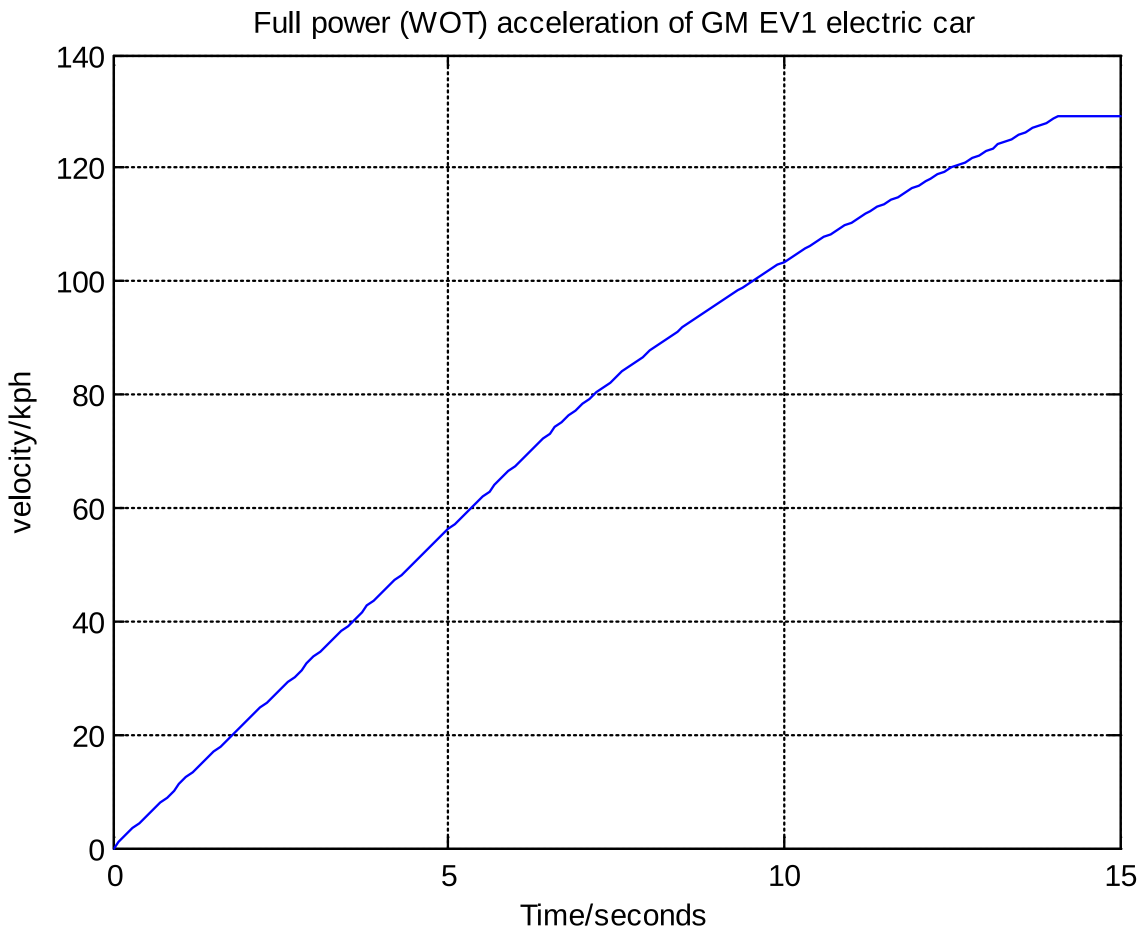

GM EV1 : from zero to 60 mph (96 kph), EV1 takes 9 s.

Electric vehicle range modelling

Electric vehicle range modelling

$$\text{EV tests}\begin{cases}\text{constant speed at level ground}\\ \text{realistic driving patterns (driving cycles)}\end{cases}$$

Well know driving cycle from Los Angeles (LA-4), called, Federal Urban Driving Schedule (FUDS), are used for emission testing by the United States Environmental Protection Agency.

MATLAB: fuds.m

Electric vehicle range modelling

Federal Urban Driving Schedule (FUDS)

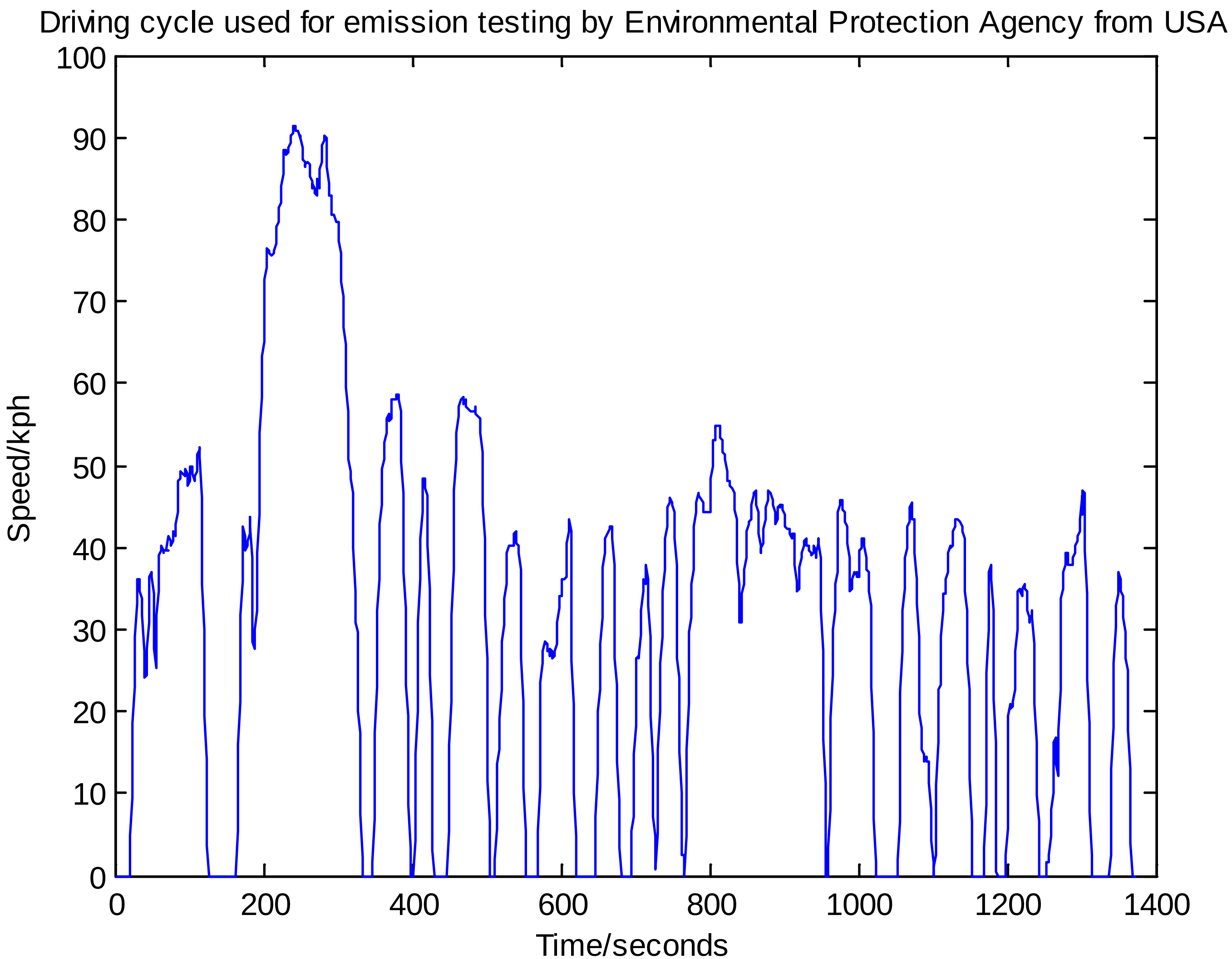

Electric vehicle range modelling

Simplified Federal Urban Driving Schedule (SFUDS)

MATLAB: sfuds.m

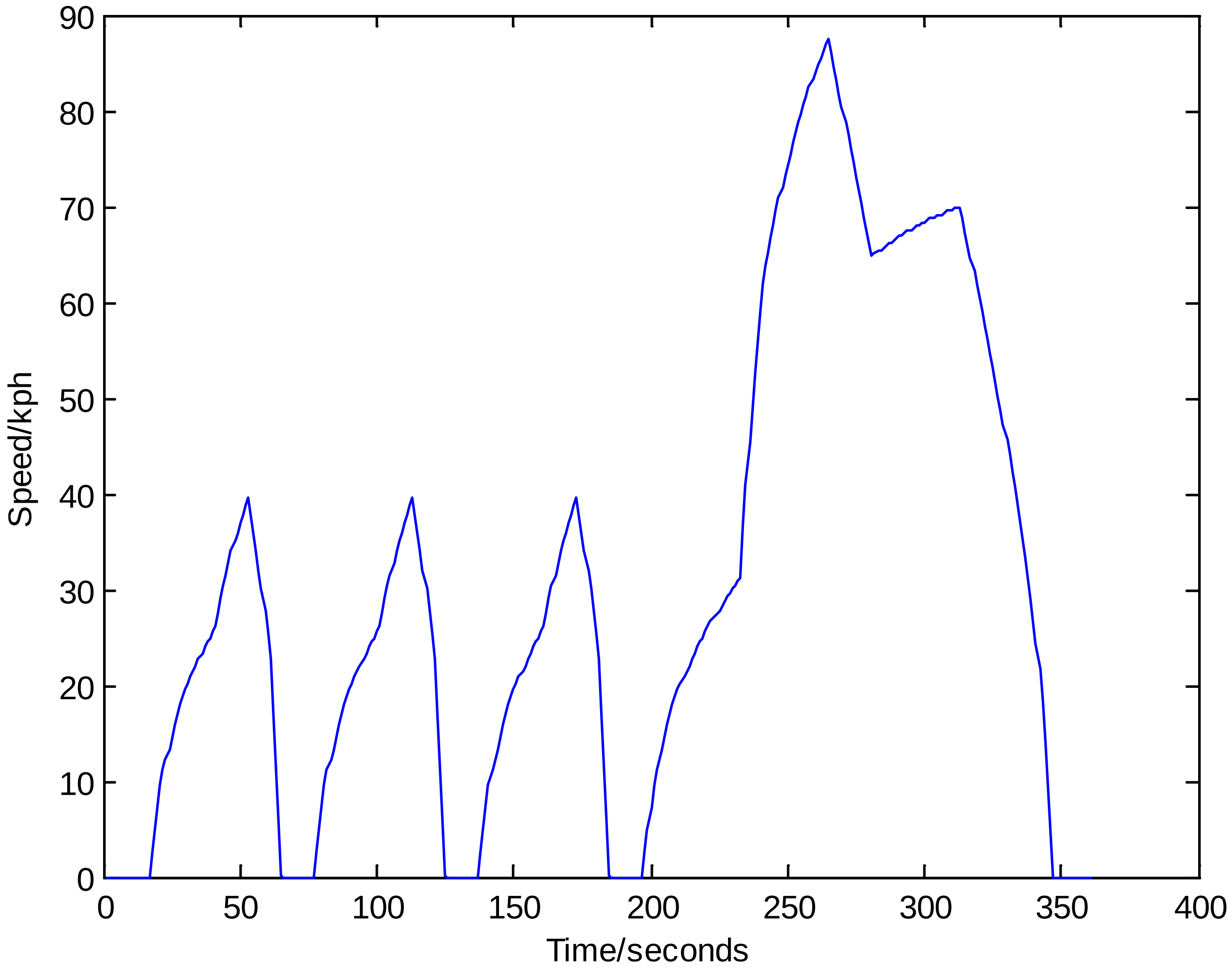

Electric vehicle range modelling

European urban driving schedule - ECE-15

MATLAB: ciclo.m

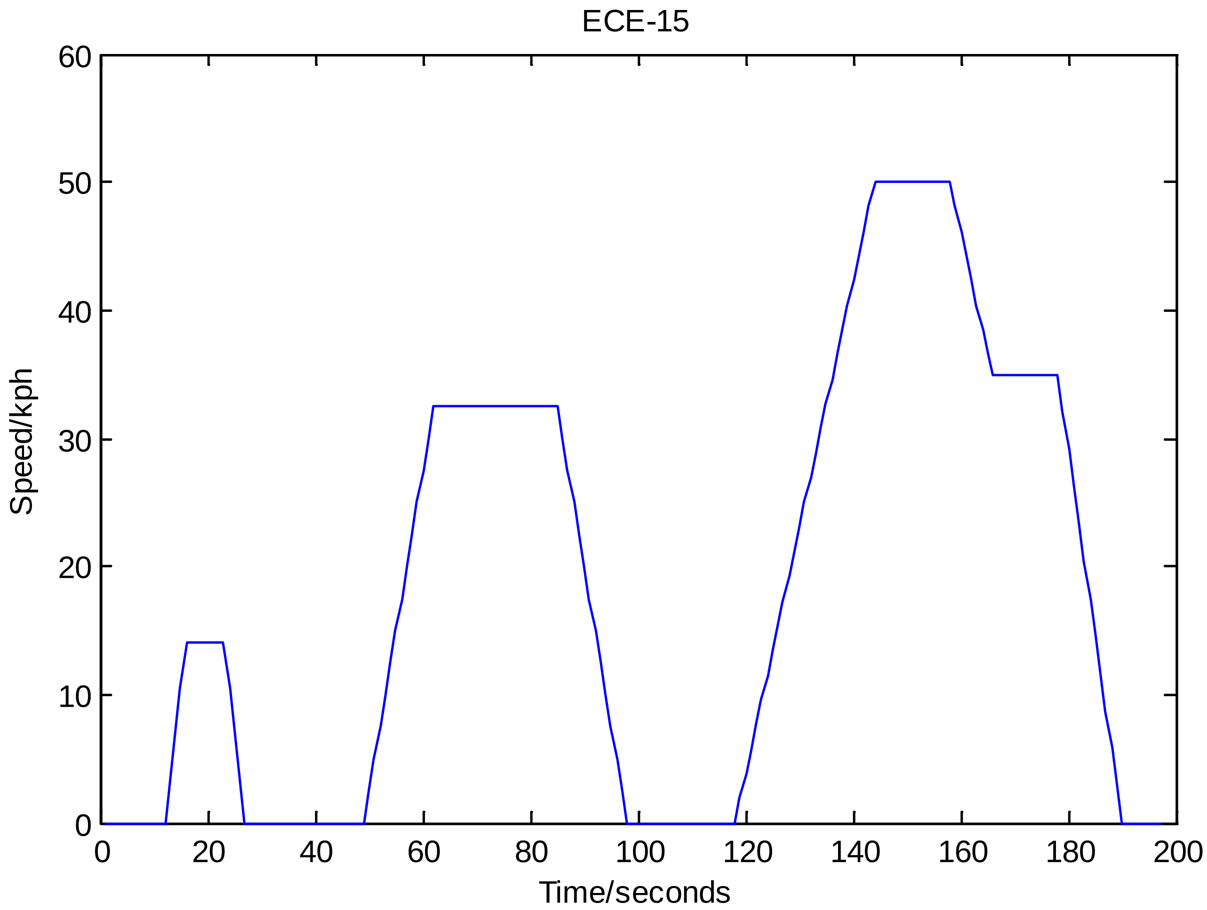

Electric vehicle range modelling

European driving cycle (ECE-47) for emission testing of mopeds and motorcycles with engine capacity less than 50 cm^3, also used for electric scooters.

MATLAB: ECE47.m

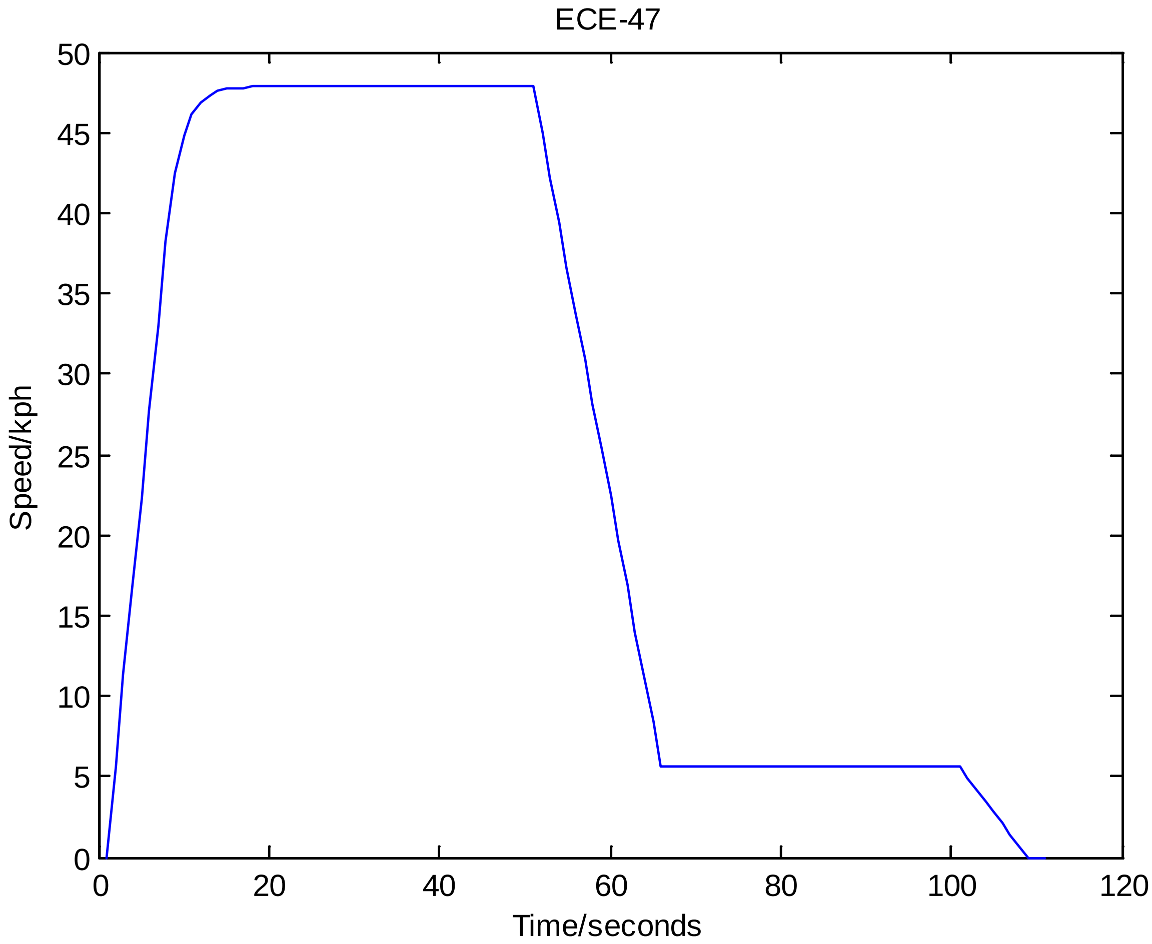

Electric vehicle range modelling

Out-of-town or highway driving:

FHDS = Federal highway driving schedule

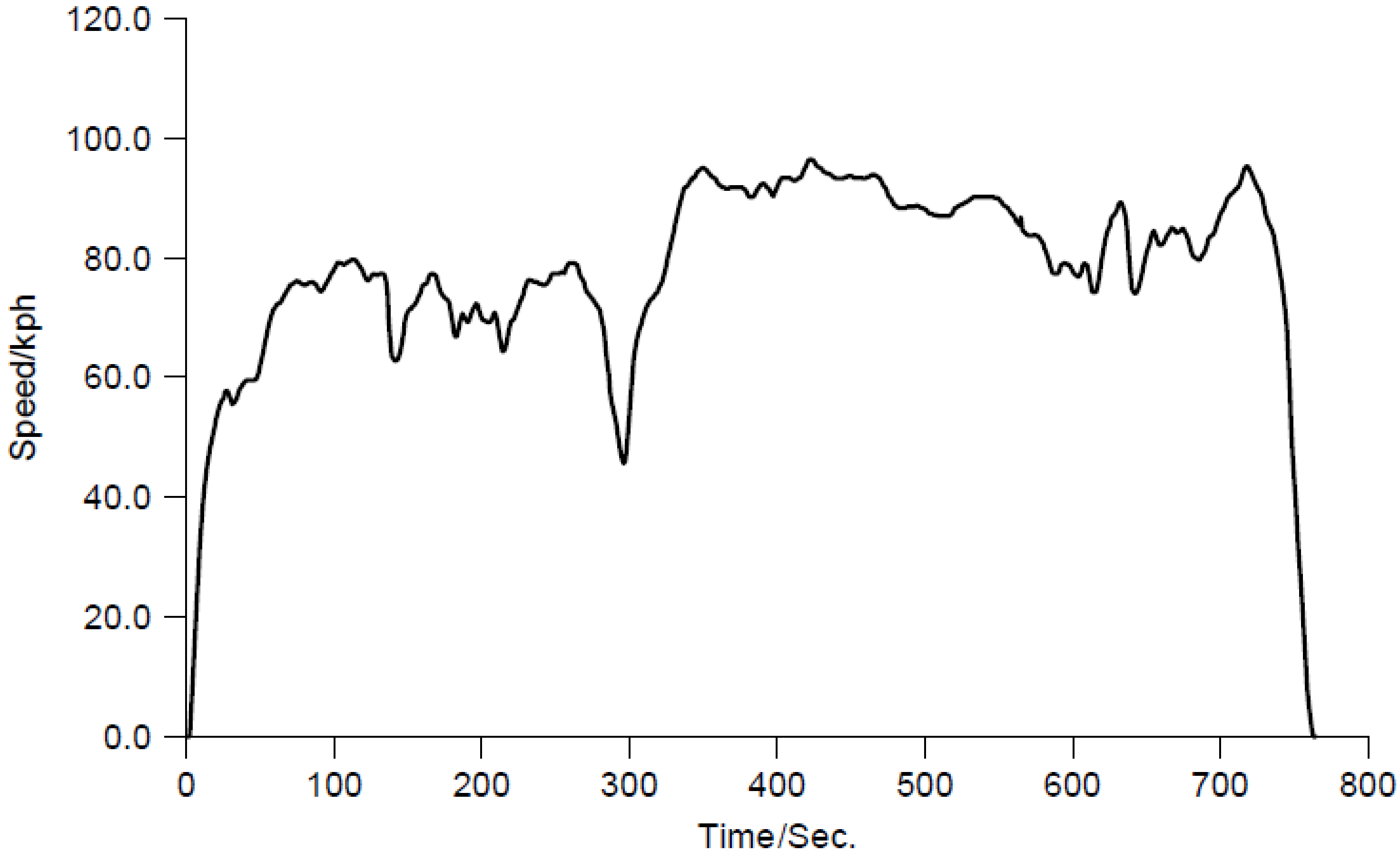

Electric vehicle range modelling

Range modelling of battery electric vehicles

To **predict the range**, the energy required to move the vehicle for **each second** of the **driving cycle** is calculated, and the effect of this **energy drain** is calculated. The process is **repeated** until the **battery is flat**. It is important to remember that if we use **one-second** time intervals, then the **power** and the **energy** consumed are **equal**.

Electric vehicle range modelling

Range modelling of battery electric vehicles

$$P = \frac{dU}{dt}$$

$$P = \frac{d(F \cdot x)}{dt} = F\frac{dx}{dt}$$

$$P = Fv$$

$$P = (F \cdot r)\omega$$

$$P = T \cdot \omega$$

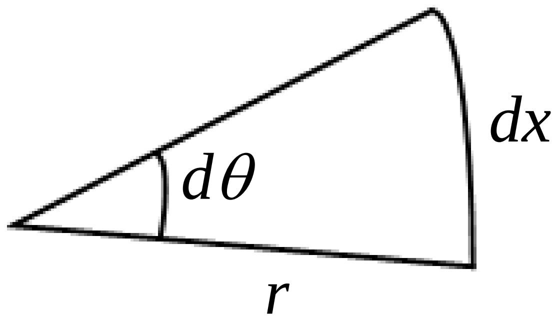

$$d\theta = \frac{dx}{r}$$

$$\frac{d\theta}{dt} = \frac{1}{r}\frac{dx}{dt}$$

$$\omega = \frac{1}{r}v$$

$$v = \omega \cdot r$$

Electric vehicle range modelling

Range modelling of battery electric vehicles

Energy required each second $\rightarrow$ $$P_{te} = F_{te} \cdot v$$

where, $$F_{te} = F_{rr} + F_{ad} + F_{hc} + F_{la} + F_{\omega a}$$

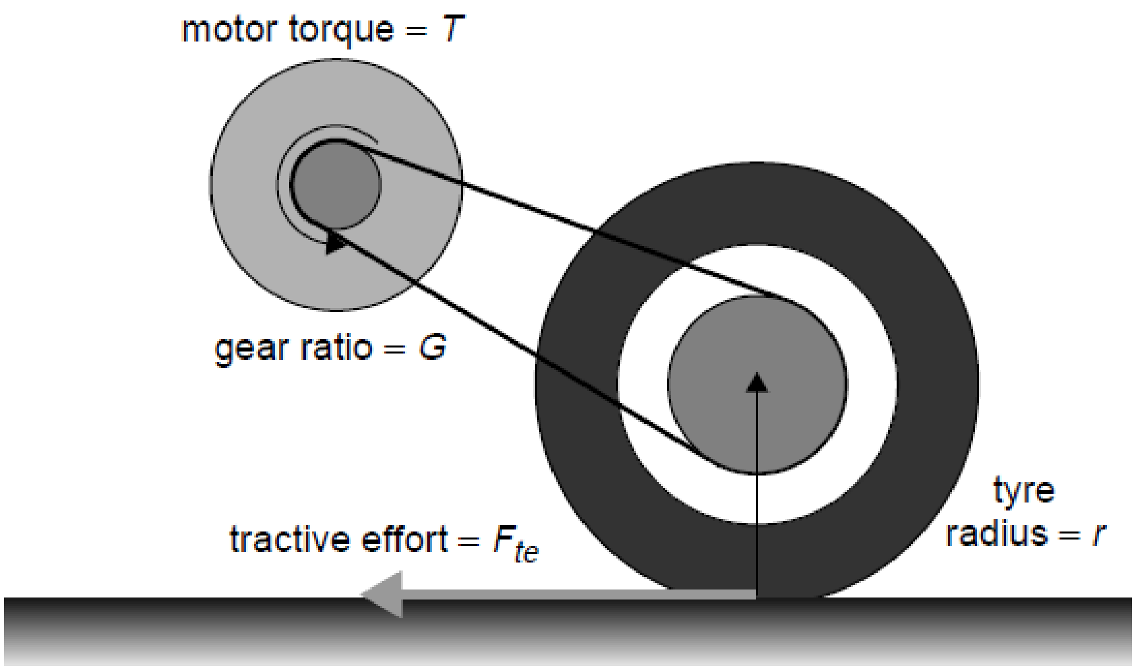

Electric vehicle range modelling

Range modelling of battery electric vehicles

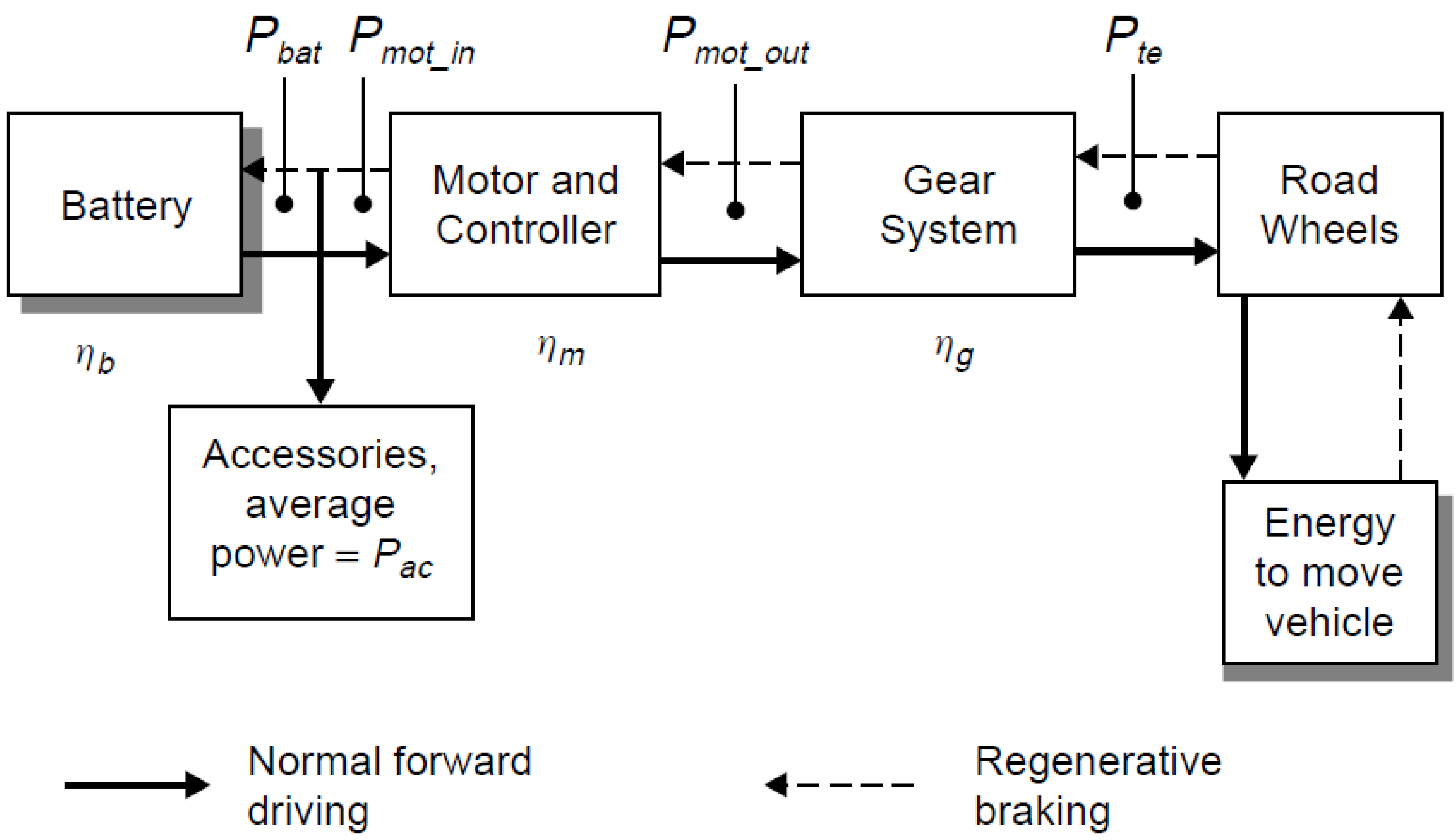

Start

Use v_{n+1} and v_n to find the acceleration

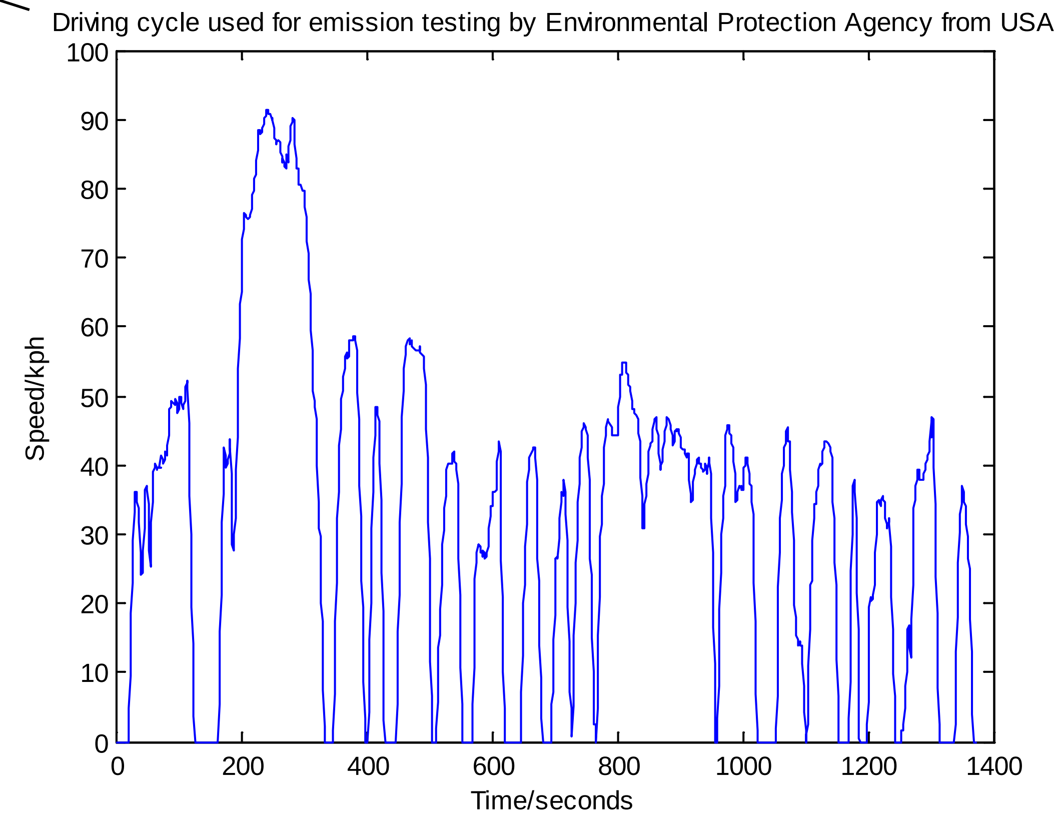

INEP

Start

Use v_{n+1} and v_n to find the acceleration

Using a and v, calculate F_{te} and P_{te}

Calculate the motor power

Calculate motor angular speed and toque

Find the motor efficiency

Rolling resistance force $\longrightarrow$ $F_{rr} = \mu_{rr} mg$

Aerodynamic drag $\longrightarrow$ $F_{ad} = 0.5\rho A C_d v^2$

Hill climbing force $\longrightarrow$ $F_{hc} = mg\sin(\psi)$

Linear acceleration force $\longrightarrow$ $F_{la} = ma$

Angular acceleration force $\longrightarrow$ $F_{\omega a} = I\left(G/r\right)^2 a$

Total tractive effort

$$F_{te} = F_{rr} + F_{ad} + F_{hc} + F_{la} + F_{\omega a}$$

$$P_{te} = F_{te} \cdot v$$

$$P_{mot\_out} = P_{te} / \eta_g$$

$$\omega = v / r \quad \& \quad T = P_{mot\_out} / \omega$$

$$\eta_m = \frac{P_o}{P_i} = \frac{\tau\omega}{\tau\omega + k_c\tau^2 + k_i\omega + k_\varpi\omega^3 + C}$$

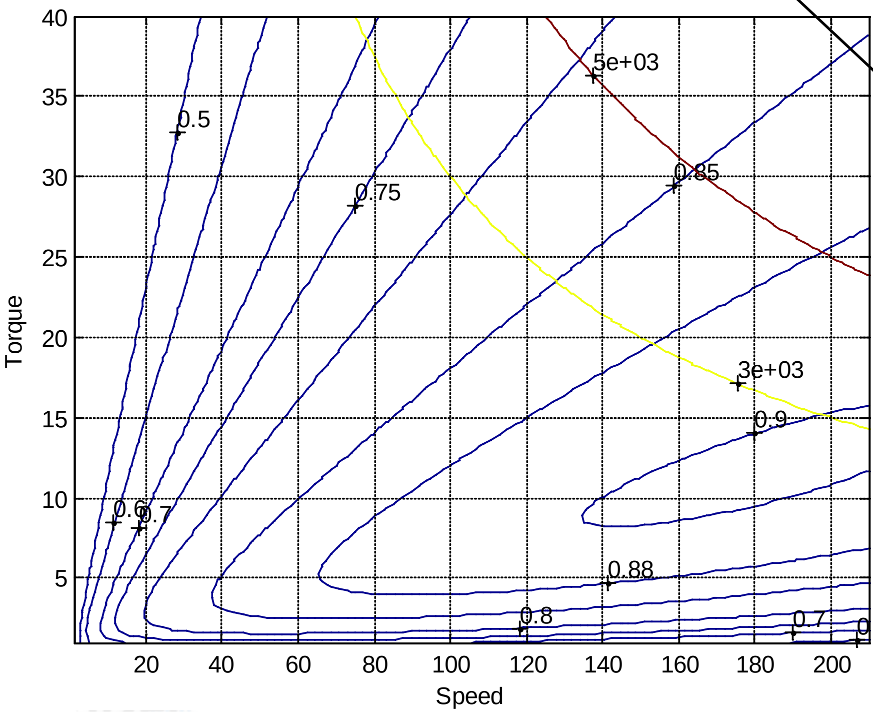

Start

1. Use v_{n+1} and v_n to find the acceleration
2. Using a and v, calculate F_{te} and P_{te}
3. Calculate the motor power
4. Calculate motor angular speed and toque
5. Find the motor efficiency
6. Find the power into the motor
7. Add the average accessory power P_{ac} to give the total value of battery
8. Find the battery current

$$P_{mot\_in} = P_{mot\_out} / \eta_{mot}$$

$$P_{bat} = P_{mot\_in} + P_{ac}$$

$$I = \frac{E - \sqrt{E^2 - 4RP}}{2R}$$

Where E depend of the battery type, for instance:

- Lead acid battery:

$$E = n \times (2.15 - DoD \times (2.15 - 2.00))$$

- NiCad battery

$$E = n \times \begin{pmatrix} -8.2816 DoD^7 + 23.5749 DoD^6 - 30 DoD^5 + 23.7053 DoD^4 \\ -12.5877 DoD^3 + 4.1315 DoD^2 - 0.8658 DoD + 1.37 \end{pmatrix}$$

INEP

Start

Use v_{n+1} and v_n to find the acceleration

Using a and v, calculate F_{te} and P_{te}

Calculate the motor power

Calculate motor angular speed and toque

Find the motor efficiency

Find the power into the motor

Add the average accessory power P_{ac} to give the total value of battery

Find the battery current

Update *DoD*

$$P_{mot\_in} = P_{mot\_out} / \eta_{mot}$$

$$P_{bat} = P_{mot\_in} + P_{ac}$$

$$I = \frac{E - \sqrt{E^2 - 4RP}}{2R}$$

$$CR_{n+1} = CR_n + \frac{\delta t \times I^k}{3600}\ [Ah]$$

→ Charge removed from the **plates** of battery

$$CS_{n+1} = CS_n + \frac{\delta t \times I}{3600}\ [Ah]$$

→ Total charge actually supplied by the battery to the vehicle's electrics

$$DoD_n = \frac{CS_n}{C_p}$$

C_p → Peukert Capacity

Obs.: This difference is caused by self-discharge reactions taking place *within* the battery.

INEP

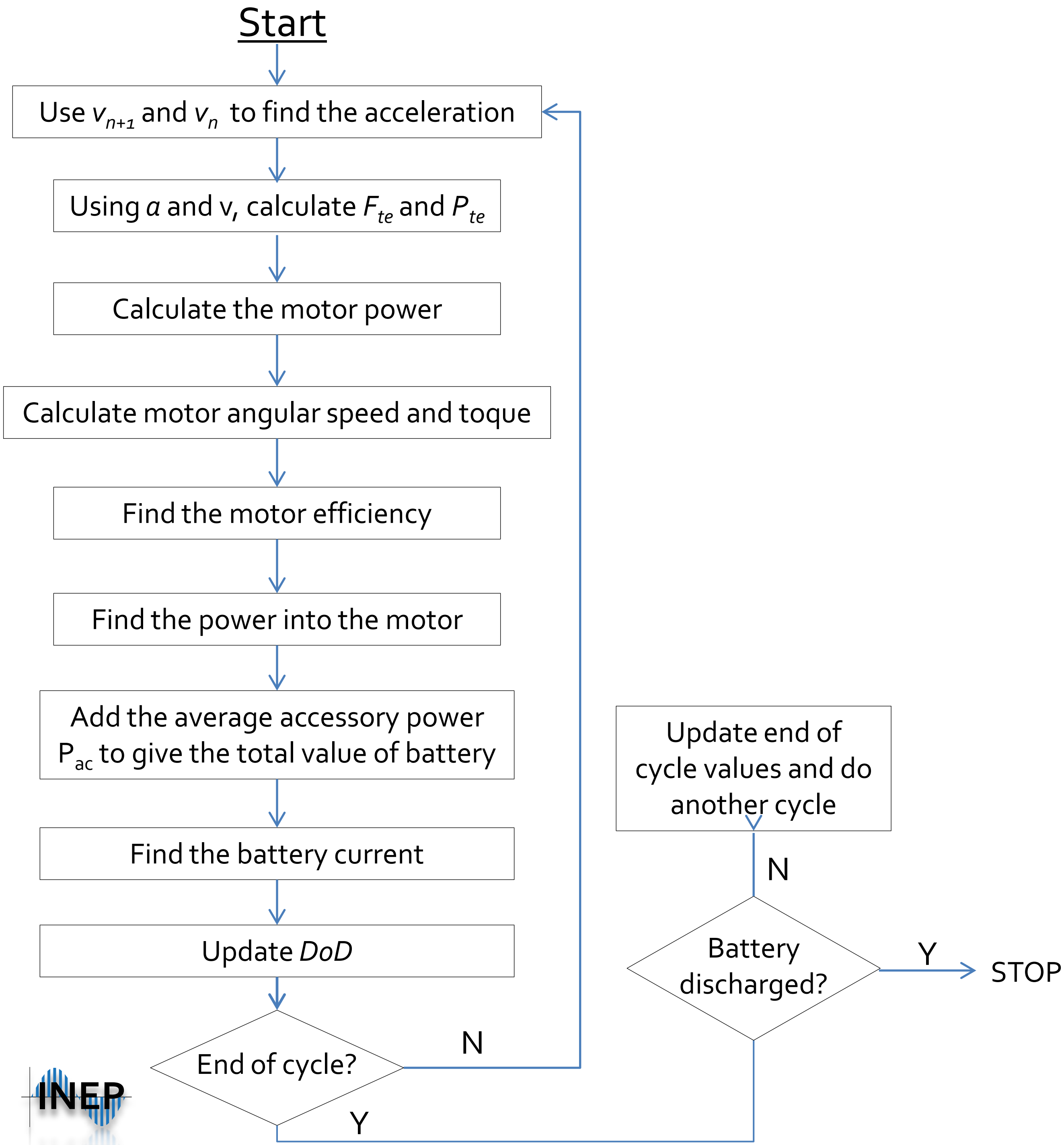
Start
Use v_{n+1} and v_n to find the acceleration
Using a and v, calculate F_{te} and P_{te}
Calculate the motor power
Calculate motor angular speed and toque
Find the motor efficiency
Find the power into the motor
Add the average accessory power P_{ac} to give the total value of battery
Find the battery current
Update *DoD*
End of cycle?
N
Y
Battery discharged?
Y
STOP
N
Update end of cycle values and do another cycle

Electric vehicle range modelling

Results obtained from the simulation:

- Distance travelled
- Vehicle acceleration
- Tractive effort
- Motor power
- Motor torque
- Motor angular speed
- Motor efficiency
- Current out of (or into) the battery

MATLAB: GM_EV1_Range.m

Electric vehicle range modelling

Results obtained from the simulation:

- Distance travelled

SFUDS driving cycle, and radio, head light and heater on.

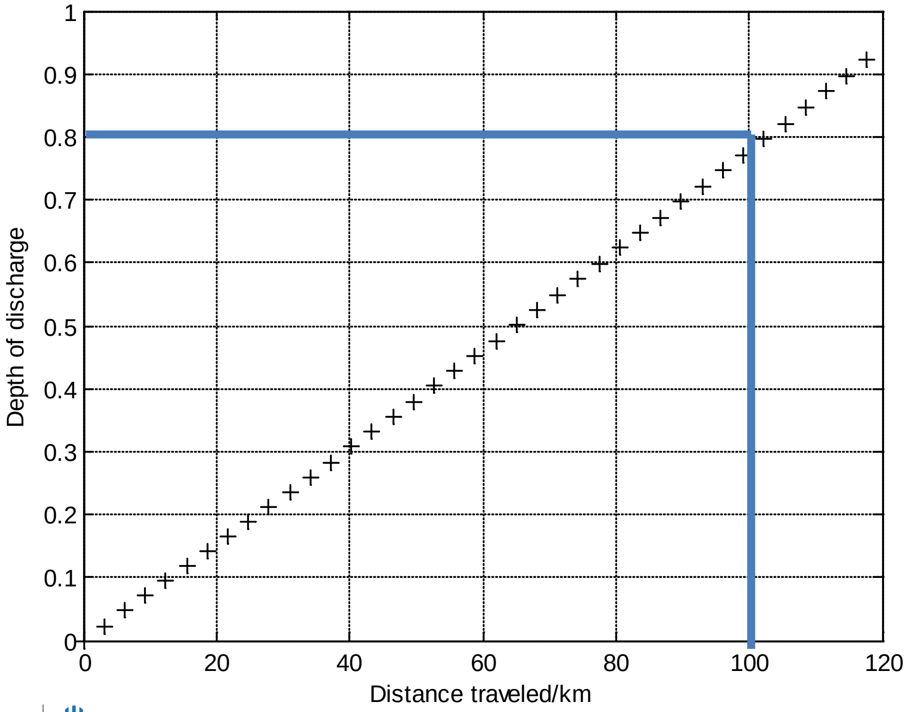

Constant speed, and radio on.

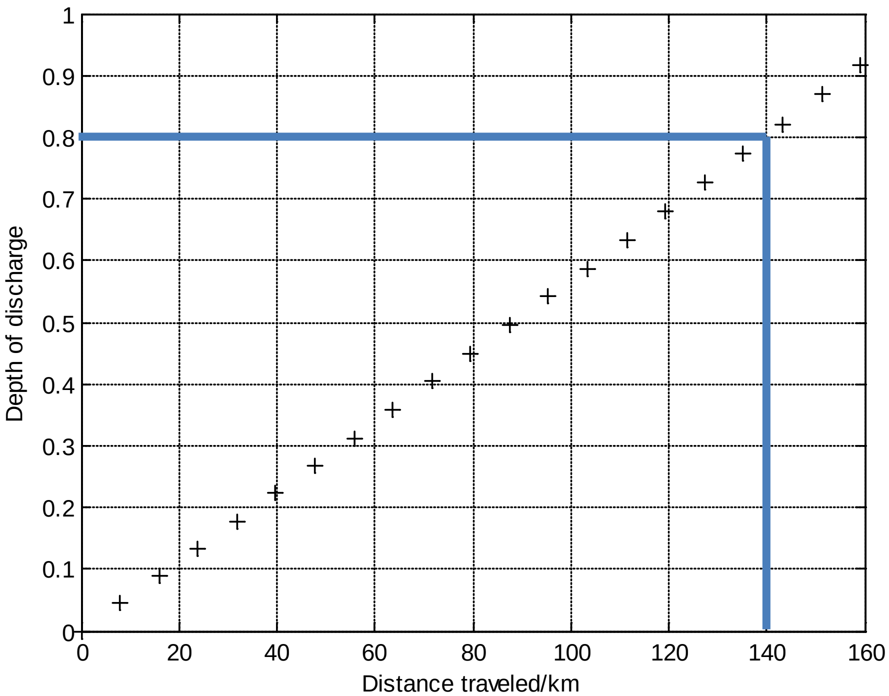

Electric vehicle range modelling

Results obtained from the simulation:

- Vehicle acceleration

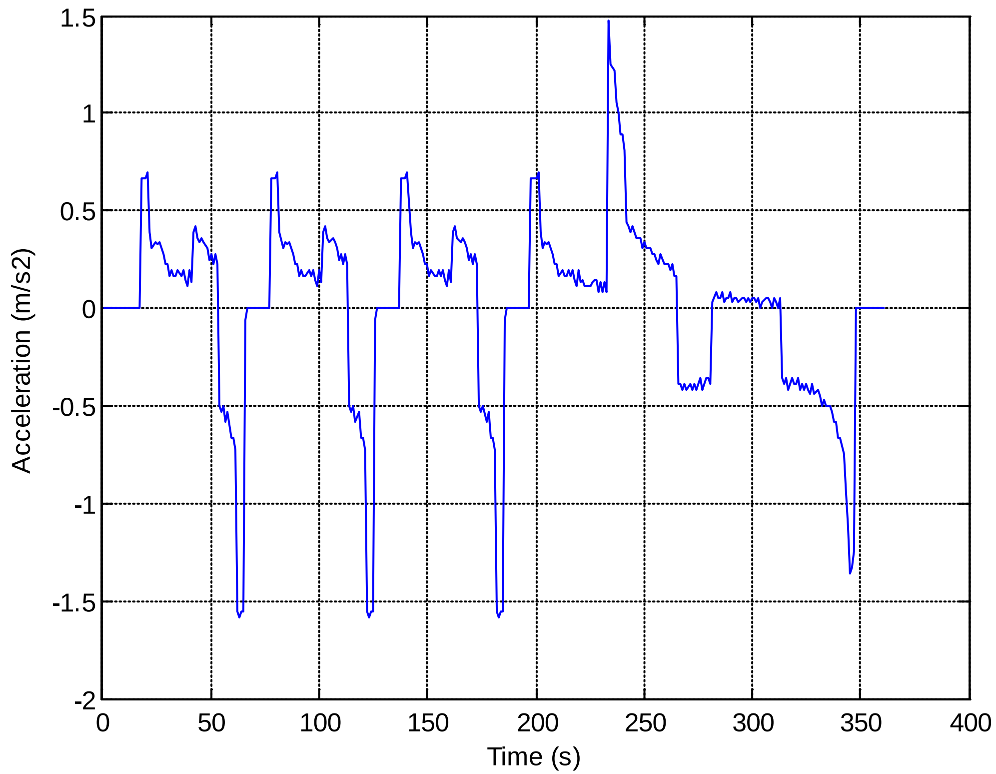

Electric vehicle range modelling

Results obtained from the simulation:

- Tractive effort

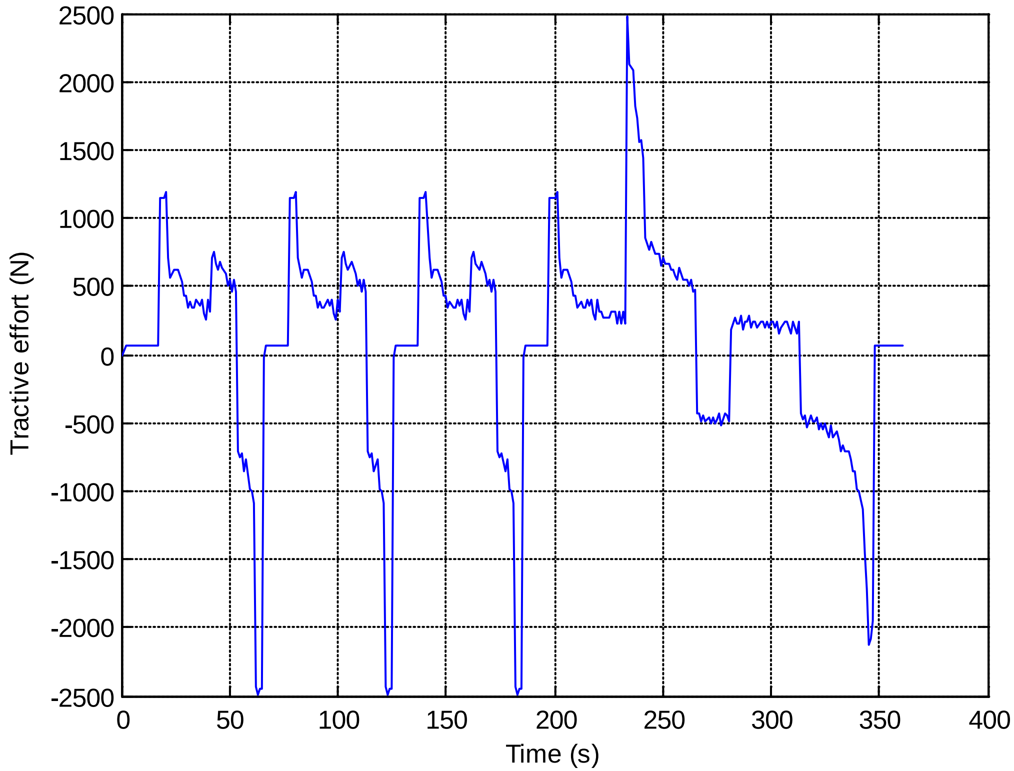

Electric vehicle range modelling

Results obtained from the simulation:

- Power into the motor

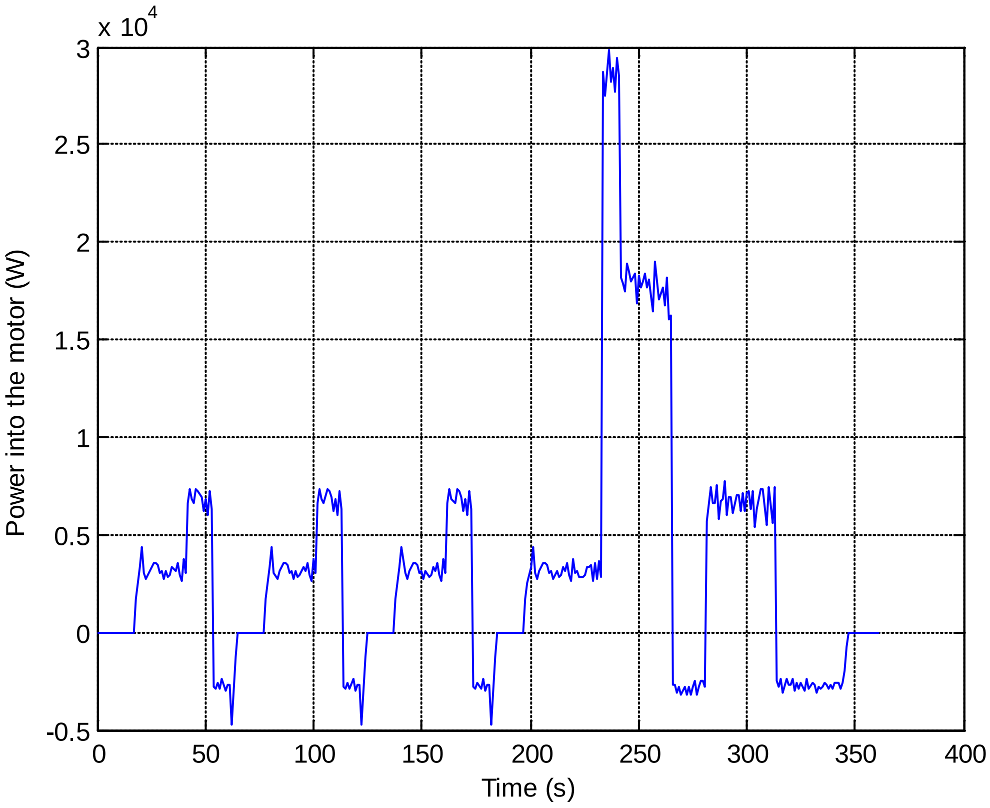

Electric vehicle range modelling

Results obtained from the simulation:

- Motor torque

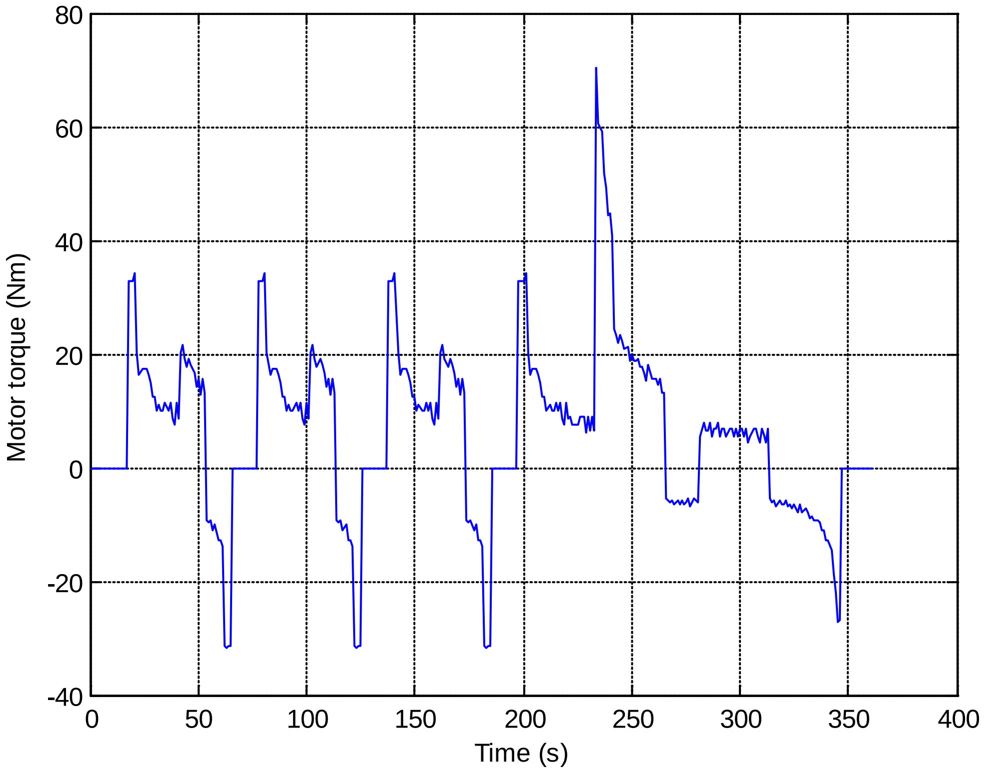

Electric vehicle range modelling

Results obtained from the simulation:

- Motor speed

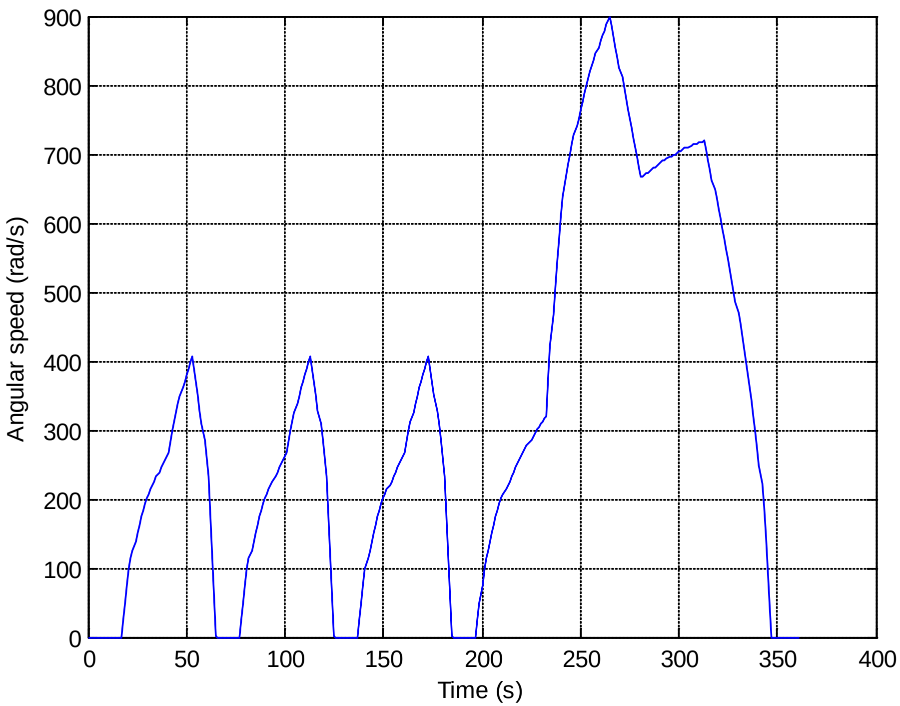

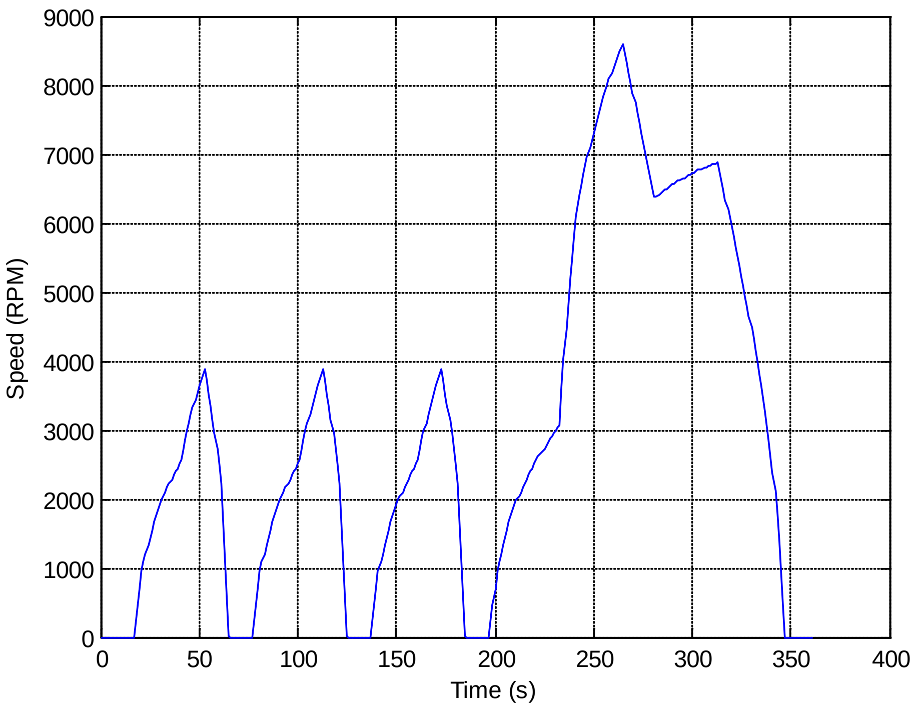

INEP

Electric vehicle range modelling

Results obtained from the simulation:

- Motor efficiency

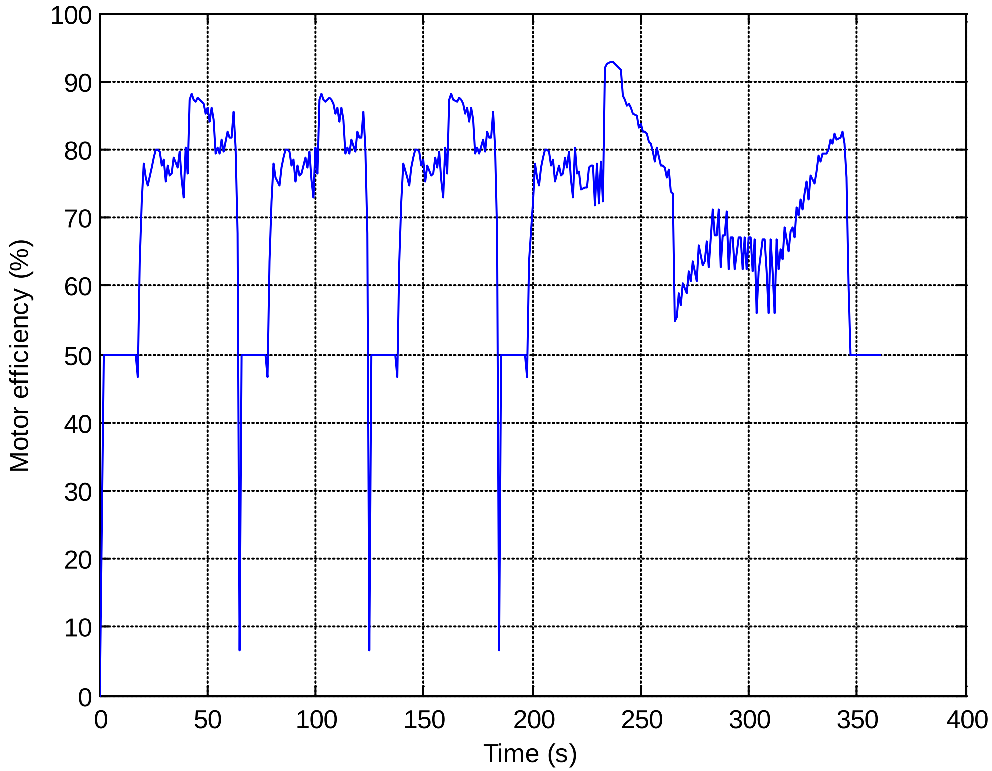

Electric vehicle range modelling

Results obtained from the simulation:

- Current into motor and controllers

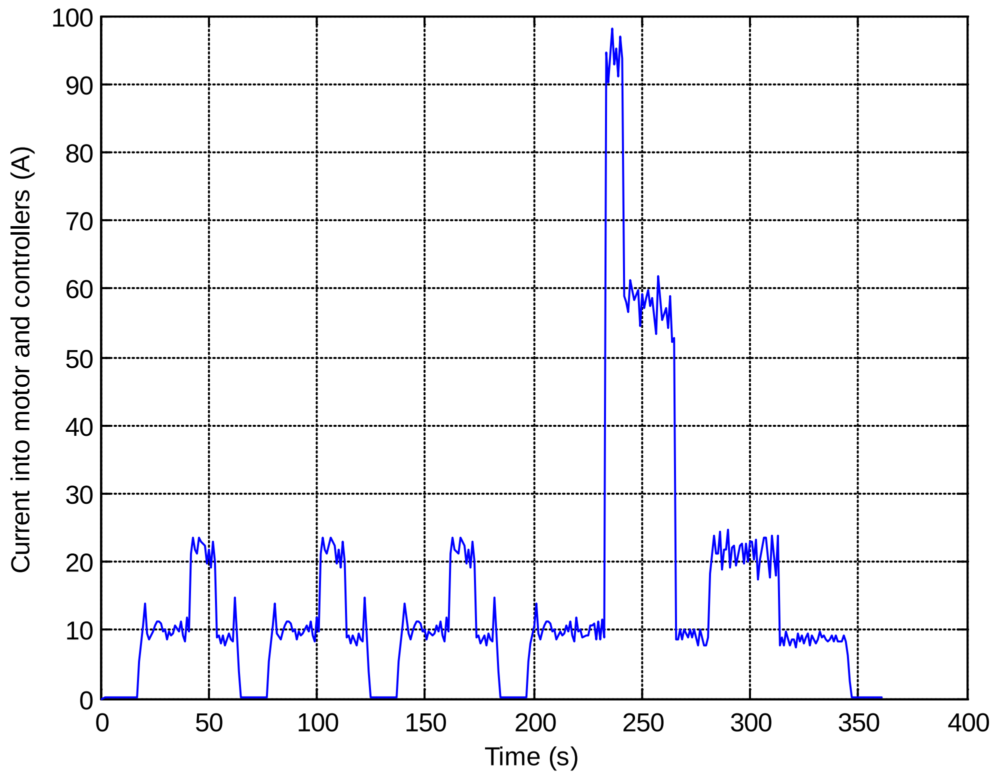

Electric vehicle range modelling

- Torque vs speed (Scooter)

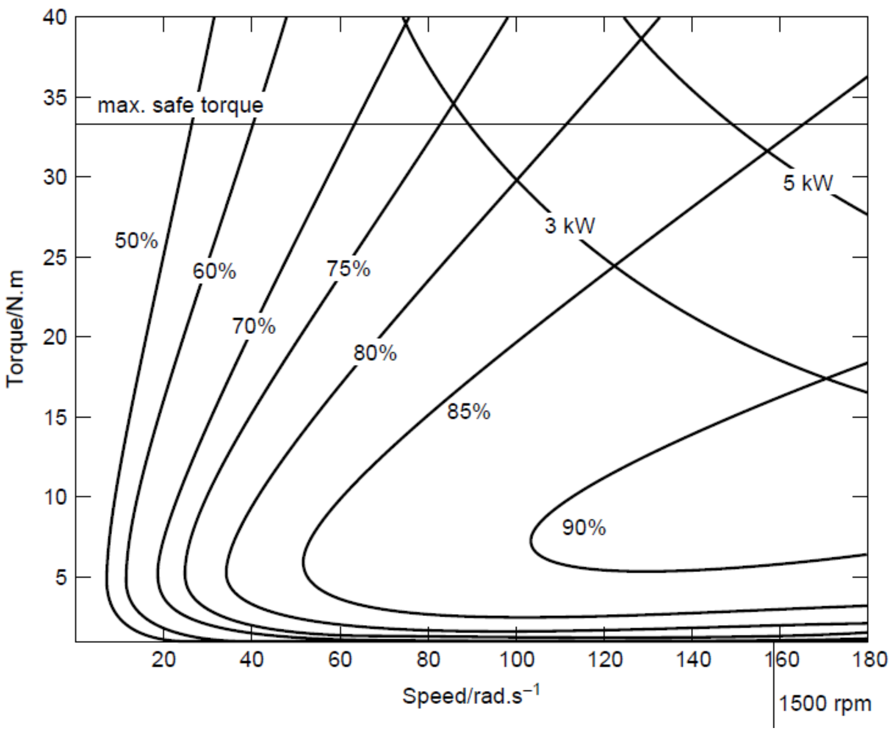

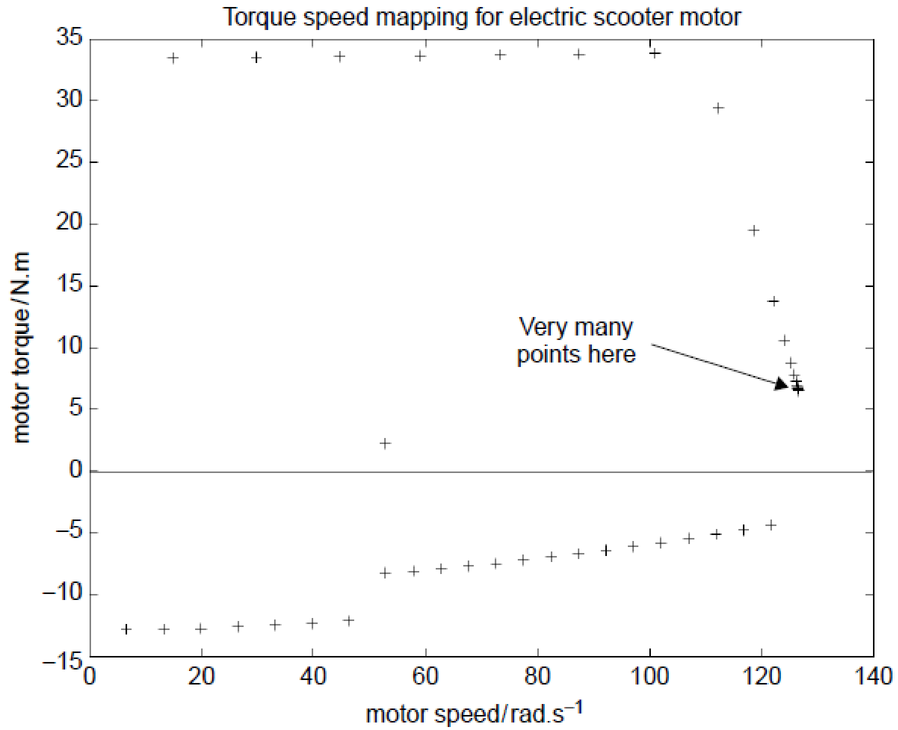

Electric vehicle modelling

UFSC

Final considerations

Other aspects might also be considered, for instance:

- Better batteries models
- Driving cycles using hill climbing forces
- Vehicle aerodynamics
- Rolling resistances
- Transmissions efficiency and others systems (in-wheel motors)
- Different converter types
- Other power trains (series, parallel, hybrid, etc)
- Carbon emission comparison between EVs
- Hybrid vehicle with intelligent systems

INEP

UFSC

INEP

Thank You!

COBEP 2015

NOVEMBER 29th TO DECEMBER 2nd, 2015

SPEC IEEE Power Electronics Society

SOUTHERN POWER ELECTRONICS CONFERENCE

www.ufsc.br

UFSC